

UC Davis

UC Davis Electronic Theses and Dissertations

Title

The Genetic Underpinning of Insidious Uveitis in LP Spotted Breeds of the Domestic Horse, Equus caballus

Permalink

<https://escholarship.org/uc/item/3263z44c>

Author

Kingsley, Nicole B.

Publication Date

2022

Peer reviewed|Thesis/dissertation

The Genetic Underpinning of Insidious Uveitis in *LP* Spotted Breeds of the
Domestic Horse, *Equus caballus*

By

NICOLE BREANN KINGSLEY
DISSERTATION

Submitted in partial satisfaction of the requirements of the degree of

DOCTOR OF PHILOSOPHY

in

Integrative Genetics and Genomics

in the

OFFICE OF GRADUATE STUDIES

of the

UNIVERSITY OF CALIFORNIA

DAVIS

Approved:

Rebecca R. Bellone, Chair

Carrie J. Finno

C. Titus Brown

Lynne S. Sandmeyer

Committee in Charge

2022

Abstract:

Insidious uveitis is a form of equine recurrent uveitis (ERU), an inflammatory eye disease, that disproportionally affects the Appaloosa horse breed. Previous research indicates that these horses are eight times more likely to be affected by ERU and four times more likely to become blind as a direct result of the disease compared to other breeds studied. Previous research also suggests that an insertion in *TRPM1* (*LP*), which leads to the breed's characteristic leopard complex spotting pattern (*LP*), is a risk factor for ERU. *TRPM1* plays a known role within normal eye function as an ion channel that is necessary for transmission of the light detection signals between rod photoreceptor cells and ON-bipolar nerve cells. Specifically, TRPM1 is needed for proper vision in low light (scotopic) conditions, and lack of the functional protein in homozygous *LP* horses, therefore, causes congenital stationary night blindness (CSNB). Several investigations in the Appaloosa breed also indicate that *LP* is associated with ERU disease status; however, *LP* genotype is not sufficient to explain the distribution of insidious uveitis among Appaloosa horses. It is, therefore, suspected that additional genetic loci may contribute to disease risk.

Investigations of the cellular mechanisms of uveitis and genetic investigations in humans suggest that regulatory elements may play a large role in ocular immune privilege and intraocular inflammation. While extensive efforts have focused on annotating genes since the sequencing of the equine genome, recent efforts have focused on functionally annotating non-coding elements in the horse genome in a tissue-specific manner as part of the Functional Annotation of Animal Genomes (FAANG) initiative. The aim of the equine portion of the FAANG project is to generate publicly available data to improve upon the existing annotation of the equine genome and thereby advance research of putative functional variants outside of coding regions for investigations of equine diseases and traits of interest. Toward this aim, chromatin immunoprecipitation sequencing

(ChIP-Seq) was chosen to evaluate four chemical modifications (H3K4me1, H3K4me3, H3K27ac, and H3K27me3) of histones proteins within eight prioritized tissues and four additional “adopted” tissues. The four histone modifications are associated with key genomic regulatory elements, such as promoters (H3K4me3) and enhancers (H3K4me1), and transcriptional activity, such as active (H3K27ac) and inactive (H3K27me3) genomic elements. Through these efforts, thousands of novel putative regulatory elements from two Thoroughbred mares were identified within the equine genome, and these histone mark peaks represent a region of increased interest outside of gene boundaries for variant identification in research on ERU and other equine diseases.

Prior to any variant investigations for insidious uveitis, a prospective observational study was performed in the Appaloosa breed to better understand the major characteristics of ERU. In that investigation, we identified increasing age as a significant risk factor for disease (OR = 1.15, 95% CI [1.06 - 1.24], P = 0.001) and recapitulated the association with the *LP* locus when comparing *LP/LP* and *lp/lp* horses (OR = 19, 95% CI [2.8 - +INF], P = 0.009). Although uveitis cases were more likely to share common ancestors compared to the control horses as determined by coancestry coefficients (P = 0.02), affected horses did not have higher levels of inbreeding (P = 0.8), and a pedigree analysis did not identify a clear mode of inheritance from the data available.

Heritability was estimated to understand the role of genetic variance in the distribution of insidious uveitis among Appaloosa horses. Using a combined and imputed dataset of 142 Appaloosas (59 cases and 83 controls) genotyped on either the Illumina Equine SNP70 BeadChip (n = 46) or the Axiom Equine 670K Genotyping Array (n = 96), SNP-based narrow-sense heritability of insidious uveitis was estimated to be 1.09 (SE = 0.16, P = 1.56x10⁻⁴). The h² estimate accounted for sex and age as covariates and incorporated *LP* genotype as a fixed effect in the model, which contributed 0.20 of the overall heritability of ERU. The high estimate indicates that

additional genetic loci outside of *LP* may be contributing to ERU in the dataset, warranting further investigation of genetic risk factors.

Using genotyping array data (Axiom Equine Genotyping Array) from 96 Appaloosas (36 cases and 60 controls), a genome-wide association study (GWAS) with *LP* genotype, sex, age, and relatedness as covariates in a mixed linear model (MLM) identified a significantly associated region on the X chromosome after multiple testing correction (ECA X: 14.5 Mb, $P = 2.11 \times 10^{-8}$), and the association was still significantly associated with disease phenotype in a sex-stratified analysis ($P = 1.35 \times 10^{-8}$). Furthermore, a Cochran-Mantel-Haenszel test for genetic interaction indicated that *LP* is epistatic to the locus on ECA X ($P = 1.72 \times 10^{-6}$). To interrogate the X locus further, whole genome sequencing (WGS) data from 18 Appaloosas (nine cases and nine controls) were evaluated for potential causal single-nucleotide variants (SNVs). SNVs within 150 Kb of the locus of interest were prioritized if they were identified by both variant callers (Freebayes and BCFtools) and had genotype frequency differences of 30% or greater in cases compared to controls. To investigate the association further, 130 prioritized variants from the region of interest were genotyped in a larger cohort of 157 horses (70 cases and 87 controls). One variant was identified within a coding region, and four variants were found within histone mark peaks based on the publicly available FAANG data. However, no SNVs were perfectly concordant with phenotype in the region of interest. Although the original GWAS SNPs remained significant in this larger cohort ($P = 4.06 \times 10^{-5}$), none of the 102 SNVs that passed quality filtering were significantly associated with disease. Based on these results, it is suspected that the top three markers may be tagging a structural variant or another uncharacterized mutation, and additional work is needed to further characterize the association on ECA X for putative causal variants.

To compliment the clinical investigation of insidious uveitis in Appaloosas, a prospective observational study was performed in the Knabstrupper breed, and we discovered that the characteristics of ERU are similar between the Appaloosa and the Knabstrupper. In particular, signs of ocular discomfort and inflammation, such as aqueous flare, conjunctival hyperemia, hypotony, and miosis, were more common in uveitis affected Appaloosas and Knabstruppers compared to controls ($P < 0.001$), while two “historic” indicators of ERU were not significantly more common (bullet-hole lesions, $P > 0.2$ and butterfly lesions, $P > 0.3$). Furthermore, *LP/LP* Knabstruppers were at significantly higher odds of developing ERU compared to true solid horses (*lp/lp*) (OR = 7.64, 95% CI [0.8 - +INF], $P = 0.04$), and horses in the age range of 11-20 years old had significantly higher odds of ERU compared to the reference age group (< 5 years old) (11-15 years OR = 8.19, 95% CI [1.2 – 105.6], $P = 0.02$ and 16-20 years OR = 13.36, 95% CI [1.4 – 213.4], $P = 0.009$). These results are consistent with findings from the Appaloosa breed. Additionally, modes of inheritance were investigated in a pedigree analysis, yet it was not possible to conclusively exclude any simple models of inheritance. The data suggest that a simple sex-linked or maternal effect mechanism does not explain the inheritance pattern of ERU in the Knabstrupper; however, investigations of additional families with phenotyping across multiple generations is necessary. Although inbreeding was not significantly different between the cases and the control horses ($P > 0.9$), Knabstruppers with ERU were more likely to share common relatives compared to the controls ($P = 0.01$).

Given the similarities between the disease phenotype identified across breeds with LP, a GWAS for insidious uveitis was performed on a combined dataset of 250 horses (111 cases and 139 controls) from the Appaloosa, Pony of the Americas (POA), and Knabstrupper breeds. The only region to reach genome-wide significance contained the *LP* locus on ECA 1 ($P = 6.58 \times 10^{-9}$),

and a haplotype analysis identified a 76 Kb haplotype, termed “Haplotype A,” in all affected horses. However, Haplotype A was also present in many unaffected horses and was not more concordant with ERU compared to the *LP* locus ($P_{\text{HapA}} = 9.04 \times 10^{-21}$ versus $P_{LP} = 1.08 \times 10^{-27}$). While it is suspected that the *LP* allele itself may play a role in ERU, further refinement and functional assessments of the associated region are needed to determine the underlying role of that locus in insidious disease.

Taken together, all these data support that there is a strong genetic underpinning to insidious uveitis, and the *LP* locus is a major risk marker for insidious uveitis across *LP* breeds. However, the causative variant in the region containing *LP* is suspected to have incomplete penetrance for ERU, and identification of other breed-specific risk factors, such as the associated region on ECA X, will help to better explain the distribution of insidious uveitis within the Appaloosa, Knabstrupper, and POA breeds.

Dedication:

It is hard to know how far back to go to thank the people in my life who have made this dissertation possible. I am sure that I will leave out key players, so I would like to start by saying to all the people who encouraged and believed in me, to the people who supported me, and to the people who pushed and challenged me – Thank you.

In particular, I want to acknowledge the love and support from my big sister, my mom, and my dad. These three people are my front-line. Any time there was danger of my life or sanity going up in flames, they were there for me. Mom, Dad, and Sis, you are irreplaceable to me, and I am lucky to have you and your love in my life. Thank you for believing in me and teaching me to be the person who I am.

I also want to thank two people who let me into their lives with open arms and open hearts. Aunt Cathy and Aunt Shakey, I would never have finished my degree without the two of you. This thesis is a testament to the love and support that you gave me every single day. Thank you for helping me weather this storm and keep my little ship afloat. I love you both, and if I had a million dollars, I would give you each a half.

To my friends, especially Lia, Moriel, Jocelyn, Sam, Elizabeth, Emily, and Pilar, thank you for listening and reorienting me when my compass stopped pointing true north. Thank you for sticking with me and keeping me from going through this journey alone. I love you all, and I am thankful to have all of you in my life.

To my thesis mentor, Dr. Rebecca Bellone – DrB, thank you for teaching me how to turn my questions into science, how to build collaborations through genuine care and respect, and how to laugh even when things are tough. As big as this thesis is, the things that you have taught me could fill even more volumes. Thank you for mentoring and encouraging me, for pushing me when I needed it, and for guiding me when I got lost.

Finally, I want to acknowledge my biggest supporters – Ann and Kokomo. I would never have dreamed of researching an equine disease, but I fell in love with two horses many years ago. The rest is history. My old mare was as smart as a whip, and one of the best teachers I have ever had. Thank you, bun bun. My old gelding, Kokomo, is a big goober, but he teaches me patience every day. He means the world to me, and love for my horses pushed me to work hard, even when I faced intimidating challenges.

I have been fortunate to meet many wonderful horse-people during my degree, and I hope this research and my future work can help keep our horses happy and healthy for many years.



Preface:

In the 2,000 years since it was described by Pliny the Elder, equine recurrent uveitis (ERU) has been a devastating disease for horses, yet the cause of ERU, also known as moon blindness and periodic ophthalmia, is not completely understood. It is suspected that genetics contributes to disease onset for some forms of uveitis, and this dissertation focuses on evaluating the role of genetic variation in triggering a form of ERU known as insidious uveitis in horses with the leopard complex spotting coat color pattern (LP). A detailed evaluation of the current understanding of ERU risk factors is provided in Chapter 1, and the manuscript, “A Review of Investigated Risk Factors for Developing Equine Recurrent Uveitis,” was submitted as a review to *Veterinary Ophthalmology* (March 3, 2022).

Advances in human uveitis research, as well as experimental autoimmune uveitis (EAU) rat models, indicate that gene dysregulation may play a role in chronic interocular inflammation. Compared to human and rodent models, little is known about the horse genome outside of coding regions. Therefore, the first part of the thesis focused on building upon the existing annotation of the equine reference genome in order to improve our ability to identify potential non-coding variants in equine genetic studies, including our own investigation of insidious uveitis. Following in the wake of the ENCODE project for annotating the human genome, the Functional Annotation of Animal Genomes (FAANG) initiative was created to characterize functional elements in the genomes of major agricultural species. From the outset, the FAANG consortium selected a core set of genome-wide assays and tissues to efficiently uncover information about the role of non-coding DNA. In particular, chromatin immunoprecipitation sequencing (ChIP-Seq) was chosen to evaluate chemical modifications of the histone proteins that are necessary for DNA organization and storage. Many of these chemical signatures or histone marks are strongly associated with

specific regulatory states, and mapping histone marks through ChIP-Seq is a valuable method to identify putative distal and proximal regulatory regions, such as enhancers and promoters, as well as transcription start sites for active and inactive genes.

Like ENCODE, the core assays of FAANG were performed on prioritized tissues to identify tissue-specific aspects of genome function. Through the initial round of funding, the equine FAANG group selected eight tissues of interest (TOI) to evaluate with histone mark ChIP-Seq based on relevance to key disease and performance characteristics in the horse. To contribute to this effort, a thorough analysis of the ChIP data to identify the regions of enrichment, known as peaks, was performed, and the results of this work were published as “Functionally Annotating Regulatory Elements in the Equine Genome Using Histone Mark ChIP-Seq” in *Genes* in 2020. The paper is reproduced fully in the second chapter of this dissertation, including the supplemental figure (Figure S1) and three of the original supplemental tables (Tables S1-S3). These supplemental materials were considered necessary for evaluating the original manuscript and were, therefore, included in the chapter. All supplemental materials, including the other supplemental tables (Tables S4-S19), are available at <https://www.mdpi.com/2073-4425/11/1/3/s1>.

Following the TOI work, an initiative that harnessed equine genomics community funding to advance the annotation effort was pioneered by the equine FAANG group. The effort, termed “Adopt-a-Tissue,” aimed at continuing to evaluate equine tissues through sponsorship by researchers with special interests in tissues outside of the original TOI, and it supported the evaluation of four additional tissues for histone mark ChIP-Seq in the mare. As part of this dissertation, a complete analysis of the data was performed to generate peak calls, and a data report titled, “‘Adopt-a-Tissue’ Initiative Advances Efforts to Identify Tissue-Specific Histone Marks in

the Mare,” was published in *Frontiers in Genetics* in 2021. The full manuscript is included in this thesis as the first addendum since it builds upon Chapter 2.

To continue to advance our understanding of insidious uveitis, several clinical investigations and genomic studies were conducted in Appaloosas and related breeds. First, an investigation of Appaloosa horses in western Canada was performed to characterize the clinical manifestations of insidious uveitis and evaluate potential risk factors. Building on previous work, this investigation aimed at identifying the mode of inheritance for insidious uveitis and testing a previously associated genetic variant, known as *LP*, that causes the characteristic Appaloosa spotting pattern. For this dissertation, a pedigree analysis was carried out to evaluate the mode of inheritance, the level of inbreeding, and the role of recent shared ancestry in the distribution of ERU within the dataset. The results were published in *Veterinary Ophthalmology* in 2020 with the title “Risk Factors for Equine Recurrent Uveitis in a Population of Appaloosa Horses in Western Canada,” and the full paper is included as the second addendum in this dissertation.

Following the clinical evaluation, the heritability of ERU in Appaloosas was investigated. Despite the strong breed predisposition for insidious uveitis in Appaloosas, previous efforts to estimate the role of genetic variation in disease onset have been hindered by small sample size. By combining two genotyping datasets, SNP-based narrow-sense heritability was estimated for insidious uveitis in Appaloosas. From this work, we determined that risk for ERU was highly heritable, and the *LP* locus only explained a small proportion of the risk, which supported performing additional genome-wide association studies (GWAS). The efforts were recently submitted as a short communication to *Animal Genetics* (March 18, 2022), and the entire manuscript, titled “Heritability of Insidious Uveitis in Appaloosa Horses” can be found in Chapter 3. Building upon that work, a genome-wide association study (GWAS) of 96 Appaloosa horses,

including 36 cases and 60 controls, was used to identify additional genetic loci in the Appaloosa for further investigation. Using a mixed linear model (MLM) with covariates for *LP* genotype, sex, age, and relatedness, we identified a 9.7 Kb region on ECA X that was significantly associated with insidious disease ($p\text{-value} = 2.11 \times 10^{-8}$). The full investigation, titled “Identifying Genetic Risk Loci for Insidious Uveitis in Appaloosa Horses,” is detailed in the 4th chapter.

In addition to the Appaloosa, predisposition for insidious uveitis is recognized in other LP-patterned breeds, including the Knabstrupper and Pony of the Americas (POA). For that reason, a clinical evaluation of insidious uveitis in Knabstrupper horses from Denmark, Sweden, and the USA was undertaken, including investigation of the most promising risk factors. The submitted manuscript summarizing the analyses and findings is reproduced fully in Chapter 5, “Risk Factors for Equine Recurrent Uveitis in the Knabstrupper Breed.” The major findings of this work, such as average age, clinical manifestations, and risk factors, support a strong similarity between insidious uveitis in Appaloosas and Knabstrupper. Based on the preceding investigations, we determined that a large multibreed GWAS was warranted for further investigation of ERU in LP spotted horses. Using a combined dataset of 250 horses (111 cases and 139 controls), we identified the region containing the *LP* insertion as the only major risk locus that was shared across the Appaloosa, Knabstrupper, and POA breeds ($P = 6.58 \times 10^{-9}$). The work is summarized in Chapter 6 in this thesis, under the title, “Genome-wide Investigation of Genetic Risk Factors for Insidious Uveitis in Horses with LP Spotting.” Altogether, these investigations increase our understanding of ERU in the Appaloosa and other LP breeds, and they will lead to new research on insidious uveitis that may improve disease management and breeding practices in the future.

Table of Contents:

Chapter 1: Risk Factors for Developing Equine Recurrent Uveitis

Abstract -----	1
Introduction -----	1
Environmental Risk Factors -----	6
Genetic Risk Factors -----	13
Future Directions -----	22
References -----	24

Chapter 2: Functionally Annotating Regulatory Elements in the Equine Genome Using Histone ChIP-Seq

Abstract -----	43
Introduction -----	44
Materials and Methods -----	47
Results -----	52
Discussion -----	68
Supplemental Material -----	75
References -----	83

Chapter 3: Heritability Estimates of Insidious Uveitis among Appaloosa Horses

Summary -----	91
Main Text -----	92
References -----	98

Chapter 4: Identifying Genetic Risk Loci for Insidious Uveitis in Appaloosa Horses

Abstract -----	102
----------------	-----

Introduction -----	103
Materials and Methods -----	106
Results -----	109
Discussion -----	113
Conclusion -----	117
Supplemental Material -----	117
References -----	125
Chapter 5: Risk factors for equine recurrent uveitis in Knabstrupper horses	
Summary -----	132
Introduction -----	134
Methods -----	136
Results -----	142
Discussion -----	152
Supplemental Material -----	158
References -----	160
Chapter 6: Genome-wide Investigation of Genetic Risk Factors for Insidious Uveitis in Horses with <i>LP</i> Spotting	
Summary -----	165
Main Text -----	165
References -----	175
Conclusion -----	179
Addendum 1: “Adopt-a-Tissue” Initiative Advances Efforts to Identify Tissue-Specific Histone Marks in the Mare	

Introduction -----	181
Methods -----	183
Quality Assessment -----	185
Data Metrics -----	191
Data Accessibility -----	192
Discussion -----	192
Supplemental Material -----	198
References -----	204

Addendum 2: Risk factors for equine recurrent uveitis in a population of Appaloosa horses in western Canada

Abstract -----	213
Introduction -----	214
Materials and Methods -----	217
Results -----	221
Discussion -----	227
References -----	232

Table of Figures and Tables:

Chapter 1	Chapter 4
Figure 1 ----- 3	Figure 1 ----- 105
Figure 2 ----- 4	Table 1 ----- 109
Table 1 ----- 16	Figure 2 ----- 110
Table 2 ----- 18	Table 2 ----- 111
Figure 3 ----- 21	Table 3 ----- 111
Chapter 2	Table 4 ----- 113
Table 1 ----- 48	Table S1 ----- 117
Table 2 ----- 50	Table S2 ----- 121
Figure 1 ----- 53	Chapter 5
Table 3 ----- 54	Figure 1 ----- 135
Table 4 ----- 56	Table 1 ----- 143
Figure 2 ----- 59	Table 2 ----- 145
Figure 3 ----- 60	Table 3 ----- 149
Figure 4 ----- 61	Table 4 ----- 149
Figure 5 ----- 62	Figure 2 ----- 150
Figure 6 ----- 63	Figure 3 ----- 151
Table 5 ----- 64	Table S1 ----- 158
Figure 7 ----- 67	Table S2 ----- 158
Figure 8 ----- 68	Table S3 ----- 158
Figure S1 ----- 76	Chapter 6
Table S1 ----- 76	Figure 1 ----- 167
Table S2.1 ----- 77	Figure 2 ----- 170
Table S2.2 ----- 78	Table 1 ----- 172
Table S3 ----- 80	Table 2 ----- 173
Chapter 3	Addendum 1
Figure 1 ----- 93	Table 1 ----- 188
Table 1 ----- 96	Table 2 ----- 190

Addendum 1 continued

Supplementary Table 1 ----- 198
Supplementary Table 2 ----- 198
Supplementary Figure 1 ----- 200
Supplementary Figure 2 ----- 201
Supplementary Figure 3 ----- 202
Supplementary Figure 4 ----- 203
Supplementary Figure 5 ----- 204

Addendum 2

Figure 1 ----- 216
Table 1 ----- 222
Table 2 ----- 223
Table 3 ----- 223
Table 4 ----- 223
Table 5 ----- 224
Figure 2 ----- 226

Chapter 1: A Review of Investigated Risk Factors for Developing Equine Recurrent Uveitis

Authors: N. B. Kingsley, Lynne Sandmeyer, and Rebecca R. Bellone

Keywords: ocular, inflammation, ERU, predisposition, horse, genetics

Reference: Kingsley, N.B.; Sandmeyer, L.; Bellone, R.R. A Review of Investigated Risk Factors for Developing Equine Recurrent Uveitis. *Vet Ophthalmol.* Submitted 2022.

Submitted: March 3, 2022

Abstract: Equine recurrent uveitis (ERU) is an ocular inflammatory disease that can be difficult to manage clinically. As such, it is the leading cause of bilateral blindness for horses. ERU is suspected to have a complex autoimmune etiology, with both environmental and genetic risk factors contributing to onset and disease progression in some or all cases. Work in recent years has aimed at unraveling the primary triggers, such as infectious agents and inherited breed-specific risk factors, for disease onset, persistence, and progression. This review has aimed at encompassing those factors that have been associated, implicated, or substantiated as contributors to ERU, as well as identifying areas for which additional knowledge is needed to better understand risk for disease onset and progression. A greater understanding of the risk factors for ERU will enable earlier detection and better prognosis through prevention and new therapeutics.

Introduction:

Equine recurrent uveitis (ERU) is a vision-threatening ocular syndrome characterized by inflammation of the uvea and historically classified into three subtypes based on location and duration of inflammation within the inner eye.¹ Baumgart *et al* (2014) has challenged the historical classification scheme of ERU; however, widespread acceptance of reclassification has not yet taken place.²⁻⁵ The classic and posterior subtypes of ERU are characterized by repeated

inflammatory episodes with intermittent periods of quiescence, while the insidious form usually presents with subtle or no outward signs of continuous intraocular inflammation. Both classic and insidious forms can manifest as inflammation throughout the vascular uveal tract (iris, ciliary body, and choroid).⁵ Posterior ERU, on the other hand, is characterized by recurring bouts of inflammation, predominantly within the posterior segment of the eye. A 2015 retrospective study identified a novel equine ocular disease known as heterochromic iridocyclitis (HIK) that presents with anterior uveitis, as well as other pathologies.⁶ The authors argue, however, that this disease is distinct from ERU by lacking periods of quiescence and presenting with uncharacteristic symptoms, such as pigmented keratic precipitates and retrocorneal membranes. To date, risk factors for this form of uveitis have not been evaluated in horses, and further discussion of HIK is outside the purview of this review of ERU. Regardless of the form, recurrent or persistent uveitis can damage the uveal tract itself and other important ocular structures, such as the cornea, lens, and retina, leading to visual impairment that may progress to complete blindness of an affected eye.^{1,5,7}

Overt signs of acute ocular inflammation include blepharospasm, epiphora, enophthalmos, photophobia, and conjunctivitis.^{8,9} While these symptoms are obvious signs of ocular discomfort, they are not specific to uveitis. Several other ocular conditions, such as corneal ulceration, can lead to similar signs of eye pain, and thorough examination is required to diagnose uveitis prior to treatment. For the anterior segment, inflammation is identified by the presence of aqueous flare or, more rarely, hypopyon (Fig. 1).^{9,10} Conversely, posterior segment uveitis is distinguished by vitritis and chorioretinitis and may not cause any of the overt signs of ocular discomfort already discussed.^{9,11} Although it is not as outwardly obvious compared with acute anterior disease, posterior inflammation is recognizable if a complete ocular examination is performed. Anterior

segment changes from inflammation can include miosis, corneal edema, corpora nigra atrophy, and irideal variation, and posterior segment changes from inflammation include vitreal degeneration and retinal edema, degeneration, or detachment.^{1,5,8,9} Although uveitis may be solely posterior or anterior at onset, it is not unusual for inflammation to spread to both ocular segments (panuveitis) in any clinical classification of ERU.^{9,11} Synechia, cataracts, and lens luxation can result from inflammation in either segment (Fig. 2). Additionally, glaucoma and phthisis bulbi are potential end-stage sequela of chronic ERU regardless of the classification, and ultimately, destructive inflammation anywhere within the eye can lead to visual loss and eventual blindness.^{9,11}

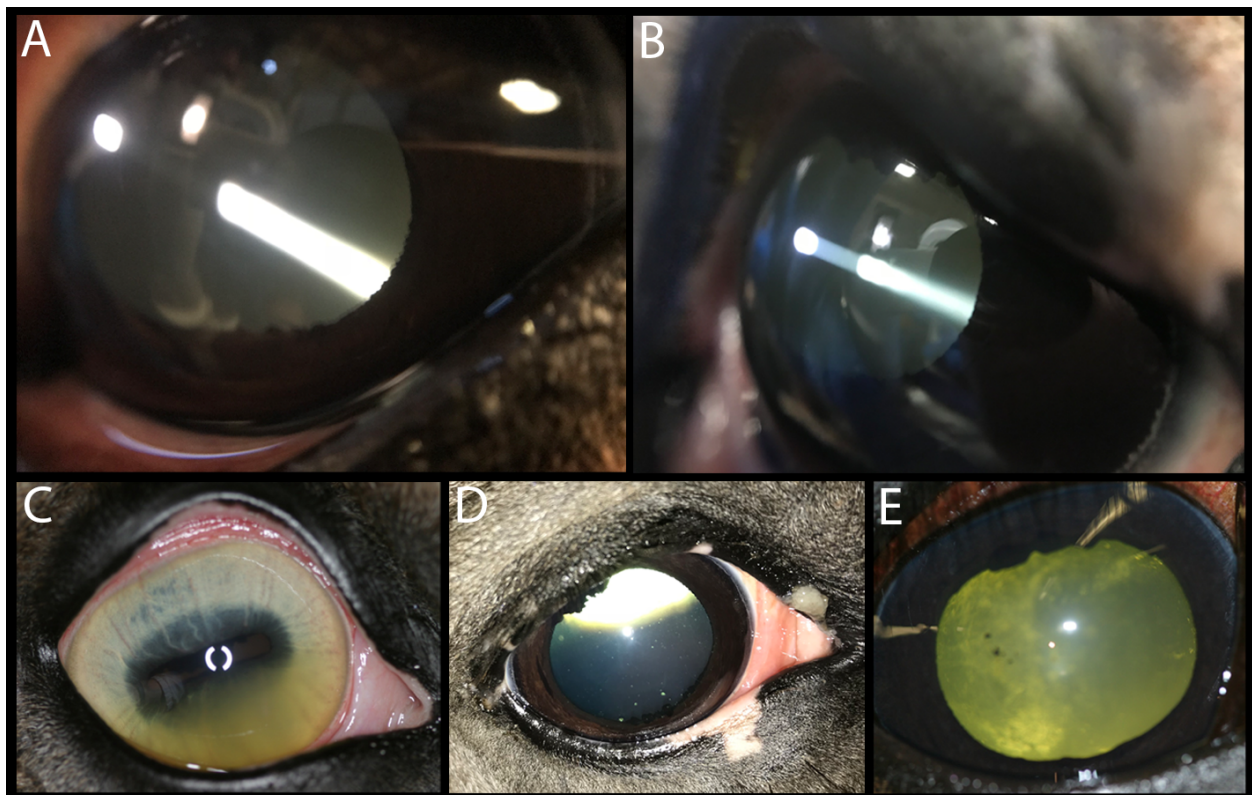


Figure 1: Ocular indications of inflammatory activity within the equine eye. (A) Normal left eye under slit lamp evaluation for aqueous flare. Note that the beam of light is scattered (visible) when passing through the cornea and lens, but not while passing through the aqueous humor of the anterior segment. (B) An affected left eye under slit lamp evaluation for aqueous flare. Note that the beam of light is unusually scattered (visible and hazy) when passing through the aqueous humor, indicating the presence of proteins and other macroscopic particles within the anterior segment (known commonly as aqueous flare). (C) An affected right eye with signs of active

inflammation in the anterior chamber including conjunctival hyperemia, iridial color change from blue to yellow, iris hyperemia, miosis, and fibrin in the ventral anterior chamber. (D) Normal right equine eye with posterior segment visible through the dilated pupil and no evidence of vitritis. (E) An affected right eye with vitreal opacities due to vitritis noted through the dilated pupil.

Unlike the episodic forms of ERU, insidious uveitis rarely develops obvious signs of ocular discomfort or dysfunction until significant damage has resulted in visual deficits or complete blindness of an affected eye.^{5,7,12} It predominantly manifests as bilateral disease with differential progression rates for a pair of eyes.⁷ The subtle character of insidious inflammation makes identification, even during an ophthalmic examination, more difficult at early stages of disease. Additionally, extensive time between onset and diagnosis seems to be common, making this form of ERU especially challenging to manage.

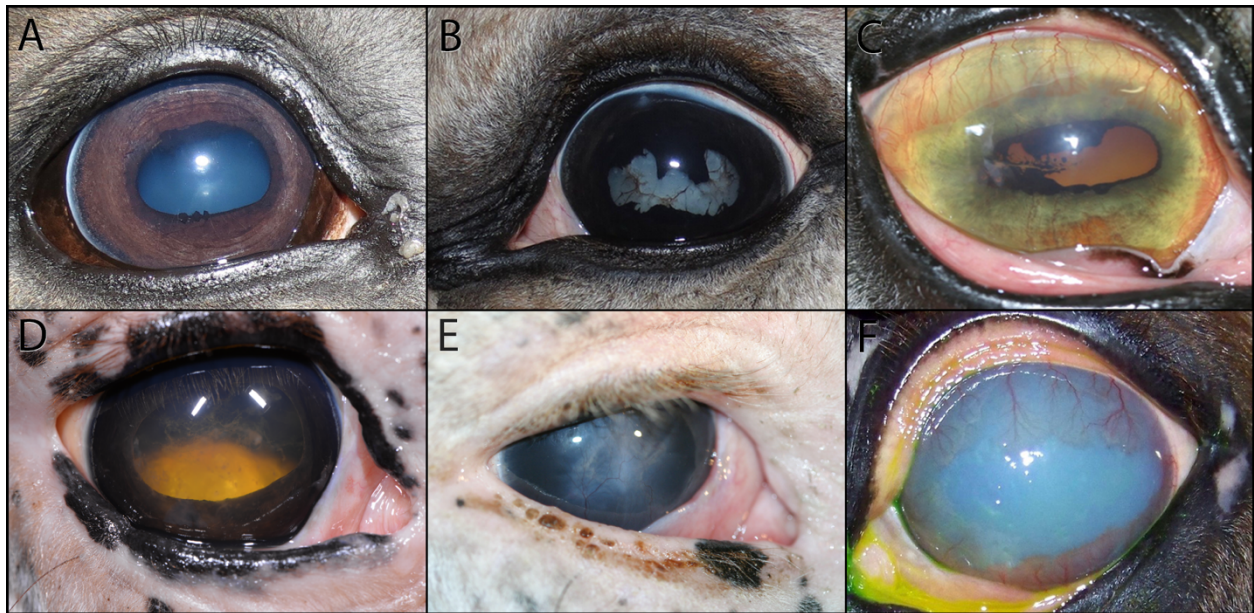


Figure 2: Common sequelae associated with ERU. (A) Unaffected right eye that is within normal limits on all measures by ocular examination. (B) Affected left eye with dense mature cataract and 360-degree anterior synechia secondary to ERU. This eye is not visual. (C) Same right eye as Fig 1C at a later date following minimal response to therapy. The eye has developed corneal vascularization, iris hyperemia, and synechia. (D) Affected right eye with posterior lens luxation and 3-4+ aqueous flare. This eye shows evidence of impaired vision. (E) Affected right eye with phthisis bulbi along with superficial neovascularization and plaque material on the central region of the cornea. This eye is not visual. (F) Affected left eye with glaucoma secondary to ERU, extensive corneal edema and corneal neovascularization. This eye is not visual. Photographs courtesy of Dr. Ann Dwyer (A, B, and F) and Dr. Mary Lassaline (D).

ERU has been described as a complex inflammatory disease with multiple genetic and environmental factors that may play roles in onset and progression, and the majority of ERU cases are thought to occur without comorbidity.¹³⁻¹⁵ Using owner reporting, researchers found that ERU was concurrent with gastrointestinal disease for 31 of 163 ERU-affected horses and with orthopedic disease for 28 of 166 ERU-affected horses, yet true comorbidity was suspected in only 21 and seven horses, respectively.⁵ For that reason, ERU is usually evaluated as a primary disease. While the exact etiology is not known, immunological research supports that ERU is immune-mediated with involvement of CD4+ T-cells triggering both Th17 and Th1 pro-inflammatory responses from the adaptive immune system.^{16,17} Similar research in experimental autoimmune uveitis (EAU) models and humans with uveitis found evidence of consistent adaptive immune responses across species.^{18,19} Horses are, therefore, considered an excellent spontaneous model for understanding uveal inflammation and disease progression.^{20,21} Additionally, investigation of antibody cross-reactivity first identified in EAU models was also found to trigger an immune response in humans and horses, indicating that uveitis involves autoimmunity against antigens normally expressed in the eye.^{16,22-26} For the disease mechanism, it is suspected that, after sensitization by an inciting factor from the environment or from genetic predisposition, one or more activated antibodies lead to an autoimmune response against proteins normally present within the eye.²⁷ It is not clear at this time if genetic predisposition is sufficient to incite disease or if molecular mimicry between foreign- and autoantigens is necessary for onset in all cases. Other possible mechanisms causing or contributing to disease onset and progression may involve epitope spreading, in which the immune response becomes sensitized to other motifs, or bystander activation, in which immune cells are triggered to respond without antigen activation.^{24,28}

Environmental risk factors:

Some environmental factors, primarily infection by a spirochete bacterium from the genus *Leptospira*, have been implicated in the onset, progression, and severity of ERU.²⁹⁻³¹ In fact, case reports indicate that uveitis is also a sequela to leptospirosis in humans, dogs, and other mammals.³²⁻³⁹ In addition to *Leptospira*, several other less common infectious agents, such as *Rhodococcus equi* (bacillus), *Borrelia burgdorferi* (spirochete), and some nematode parasites and viruses, have been associated with uveitis.⁴⁰⁻⁴⁶ Outside of infectious organisms and viruses, little is known about the environmental conditions that may contribute to development and progression of recurrent uveitis.

Leptospira interrogans

Several methods exist for detecting *Leptospira* including serological testing, SNAP Lepto rapid testing (IDEXX), PCR detection, or culture from blood (serum), aqueous humor, or vitreous.⁴⁷⁻⁴⁹ Currently, there is limited consensus about the best method to assess exposure to *Leptospira* in relation to ERU risk.⁴⁷ Both PCR and culture can be used to detect the bacterium; however, they are mainly informative when used within the timeframe of a suspected infection. Serological evaluation using a microscopic agglutination test (MAT) or an enzyme-linked immunosorbent assay (ELISA) is valuable for assessing the ramifications of *Leptospira* exposure based on host immune system response, yet both techniques are prone to false positives or false negatives depending on sample quality and the timeframe since exposure.^{48,50} Additionally, tissue sample type may have a large impact on test accuracy, regardless of detection method.^{48,51,52} For example, *Leptospira* has been cultured from vitreous samples taken from ERU-affected horses that were negative by MAT evaluation of serum.⁵³ By testing both serum and ocular fluids (aqueous or vitreous humor), it is possible to calculate the Goldmann-Whitmer coefficient (GWC), often

used synonymously with c-value, to determine if there is a local antibody response within the eye.^{54,55} A recent review emphasized the distinction between the GWC and a standard c-value in that GWC takes into account the relative protein content of the two fluids when comparing antibody concentrations.³ While informative, obtaining ocular fluids is more invasive than venipuncture and such methods can be a challenge to perform in studies that examine horses in the field. For these reasons, using a combination of detection methods and sample types, when possible, will provide researchers and clinicians with the best prospect of accurately detecting evidence of *Leptospira* exposure or infection. To confirm *Leptospira* involvement in ERU, the current gold standard combines PCR on ocular fluids and MAT evaluation of both serum and ocular fluids to calculate a GWC.^{3,56}

Although a link between uveitis and *Leptospira* has been recognized since 1886, researchers first identified evidence of a causal relationship between *Leptospira* infection and chronic intraocular inflammation in 1971 by inoculating eighteen Shetland ponies with serovar *pomona* and monitoring ocular changes for several years.^{57,58} Consistent with subsequent studies in humans and horses,^{34,58-60} this investigation found an extensive latency period of approximately one to two years between infection and onset of ocular inflammation.⁵⁷ A subsequent retrospective study found that there was a significant association between positive *Leptospira* titers from blood serum and presence of ERU in a clinical population in the Genesee River Valley, New York,²⁹ and additional retrospective and case-control investigations across North America and Europe have continued to support that association.^{47,56,61} Furthermore, immunological research found that there is cross-reactivity between antibodies for *Leptospira* and proteins of major ocular structures including S-antigen, interphotoreceptor binding protein, and cellular retinaldehyde-binding protein.^{23,25,26,62-64} These findings suggest that exposure to *Leptospira* may train the immune

system to target structures of the eye by molecular mimicry and thereby trigger development of ERU.⁶⁴ Additionally, there is evidence that the spirochetes themselves may be able to breach the blood-ocular barrier and open previously inaccessible territory within the eye to the immune system.^{1,16,21,56} Once inside ocular structures, *Leptospira* may be able to survive for long periods of time.³ Recent evidence suggests that the bacteria can form biofilms within the vitreous humor and potentially thwart indirect detection methods and resist antibiotic treatments.^{65,66} More work is needed to replicate these findings in other geographic areas and to determine what factors may influence biofilm formation and antibiotic resistance.

While there is a growing body of knowledge supporting *Leptospira* involvement in ERU, some studies suggest otherwise. Two independent investigations in 1987 and 2017 using MAT evaluation of serum or ocular fluids found that seroprevalence was not different between ERU affected and unaffected horses in the United Kingdom.^{31,67} Using PCR and serology, a 2008 study in the southeastern United States identified definitive intraocular exposure to *Leptospira* in only one case out of 24 horses affected with ERU.⁶⁸ Another investigation in the midwestern United States in 2007 similarly found that two of ten fixed ocular samples from horses with end-stage disease had evidence of *Leptospira* involvement when assessed by immunohistochemical staining.³⁰ It is not clear at this time if the biofilm activity or the latency between infection and onset of uveitis may be contributing to the contradictory results for involvement of *Leptospira* in ERU.^{3,16} Regardless, the complex relationship between infection and disease progression makes it especially challenging to accurately measure the role of *Leptospira* as an environmental risk factor in all ERU cases.

Altogether, the results from numerous investigations indicate that infection with the spirochete bacterium is sufficient for ERU to develop but may not be required to initiate disease

in all horses.^{5,47,68-70} Instead, exposure to *Leptospira* may act as one of several possible triggers for uveitis onset, and it may also play a role in disease severity. A 2016 retrospective study in the southeastern United States found that ERU affected horses with evidence of *Leptospira* infection (either positive titers or high c-values) were more likely to become blind than other ERU affected horses.^{5,68} In particular, horses stabled within river valleys and other areas with higher environmental *Leptospira* load appear to have an increased risk of contracting *Leptospira* infection during the wet season.²⁹ These horses are, therefore, suspected to be at a higher risk of developing *Leptospira*-associated uveitis, which may progress to recurrent inflammation after onset.

Other infectious risk factors

Although *R. equi* is predominantly known for causing a respiratory disease in foals, the infection can have numerous extrapulmonary manifestations, affecting various organ systems like the eye. A retrospective study spanning twenty years in the southwestern United States found that 11% of the 150 foals with confirmed *R. equi* infection had evidence of uveitis, and the survival rate among these foals was 18.8%.⁴¹ Thus, high mortality could prevent *R. equi* infection from being a major risk factor for recurrent ocular inflammation, although this relationship remains to be evaluated. While four of the foals were suspected to have immune-mediated disease since bacteria could not be isolated from their ocular samples, it was not clear as to the exact mechanism triggering uveitis in these infected foals.⁴¹ To investigate whether infection causes septic or immune-mediated uveitis, a 2018 study intratracheally inoculated foals with either high or low concentrations of *R. equi*.⁴² Fourteen days after infection, uveitis was identified in 56% of foals, and the presence of *R. equi* was confirmed by culture of aqueous humor in five out of fourteen uveitic and six out of eleven non-uveitic foals. Although positive culture was not predictive of uveitis, the researchers considered all ocular disease to be septic in this study as the presence of

uveitis was associated with more extensive histopathological changes in the lungs.⁴² Even though early investigations indicated that foals with *Rhodococcus*-associated uveitis have lower survival rates than other cases,⁴¹ a more recent 15-year retrospective study in Spain identified a higher survival rate (66.7%) for infected foals with uveitis.⁷¹ Furthermore, the surviving foals in the recent study were characterized as visual with no indications of ocular disease at discharge, yet no longitudinal data are available from these or other cases to characterize the presence or absence of any long-term impacts, such as recurrent uveitis, in survivors of *R. equi* infection.

The bacteria responsible for Lyme disease, *Borrelia* species (primarily *B. burgdorferi*), have also been associated with cases of equine and human uveitis.^{43,45,72–75} Although exposure to *B. burgdorferi* appears to be widespread in horses, rates of borreliosis and *Borellia*-associated uveitis are not correspondingly high.^{44,73,76} In fact, experimental exposure of seven ponies to *B. bergdorferi* via a tick vector failed to trigger any notable histopathologic changes aside from skin lesions near the site of infection.⁷⁷ Furthermore, horses with *Borellia*-associated uveitis often display other signs of borreliosis, including neurologic deficits, lameness, arthritis, or muscle wasting.⁴⁴ Together, these studies suggest that *B. bergdorferi* is currently not a major risk factor for ERU, especially when ocular inflammation presents without other pathologies.

Although several parasites have also been implicated for inciting equine uveitis, current evidence suggests that uveitis secondary to infection is usually rare as the parasitic organisms must infiltrate ocular structures to trigger inflammation within the eye.⁴⁰ In particular, *Onchocerca cervicalis* and other *Onchocerca* species have been linked with uveitis in humans and horses.^{8,78,79} Connections between uveitis and infection of *Setaria* or *Halicephalobus* species have also been reported in horses.^{46,80–84} However, case reports indicate that infections of *Setaria*, *Halicephalobus*, and *Onchocerca* species are not major risk factors for recurrent uveitis in horses

as inflammation often resolves after treatment (*Setaria* and *Onchocerca*) or affected individuals do not survive the infection (*Halicephalobus*).^{46,85,86}

Viruses, such as the equine arteritis virus (EAV), influenza, and the equine herpes viruses (EHV-1, in particular) have been included as possible causes of uveitis for decades; however, few case reports or retrospective studies link ERU with viral infections.^{8,87,88} Both EAV and influenza are reported to trigger conjunctivitis, periocular edema, and lacrimation, but further discussion of associated ocular pathology appears to be absent from the literature.⁸⁹⁻⁹³ EHV-1, however, has been reported to infect ocular tissues and trigger uveitis.⁹⁴ Pathological investigation of a 1988 outbreak found that the virus was detectable by indirect immunoperoxidase stain within uveal tissues from horses with clinical signs of infection.⁹⁵ Infected foals from another outbreak in 1995 developed uveitis; however, persistence or recurrence of inflammation cannot be determined from this study due to lack of longitudinal data.⁹⁶ Using experimentally infected animals, researchers discovered that a large proportion (50-90%) of the horses without equine herpesvirus myeloencephalopathy developed visible choroidal lesions within three months after infection and chorioretinitis was common, although not ubiquitous, among both clinically and subclinically infected horses.^{97,98} Without retrospective studies and longitudinal data, it is not clear at this time if viral infection is a major risk factor for recurrent uveitis in horses.

Noninfectious risk factors

In addition to infectious agents, other environmental factors are suspected to impact ERU onset and progression. For example, previous studies have found that increased age is a risk factor for onset and severity, which is consistent with the progressive nature of ERU.^{5,7,69,99} Across these investigations, the average age of disease has been identified as 11.6 – 12.3 years. However, the averages listed represent the age of presentation or diagnosis and are likely inflated estimates for

the age of onset as horses may not be seen at the start of inflammation.^{5,7,29,69} Although the exact age of onset has not been thoroughly investigated within or across breeds, several studies have demonstrated that age is important for ERU risk assessments.^{69,100} For example, one study that evaluated 1014 horses from more than 40 breeds for ERU found 25-30% of the examined horses over 15 years old were affected.⁹⁹ Sex has also been identified in some studies as being associated with ERU, as more geldings than mares were affected compared to the reference population.^{5,99} However, other investigations do not support a link between sex and recurrent disease.^{7,29,69,101} It is possible that factors, such as sex-specific hormones or sex-linked genes, may be contributing to ERU risk, but these factors require more investigation. In particular, prospective studies are needed to measure an accurate average age of onset and to determine if the significant associations between sex and ERU are the result of a true causal factor or sampling bias.

Limited information is currently known about the role of management factors in ERU onset and progression. In humans, investigations into diet, obesity, activity level, and microbiome composition have not identified any other prominent environmental characteristics affecting uveitis onset, although some results suggest that these factors may have a role in disease progression.¹⁰²⁻¹⁰⁴ A recent investigation comparing microbiota in ERU affected and unaffected horses did not identify a significant difference in gut microbe diversity or composition, suggesting that dysbiosis may not be a risk factor for ERU.¹⁰⁵ However, the study did not distinguish between the different forms of ERU among the affected horses, and further investigations of ERU and gut microbiota should evaluate affected horses with a specific classification of ERU (posterior, classic, or insidious) or use a breed-specific analysis. Additionally, a possible role of gut microbiota in distinguishing between active and quiescent phases of the recurrent forms of ERU (posterior and classic) remains to be investigated.

With regard to other management factors, anecdotal evidence suggests that multivalent or many single vaccines may trigger recurrence in horses already affected by ERU;¹ however, a recent case-control study in the UK did not identify an association between recent vaccination history and a first episode or recurrence of idiopathic uveitis (n = 22 and 4, respectively).¹⁰¹ Similarly, one experimental investigation compared the rate of recurrence between *Leptospira* vaccinated and unvaccinated horses previously diagnosed with ERU, and the study found no statistical difference in recurrence rates between the two groups.¹⁰⁶ To date, no other studies have experimentally evaluated the effect of vaccinations in ERU recurrence in horses. Thus, additional experimental and observational studies are needed to determine if an immune system challenge like vaccinations impacts progression and recurrence of ERU.

In addition to assessing an association to vaccinations, the case-control study in the UK investigated more than 20 horse characteristics (age, sex, breed, etc.) and husbandry-level factors (years at barn, availability and type of turnout, proximity to other livestock, deworming, etc.) for association with the first episode of idiopathic uveitis and recurrence of inflammation.¹⁰¹ The study identified turnout on a recently flooded pasture and proximity to a pig farm as two factors that were associated with the primary incidence of uveitis. Although *Leptospira* was suspected to have a possible connection to both factors, assessments of bacterial exposure were not performed in the study. Additionally, only five of the 22 horses had recurrence upon follow-up evaluations within the timeframe of the study (< 5 years).¹⁰¹ Thus, additional work is needed to more thoroughly characterize any potential role of management or husbandry that might impact recurrent uveal disease in horses.

Genetic Risk Factors:

Breed predisposition provides evidence of a genetic component for the development of ERU. For example, classic ERU has been recognized to occur more commonly among warmblood and Icelandic horses, although limited information about prevalence of the classic subtype is available for these breeds.^{9,107} For posterior ERU, previous investigations identified an overrepresentation of warmblood horses among ERU cases, but limited information is available about the propensity or relative risk for developing posterior uveitis for any one breed.^{4,7}

The Appaloosa and breeds with similar coat spotting patterns, along with Icelandic horses and draft breeds, have been reported to have a predisposition for insidious uveitis.^{29,108,109} The prevalence for insidious uveitis among Icelandic horses over 8 years old was 6.7% in a recent investigation with horses from Denmark and the USA.¹⁰⁹ No information is available about the rate of insidious uveitis among draft breeds in the scientific literature, therefore, investigations of ERU in draft breeds is warranted. Appaloosas, on the other hand, are known to be significantly more likely to develop ERU and become blind as a direct result of the insidious uveitis.^{7,29} Several retrospective studies found that the odds of an Appaloosa developing uveitis were between 8.3-65.8 compared to the patient population without the leopard complex spotting pattern (LP), for which the Appaloosa is well known.^{7,29} Although specific information about relative risk is not available for Pony of the Americas (POA), Knabstrupper, and other LP patterned breeds, these horses have also been reported to have a higher incidence of insidious uveitis compared to other unrelated breeds.^{2,7}

Genetic studies in warmblood breeds

Although breed predisposition for recurrent uveitis is a valuable marker of potential genetic risk factors, limited information is currently known about the genetic architecture underlying ERU propensity across warmblood breeds. A previous investigation using a microcytotoxicity test

identified an association between ERU status and the MHC serological haplotype known as ELA-A9 in a sample of German Warmbloods.¹¹⁰ The MHC, or the major histocompatibility complex, is the set of immune genes that are primarily involved in antibody formation. Despite concerted effort, the recognized serological haplotypes of the class I region of the MHC, first characterized in 1988, have not been entirely mapped to physical locations within the equine reference sequence due to the complexity of the MHC region and antigen class switching.¹¹¹⁻¹¹⁴ Without a physical mapping location for the class I haplotypes, it is not currently possible to translate the serological association from Deeg *et al.* (2004) into a specific genomic location on ECA 20 for further targeted investigation and genetic testing. Subsequently, a genome-wide association study (GWAS), also in German Warmbloods, uncovered an association between disease status and a SNP marker (BIEC2-536712, NC_009163.3:g.50364059G>A) near two immune genes, IL17A and IL17F, located on the same chromosome as the MHC.¹¹⁵ While not considered part of the complex, BIEC2-536712 is located within 20 Mb of the putative MHC class I and class II genes.^{116,117} Together, the two independent associations to the MHC and a nearby region on ECA 20 suggest variants affecting immune-related genes on this chromosome may play a role in the pathogenesis of posterior uveitis. While these SNPs were associated with ERU affection status, no casual risk alleles at these associated loci have been identified. Thus, further work is needed to investigate putative causal variants and to determine if similar associations exist within other warmblood breeds before genetic testing of this region is warranted.

In addition to investigating risk factors for disease onset, Kulbrock *et al.* (2013) also evaluated genetic factors contributing to ERU severity, and cases were classified as mild, moderate, or severe based on clinical signs of disease in the most affected eye (Table 1). A GWAS for severity identified a significantly associated SNP marker (BIEC2-421990, NC_009161.3:

g.81963620A>G) within an intron of *PLEKHM3*.¹¹⁵ The authors suspect, however, that the association is due to effects on a nearby crystalline gene called *CRYGB* that is located within 1 Mb of the associated SNP. There have not been any subsequent studies to replicate this association or to identify and characterize a causal genetic variant on ECA 18 responsible for disease severity. Such follow-up work is limited by the difficulty in characterizing severity for a highly variable disease like posterior uveitis, which has many secondary sequelae. Furthermore, environmental variation may play a large role in ERU progression; however, such factors are not well understood at this time.

Table 1: Summary of the clinical classification of ERU severity used in Kulbrock *et al* (2013).¹¹⁵

	Mild	Moderate	Severe
<u>Anterior segment changes:</u>			
Intraocular pressure	No change	Slight increase	High-grade increase
Cornea	No change	Slight local opacity	Descemet's membrane tears
Iris/pupil	Focal residue; slight depigmentation; small focal synechia	Multifocal residue; moderate depigmentation; large focal or multifocal synechia	Atrophy; high-grade depigmentation; circular or seclusion pupillae synechia
<u>Lens changes:</u>	Capsular cataract	Multifocal, local vesicular; local reticular capsular; subcapsular; or local immature cortical or nuclear cataract	Luxation or subluxation; diffuse immature, mature, or hypermature cataract
<u>Posterior segment changes:</u>			

Vitreous	Slight liquification	Moderate liquification	High-grade liquification
Retina	Focal chorioretinopathy	Multiple focal or peripapillary chorioretinopathies	Large chorioretinopathies; wrinkled or detached
Infiltrate	Slight inflammatory products	Moderate inflammatory products	High-grade inflammatory products; yellow haze
<u>Other changes:</u>	None	None	Phthisis bulbi

Genetic studies in Icelandic horses

A recent descriptive cross-sectional study identified 6/75 Icelandic horses over the age of eight years old as affected with ERU.¹⁰⁹ Five of the six affected animals were characterized as displaying subtle signs of intraocular inflammation characteristic of insidious uveitis, while the other affected horse was phenotyped as having the classic form of ERU.¹⁰⁹ Additional investigations are needed to determine the relative risk of these two classifications of ERU among Icelandic horses. A genome-wide association study using the same population of Icelandic horses identified an association on ECA 11, but no causal genetic risk factors have been identified at this time.¹⁰⁷ Additional investigations are needed to replicate these findings and identify potential variants for further investigations to understand the role of genetics in the onset of ERU among Icelandic horses.

Genetic studies in breeds with leopard complex spotting (LP)

Interestingly, insidious uveitis is known to disproportionately affect the Appaloosa breed, which has been selected for a particular coat color pattern known as the leopard complex spotting pattern or LP.^{7,12,29,100,118} It has been proposed that a new designation of “leopard coat pattern uveitis” be used to describe insidious uveitis;^{2,3} however, other non-LP spotted breeds, such as Icelandic horses, have been characterized with chronic low-grade uveitis consistent with insidious

disease.¹⁰⁹ Additionally, not all horses with LP will develop uveitis,^{29,69} and the term “leopard coat pattern” describes one of several possible spotting phenotypes that result from *LP*, the genetic variant leading to the LP spotting patterns (Fig. 3). We are, therefore, not in support of changing the nomenclature of insidious uveitis as further research is needed to understand the complete etiology of the disease in these breeds.

A seven year retrospective investigation in the United States discovered that Appaloosas represented 25% of the horses affected with ERU in the study population and had higher odds of becoming blind as a result of ERU compared to other breeds (OR = 3.8).²⁹ A subsequent retrospective investigation extending for more than ten years in western Canada found that Appaloosa horses had significantly higher odds of presenting with ERU (OR = 65.8) when compared with all other breeds except Pony of the Americas (OR = 3.09 relative to Appaloosa, P = 0.2) and Hanoverians (OR = 0.20 relative to Appaloosa, P = 0.1), when the form of ERU was not considered.⁷ Interestingly, POAs are also bred for the LP spotting pattern.¹¹⁹ Although the total number of POAs presenting to the hospital was low (n = 6), this study suggests that there is a potential predisposition for ERU within a second LP breed, which warrants further investigation.⁷ Sandmeyer *et al* (2017) also evaluated disease severity, although there was not a significant difference in severity between the Appaloosa and other breeds based on the criteria used (Table 2).⁷

Table 2: Summary of the clinical classification of ERU severity used in Sandmeyer *et al* (2017).⁷

	Mild	Moderate	Severe
<u>Anterior segment changes:</u>	Aqueous flare	Aqueous flare	Aqueous flare
Intraocular pressure	Slight decrease	Slight decrease	Change
Cornea	No change	No change	Edema

Iris/pupil	Miosis	Miosis; pigmentation changes; synechia	Miosis; pigmentation changes; synechia
<u>Lens changes:</u>	No change	Cataract	Cataract
<u>Posterior segment changes:</u>			
Vitreous	No change	Vitritis	Vitritis
Retina	No change	Pigmentation changes	Pigmentation changes; detachment
Infiltrate	None	None	None
<u>Other changes:</u>	Conjunctival hyperemia	Conjunctival hyperemia	Conjunctival hyperemia; secondary glaucoma; phthisis bulbi

An investigation in Germany found that Appaloosa and Knabstrupper horses had a higher rate of insidious uveitis (45.5% and 33.3%, respectively) compared to horses from other breeds (3.2%).² The Knabstrupper breed originated in Denmark and has also been selected for the LP spotting patterns.¹²⁰ More generally, Baumgart *et al.* (2014) found that horses with a coat pattern that was identified as *Tigerschecken* or leopard spotted experienced insidious uveitis at a higher frequency (40.8%) than horses with other coat patterns.² Together these investigations indicate that several leopard complex spotted breeds share a predisposition for insidious uveitis and provide evidence that the genetics governing this spotting pattern may play a role in disease risk. Several human disorders also feature comorbidity of uveitis and depigmentation, including Behçet's disease (BD), Voyt-Koyanagi-Harada disease (VKH), and some forms of vitiligo, thus investigation of disease mechanisms underlying insidious uveitis of LP horses may provide insights into mechanisms underlying similar uveitis disorders among humans.^{18,100,121}

The LP phenotype is characterized by a white pattern centered over the hips that varies in size from minimal to an entirely unpigmented coat (Fig. 3). The LP coat pattern is inherited as an incomplete dominant phenotype caused by a long terminal repeat (LTR) insertion in an intron of the *Transient Receptor Potential Cation M1 Channel (TRPM1)* gene, which is located on ECA 1.^{122,123} This LTR insertion has been shown to cause premature polyadenylation of the *TRPM1* mRNA, therefore, it is suspected to prevent normal protein production in homozygotes.¹²² Although *LP* is suspected to be epistatic with other modifying loci to produce the range in amount of white patterning observed, heterozygotes (*LP/lp*) tend to have pigmented oval spots within the unpigmented region while homozygotes (*LP/LP*) have few or no pigmented spots in the white patterned area. One modifying locus known as *Pattern 1 (PATN1)* has been characterized as leading to increased levels of white patterning (60% or greater at birth) for horses with at least one copy of *LP*.¹²⁴ In addition to affecting coat color, the *LP* allele is also known to affect the function of the ON-bipolar cell signaling pathway responsible for vision in low light conditions as *TRPM1* is a calcium ion channel that is responsible for proper signal transduction following photon detection by the rod cells.^{122,125} Horses homozygous for the *LP* insertion lack the full length *TRPM1* transcript, and therefore, are unable to see when the rod cells are primarily responsible for vision, a condition known as Congenital Stationary Night Blindness (CSNB).¹²²

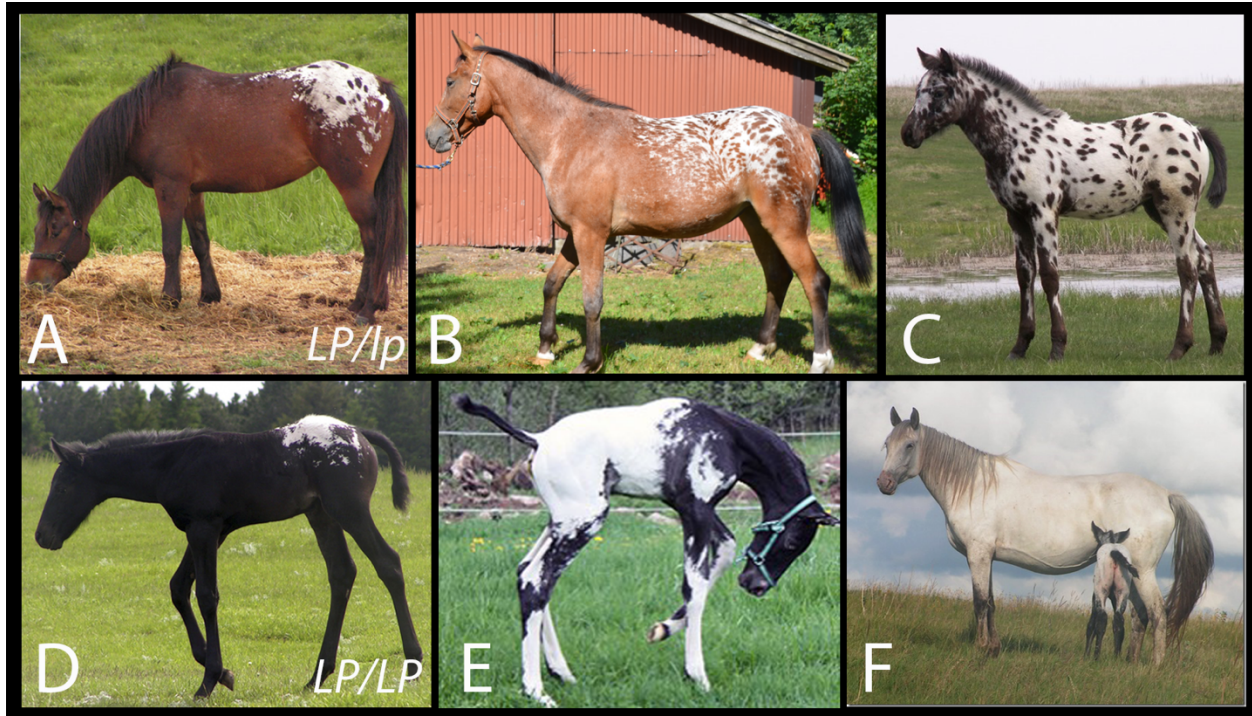


Figure 3: Leopard complex spotting patterns in the horse. In general, horses with the *LP* insertion have white spotting patterns that vary in the extent of unpigmented coat as displayed in A-F. Horses with one copy of *LP* usually display pigmented spots within the white region, although the pattern may vary from minimal white patterning over the rump (A) extending to a blanket (B) or to white patterning over most of the coat (C). Homozygotes usually display few to no pigmented spots in the white area, but their patterning can also range from a minimal area over the rump (D) to a blanket (E) or to white patterning over the entire animal (F). Photographs courtesy of Anna Larson and Dr. Sanna Heden (E) and Cheryl Woods (C and F).

Previous research using a candidate gene approach found that insidious uveitis in a sample of Appaloosas was associated with alleles at two microsatellite markers in the MHC and one SNP marker in the 11th intron of *TRPM1* (NC_009144.3:g.109163268C>T).¹² Subsequent testing of the same population using the Illumina Equine SNP70 BeadChip genotyping array, with approximately 70K SNP markers, recapitulated the association at the *LP* locus but did not support the association on ECA 20.¹⁰⁰ It is suspected, however, that evaluation on an array with a higher marker density may be necessary to properly tag the variability within the MHC. The Axiom Equine 670K genotyping array contains 7,394 additional markers within the MHC compared to the marker set on the SNP70 BeadChip, making the 670K genotyping array a more robust tool for

closely evaluating the MHC.¹²⁶ The 70K marker GWAS also identified associations with loci on ECA 12 and 29, but replication testing with a second population only supported the association for the *LP* locus on ECA 1.¹⁰⁰ These investigations indicate that the *LP* insertion or a closely linked variant is involved in the development of insidious uveitis within the Appaloosa breed; however, *LP* genotype is not sufficient to explain the distribution of the disease among Appaloosas. It is, therefore, suspected that additional genetic loci are involved in the development of insidious uveitis.

Due to its epistatic interaction with *LP*, *PATNI* was also evaluated for association to ERU, and a risk model with *LP* and *PATNI* genotypes as well as age explained 30% of the phenotypic variance of ERU in a study population.⁸⁵ Furthermore, an observational study involving 145 Appaloosas from western Canada further supported age and *LP* genotype as risk factors for ERU, and horses with a larger amount of white patterning at birth also appeared to be at the greatest risk.⁴⁷ The *LP* and *PATNI* loci are of particular interest given selection for the LP coat patterns in Appaloosa and similarly spotted breeds. Additional investigations are, therefore, needed to evaluate the role of *LP* and *PATNI* in ERU development across spotted horse breeds.

Future Directions:

Although the complete mechanism underlying ERU is not known, part of the pathology must involve the breakdown of the blood-ocular barrier, which maintains immune privilege within the eye by both physical and regulatory means. The physical barrier leverages tight junctions between cells to prevent intrusion of migratory immune cells into ocular tissues. In the event that immune cells are able to pass the physical barrier, there are negative regulatory signals, such as transforming growth factor β 2 (TGF- β 2), programmed death-ligand 1 (PD-L1), α -melanocyte stimulating hormone, and Fas ligand, that trigger immunosuppressive actions (apoptosis) or

immune tolerance.¹²⁷ Similar to rodents that are not susceptible to EAU, an autoimmune attack that overwhelms both aspects of the blood-ocular barrier should resolve for any individuals with normal immune system function through an immunosuppression mechanism, such as the activity of regulatory T cells and B cells.^{128,129} For horses with recurrent uveitis, however, one or more aspects of these regulatory pathways are likely ineffective and lead to chronic disease. Thus, further investigation of the regulatory mechanisms of the immune system will provide new insights into autoimmune diseases, such as ERU.

Following advancements in molecular genomics, investigations into mammalian immune system regulation indicate that there is a complex interplay of regulatory RNAs and epigenetic signals, such as histone modifications and DNA methylation, that play key roles in the maturation and differentiation of lymphocytes.¹³⁰ In fact, several forms of recurrent uveitis in humans have been associated with epigenetic changes.¹³¹ For example, differences in both tissue-specific histone modifications and genome-wide DNA methylation levels between BD affected and unaffected individuals have been detected, suggesting that epigenetic dysfunction may play a role in uveitis.^{131–133} Additional research identified associations between aberrant expression of key regulatory miRNAs and many autoimmune diseases, including rheumatoid arthritis, BD, and VKH, along with EAU models.^{134–136} Previous investigations also found that copy number variants of non-coding RNA genes were associated with both BD and VKH.^{137,138} Few disease investigations in the horse have evaluated noncoding variants, yet work in humans indicate that evaluating these potential regulatory regions would be an obvious next avenue to explore for ERU.

In order to investigate the role of regulatory pathways in the etiology of ERU, more work is needed to characterize the equine genomic landscape, including annotating tissue-specific regulatory marks and further characterizing regulatory RNAs. For the horse, there is limited

information known about regulatory regions and other functional elements driving gene regulation in a tissue-specific manner. Due to advancements in human disease research following the ENCODE annotation effort, an initiative known as the Functional Annotation of ANimal Genomes (FAANG) consortium was created in 2015 to annotate the reference genome of the horse and other major agricultural species.^{139–145} These efforts will improve the characterization of genomic regulatory changes that contribute to complex diseases and other traits of interest. Equine FAANG contributors have used several genome-wide assays, such as RNA- and ChIP-Seq, to evaluate tissue-specific differences in four Thoroughbred horses to compile an atlas of normal genomic function.^{141,146–152} Further tissue-specific annotation of the equine reference genome, including work on additional ocular tissues, through FAANG and similar efforts is, therefore, a necessary step to understand the risk factors contributing to ERU in the horse.

Acknowledgments:

The authors' ERU research has been funded by the University of California – Davis, Center for Equine Health, the Townsend Equine Health Research Fund (TEHRF), and the Morris Animal Foundation (D16EQ-028). The mission of the Morris Animal Foundation is to bridge science and resources to advance the health of animals. N. B. K. was also supported in part by the University of California –Davis, Center for Equine Health Fellowship.

Conflict of Interest:

N. B. Kingsley and R. R. Bellone are affiliated with the Veterinary Genetics Laboratory, a service laboratory offering diagnostic genetic tests for horses and other animal species.

References:

1. Gilger BC, Hollingsworth SR. Diseases of the uvea, uveitis, and recurrent uveitis. In: Gilger BC, ed. *Equine Ophthalmology*. 3rd ed. John Wiley & Sons, Ltd; 2017:376-422.

2. Baumgart A, Gerhards H. Besonderheiten der Tigerschecken-Uveitis und möglicher Cyclosporin A-Einsatz in deren Therapie in Deutschland. *Pferdeheilkunde*. 2014;30(6):626-632.
3. Wollanke B, Gerhards H, Ackermann K. Infectious Uveitis in Horses and New Insights in Its Leptospiral. *Microorganisms*. 2022;10(2):387.
4. Malalana F. What's new in equine recurrent uveitis? *In Pract*. 2020;42(6):348-354. doi:10.1136/inp.m2464
5. Gerding JC, Gilger BC. Prognosis and impact of equine recurrent uveitis. *Equine Vet J*. 2016;48(3):290-298. doi:10.1111/evj.12451
6. Pinto NI, McMullen RJ, Linder KE, Cullen JM, Gilger BC. Clinical, histopathological and immunohistochemical characterization of a novel equine ocular disorder: Heterochromic iridocyclitis with secondary keratitis in adult horses. *Vet Ophthalmol*. 2015;18(6):443-456. doi:10.1111/vop.12234
7. Sandmeyer LS, Bauer BS, Feng CX, Grahn BH. Equine recurrent uveitis in western Canadian prairie provinces : A retrospective study (2002–2015). *Can Vet J*. 2017;58:717-722.
8. Schwink KL. Equine Uveitis. *Vet Clin North Am - Equine Pract*. 1992;8(3):557-574. doi:10.1016/S0749-0739(17)30441-8
9. McMullen RJ, Fischer BM. Medical and Surgical Management of Equine Recurrent Uveitis. *Vet Clin North Am - Equine Pract*. 2017;33(3):465-481. doi:10.1016/j.cveq.2017.07.003
10. Zaidi AA, Ying GS, Daniel E, et al. Hypopyon in Patients with Uveitis. *Ophthalmology*. 2010;117(2):366-372. doi:10.1016/j.ophtha.2009.07.025

11. Gilger BC, Michau TM. Equine recurrent uveitis: New methods of management. *Vet Clin North Am - Equine Pract.* 2004;20(2):417-427. doi:10.1016/j.cveq.2004.04.010
12. Fritz KL, Kaese HJ, Valberg SJ, et al. Genetic risk factors for insidious equine recurrent uveitis in Appaloosa horses. *Anim Genet.* 2014;45(3):392-399. doi:10.1111/age.12129
13. Gilger BC, Deeg CA. Equine recurrent uveitis. In: Gilger BC, ed. *Equine Ophthalmology*. 2nd ed. Elsevier Saunders; 2011:317-349.
14. Gilger BC, Malok E, Cutter K V., Stewart T, Horohov DW, Allen JB. Characterization of T-lymphocytes in the anterior uvea of eyes with chronic equine recurrent uveitis. *Vet Immunol Immunopathol.* 1999;71(1):17-28. doi:10.1016/S0165-2427(99)00082-3
15. Romeike A, Brugmann M, Drommer W. Immunohistochemical Studies in Equine Recurrent Uveitis (ERU). *Vet Pathol.* 1998;35:515-526.
16. Malalana F, Stylianides A, McGowan C. Equine recurrent uveitis: Human and equine perspectives. *Vet J.* 2015;206(1):22-29. doi:10.1016/j.tvjl.2015.06.017
17. Saldinger LK, Nelson SG, Bellone RR, et al. Horses with equine recurrent uveitis have an activated CD4+ T-cell phenotype that can be modulated by mesenchymal stem cells in vitro. *Vet Ophthalmol.* 2020;23(1):160-170. doi:10.1111/vop.12704
18. Caspi RR. A look at autoimmunity and inflammation in the eye. *J Clin Invest.* 2010;120(9):3073-3083. doi:10.1172/JCI42440
19. Guedes MCE, Borrego LM, Proença RD. Roles of interleukin-17 in uveitis. *Indian J Ophthalmol.* 2016;64(9):628-634. doi:10.4103/0301-4738.194339
20. Deeg CA, Hauck SM, Amann B, et al. Equine recurrent uveitis - A spontaneous horse model of uveitis. *Ophthalmic Res.* 2008;40(3-4):151-153. doi:10.1159/000119867
21. Witkowski L, Cywinska A, Paschalis-Trela K, Crisman M, Kita J. Multiple etiologies of

- equine recurrent uveitis – A natural model for human autoimmune uveitis: A brief review. *Comp Immunol Microbiol Infect Dis*. 2016;44:14-20. doi:10.1016/j.cimid.2015.11.004
22. Wildner G, Thureau SR. Cross-reactivity between an HLA-B27-derived peptide and a retinal autoantigen peptide: a clue to major histocompatibility complex association with autoimmune disease. *Eur J Immunol*. 1994;24(11):2579-2585. doi:10.1002/eji.1830241103
23. Deeg CA, Thureau SR, Gerhards H, Ehrenhofer M, Wildner G, Kaspers B. Uveitis in horses induced by interphotoreceptor retinoid-binding protein is similar to the spontaneous disease. *Eur J Immunol*. 2002;32(9):2598-2606.
24. Deeg CA, Amann B, Raith AJ, Kaspers B. Inter- and intramolecular epitope spreading in equine recurrent uveitis. *Investig Ophthalmol Vis Sci*. 2006;47(2):652-656. doi:10.1167/iovs.05-0789
25. Deeg CA, Reese S, Gerhards H, Wildner G, Kaspers B. The uveitogenic potential of retinal S-antigen in horses. *Investig Ophthalmol Vis Sci*. 2004;45(7):2286-2292. doi:10.1167/iovs.03-1226
26. Deeg CA, Hauck SM, Amann B, Kremmer E, Stangassinger M, Ueffing M. Major retinal autoantigens remain stably expressed during all stages of spontaneous uveitis. *Mol Immunol*. 2007;44(13):3291-3296. doi:10.1016/j.molimm.2007.02.027
27. Deeg CA. A proteomic approach for studying the pathogenesis of spontaneous equine recurrent uveitis (ERU). *Vet Immunol Immunopathol*. 2009;128(1-3):132-136. doi:10.1016/j.vetimm.2008.10.302
28. Deeg CA, Ehrenhofer M, Thureau SR, Reese S, Wildner G, Kaspers B. Immunopathology of recurrent uveitis in spontaneously diseased horses. *Exp Eye Res*. 2002;75(2):127-133. doi:10.1006/exer.2002.2011

29. Dwyer AE, Crockett RS, Kalsow CM. Association of leptospiral seroreactivity and breed with uveitis and blindness in horses: 372 cases (1986-1993). *J Am Vet Med Assoc.* 1995;207(10):1327-1331. <http://www.ncbi.nlm.nih.gov/pubmed/7591929>
30. Pearce JW, Galle LE, Kleiboeker SB, et al. Detection of *Leptospira interrogans* DNA and antigen in fixed equine eyes affected with end-stage equine recurrent uveitis. *J Vet Diagnostic Investig.* 2007;19(6):686-690. doi:10.1177/104063870701900611
31. Matthews AG, Palmer MF. Serological study of leptospiral infections and endogenous uveitis among horses and ponies in the United Kingdom. *Equine Vet J.* 1987;19(2):125-128. doi:10.1111/j.2042-3306.1987.tb02605.x
32. Hanno HA, Cleveland AF. Leptospiral uveitis. *Am J Ophthalmol.* 1949;32(11):1564-1566. doi:10.1016/s0002-9394(49)90377-3
33. Davidson MG, Nasiss MP, Roberts SM. Immunodiagnosis of leptospiral uveitis in two horses. *Equine Vet J.* 1987;19(2):155-157. doi:10.1111/j.2042-3306.1987.tb02615.x
34. Rathinam SR, Rathnam S, Selvaraj S, Dean D, Nozik RA, Namperumalsamy P. Uveitis associated with an epidemic outbreak of Leptospirosis. *Am J Ophthalmol.* 1997;124(1):71-79. doi:10.1016/S0002-9394(14)71646-0
35. Straub MH, Church M, Glueckert E, Foley JE. Raccoons (*Procyon lotor*) and striped skunks (*Mephitis mephitis*) as potential reservoirs of *Leptospira* spp. in California. *Vector-Borne Zoonotic Dis.* 2020;20(6):418-426. doi:10.1089/vbz.2019.2528
36. Gallagher A. Leptospirosis in a dog with uveitis and presumed cholecystitis. *J Am Anim Hosp Assoc.* 2011;47(6):162-167. doi:10.5326/JAAHA-MS-5590
37. Chu KM, Rathinam R, Namperumalsamy P, Dean D. Identification of *Leptospira* species in the pathogenesis of uveitis and determination of clinical ocular characteristics in South

- India. *J Infect Dis.* 1998;177(5):1314-1321. doi:10.1086/515273
38. Townsend WM. Canine and Feline Uveitis. *Vet Clin North Am - Small Anim Pract.* 2008;38(2):323-346. doi:10.1016/j.cvsm.2007.12.004
 39. Townsend WM, Stiles J, Krohne SG. Leptospirosis and panuveitis in a dog. *Vet Ophthalmol.* 2006;9(3):169-173. doi:10.1111/j.1463-5224.2006.00464.x
 40. Wotman KL, Johnson AL. Ocular Manifestations of Systemic Disease in the Horse. *Vet Clin North Am - Equine Pract.* 2017;33(3):563-582. doi:10.1016/j.cveq.2017.08.002
 41. Reuss SM, Chaffin MK, Cohen ND. Extrapulmonary disorders associated with *Rhodococcus equi* infection in foals: 150 cases (1987–2007). *JAVMA.* 2009;235(7):855-863.
 42. Huber L, Giguère S, Berghaus LJ, Hanafi A, Vitosh-Sillman S, Czerwinski SL. Development of septic polysynovitis and uveitis in foals experimentally infected with *Rhodococcus equi*. *PLoS One.* 2018;13(2):1-11. doi:10.1371/journal.pone.0192655
 43. Priest HL, Irby NL, Schlafer DH, et al. Diagnosis of *Borrelia*-associated uveitis in two horses. *Vet Ophthalmol.* 2012;15:398-405. <https://doi.org/10.1111/j.1463-5224.2012.01000.x>
 44. Divers TJ, Gardner RB, Madigan JE, et al. *Borrelia burgdorferi* Infection and Lyme Disease in North American Horses: A Consensus Statement. *J Vet Intern Med.* 2018;32(2):617-632. doi:10.1111/jvim.15042
 45. Burgess E, Gillette D, Pickett J. Arthritis and panuveitis as manifestations of *Borrelia burgdorferi* infection in a Wisconsin pony. *J Am Vet Med Assoc.* 1986;189:1340-1342.
 46. Kinde H, Mathews M, Ash L, St Leger J. *Halicephalobus gingivalis* (*H. deletrix*) infection in two horses in southern California. *J Vet Diagn Invest.* 2000;12(2):162-165.

doi:10.1177/104063870001200213

47. Divers TJ, Chang Y -F., Irby NL, Smith JL, Carter CN. Leptospirosis: An important infectious disease in North American horses. *Equine Vet J.* 2019;51(3):287-292. doi:10.1111/evj.13069
48. Marquez A, Djelouadji Z, Lattard V, Kodjo A. Overview of laboratory methods to diagnose leptospirosis and to identify and to type leptospire. *Int Microbiol.* 2017;20(4):184-193. doi:10.2436/20.1501.01.302
49. Geiger T, Gerhards H, Wollanke B. Detection of anti-lip132 antibodies in serum samples from horses with chronic intraocular infection with *Leptospira* spp. *Pathogens.* 2021;10(10). doi:10.3390/pathogens10101325
50. Ye C, Yan W, McDonough PL, et al. Serodiagnosis of equine leptospirosis by enzyme-linked immunosorbent assay using four recombinant protein markers. *Clin Vaccine Immunol.* 2014;21(4):478-483. doi:10.1128/CVI.00649-13
51. Miller MD, Annis KM, Lappin MR, Lunn KF. Variability in Results of the Microscopic Agglutination Test in Dogs with Clinical Leptospirosis and Dogs Vaccinated against Leptospirosis. *J Vet Intern Med.* 2011;25(3):426-432. doi:10.1111/j.1939-1676.2011.0704.x
52. Halliwell RE, Brim TA, Mines MT, Wolf D, White FH. Studies on equine recurrent uveitis. II: The role of infection with *Leptospira interrogans* serovar Pomona. *Curr Eye Res.* 1985;4(10):1033-1040. doi:10.3109/02713688509003348
53. Wollanke B, Gerhards H, Brem S, Meyer P, Kopp H. Ätiologie der equinen rezidivierenden uveitis (ERU): Autoimmunkrankheit oder intraokulare leptospireninfektion? *Pferdeheilkunde.* 2004;20(4):327-340. doi:10.21836/PEM20040403

54. Gilger BC. Association of acute leptospirosis with systemic disease and uveitis in horses. *Equine Vet Educ.* 2018;30(3):137-138. doi:10.1111/eve.12693
55. De Groot-Mijnes JDF, Rothova A, Van Loon AM, et al. Polymerase chain reaction and goldmann-witmer coefficient analysis are complimentary for the diagnosis of infectious uveitis. *Am J Ophthalmol.* 2006;141(2):313-318. doi:10.1016/j.ajo.2005.09.017
56. Sauvage AC, Monclin SJ, Elansary M, Hansen P, Grauwels MF. Detection of intraocular *Leptospira* spp. by real-time polymerase chain reaction in horses with recurrent uveitis in Belgium. *Equine Vet J.* 2019;51(3):299-303. doi:10.1111/evj.13012
57. Williams RD, Morter RL, Freeman MJ, Lavignette AM. Experimental chronic uveitis. Ophthalmic signs following equine leptospirosis. *Invest Ophthalmol.* 1971;10(12):948-954.
58. Verma A, Stevenson B. Leptospiral Uveitis - There Is More to It Than Meets the Eye! *Zoonoses Public Health.* 2012;59(SUPPL.2):132-141. doi:10.1111/j.1863-2378.2011.01445.x
59. Rathinam SR. Ocular manifestations of leptospirosis. *J Postgrad Med.* 51(3):189-194. <http://www.ncbi.nlm.nih.gov/pubmed/16333191>
60. Verma A, Stevenson B, Adler B. Leptospirosis in horses. *Vet Microbiol.* 2013;167(1-2):61-66. doi:10.1016/j.vetmic.2013.04.012
61. Voelter K, Vial Z, Pot SA, Spiess BM. Leptospiral antibody prevalence and surgical treatment outcome in horses with Equine Recurrent Uveitis (ERU) in Switzerland. *Vet Ophthalmol.* 2020;23(4):648-658. doi:10.1111/vop.12767
62. Verma A, Kumar P, Babb K, Timoney JF, Stevenson B. Cross-reactivity of antibodies against leptospiral recurrent uveitis-associated proteins A and B (LruA and LruB) with eye proteins. *PLoS Negl Trop Dis.* 2010;4(8):1-9. doi:10.1371/journal.pntd.0000778

63. Deeg CA, Pompetzki D, Raith AJ, et al. Identification and functional validation of novel autoantigens in equine uveitis. *Mol Cell Proteomics*. 2006;5(8):1462-1470. doi:10.1074/mcp.M500352-MCP200
64. Deeg CA, Kaspers B, Gerhards H, Thureau SR, Wollanke B, Wildner G. Immune responses to retinal autoantigens and peptides in equine recurrent uveitis. *Investig Ophthalmol Vis Sci*. 2001;42(2):393-398.
65. Ristow P, Bourhy P, Kerneis S, et al. Biofilm formation by saprophytic and pathogenic leptospire. *Microbiology*. 2008;154(5):1309-1317. doi:10.1099/mic.0.2007/014746-0
66. Ackermann K, Kenngott R, Settles M, Gerhards H, Maierl J, Wollanke B. In vivo biofilm formation of pathogenic *Leptospira* spp. In the vitreous humor of horses with recurrent uveitis. *Microorganisms*. 2021;9(9):1-14. doi:10.3390/microorganisms9091915
67. Malalana F, Blundell RJ, Pinchbeck GL, McGowan CM. The role of *Leptospira* spp. in horses affected with recurrent uveitis in the UK. *Equine Vet J*. 2017;49(6):706-709. doi:10.1111/evj.12683
68. Gilger BC, Salmon JH, Yi NY, et al. Role of bacteria in the pathogenesis of recurrent uveitis in horses from the southeastern United States. *Am J Vet Res*. 2008;69(10):1329-1335. doi:10.2460/ajvr.69.10.1329
69. Sandmeyer LS, Kingsley NB, Walder C, et al. Risk factors for equine recurrent uveitis in a population of Appaloosa horses in western Canada. *Vet Ophthalmol*. 2020;23(3):515-525. doi:10.1111/vop.12749
70. Frellstedt L. Equine recurrent uveitis: A clinical manifestation of leptospirosis. *Equine Vet Educ*. 2009;21(10):546-552. doi:10.2746/095777309X467853
71. Tarancón I, Leiva M, Jose-Cunilleras E, Ríos J, Peña T. Ophthalmologic findings associated

- with *Rhodococcus equi* bronchopneumonia in foals. *Vet Ophthalmol.* 2019;22(5):660-665.
doi:10.1111/vop.12637
72. Sommerauer S, Blohm KO, Spergser J, Buchner HHF. Arthritis, panuveitis and hyperaesthesia associated with *Borrelia afzelii* infection in a warmblood gelding. *Vet Rec Case Rep.* 2019;7:e000911. <https://doi.org/10.1136/vetreccr-2019-000911>
73. Gerhards H, Wollanke B. Antibody titers against *Borrelia* in horses in serum and in eyes and occurrence of equine recurrent uveitis. *Berl Munch Tierarztl Wochenschr.* 1996;109(8):273-278.
74. Breeveld J, Kuiper H, Spanjaard L, Luyendijk L, Rothova A. Uveitis and Lyme borreliosis. *Br J Ophthalmol.* 1993;77(8):480-481. doi:10.1136/bjo.77.8.480
75. Mikkilä H, Seppälä I, Leirisalo-Repo M, Immonen I, Karma A. The etiology of uveitis: The role of infections with special reference to Lyme borreliosis. *Acta Ophthalmol Scand.* 1997;75(6):716-719. doi:10.1111/j.1600-0420.1997.tb00637.x
76. Neely M, Arroyo LG, Jardine C, et al. Seroprevalence and evaluation of risk factors associated with seropositivity for *Borrelia burgdorferi* in Ontario horses. *Equine Vet J.* 2020;53:331-338.
77. Chang YF, Novosol V, McDonough SP, et al. Experimental infection of ponies with *Borrelia burgdorferi* by exposure to ixodid ticks. *Vet Pathol.* 2000;37(1):68-76.
doi:10.1354/vp.37-1-68
78. Cambra-Pellejà M, Gandasegui J, Balaña-Fouce R, Muñoz J, Martínez-Valladares M. Zoonotic implications of *Onchocerca* species on human health. *Pathogens.* 2020;9(9):1-17.
doi:10.3390/pathogens9090761
79. Attenburrow DP, Donnelly JJ, Soulsby E JL. Periodic ophthalmia (recurrent uveitis) of

- horses: An evaluation of the aetiological role of microfilariae of *Onchocerca cervicalis* and the clinical management of the condition. *Equine Vet J.* 2010;15(S2):48-56. doi:10.1111/j.2042-3306.1983.tb04559.x
80. Boswinkel M, Neyens IJS, van Oldruitenborgh-Oosterbaan MM. *Halicephalobus gingivalis* infection in a 5-year-old Tinker gelding. *Tijdschr Diergeneeskd.* 2006;131(3):74—80. <http://europepmc.org/abstract/MED/16502977>
 81. Yu F, Liu B, Chen S, et al. First molecular confirmation of equine ocular *Setaria digitata* in China. *Vet Sci.* 2021;8(4):4-9. doi:10.3390/vetsci8040055
 82. Shin J, Ahn KS, Suh GH, et al. First blindness cases of horses infected with *Setaria Digitata* (nematoda: Filarioidea) in the republic of Korea. *Korean J Parasitol.* 2017;55(6):667-671. doi:10.3347/kjp.2017.55.6.667
 83. Rafee MA, Amarpal A. Equine ocular setariasis and its management. *J Exp Biol Agric Sci.* 2016;4(Spl-4-EHIDZ):S139-S143. doi:10.18006/2016.4(spl-4-ehidz).s139.s143
 84. Aroch I, Ofri R, Sutton GA. Ocular Manifestations of Systemic Diseases. *Slatter's Fundam Vet Ophthalmol.* 2008;(January):374-418. doi:10.1016/B978-072160561-6.50021-6
 85. Davis JL. *Ocular Manifestations of Systemic Disease.* Second Edi. Elsevier Inc.; 2016. doi:10.1002/9781119047919.ch15
 86. Muhammad G, Saqib M. Successful treatment of ocular equine microfilariasis (*Setaria* species) with ivermectin. *Vet Rec.* 2007;160(1):25-26. doi:10.1136/vr.160.1.25
 87. Gilger BC. Recurrent Uveitis. In: Felipe M, ed. *Equine Clinical Immunology.* John Wiley & Sons, Ltd; 2016:121-126.
 88. Sandmeyer LS, Bowen G, Grahn BH. Diagnostic ophthalmology. *Can Vet J.* 2007;48(9):975-976.

89. Glaser AL, de Vries AAF, Rottier PJM, Horzinek MC, Colenbrander B. Equine arteritis virus: A review of clinical features and management aspects. *Vet Q.* 1996;18(3):95-99. doi:10.1080/01652176.1996.9694625
90. Balasuriya UBR, Go YY, MacLachlan NJ. Equine arteritis virus. *Vet Microbiol.* 2013;167(1-2):93-122. doi:10.1016/j.vetmic.2013.06.015
91. Timoney PJ. Equine influenza. *Comp Immunol Microbiol Infect Dis.* 1996;19(3):205-211. doi:10.1016/0147-9571(96)00006-9
92. van Maanen C, Cullinane A. Equine influenza virus infections: An update. *Vet Q.* 2002;24(2):79-94. doi:10.1080/01652176.2002.9695127
93. Landolt GA. Equine influenza virus. *Vet Clin North Am - Equine Pract.* 2014;30(3):507-522. doi:10.1016/j.cveq.2014.08.003
94. Wilson WD. Equine herpesvirus 1 myeloencephalopathy. *Vet Clin North Am Equine Pract.* 1997;13(1):53-72. doi:10.1016/S0749-0739(17)30255-9
95. Whitwell KE, Bluden AS. Pathological findings in horses dying during an outbreak of the paralytic form of Equid herpesvirus type 1 (EHV-1) infection. *Equine Vet J.* 1992;24:13-19. <https://doi.org/10.1111/j.2042-3306.1992.tb02771.x>
96. McCartan C, Russell M, Wood J, Mumford J. Clinical, serological and virological characteristics of an outbreak of paresis and neonatal foal disease due to equine herpesvirus-1 on a stud farm. *Vet Rec.* 1995;136(1):7-12. doi:10.1136/vr.136.1.7
97. Hussey GS, Goehring LS, Lunn DP, et al. Experimental infection with equine herpesvirus type 1 (EHV-1) induces chorioretinal lesions. *Vet Res.* 2013;44(1):1-15. doi:10.1186/1297-9716-44-118
98. Holz CL, Sledge DG, Kiupel M, Nelli RK, Goehring LS, Hussey GS. Histopathologic

- findings following experimental equine herpesvirus 1 infection of horses. *Front Vet Sci.* 2019;6(MAR):1-10. doi:10.3389/fvets.2019.00059
99. Szemes P, Gerhards H. Untersuchungen zur Prävalenz der equinen rezidivierenden Uveitis im Großraum Köln-Bonn. *Prakt Tierarzt.* 2000;81:408-420.
 100. Rockwell H, Mack M, Famula T, et al. Genetic investigation of equine recurrent uveitis in Appaloosa horses. *Anim Genet.* 2020;51(1):111-116. doi:10.1111/age.12883
 101. Malalana F, Ireland JL, Pinchbeck GL, McGowan CM. Risk factors for a first episode of primary uveitis in the UK and proportion of cases that experience recurrence following this first episode. *Equine Vet J.* 2022;(March):1-6. doi:10.1111/evj.13576
 102. Guo X, Chen Z, Xing Y. Immune-Mediated Uveitis and Lifestyle Factors: A Review. *Ophthalmic Res.* 2021;64(5):687-695. doi:10.1159/000518496
 103. Fu X, Chen Y, Chen D. The Role of Gut Microbiome in Autoimmune Uveitis. *Ophthalmic Res.* 2021;64(2):168-177. doi:10.1159/000510212
 104. Muhammad FY, Peters K, Wang D, Lee DJ. Exacerbation of autoimmune uveitis by obesity occurs through the melanocortin 5 receptor. *J Leukoc Biol.* 2019;106(4):879-887. doi:10.1002/JLB.MA0119-030RR
 105. de Bustamante MM, Gomez D, Macnicol J, Hamor R, Plummer C. The fecal bacterial microbiota in horses with equine recurrent uveitis. *Animals.* 2021;11(3):1-16. doi:10.3390/ani11030745
 106. Rohrbach BW, Ward DA, Hendrix DVH, Cawrse-Foss M, Moyers TD. Effect of vaccination against leptospirosis on the frequency, days to recurrence and progression of disease in horses with equine recurrent uveitis. *Vet Ophthalmol.* 2005;8(3):171-179. doi:10.1111/j.1463-5224.2005.00367.x

107. Hack Y, Henriksen M de L, Pihl TH, Nielsen RK, Dwyer AE, Bellone RR. A genetic investigation of equine recurrent uveitis in the Icelandic horse breed. *Anim Genet.* 2022;00:1-5. doi:DOI: 10.1111/age.13200
108. Kulbrock M, Von Borstel M, Rohn K, Distl O, Ohnesorge B. Studie zu Häufigkeit und Schweregrad der Equinen Rezidivierenden Uveitis bei Warmblütern. *Pferdeheilkunde.* 2013;29(1):27-36. doi:10.21836/PEM20130105
109. Henriksen M de L, Dwyer AE, Krarup Nielsen R, Bäcklund S, Dahlmann Christensen N, Holberg Pihl T. Ocular abnormalities in the Icelandic horse with a focus on equine recurrent uveitis: 112 Icelandic horses living in Denmark and 26 Icelandic horses living in the United States. *Vet Ophthalmol.* 2021;(November):1-15. doi:10.1111/vop.12961
110. Deeg CA, Marti E, Gaillard C, Kaspers B. Equine recurrent uveitis is strongly associated with the MHC class I haplotype ELA-A9. *Equine Vet J.* 2004;36(1):73-75. doi:10.2746/0425164044864651
111. Lazary S, Antczak DF, Bailey E, et al. Joint Report of the Fifth International Workshop on Lymphocyte Alloantigens of the Horse, Baton Rouge, Louisiana, 31 October-1 November 1987. *Anim Genet.* 1988;19(4):447-456. doi:10.1111/j.1365-2052.1988.tb00836.x
112. Tseng CT, Miller D, Cassano J, Bailey E, Antczak DF. Identification of equine major histocompatibility complex haplotypes using polymorphic microsatellites. *Anim Genet.* 2010;41(SUPPL. 2):150-153. doi:10.1111/j.1365-2052.2010.02125.x
113. Tallmadge RL, Campbell JA, Miller DC, Antczak DF. Analysis of MHC class I genes across horse MHC haplotypes. *Immunogenetics.* 2010;62(3):159-172. doi:10.1007/s00251-009-0420-9
114. Tallmadge RL, Lear TL, Antczak DF. Genomic characterization of MHC class I genes of

- the horse. *Immunogenetics*. 2005;57(10):763-774. doi:10.1007/s00251-005-0034-9
115. Kulbrock M, Lehner S, Metzger J, Ohnesorge B, Distl O. A Genome-Wide Association Study Identifies Risk Loci to Equine Recurrent Uveitis in German Warmblood Horses. *PLoS One*. 2013;8(8):1-6. doi:10.1371/journal.pone.0071619
116. Miller D, Tallmadge RL, Binns M, et al. Polymorphism at Expressed DQ and DR Loci in Five Common Equine MHC Haplotypes. *Immunogenetics*. 2017;69(3):145-156. doi:10.1007/s00251-016-0964-4
117. Wade CM, Giulotto E, Sigurdsson S, et al. Genome sequence, comparative analysis, and population genetics of the domestic horse. *Science (80-)*. 2009;326(5954):865-867. doi:10.1126/science.1178158
118. Deeg CA. Ocular immunology in equine recurrent uveitis. *Vet Ophthalmol*. 2008;11(SUPPL.1):61-65. doi:10.1111/j.1463-5224.2008.00625.x
119. Sponenberg DP, Carr G, Simak E, Schwink K. The inheritance of the leopard complex of spotting patterns in horses. *J Hered*. 1990;81(4):323-331. doi:10.1093/oxfordjournals.jhered.a110997
120. Thirstrup JP, Pertoldi C, Loeschke V. Genetic analysis, breed assignment and conservation priorities of three native Danish horse breeds. *Anim Genet*. 2008;39(5):496-505. doi:10.1111/j.1365-2052.2008.01767.x
121. Iannella G, Greco A, Didona D, et al. Vitiligo: Pathogenesis, clinical variants and treatment approaches. *Autoimmun Rev*. 2016;15(4):335-343. doi:10.1016/j.autrev.2015.12.006
122. Bellone RR, Holl H, Setaluri V, et al. Evidence for a Retroviral Insertion in *TRPM1* as the Cause of Congenital Stationary Night Blindness and Leopard Complex Spotting in the Horse. *PLoS One*. 2013;8(10):1-14. doi:10.1371/journal.pone.0078280

123. Bellone RR, Forsyth G, Leeb T, et al. Fine-mapping and mutation analysis of *TRPM1*: A candidate gene for leopard complex (LP) spotting and congenital stationary night blindness in horses. *Briefings Funct Genomics Proteomics*. 2010;9(3):193-207. doi:10.1093/bfgp/elq002
124. Holl HM, Brooks SA, Archer S, et al. Variant in the *RFWD3* gene associated with PATN1, a modifier of leopard complex spotting. *Anim Genet*. 2016;47(1):91-101. doi:10.1111/age.12375
125. Bellone RR, Brooks SA, Sandmeyer L, et al. Differential gene expression of *TRPM1*, the potential cause of congenital stationary night blindness and coat spotting patterns (LP) in the Appaloosa horse (*Equus caballus*). *Genetics*. 2008;179(4):1861-1870. doi:10.1534/genetics.108.088807
126. Schaefer RJ, Schubert M, Bailey E, et al. Developing a 670k genotyping array to tag ~2M SNPs across 24 horse breeds. *BMC Genomics*. 2017;18(1):1-18. doi:10.1186/s12864-017-3943-8
127. Taylor AW, Ng TF. Negative regulators that mediate ocular immune privilege. *J Leukoc Biol*. 2018;103(6):1179-1187. doi:10.1002/JLB.3MIR0817-337R
128. Agarwal RK, Silver PB, Caspi RR. Rodent Models of Experimental Autoimmune Uveitis. *Methods Mol Biol*. 2012;900. doi:10.1007/978-1-60761-720-4_22
129. Egwuagu CE, Alhakeem SA, Mbanefo EC. Uveitis: Molecular Pathogenesis and Emerging Therapies. *Front Immunol*. 2021;12(April):1-11. doi:10.3389/fimmu.2021.623725
130. Wu H, Deng Y, Feng Y, et al. Epigenetic regulation in B-cell maturation and its dysregulation in autoimmunity. *Cell Mol Immunol*. 2018;15(7):676-684. doi:10.1038/cmi.2017.133

131. Hou S, Li N, Liao X, Kijlstra A, Yang P. Uveitis genetics. *Exp Eye Res.* 2020;190(May 2019). doi:10.1016/j.exer.2019.107853
132. Ortiz-Fernández L, Sawalha AH. Genetics of Behçet's Disease: Functional Genetic Analysis and Estimating Disease Heritability. *Front Med.* 2021;8(February). doi:10.3389/fmed.2021.625710
133. Hughes T, Ture-Ozdemir F, Alibaz-Oner F, Coit P, Direskeneli H, Sawalha AH. Epigenome-wide scan identifies a treatment-responsive pattern of altered dna methylation among cytoskeletal remodeling genes in monocytes and CD4+ T cells from patients with behçet's disease. *Arthritis Rheumatol.* 2014;66(6):1648-1658. doi:10.1002/art.38409
134. Jin F, Hu H, Xu M, et al. Serum microRNA profiles serve as novel biomarkers for autoimmune diseases. *Front Immunol.* 2018;9(OCT):1-9. doi:10.3389/fimmu.2018.02381
135. Wei Y, Li N, Zhao L, et al. MicroRNAs and Autoimmune-Mediated Eye Diseases. *Front Cell Dev Biol.* 2020;8(August):1-11. doi:10.3389/fcell.2020.00818
136. Guo D, Li J, Liu Z, Tang K, Song H, Bi H. Characterization of microRNA expression profiling in peripheral blood lymphocytes in rats with experimental autoimmune uveitis. *Inflamm Res.* 2015;64(9):683-696. doi:10.1007/s00011-015-0848-3
137. Zhou Q, Xiao X, Wang C, et al. Decreased microRNA-155 expression in ocular Behçet's disease but not in Vogt-Koyanagi-Harada syndrome. *Investig Ophthalmol Vis Sci.* 2012;53(9):5665-5674. doi:10.1167/iovs.12-9832
138. Hou S, Ye Z, Liao D, et al. MiR-23a, miR-146a and miR-301a confer predisposition to Vogt-Koyanagi-Harada syndrome but not to Behçet's disease. *Sci Rep.* 2016;6(January):2-10. doi:10.1038/srep20057
139. Andersson L, Archibald AL, Bottema CD, et al. Coordinated international action to

- accelerate genome-to-phenome with FAANG, the Functional Annotation of Animal Genomes project. *Genome Biol.* 2015;16(1):4-9. doi:10.1186/s13059-015-0622-4
140. Tuggle CK, Giuffra E, White SN, et al. GO-FAANG meeting: a Gathering On Functional Annotation of Animal Genomes. *Anim Genet.* 2016;47(5):528-533. doi:10.1111/age.12466
141. Burns EN, Bordbari MH, Mienaltowski MJ, et al. Generation of an equine biobank to be used for Functional Annotation of Animal Genomes project. *Anim Genet.* 2018;49(6):564-570. doi:10.1111/age.12717
142. Farh KKH, Marson A, Zhu J, et al. Genetic and epigenetic fine mapping of causal autoimmune disease variants. *Nature.* 2015;518(7539):337-343. doi:10.1038/nature13835
143. Moraes F, Góes A. A decade of human genome project conclusion: Scientific diffusion about our genome knowledge. *Biochem Mol Biol Educ.* 2016;44(3):215-223. doi:10.1002/bmb.20952
144. Encode Consortium, Carolina N, Hill C. For Junk DNA. *Nature.* 2013;489(7414):57-74. doi:10.1038/nature11247.An
145. Dunham I, Kundaje A, Aldred SF, et al. An integrated encyclopedia of DNA elements in the human genome. *Nature.* 2012;489(7414):57-74. doi:10.1038/nature11247
146. Kingsley NB, Kern C, Creppe C, et al. Functionally Annotating Regulatory Elements in the Equine Genome Using Histone Mark ChIP-Seq. *Genes (Basel).* 2020;11(1):3. doi:10.3390/genes11010003
147. Peng S, Bellone R, Petersen JL, Kalbfleisch TS, Finno CJ. Successful ATAC-Seq From Snap-Frozen Equine Tissues. *Front Genet.* 2021;12(June):1-10. doi:10.3389/fgene.2021.641788
148. Donnelly CG, Bellone RR, Hales EN, et al. Generation of a Biobank From Two Adult

- Thoroughbred Stallions for the Functional Annotation of Animal Genomes Initiative. *Front Genet.* 2021;12(March):1-6. doi:10.3389/fgene.2021.650305
149. Dahlgren AR, Scott EY, Mansour T, et al. Comparison of poly-A⁺ selection and rRNA depletion in detection of lncRNA in two equine tissues using RNA-seq. *Non-coding RNA.* 2020;6(3). doi:10.3390/ncrna6030032
150. Finno CJ, Petersen JL, Bellone RR, MacLeod JN. Functional annotation of the equine genome. *J Anim Sci Suppl 4.* 2016;94:51-53.
151. Horvath S, Haghani A, Peng S, et al. DNA methylation aging and transcriptomic studies in horses. *Nat Commun.* 2022;13(1):1-13. doi:10.1038/s41467-021-27754-y
152. Kingsley NB, Hamilton NA, Lindgren G, et al. “Adopt-a-Tissue” Initiative Advances Efforts to Identify Tissue-Specific Histone Marks in the Mare. *Front Genet.* 2021;12(March):1-9. doi:10.3389/fgene.2021.649959

Chapter 2: Functionally Annotating Regulatory Elements in the Equine Genome Using Histone Mark ChIP-Seq

Authors: N. B. Kingsley, Colin Kern, Catherine Creppe, Erin N. Hales, Huaijun Zhou, T. S. Kalbfleisch, James N. MacLeod, Jessica L. Petersen, Carrie J. Finno, and Rebecca R. Bellone.

Keywords: FAANG; epigenetics; horse; genome regulation; H3K4me1; H3K4me3; H3K27ac; H3K27me3; tissue-specific; annotation.

Reference: Kingsley, N.B.; Kern, C.; Creppe, C.; Hales, E.N.; Zhou, H.; Kalbfleisch, T.S.; MacLeod, J.N.; Petersen, J.L.; Finno, C.J.; Bellone, R.R. Functionally Annotating Regulatory Elements in the Equine Genome Using Histone Mark ChIP-Seq. *Genes* **2020**, *11*, 3. <https://doi.org/10.3390/genes11010003>.

Accepted: December 16, 2019

Abstract: One of the primary aims of the Functional Annotation of ANimal Genomes (FAANG) initiative is to characterize tissue-specific regulation within animal genomes. To this end, we used Chromatin Immunoprecipitation followed by sequencing (ChIP-Seq) to map four histone modifications (H3K4me1, H3K4me3, H3K27ac, and H3K27me3) in eight prioritized tissues collected as part of the FAANG equine biobank from two Thoroughbred mares. Data were generated according to optimized experimental parameters developed during quality control testing. To ensure that we obtained sufficient ChIP and successful peak-calling, data and peak-calls were assessed using six quality metrics, replicate comparisons, and site-specific evaluations. Tissue specificity was explored by identifying binding motifs within unique active regions, and motifs were further characterized by gene ontology (GO) and protein-protein interaction analyses. The histone marks identified in this study represent some of the first resources for tissue-specific regulation within the equine genome. As such, these publicly available annotation data can be used

to advance equine studies investigating health, performance, reproduction, and other traits of economic interest in the horse.

1. Introduction

In 1992, researchers discovered the first disease mutation in horses, conferring hyperkalemic periodic paralysis (HYPP) in Quarter Horses [1], yet identification of additional equine genetic diseases progressed slowly, with only nine disease-associated variants discovered prior to 2007 [2,3]. Since the release of the equine reference genome in 2007 [4], twenty-two additional genes were found to cause or be associated with equine diseases, yet there are at least two hundred described genetic disorders for which causal variants are unknown [2,5]. While the majority of characterized equine disease variants are located within coding regions, an increasing amount of research in humans and other animal species suggests that a large number of disease mutations are harbored within regulatory elements and other functional but non-coding regions of the genome [6-9]. Current genomic annotations for the horse have limited information about the functions of these non-coding regions, making it difficult to identify variants that alter gene regulation. While there is a high degree of conservation within coding regions across species, increasing evidence suggests that regulatory regions, especially tissue-specific elements, are not as well conserved in terms of sequence or function across species [7-10].

Using improved annotations of regulatory networks for humans and other mammals, researchers have begun to identify causal variants outside of coding regions. For example, a super-enhancer that significantly contributes to the risk of Type II diabetes in humans was identified by combining a genome-wide association study (GWAS) with locations of regulatory elements and other functional regions across the genome [11]. Additionally, cattle researchers used annotations from both genomic assays on bovine tissue and homology-based methods to investigate complex

traits. They found that the annotation from the homology-based method provided less relevant information than the bovine-specific annotation when combined with GWAS pertaining to milk production [8]. Along with the increasing number of regulatory GWAS, researchers are also expanding efforts to look at large-scale changes in the epigenome, such as associations between genome-wide changes in active regulatory elements and autism spectrum disorder [12]. With the increasing focus on the importance of regulatory elements in the pathogenesis of many diseases, it is clear that annotations of the equine genome need to encompass both coding and noncoding functional elements in order to understand complex genetic diseases and other traits affecting horses and the equine industry.

Similar to the Encyclopedia of DNA Elements (ENCODE), the Functional Annotation of ANimal Genomes (FAANG) initiative was established to improve the reference annotation of animal species, including characterization of genomic regulatory regions [13-15]. The link between chromatin modifications and regulatory regions, such as enhancers and promoters, has been well established for several decades [16]. Four histone tail modifications, also known as histone marks, were selected by the FAANG consortium to characterize promoters (H3K4me3) and enhancers (H3K4me1), as well as distinguish between active (H3K27ac) and inactive (H3K27me3) genomic elements [15].

Histone tail modifications were first hypothesized to affect genomic regulation in 1964 [17]. Since that time, associations between histone marks and regulatory elements have continued to expand. However, it is still unclear if the associations are the result of underlying functional roles in all cases or if the histone marks are the by-products of regulatory activities [18]. There is evidence that monomethylation of H3K4 recruits chromatin-modifying proteins to enhancer regions leading to enhancer priming and recognition [19]. Conversely, H3K4me3 is associated

with promoters and the transcription start site, but some research suggests that the mark may actually be a signature left by frequent transcriptional activity to create cellular memory rather than acting as a pioneer factor [18]. In conjunction with the H3K4 modifications, acetylation of H3K27 is found at active enhancers and promoters [20]. Trimethylation of the same residue, however, is strongly associated with facultative heterochromatin leading to inactive regulatory elements and silenced genes [20]. In fact, these two H3K27 marks are thought to be antagonistic to one another such that acetylation may physically prevent Polycomb silencing [21]. Acetylation of H3K27 also decreases the overall positive charge of the histone proteins leading to fewer interactions with DNA and more open chromatin structure [22]. Since H3K27ac has been strongly associated with active regulatory elements across the genome, presence of this mark can be used to distinguish between active and poised regulatory elements [23]. While research into the functional roles of histone tail modifications continues, the associations between these four marks and patterns of regulatory elements are well established. For more than a decade, chromatin immunoprecipitation (ChIP) assays have remained the primary method for identifying genomic sites enriched with histone marks to conduct large-scale regulatory mapping [24,25].

As part of the international FAANG collaboration, we performed ChIP-Seq on four major histone modifications (H3K4me1, H3K4me3, H3K27ac, and H3K27me3) in eight equine tissues (adipose, brain (parietal cortex), heart, lamina, liver, lung, (skeletal) muscle, and ovary). These tissues were collected as part of the FAANG equine biobank, which includes samples from eighty tissues, six fluids, and two cell lines that were collected from two healthy adult Thoroughbred mares [26]. The eight tissues evaluated in this study were prioritized for thorough investigation based on (1) continuity with other FAANG species to enable across species comparisons and/or (2) the primary needs of the equine community in terms of health, performance, and reproduction.

2. Materials and Methods

Due to the limited number of previous histone ChIP-Seq experiments across equine tissues, we first performed quality control (QC) testing to determine appropriate experimental parameters for each tissue and mark. All ChIP-Seq experiments, including QC, were conducted by Diagenode ChIP-Seq Profiling Service (Diagenode, Cat# G02010000), and a complete summary of the final protocols used for all tissues can be accessed at <ftp://ftp.faang.ebi.ac.uk/ftp/protocols/assays/>. QC involved chromatin extraction, ChIP, library preparation, and sequencing of one training sample from each of the eight tissues investigated. QC training samples were obtained from previously banked tissues collected at the University of California, Davis. Bioinformatic analysis was performed on the QC data in order to calculate library complexity and ChIP enrichment metrics and to call peaks and evaluate the genomic distribution of detected marks. Library complexity metrics included Non-Redundant Fraction (NRF) and PCR Bottleneck Coefficients 1 and 2 (PBC1 & PBC2). ChIP enrichment metrics included Normalized Strand Cross-Correlation Coefficient (NSC), Relative Strand Cross-Correlation Coefficient (RSC), and Jensen-Shannon Distance (JSD). NRF, PBC1&2, NSC, and RSC are all standardized metrics of the ENCODE project [27] and were compared against ENCODE standards to determine the efficacy of the ChIP protocols. JSD is a common statistic used to compare two distributions that can be applied to ChIP datasets using deepTools version 2.4.3 [28], and a threshold was determined by agreement among FAANG collaborators. Tissues of interest (TOI) used in the final experiments that generated combined peak-calls were collected from two Thoroughbred mares (referred to in this manuscript as ECA_UCD_AH1 and ECA_UCD_AH2) as part of the FAANG equine biobank [26], and all protocols for this work were

approved by the University of California, Davis Institutional Animal Care and Use Committee (Protocol #19037). Laboratory procedures that varied based on tissue are summarized in Table 1.

Table 1: Optimized ChIP-Seq experimental procedures for each tissue.

Parameter	Adipose	Brain	Heart	Lamina	Liver	Lung	Muscle	Ovary
Starting Tissue (mg)	220	90	105	100	40	40	100	85
Homogenization Time (min)	8	5	5	9	n/a	5	5	5
Duration Fixed (min)	10	9	9	9	9	9	9	9
Fixation Temp. (°C)	37	23	23	23	23	23	23	23
Shearing Volume (ul)	400	1500	1800	1800	1500	1500	1800	1800
Shearing Cycles	5 x 8 ¹	10	13	10	12	10	12	10
Chromatin per IP (ng)	700	300	500	700	450	800	260	1200

¹ Samples were sonicated for five sets of eight cycles.

2.1. Chromatin Extraction

Chromatin was extracted from adipose using the True MicroChIP Kit (Diagenode, Cat# C01010130) and from the other seven tissues following the iDeal ChIP-Seq Kit for histones (Diagenode, Cat# C01010059) with the modifications or specifications described in this paper. The starting amount varied depending on tissue, such that those with extensive extracellular matrices and/or low ratio of nuclei to cellular matter required larger amounts of starting material compared to those tissues that homogenized easily. Samples were homogenized either by douncing (liver) or grinding with the Tissue Lyser II (Qiagen, Germany) at 25 strokes/minute for a length of time that varied by tissue (Table 1).

In order to reach the desired fragment length (approximately 200 bp), chromatin was sheared with the Bioruptor Pico (Diagenode, Cat# B01060001) combined with the Bioruptor® Water cooler for 8-12 cycles of 30 seconds with 30 seconds rest between cycles. The temperature was

maintained at 10°C for adipose and 4°C for all other tissues during shearing. The number of cycles varied based on tissue (Table 1), and the chromatin quality was assessed using the Fragment Analyzer (Aligent, USA).

2.2. Immunoprecipitation

Immunoprecipitation (IP) of the four histone marks, along with a negative IP control (IgG), was performed on tissue-specific amounts of chromatin using the IP-Star Compact Automated System (Diagenode, Cat# B03000002). The antibodies used were all previously validated by Diagenode, and antibody concentrations were determined during QC for every tissue and histone mark combination (Table S1). An aliquot of chromatin from each tissue was set aside for the input to characterize sequencing background and identify true ChIP enrichment.

2.3. Sequencing

Libraries were prepared using the IP-Star® Compact Automated System (Diagenode, Cat# B03000002) and the MicroPlex Library Preparation Kit v2 (Diagenode, Cat# C05010013) for the input and four ChIPs per tissue. Libraries were amplified prior to sequencing for at least ten cycles, and additional cycles were performed as needed to reach a concentration of 3-10 nM. Using Agencourt AMPure XP (Bechman Coulter, USA), libraries were purified, and fragments were size-selected for approximately 200 bp. Libraries were sequenced as 50 bp, single-end reads on the HiSeq 4000 platform (Illumina, USA) to generate approximately 55-80M raw reads for H3K27me3 and 30-50M raw reads for the other marks and inputs.

2.4. Data Processing

A complete summary of the bioinformatic workflow can be accessed at <ftp://ftp.faang.ebi.ac.uk/ftp/protocols/analysis/>, and bioinformatic parameters that varied by mark are summarized in Table 2. Reads were trimmed using Trim-Galore version 0.4.0 [29,30]

under the default parameters and aligned to EquCab3.0 [31] with BWA-MEM version 0.7.9a [32] such that split hits were marked as secondary alignments. Alignments were converted to BAM file format, processed, and filtered using SAMtools version 1.9 [33]. For strict quality filtering, reads were removed if they did not map, had secondary alignments, failed platform/vendor quality tests, were identified as optical duplicates, or had an alignment quality score lower than 30. PCR duplicates were marked with PicardTools version 2.7.1 [34] and then removed with SAMtools. For peak-calling, MACS2 version 2.1.1.20160309 [35] was used to call peaks for all marks, and SICERpy version 0.1.1 [36], which is a wrapper for executing SICER [37], was also used to call peaks for the broad mark, H3K27me3. Combining peak-calls involved identifying overlapping regions of enrichment in both biological replicates where at least one replicate was significantly enriched based on a set of significance thresholds that varied by mark (Table 2). Additionally, enrichment tracks (bigWig) were generated using deepTools version 2.4.3, which subtracted background characterized by the input and then combined enrichment from both replicates.

Table 2: Software parameters used to analyze ChIP-Seq data for each histone mark.

Software	Parameter	H3K4me1	H3K4me3	H3K27ac	H3K27me3
MACS2	Filtering	strict	strict	strict	strict
	Size	narrow ¹	narrow	narrow	broad
	Size Flag	none	none	none	--broad
	Model	--fix-bimodal	--fix-bimodal	--fix-bimodal	--fix-bimodal
	Genome Size	2,409,143,234	2,409,143,234	2,409,143,234	2,409,143,234
both	Fragment Size	200	200	200	200
	FDR	0.05	0.01	0.01	0.1
SICERpy ²	Gap Size	n/a	n/a	n/a	4
	Window Size	n/a	n/a	n/a	200

Genome Fraction	n/a	n/a	n/a	0.63
-----------------	-----	-----	-----	------

¹ Mark was treated as broader than other narrow marks due to being categorized previously as broad by ENCODE (Calo and Wysocka 2014). ² SICERpy was only used to call peaks for the broad mark, H3K27me3.

2.5. Data Analysis

As with the QC data, the datasets from the eight TOI were assessed by calculating library complexity and ChIP enrichment metrics as well as evaluating the genomic distribution of detected marks. Identity between peaks called for ECA_UCD_AH1 and ECA_UCD_AH2 were compared to assess the similarity of the biological replicates using the Jaccard Index [38], also known as the Jaccard Similarity Coefficient, from BEDtools version 2.27.1 [39]. Unique peaks were defined as a peak for a given mark that does not have any overlap with peaks from the same mark in the other prioritized tissues. BEDtools version 2.27.1 was used to identify unique peaks as well as calculate the percent of the genome covered by peaks. Graphs were generated using ggplot2 with R software version 3.4.3 [40,41]. To characterize the average peak topology in relation to gene annotations and calculate normalized enrichment patterns, we used deepTools version 2.4.3. RNA-Seq data from the two FAANG replicates allowed for site-specific validation of the histone peaks (ERR2584116, ERR2584168, ERR2584153, ERR2584205, ERR2584194, ERR2584142, ERR2584135, ERR2584187, ERR2584195, ERR2584143, ERR2584197, ERR2584145, ERR2584144, ERR2584196, ERR2584152, and ERR2584204). Analysis of Motif Enrichment (AME) from the MEME Suite version 5.0.5 [42] was used to identify known transcription factor binding motifs within peaks based on the JASPAR 2018 vertebrate database [43], and Biological Process Gene Ontologies (GO) from Swiss Prot were used to perform a GO term analysis [44]. Novel motifs were characterized with DREME and MEME, and each of the novel motifs was manually investigated to identify additional known motifs that were not included in the JASPAR

database. The Integrated Genome Viewer [45] was used to visualize peak-calls in conjunction with the Ensembl annotation (release 95) for the EquCab3.0 reference assembly [46]. String version 11.0 was used to perform a protein-protein interaction analysis on the transcription factors implicated in each tissue based on the enriched motifs identified in the tissue-specific active enhancer elements [47].

3. Results

Quality control testing was performed to determine tissue-specific laboratory parameters such as antibody concentration and shearing time (Table 1 and Table S1) by comparing the quality metrics and peak-calls to ENCODE and FAANG standards (Table S2). The raw and processed data are available on <https://data.faang.org/home> under the study accession PRJEB35307. The processed files include read alignments to EquCab3.0 and peak-calls for each biological replicate as well as the combined peak-calls.

3.1. Assessing Data Quality

Using the Jaccard Index to compare replicates for all of the marks, we found the highest identity between the two replicates of the same tissue (Figure 1), with the exception of the brain replicates for H3K4me1 and the ovary replicates for H3K27me3. For the brain replicates, ECA_UCD_AH2 had 65,327 peaks compared to 143,328 peaks for ECA_UCD_AH1 (Table 3). In addition to a lower peak number, two of the library complexity quality scores for the ECA_UCD_AH2 brain replicate were lower than the ENCODE quality thresholds (Table 4). In terms of enrichment, however, the cross-correlation metrics for this sample were both above the established thresholds and indicate that the data had sufficient ChIP enrichment. Indeed, we were able to call 95,918 combined peaks, which is consistent with the range of H3K4me1 values from the other tissues. For the ovary replicates, two of the three library complexity metrics were below

ENCODE standards, yet all of the ChIP enrichment metrics were consistent with those for the broad mark in other tissues, indicating that we had sufficient ChIP enrichment despite lower library complexity. When comparing SICER and MACS2 peak-calls for the broad mark, the number of combined peaks (8,479 and 40,825, respectively) and the percentage of the genome covered (2.1% and 1.2%, respectively) for ovary were all consistent with the same measures for the H3K27me3 peaks from the other tissues evaluated in this study.

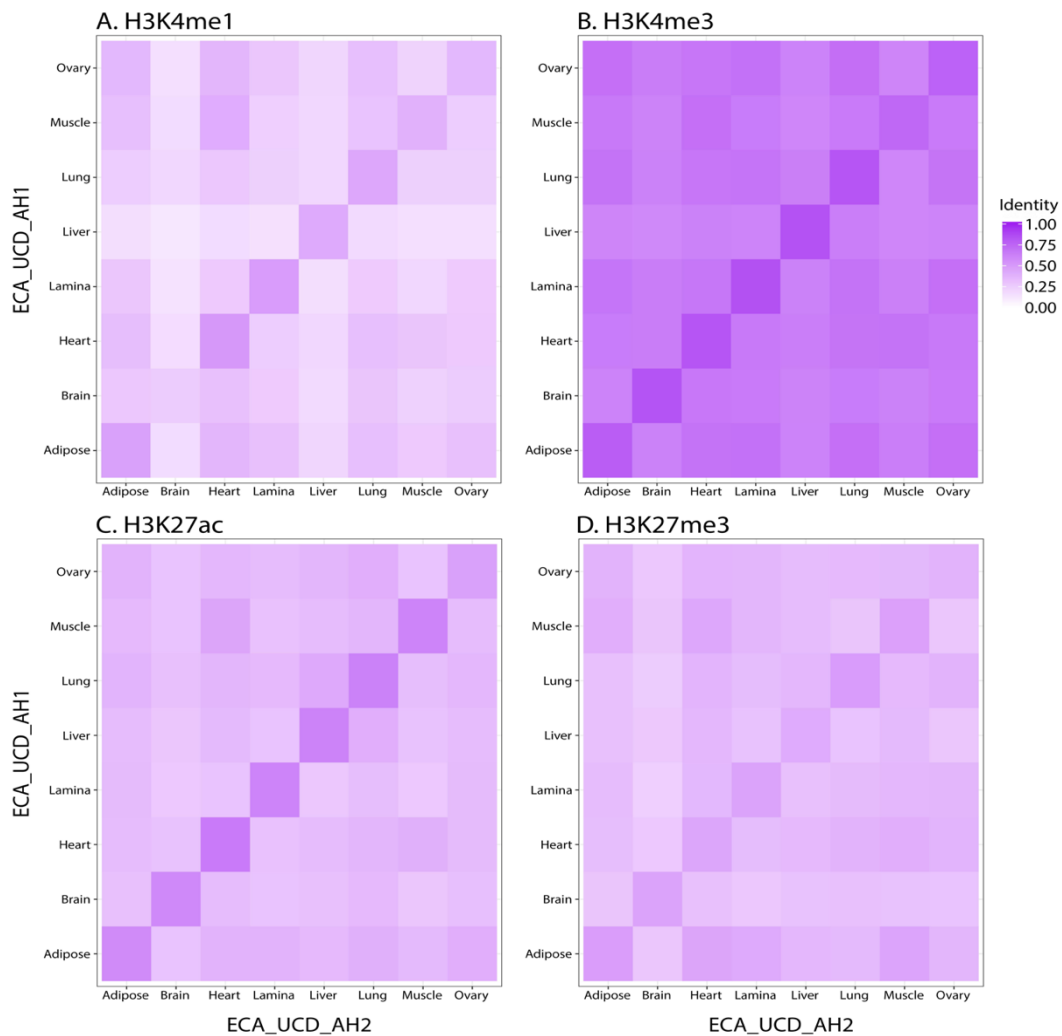


Figure 1: Jaccard Index to measure similarity of peaks called for each histone mark and tissue between biological replicates, ECA_UCD_AH1 and ECA_UCD_AH2. Each panel is a heatmap displaying the Jaccard Index for pairwise comparisons of tissues between replicates. Darker purple indicates that there are more peaks that are shared by the two tissues. A. H3K4me1 B. H3K4me3 C. H3K27ac D. H3K27me3 called by SICER.

While demonstrating more variation than the other marks, H3K27me3 had peaks called by SICER that were more similar between replicates of the same tissue compared to the H3K27me3 peaks called by MACS2 software (Figure S1). Peak-calls from the two biological replicates were combined by identifying regions of overlapping enrichment in which at least one replicate had significant enrichment based on a q-value that differed by mark (Table 2). For H3K4me1, H3K4me3, and H3K27ac, the number of combined peaks ranged from 93-121K, 26-29K, and 64-88K, respectively. The number of combined peaks called for the broad mark was lower than the three activating marks for both MACS2 and SICER (24-68K and 7-11K, respectively). Although the combined peak numbers for the MACS2-H3K27me3 datasets were more similar to the ENCODE equivalent than the number of peaks called by SICER (Table S3), the SICER-H3K27me3 combined peaks covered a larger portion of the genome, similar to that for the other marks (Table 3). Files for H3K27me3 peaks called by MACS2 and SICERpy are both publicly available for every tissue.

Table 3: Summary of peak number and percent of the genome covered for each mark and tissue.

Mark	Tissue	Software	Combined Peak Number	Percent Genome Covered	AH1 Peak Number	AH2 Peak Number
H3K4me1	Adipose	MACS2	107318	5.1	130242	157497
	Brain	MACS2	95918	3.1	143328	65327
	Heart	MACS2	121663	4.9	137385	155881
	Lamina	MACS2	114708	4.2	137575	124150
	Liver	MACS2	116760	3.6	97863	135122
	Lung	MACS2	92972	2.9	90687	109001
	Muscle	MACS2	95816	3.7	137322	100999

	Ovary	MACS2	102986	4.3	166303	133209
H3K4me3	Adipose	MACS2	26905	1.7	26286	29121
	Brain	MACS2	27101	1.6	25473	28028
	Heart	MACS2	26475	1.4	24101	27985
	Lamina	MACS2	29380	1.6	29023	19742
	Liver	MACS2	28498	1.5	28204	28222
	Lung	MACS2	28546	1.6	30048	27779
	Muscle	MACS2	28110	1.6	30428	25123
	Ovary	MACS2	28378	1.7	30522	29192
H3K27ac	Adipose	MACS2	79620	3.3	75823	99249
	Brain	MACS2	78823	3.2	89445	73795
	Heart	MACS2	68728	2.9	71462	7192
	Lamina	MACS2	82394	2.9	91345	78953
	Liver	MACS2	87589	3.1	84814	96238
	Lung	MACS2	69054	2.9	69621	75299
	Muscle	MACS2	76495	2.9	78047	86524
	Ovary	MACS2	64318	3.3	94817	82318
H3K27me3	Adipose	MACS2	25183	0.6	8948	29906
	Brain	MACS2	24243	0.6	16055	23411
	Heart	MACS2	68113	1.8	31455	88818
	Lamina	MACS2	37366	0.8	31839	28508
	Liver	MACS2	63874	1.3	93423	23888
	Lung	MACS2	30191	0.7	32385	18124
	Muscle	MACS2	42610	0.9	39076	29579
	Ovary	MACS2	40825	1.2	43036	33220
H3K27me3	Adipose	SICER	8167	4.9	13540	14571
	Brain	SICER	7860	3.4	11386	13603
	Heart	SICER	9032	3.3	12192	18903

Lamina	SICER	7072	3.8	11933	11694
Liver	SICER	11430	3.7	22270	16099
Lung	SICER	7863	2.6	12668	11715
Muscle	SICER	8437	4.6	17073	10987
Ovary	SICER	7083	3.0	14731	11124

Table 4: Quality metrics for assessing library complexity and ChIP enrichment. Thresholds for NRF, PBC1, PBC2, NSC, and RSC represent those developed by ENCODE [27]. JSD threshold was established among members of the FAANG consortium.

Mark	Tissue	Rep	NRF	PBC1	PBC2	NSC	RSC	JSD
Thresholds			(>0.5)	(>0.5)	(>1)	(>1.05)	(>0.8)	(>0.05)
H3K4me1	Adipose	AH2	0.677	0.673	3.017	1.068	1.249	0.281
	Adipose	AH1	0.621	0.617	2.595	1.067	1.147	0.239
	Brain	AH2	0.435	0.443	1.908	1.055	1.243	0.186
	Brain	AH1	0.754	0.756	4.128	1.074	1.275	0.228
	Heart	AH2	0.708	0.708	3.444	1.086	1.790	0.321
	Heart	AH1	0.497	0.496	2.023	1.071	1.657	0.259
	Lamina	AH2	0.606	0.606	2.551	1.093	1.628	0.281
	Lamina	AH1	0.561	0.562	2.311	1.088	1.809	0.283
	Liver	AH2	0.760	0.762	4.226	1.097	1.240	0.226
	Liver	AH1	0.838	0.842	6.462	1.117	1.289	0.252
	Lung	AH2	0.736	0.736	3.796	1.079	1.123	0.199
	Lung	AH1	0.667	0.665	2.980	1.069	1.063	0.178
	Muscle	AH2	0.706	0.706	3.418	1.077	1.030	0.210
	Muscle	AH1	0.576	0.573	2.338	1.084	1.200	0.259
	Ovary	AH2	0.712	0.712	3.488	1.077	1.265	0.245
	Ovary	AH1	0.692	0.691	3.240	1.085	2.117	0.313
H3K4me3	Adipose	AH2	0.595	0.604	2.581	1.322	1.391	0.382

	Adipose	AH1	0.559	0.571	2.389	1.313	1.501	0.354
	Brain	AH2	0.497	0.515	2.167	1.366	1.198	0.516
	Brain	AH1	0.333	0.362	1.813	1.360	1.249	0.528
	Heart	AH2	0.410	0.435	1.905	1.467	1.364	0.540
	Heart	AH1	0.337	0.374	1.857	1.399	1.639	0.548
	Lamina	AH2	0.529	0.551	2.345	1.384	1.188	0.467
	Lamina	AH1	0.571	0.594	2.606	1.380	1.289	0.465
	Liver	AH2	0.452	0.471	1.996	1.407	1.196	0.517
	Liver	AH1	0.421	0.444	1.926	1.385	1.282	0.537
	Lung	AH2	0.610	0.628	2.813	1.354	1.154	0.387
	Lung	AH1	0.580	0.600	2.634	1.344	1.117	0.452
	Muscle	AH2	0.240	0.277	1.818	1.340	1.354	0.441
	Muscle	AH1	0.559	0.567	2.350	1.350	1.164	0.448
	Ovary	AH2	0.633	0.646	2.926	1.315	1.191	0.428
	Ovary	AH1	0.603	0.622	2.779	1.335	1.220	0.439
H3K27ac	Adipose	AH2	0.678	0.677	3.087	1.223	1.605	0.313
	Adipose	AH1	0.537	0.532	2.129	1.250	1.800	0.333
	Brain	AH2	0.495	0.493	2.001	1.202	1.320	0.310
	Brain	AH1	0.655	0.657	2.939	1.200	1.341	0.326
	Heart	AH2	0.493	0.489	1.970	1.316	2.193	0.402
	Heart	AH1	0.573	0.573	2.361	1.331	1.856	0.376
	Lamina	AH2	0.597	0.596	2.486	1.296	1.655	0.351
	Lamina	AH1	0.657	0.662	3.006	1.304	1.711	0.345
	Liver	AH2	0.719	0.722	3.651	1.258	1.225	0.347
	Liver	AH1	0.721	0.724	3.674	1.242	1.237	0.298
	Lung	AH2	0.500	0.499	2.008	1.241	1.290	0.327
	Lung	AH1	0.654	0.658	2.956	1.208	1.281	0.299
	Muscle	AH2	0.605	0.604	2.524	1.291	1.306	0.335

	Muscle	AH1	0.510	0.511	2.072	1.285	1.335	0.381
	Ovary	AH2	0.733	0.736	3.816	1.254	1.309	0.374
	Ovary	AH1	0.678	0.678	3.112	1.224	1.461	0.391
H3K27me3	Adipose	AH2	0.646	0.641	2.751	1.057	0.659	0.101
	Adipose	AH1	0.650	0.647	2.809	1.053	0.592	0.067
	Brain	AH2	0.511	0.510	2.077	1.060	0.400	0.101
	Brain	AH1	0.616	0.614	2.587	1.067	0.477	0.088
	Heart	AH2	0.407	0.414	1.834	1.070	0.595	0.106
	Heart	AH1	0.287	0.315	1.778	1.090	0.649	0.102
	Lamina	AH2	0.459	0.460	1.919	1.069	0.656	0.071
	Lamina	AH1	0.429	0.436	1.885	1.076	0.732	0.065
	Liver	AH2	0.545	0.537	2.140	1.076	0.648	0.093
	Liver	AH1	0.454	0.451	1.871	1.084	0.661	0.123
	Lung	AH2	0.619	0.615	2.575	1.072	0.617	0.072
	Lung	AH1	0.550	0.545	2.199	1.084	0.671	0.088
	Muscle	AH2	0.534	0.526	2.098	1.070	0.597	0.070
	Muscle	AH1	0.476	0.472	1.914	1.079	0.689	0.103
	Ovary	AH2	0.524	0.520	2.103	1.071	0.587	0.066
	Ovary	AH1	0.495	0.489	1.970	1.077	0.688	0.101

As a proof-of-principle, we investigated a small number of regions near well-characterized genes to compare the histone peaks with RNA-seq data generated from the same tissues. We found consistent activating marks across all tissues for a widely expressed gene, *ACTB* (Figure 2A). Conversely, liver was the only tissue enriched for a set of active histone marks near the transcription start site (TSS) of the liver-specific gene *CYP2E1* (Figure 2B) [48].

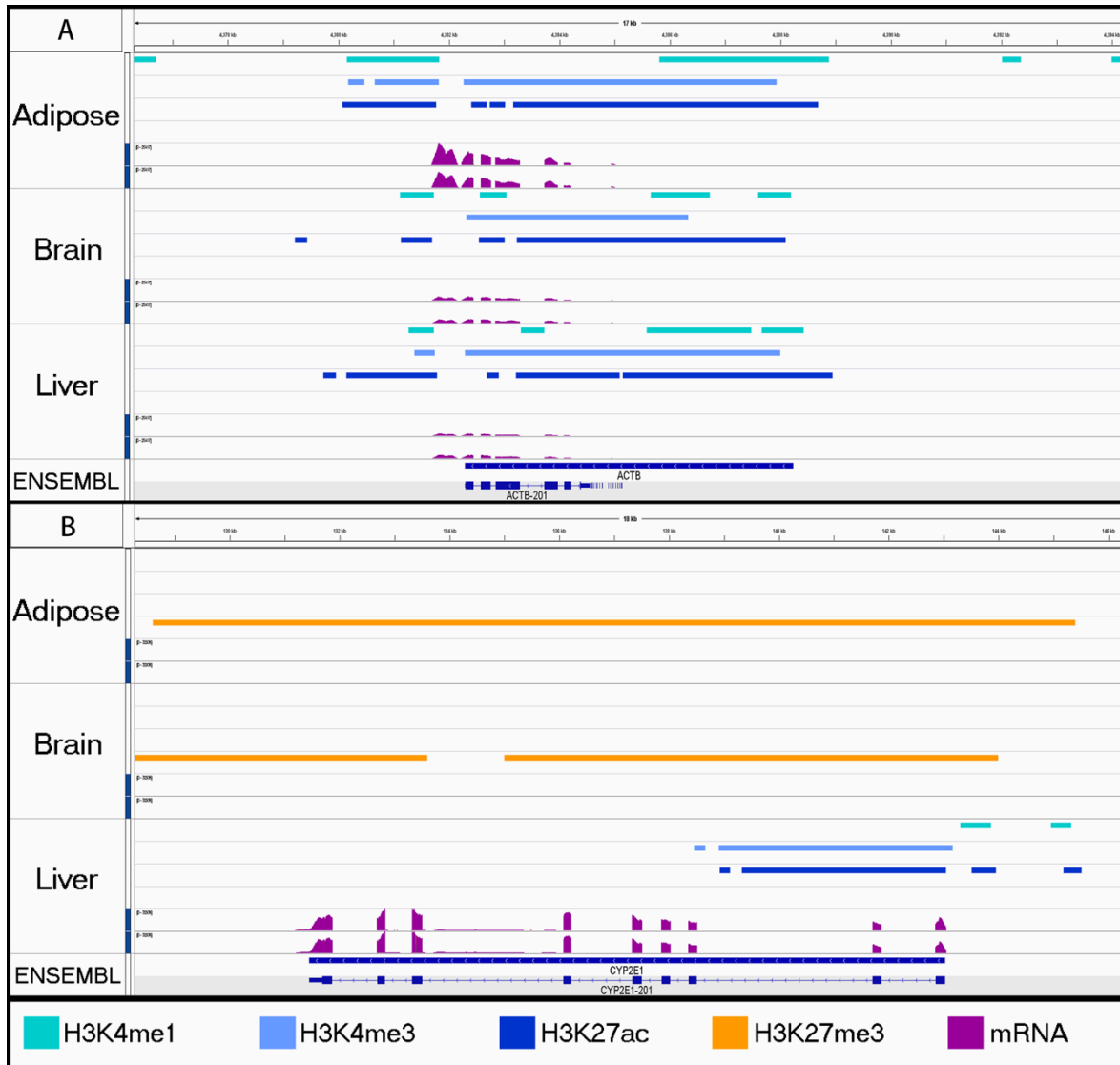


Figure 2: Proof-of-principle investigating house-keeping gene, *ACTB*, and liver-specific gene, *CYP2E1*, for appropriate regulatory elements. For adipose, brain, and liver tissue, combined peaks are displayed for H3K4me1 (aqua), H3K4me3 (light blue), H3K27ac (dark blue), H3K27me3 from SICER (orange), and mRNA expression (purple). A. *ACTB* is a housekeeping gene that is commonly expressed for many tissues. B. *CYP2E1* is a liver enzyme, which displays tissue-specific expression. Note the presence of the H3K27me3 repressive mark (orange) within adipose and brain samples.

3.2. Characterizing Tissue-Specific Features

Brain tissue had the highest percentage of unique peaks, defined as peaks that were only found in that tissue, for H3K27ac (31%) and H3K27me3 (20%), while liver had the highest percentage of unique peaks for H3K4me1 (32%) and H3K4me3 (16%), along with the second

highest for H3K27ac (26%) and H3K27me3 (14%) (Figure 3). Lamina tissue also had a high percentage of unique peaks for the three activating marks with 24, 10, and 26 percent for H3K4me1, H3K4me3, and H3K27ac, respectively.

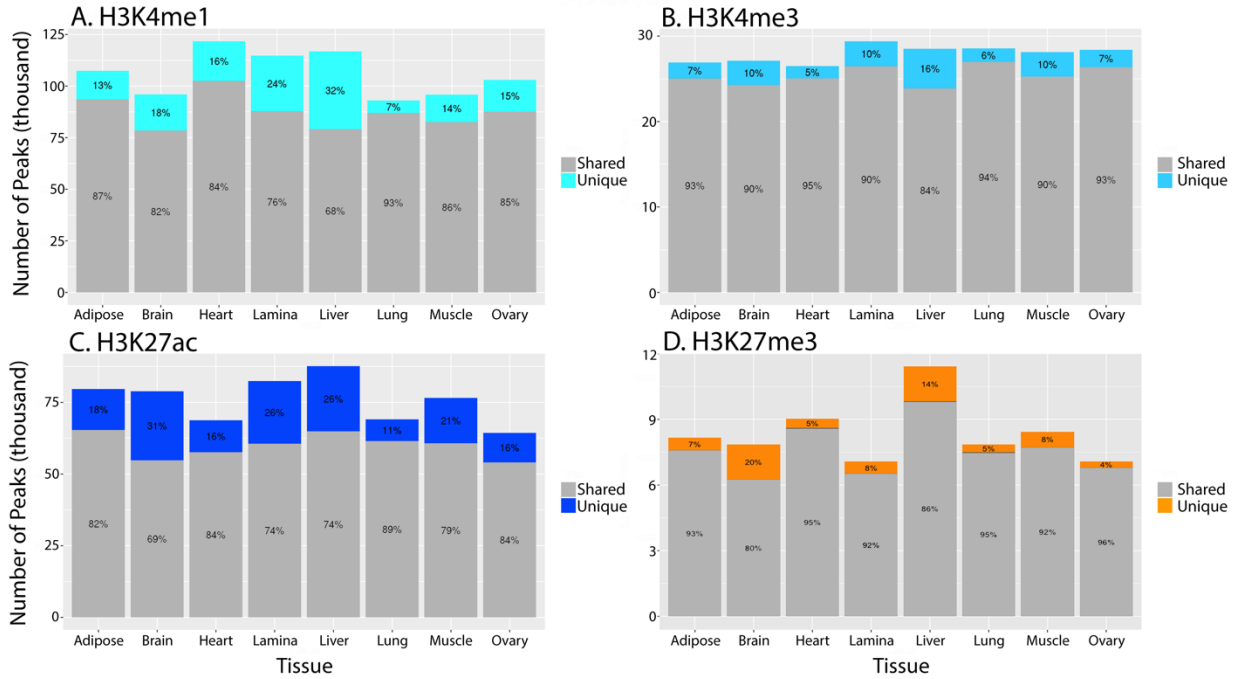


Figure 3: Tissue-specific peaks for each histone mark. Grey area indicates the number of peaks for a particular histone tail modification that are shared between at least two tissues, while the color region of each bar indicates the number of tissue-specific peaks. Percentage values are also assigned to the two segments of each bar to indicate the proportion of shared and unique peaks. A. H3K4me1 B. H3K4me3 C. H3K27ac D. H3K27me3 from SICER.

In addition to characterized genes, we also investigated a small number of genomic regions with putative tissue-specific functions in liver and muscle. For liver, a potential tissue-specific regulatory element was identified in the 59th intron of *PKHDI* (Ensembl Transcript ID: ENSECAT00000024985.1; Figure 4), a gene which has been previously associated with liver fibrosis [49]. Similarly, when considering a genomic region associated with racing ability [50], peaks for H3K4me3 in both muscle tissues were discovered at the start of a predicted lncRNA

from Ensembl genebuild [51], indicating that this uncharacterized gene may be particularly informative for the function of contractile tissues (Figure 5).

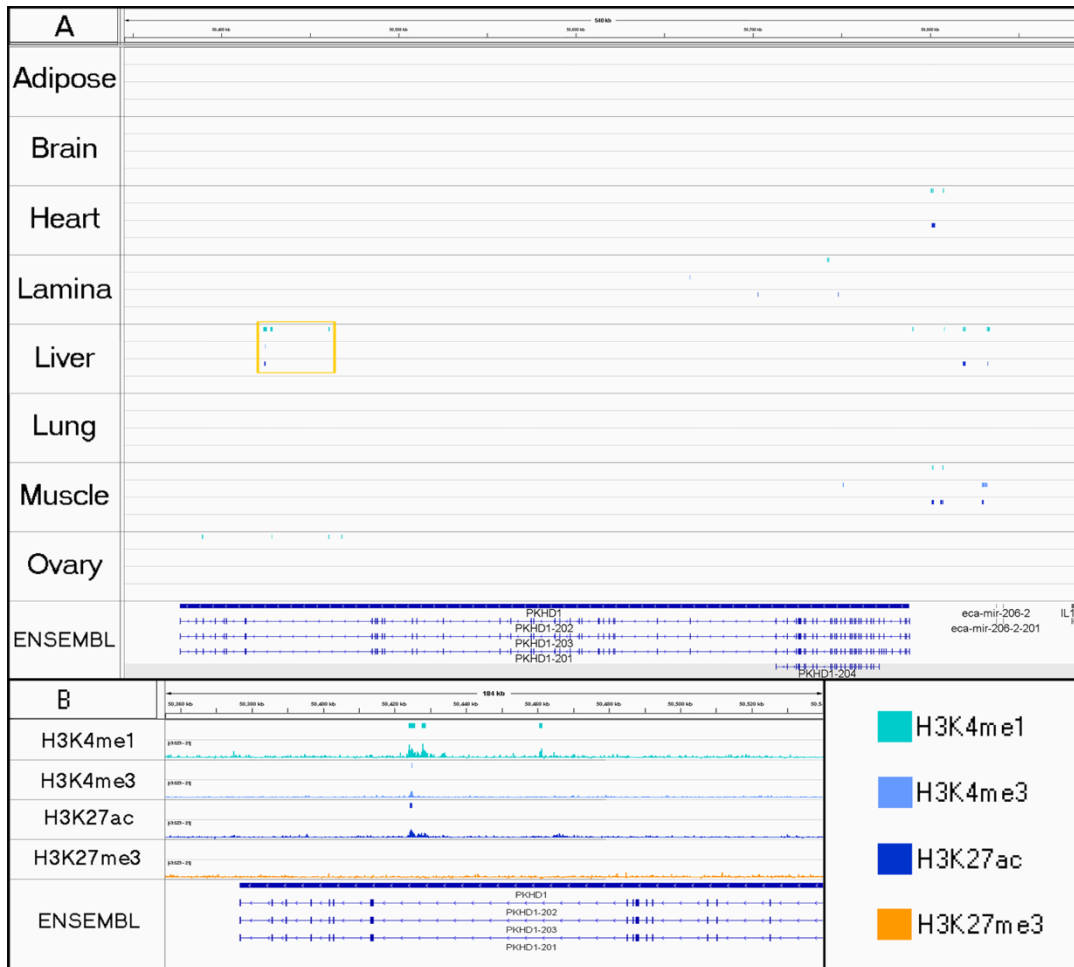


Figure 4: Evidence of a tissue-specific regulatory element found in liver tissue. For each tissue, peaks are displayed for H3K4me1 (aqua), H3K4me3 (light blue), H3K27ac (dark blue), and H3K27me3 from SICER (orange). A. Gold box highlights liver-specific active marks in the 59th intron of an annotated gene, *PKHD1* (Ensembl Transcript ID: ENSECAT00000024985.1), which is transcribed from the antisense strand. H3K4me1 marks were also detected in ovary tissue at the end of the gene, but they do not indicate the presence of an active enhancer without co-occurrence of H3K27ac. B. Enrichment profiles (BigWig) were visualized below the corresponding peak tracks for the region highlighted by the gold box in A.

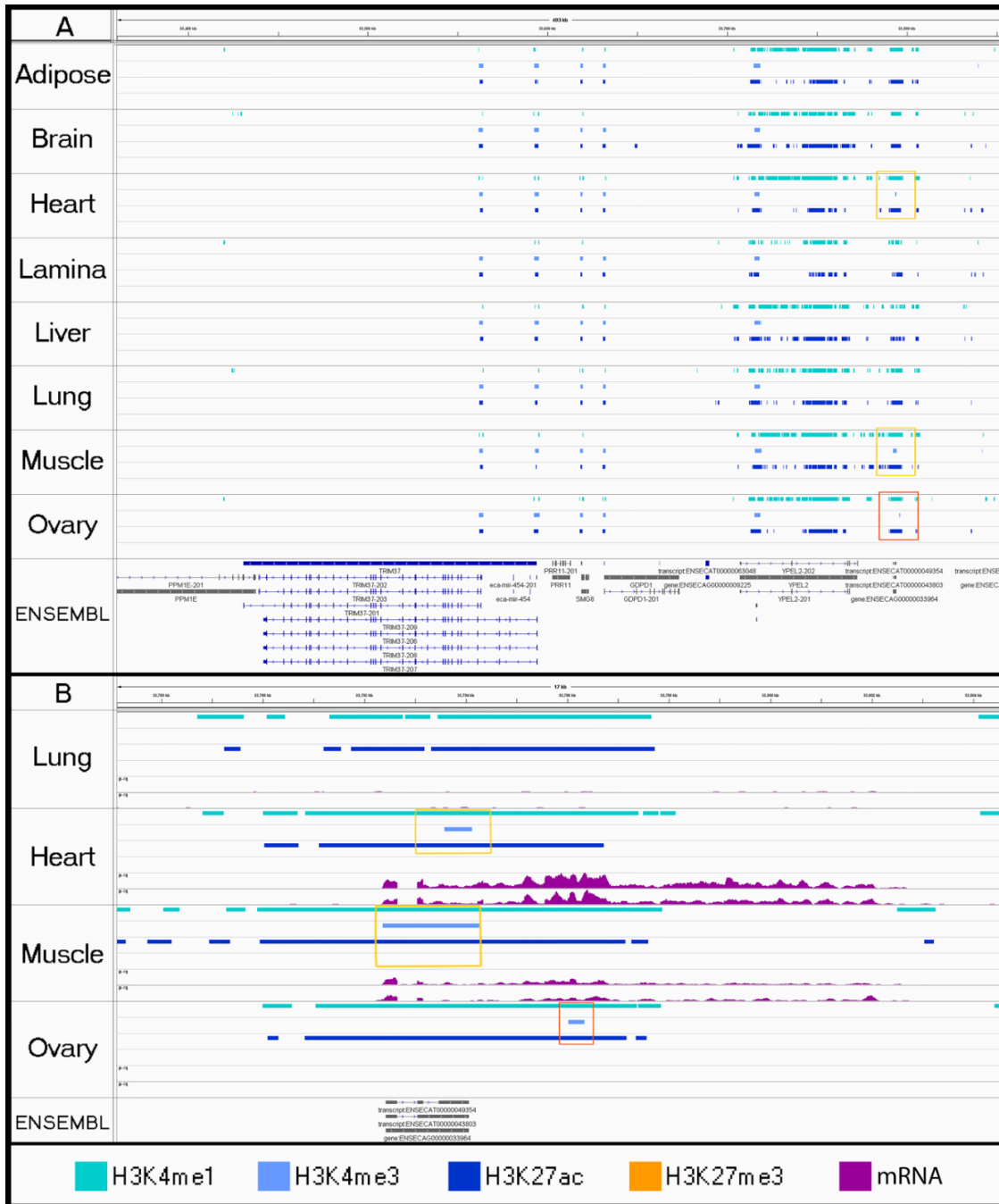


Figure 5: Visualizing tissue-specific peak-calls using the Integrated Genome Viewer. For each tissue, peaks are displayed for H3K4me1 (aqua), H3K4me3 (light blue), H3K27ac (dark blue), and H3K27me3 from SICER (orange). Gold boxes highlight active marks associated with promoters (H3K4me3) in both muscle tissues (skeletal and cardiac) for an unannotated lncRNA, *LOC111775680* (*ENSECAT00000049354*), and red box highlights an H3K4me3 peak specific to ovary tissue. B. Zoomed in view of A for relevant tissues with RNA expression shown in purple. While ovary also appears to have a peak in H3K4me3 nearby, it does not have expression of the lncRNA based on mRNA expression from these tissue samples.

Across all tissues, H3K4me1 was enriched around the TSS with a decrease in enrichment at the actual annotated start site that created a bimodal distribution across the average gene body (Figure 6A). Additionally, H3K4me1 maintained a moderate level of enrichment throughout the gene body as well as 3 Kb up- and downstream as expected for distal and proximal enhancer elements. Alternatively, H3K4me3 (Figure 6B) and H3K27ac (Figure 6C) had peaks of enrichment at the TSS, although H3K27ac also showed enrichment, to a lesser extent, just upstream of the TSS. H3K27me3 had lower enrichment than the other three marks overall, but the average enrichment was essentially constant throughout the gene body as well as 3 Kb up- and downstream (Figure 6D). While patterns of enrichment for each mark were highly consistent between tissues, the enrichment of H3K27me3 for lamina was lower at the TSS compared to the other tissues.

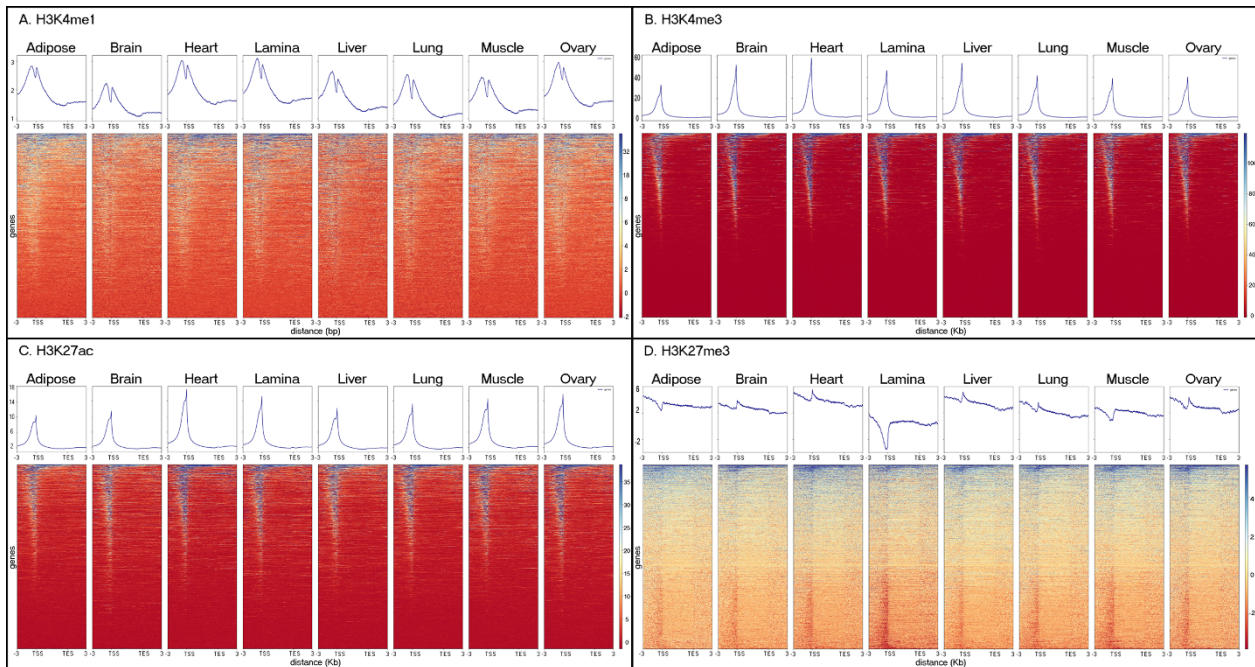


Figure 6: Histone mark enrichment across the average annotated gene body. A. H3K4me1 B. H3K4me3 C. H3K27ac D. H3K27me3 from SICER. Topology plots (top) and heat maps (bottom) show average enrichment of each histone mark in each tissue across a size-normalized gene distribution based on the Ensembl (Release 95) annotation for EquCab3.0. Each line in the heatmap represents mark enrichment across a given gene such that red indicates low relative enrichment and blue indicates high relative enrichment.

3.3. Identifying Motifs and Biological Process GO Terms

We identified between 16 and 61 transcription factor binding motifs in the unique active regions for each tissue, and the full results from the GO term analysis can be found in Tables S4-S19. While a large proportion of the identified transcription factors were still shared between tissues despite being identified in tissue-specific active regions, all of the tissues except for adipose and lung had at least one uniquely detected transcription factor binding site. A uniquely detected binding site was defined as a motif that was only identified in the tissue-specific active regions for a single tissue. The motifs were ranked based on significance of enrichment after multiple testing correction, and the top five enriched and identified motifs for each tissue are listed in Table 5. Ovary was the only tissue that had uniquely detected transcription factor motifs in this top five list, and the most significant motif was associated with FOXO3, which is a transcription factor (TF) characterized by 39 GO terms including several for tissue-specific functions such as oocyte maturation [GO:0001556] and ovulation [GO:0001542]. In fact, upon closer inspection, the FOXO3 motif was found within a tissue-specific regulatory element near a gene with recognized roles in mammalian reproduction, *NR5A1* (Figure 7) [52]. Using a network analysis for TFs implicated in each tissue, we found that six networks contained EP300 as a central node, although these networks did not link every TF for a given tissue (Figure 8A). Interestingly, MYC was the central node for brain, liver, and skeletal muscle (Figure 8B) and TP53 was the central node for lung (Figure 8C).

Table 5: Top five significantly enriched transcription factor binding motifs identified in tissue-specific active enhancers. Tissue specificity of the active enhancers was defined by overlap of H3K4me1 and H3K27ac in the same tissue and no overlap of these marks in this region in any other tissues, and tissue specificity of the binding motifs was then defined by detection of an enriched binding motif in only one tissue.

Rank	Motif ID	Consensus	Adjusted p-value	UniProt Entry
Adipose				
1	SP3	VCCACGCCCMC	1.49E-10	Q02447

2	TFDP1	VSGCGGGA AVN	1.74E-10	Q14186
3	TFAP2A	HGCCYSAGGCD	3.27E-10	P05549
4	TFAP2C	YGCCYBVRGGCA	4.56E-10	Q92754
6	KLF16	GMCACGCCCCC	5.81E-09	Q9B XK1
Brain				
1	TFAP2A(var.2)	YGCCCBVRGGCR	1.82E-16	P05549
2	TFAP2B	YGCCCBVRGGCA	1.29E-13	Q92481
3	SP3	VCCACGCCCMC	2.69E-13	Q02447
4	TFAP2C	YGCCYBVRGGCA	4.99E-13	Q92754
5	KLF16	GMCACGCCCCC	1.06E-12	Q9B XK1
Heart				
1	MZF1	BGGGGA	2.23E-05	P28698
2	Ascl2	ARCAGCTGCY	7.06E-04	Q99929
3	ASCL1	VSAGCAGCTGSNN	9.41E-4	P50553
4	SP3	VCCACGCCCMC	1.42E-03	Q02447
5	NEUROD1	NRACAGATGGYNN	1.60E-03	Q13562
Lamina				
1	SP2	GYCCCGCCYCYBSSS	8.51E-15	Q02086
2	SP1	GCCCCKCCCCC	5.98E-14	P08047
3	SP3	VCCACGCCCMC	2.84E-13	Q02447
4	KLF16	GMCACGCCCCC	3.22E-13	Q9B XK1
7	Zfx	SSSGCCBVGGCCTS	1.06E-11	P17010
Liver				
1	SP1	GCCCCKCCCCC	7.81E-13	P08047
2	TFAP2B	YGCCCBVRGGCA	4.23E-12	Q92481
3	TFAP2C	YGCCYBVRGGCA	1.87E-11	Q92754
4	TFAP2A	HGCCYSAGGCD	4.97E-11	P05549
5	ZNF740	MCCCCCCCAC	8.99E-11	Q8NDX6

Lung

1	THAP1	YTGCCDBA	5.09E-09	Q9NVV9
3	ESR2	AGGTCASVNTGMCCY	1.08E-08	Q92731
4	Zfx	SSSGCCBVGGCCTS	1.44E-08	P17010
5	ZBTB7A	NVCCGGAAGTGSV	1.46E-08	O95365
6	TFAP2A(var.2)	YGCCCBVRGGCR	6.51E-08	P05549

Muscle

1	SP1	GCCCCKCCCCC	1.45E-09	P08047
2	SP2	GYCCCGCCYCYBSSS	4.21E-09	Q02086
3	SP8	RCCACGCCCMCY	1.15E-08	Q8IXZ3
4	CTCF	CRSCAGGGGGCRSB	3.44E-08	Q8NI51
5	KLF16	GMCACGCCCCC	4.36E-07	Q9BXX1

Ovary

1	FOXO3 ¹	DAAAYA	7.23E-07	O43524
3	KLF16	GMCACGCCCCC	1.93E-04	Q9BXX1
4	FOXC1 ¹	WAWGTAAAYAW	2.39E-04	Q12948
6	CTCF	CRSCAGGGGGCRSB	4.38E-04	Q8NI51
7	Arid5a	SYAATATTGVDANH	4.99E-04	Q03989

¹TF motifs that were only detected in one tissue

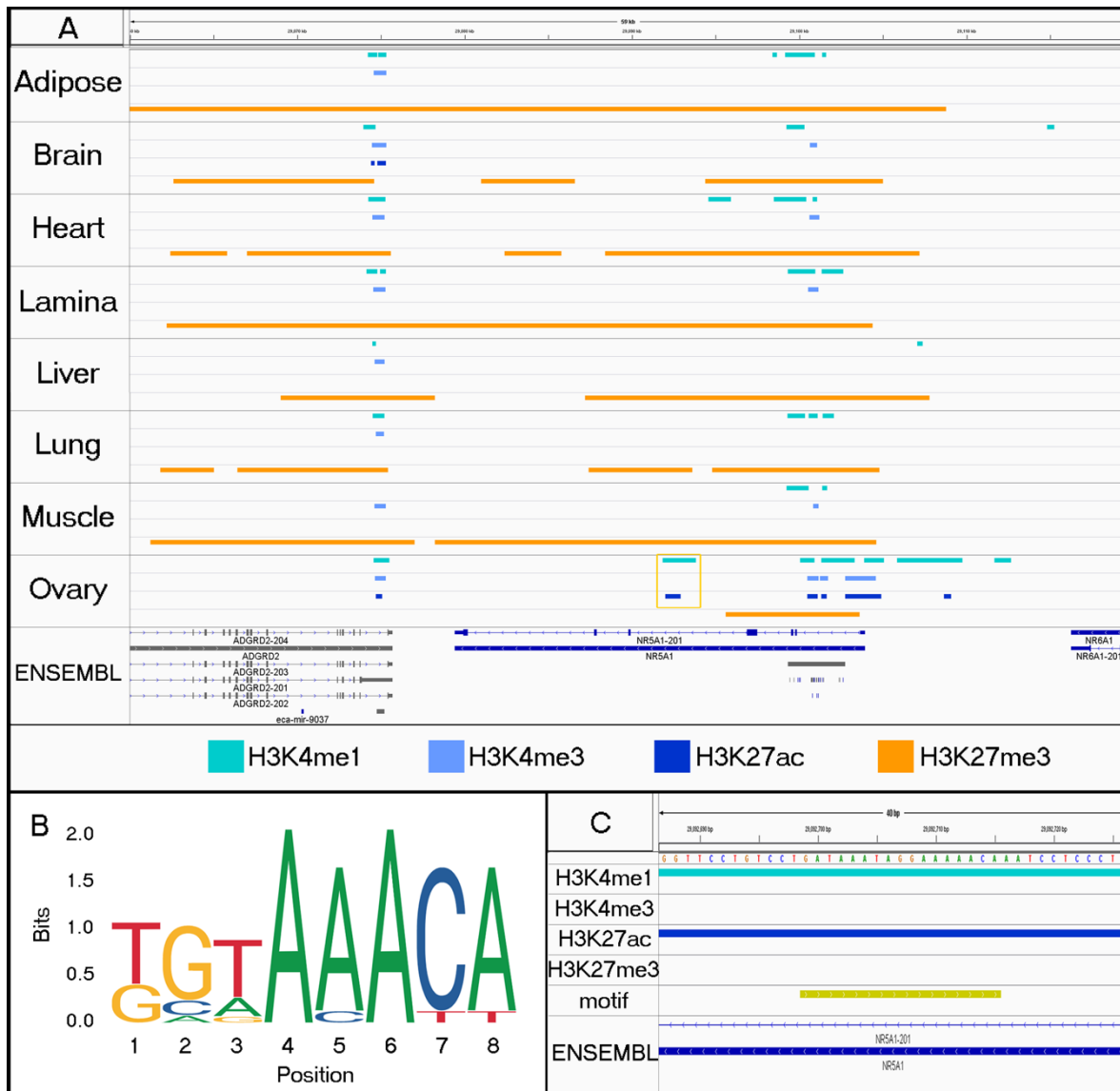


Figure 7: Localizing enriched TF binding motifs within tissue-specific peaks. For each tissue, peaks are displayed for H3K4me1 (aqua), H3K4me3 (light blue), H3K27ac (dark blue), and H3K27me3 from SICER (orange). Gold box highlights ovary specific marks in intron of *NR5A1*. B. Motif logo displays one of the major motifs for FOXO3. C. Zoomed in view of 40 bp within region highlighted in A. The gold track indicates presence of two nearly consecutive motifs for FOXO3 within the H3K4me1 and H3K27ac peaks that were detected only in ovary tissue.

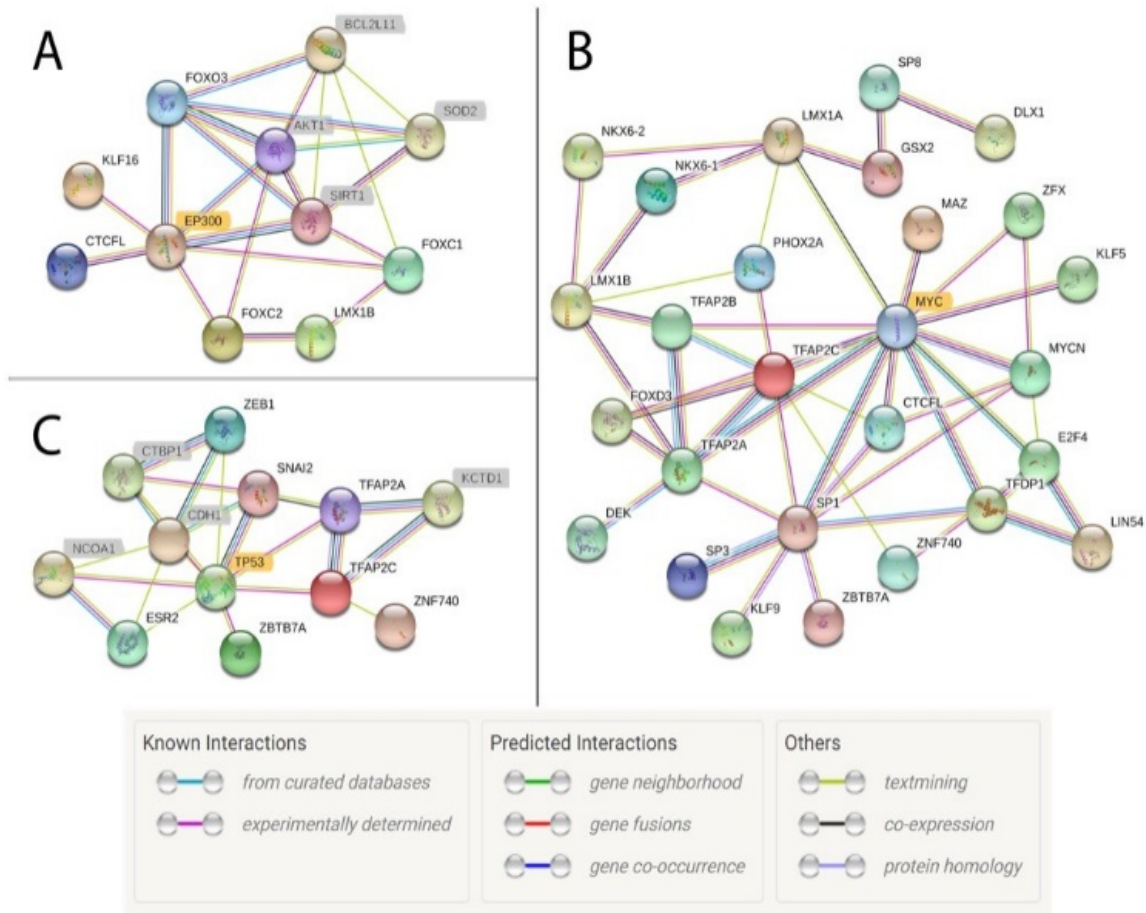


Figure 8: Network of transcription factor interactions based on active motif regions in ovary, skeletal muscle, and lung tissues. Each circle represents a protein, and lines indicate interactions between proteins. Each line color indicates a different type of evidence for the interaction. Protein names highlighted in grey were not identified in the horse ChIP-seq data but were identified as secondary factors by the network analysis based on implicated or known protein-protein interactions from research in humans and mice. A. EP300 is highlighted in gold to denote its central role in the network for ovary tissue. B. MYC is highlighted in gold to indicate its central role in the network for muscle tissue. C. TP53 is highlighted in gold to indicate its central role in the network for lung. Legend is from String Software [47].

4. Discussion

As part of the FAANG consortium, we mapped more than 1 million putative regulatory sites across the equine genome, which will contribute significantly to our understanding of genome regulation in horses as well as regulatory differences across species. To ensure that we obtained high quality data for the horse, we first performed quality control experiments to optimize tissue-specific laboratory protocols (Table S2). Sequencing, rather than targeted qPCR, was used to

assess the quality of these data due to the limited knowledge of appropriate tissue-specific control genes in the horse. Adipose tissue presented a distinct challenge based on the low number of nuclei and large amount of cellular material including lipid deposits. The True MicroChIP Kit was used to limit loss of material between steps, and the original adipose sample for each replicate was divided into smaller aliquots of 200 ml for chromatin shearing. After chromatin quality assessment with a capillary electrophoresis fragment analyzer, the best two adipose aliquots for each replicate were pooled for sequencing. From this work, we suspect that other difficult tissues (i.e. those with low nuclei density, extensive and persistent extra- or intracellular material, etc.) will also require similar alternate approaches.

To ensure accurate and relevant peak-calling, we employed MACS2 software for calling H3K4me1, H3K4me3, and H3K27ac peaks and both MACS2 and SICER for identifying peaks for the broad mark, H3K27me3. While several attempts have been made to develop a bench-marking method for ranking ChIP peak-callers, there is no established gold standard for selecting a particular application [53]. Several analyses have been performed to compare peak-callers using both real and simulated data, yet those studies cannot evaluate software performance across all types of DNA-protein interactions. Steinhauser *et al.*, for example, found that both MACS2 and SICER performed well at detecting differential peak-calls from real data for the broad histone modification H3K36me3, although SICER detected substantially more differential regions (DRs) than MACS2 [54]. Using simulated data for H3K36me3, the same group found that SICER was better able to detect true-positive DRs when the data were down-sampled to as low as ten percent while MACS2 was only effective at detecting true-positive DRs at 60 percent or higher. SICER, however, also had a higher number of false-positive DRs compared to MACS2, indicating that it may be sacrificing some specificity in order to obtain higher sensitivity while MACS2 does the

opposite. It remains unknown if these differences are the result of differing algorithms for peak-calling or for detecting differential peaks. When comparing peak-calls for H3K4me3 and H3K27me3 from previously collected data, Zang *et al.* found that SICER and MACS2 had similar abilities to detect true-positives and limit the number of false-positives [37]. In particular, SICER is known for its ability to detect regions with high specificity despite low enrichment, which makes this software particularly good at calling peaks for broad histone modifications [55]. Based upon generating peaks with higher identity between replicates (Figure S1) and higher proportions of the genome covered (Table 3), we found SICER software to be more consistent for calling broad peak-calls compared to MACS2. For that reason, we continued our investigations using the SICER-called H3K27me3 peaks. Given that peaks from both callers are supported in the literature of other species studied, both sets of peak-calls are available at <https://data.faaang.org/dataset/PRJEB35307>.

Using the Jaccard Similarity Index to compare significant peak-calls, we determined that biological replicates were highly similar for each tissue, with the exception of the brain replicates for H3K4me1 and the ovary replicates for H3K27me3 (Figure 1). While these low identity scores could be the result of underlying biological differences between the samples of brain or ovary tissue, this is unlikely given that the differences between replicates were only found in one mark for each of the tissues. In the first case, the lower number of H3K4me1 peaks called for the ECA_UCD_AH2 brain replicate likely led to decreased identity (Table 3), however, we do not suspect that this dramatically impaired our ability to call replicated peaks because our method relied on identifying overlapping enrichment rather than just the intersection of significant peaks. Additionally, the quality metrics for ECA_UCD_AH2 indicated sufficient ChIP enrichment despite having lower library complexity (Table 4). In the second case, the number of H3K27me3 peaks for both of the ovary replicates was sufficiently high; however the quality metrics for the

ECA_UCD_AH1 replicate indicate that it had lower library complexity. Nevertheless, this sample still had sufficient enrichment for a broad mark as only the RSC metric was lower than the minimum standard. In fact, all of the H3K27me3 data score below 0.8 for RSC despite having high similarity between most of the replicates, and it has been recognized previously that broad marks are especially prone to score poorly on this metric [27]. As a proof-of-principle, we assessed peak-calls surrounding genes with known expression patterns. In particular, the three active marks (H3K4me1, H3K4me3, and H3K27ac) had consistent peaks between tissues near *ACTB* (Figure 2A) and tissue-specific peaks near the liver enzyme *CYP2E1* (Figure 2B), supporting the validity of our peak-calling methods. Additionally, these peak-calls were all consistent with RNA expression from the same tissues from ECA_UCD_AH1 and ECA_UCD_AH2, further supporting the validity of the enrichment patterns detected for each histone mark.

Comparing replicated peaks between tissues, we found that liver, brain, and lamina had the highest percentage of peaks that were unique to only that tissue (Figure 3). Liver is known to have hundreds of distinct biological functions [48]. Since many of the functions are entirely unique to liver, a high proportion of unique active regulatory elements is consistent with the specialization of this tissue. Additionally, the mammalian brain is thought to have hundreds of different neuronal cell types within the cortex to coordinate numerous neurologic functions simultaneously, making it one of the most complex tissues of the body [56]. Therefore, these results are consistent with the expectation that there is a high degree of regulatory specificity to control numerous coordinated functions within complex tissues.

Interestingly, lamina was the other tissue with a high percentage of unique peaks for H3K4me1, H3K4me3, and H3K27ac (Figure 3). Due to the role of lamina in disease, this finding may be particularly impactful for research into the physiological changes associated with laminitis,

a syndrome that was established as a priority for equine research by the American Association of Equine Practitioners [57,58]. Additionally, when comparing the distribution of marks across the average gene body, we found that lamina tissue had an unusually low level of the repressive mark, H3K27me3, at the TSS (Figure 6). While all of the tissues had a portion of genes that appear to have a dip in enrichment directly at the TSS, lamina had the most extreme decrease. Perhaps the dip in enrichment for lamina is an indication of increased levels of expression across more of the genome and, when combined with the high percentage of unique peaks, could suggest that hoof lamina may perform additional biological processes that are currently uncharacterized. In order to understand all of the molecular functions of lamina tissue and its role in laminitis, more work is needed to further annotate and functionally characterize the extent of the cellular processes within healthy and diseased tissue. Without further validation, however, we cannot exclude that this decrease in enrichment may be a technical artifact such as decreased detection of H3K27me3 in lamina tissue due to low cell numbers and excess extracellular matrix.

To further characterize tissue-specific regulatory regions, we identified numerous transcription factor binding motifs within the unique active elements for each tissue (Table 5). Despite investigating elements that were only enriched in one tissue, we still identified many transcription factor motifs that were shared between tissues (Tables 4 and S19), and based on a GO term analysis, many of these factors had numerous associated biological processes (Tables S4-S18). Our network analysis identified EP300 as a central secondary factor needed to connect many implicated TFs (Figure 8A). This gene encodes a histone acetyltransferase that is known to interact with many TFs by protein-protein interactions rather than DNA binding [59,60]. Given that the TF motifs were all identified within active elements based on the presence of H3K27ac, finding a connection with EP300 supports our ability to detect relevant peaks for this histone modification.

Interestingly, there were three tissues (brain, liver, and muscle) that had MYC rather than EP300 as the central node for their TF networks (Figure 8B). We found that binding motifs for MYC were enriched in all three tissues, which is consistent with its role as a TF for many common cellular processes including growth and regulation of the cell cycle [61]. Similarly, TP53 was the central node in the protein interaction network for lung tissue (Figure 8C), which is consistent with its role as a key regulator of the cell cycle when functional and as a major tumorigenesis factor in lung cancer when dysfunctional [62].

By developing tissue-specific maps of the H3K4me1, H3K4me3, H3K27ac, and H3K27me3 histone modifications, we aimed to build upon our current knowledge about genomic regulation in the horse and provide new resources for further advancing research on health, performance, and reproduction traits. In particular, incorporating histone ChIP-seq data with current annotations is expected to lead to the discovery of more tissue-specific functional variants that are outside of protein-coding regions. For example, a genome-wide investigation of liver fibrosis in the Swiss Franches-Montagnes breed led to the identification of an associated region containing a promising candidate gene, *PKHDI*, which was also associated with kidney and liver disease in humans [49]. Sequencing the coding region of this gene identified two synonymous coding variants strongly associated with disease; however, their causal role remains unclear. Comparing peaks from multiple tissues in that region, there are also several liver-specific regulatory peaks within intron 59 of *PKHDI* (Ensembl Transcript ID: ENSECAT00000024985.1) that may affect expression of this or another hepatic gene nearby (Figure 4) and represent another avenue to explore for the molecular mechanism underlying liver fibrosis.

Tissue-specific histone modifications have also been implicated in the complex traits of performance [63] and, throughout modern horse domestication performance abilities, such as

speed, have been a major factor for selective breeding [64]. For example, recent research comparing three trotting breeds in Scandinavia (North Swedish Draught, Norwegian-Swedish Coldblooded trotter, and Standardbred trotter), found a 684 Kb genomic region associated with trotting racing ability containing numerous annotated and unannotated genes [50]. Using a protein-coding annotation, only one gene in the region, *TRIM37*, was identified as a potential candidate due to its associations with growth phenotypes in humans. Utilizing the locations of the histone mark enrichment identified in this study could help to identify other candidates such as tissue-specific regulatory regions or the genes that they regulate. In particular, there are H3K4me3 peaks at the start of a novel lncRNA predicted by Ensembl genebuild [51] within the region of interest for racing ability (Figure 5A). While uncharacterized, *LOC111775680* has a set of unique promoters found in skeletal and cardiac muscle with corresponding transcript data (as determined by RNAseq of the same tissues from ECA_UCD_AH1 and ECA_UCD_AH2) suggesting that the lncRNA may play a role in muscle physiology (Figure 5B). Additional work is needed to further characterize *LOC111775680* and investigate its potential role in muscle tissue and any corresponding effects on racing ability.

In addition to health and performance, these annotation data can also be used to identify important genomic regulatory regions for the reproductive system. Previously, homology with humans and mice was utilized to create a panel of candidate regions for determining the genetic cause of gonadal dysgenesis disorders across many breeds of horses [65], yet the panel was focused on coding variants and those within untranslated regions that may affect RNA and protein synthesis. By evaluating histone marks, we found that there are additional regulatory regions relevant to the reproductive system that were missed by the homology-based approaches. For example, *NR5A1*, a gene that is implicated in many dysgenesis cases [52,66], has a regulatory

region as identified by H3K4me1 and H3K27ac histone modifications in equine ovary tissue that is characteristic of an active enhancer (Figure 7A). Upon further inspection, we identified two FOXO3 binding sites within the region enriched with peak-calls (Figure 7B and 7C). FOXO3 is a transcription factor with known roles in oocyte maturation [GO:0001556] and ovulation [GO:0001542] that was identified as an ovary-specific TF based on our motif analysis (Tables S18).

Along with the regulatory regions identified in this study, the equine FAANG consortium is also characterizing the full RNA profile of more than fifty tissues and cell types from the FAANG equine biobank supported by a research community initiative [26] and the DNA methylation profiles for the TOI. Moreover, the equine FAANG consortium is currently mapping a major insulator protein known as CTCF with the goal of generating tissue-specific chromatin state predictions for the eight TOI. CTCF plays a key role in defining chromatin looping and, therefore, topologically associated domains and gene-enhancer interactions when combined with Histone ChIP-Seq [67,68]. The same panel of genomic investigations are also being conducted in two stallions so that males and females are represented in the annotations. We anticipate that the integration and utilization of these functional annotation datasets by the equine genomics community will lead to the identification of causal, non-coding variants underlying many traits of interest for equine medicine, performance, and reproduction.

Supplemental Material: The following are available online at www.mdpi.com/xxx/s1, Figure S1: Jaccard Index to measure similarity of peaks called for H3K27me3 peaks based on either MACS2 or SICER peak-calling; Table S1: Concentrations and catalog numbers for antibodies used during ChIP; Table S2: Quality metrics, peak-calling summary, and comparison to ENCODE data from QC testing; Table S3: Comparing peak numbers to ENCODE data.

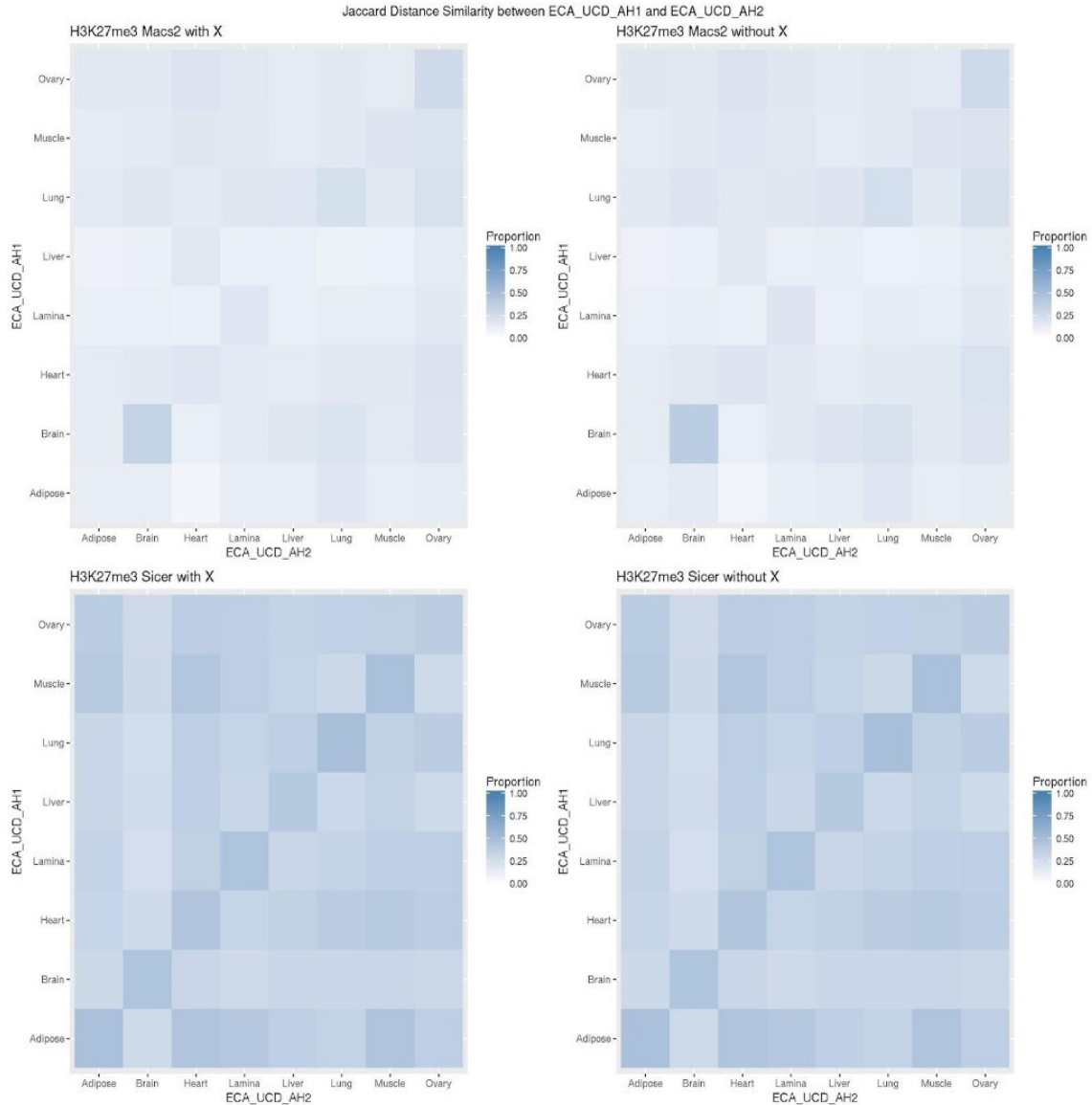


Figure S1: Jaccard Index to measure similarity of peaks called for H3K27me3 based on either MACS2 or SICER peak-calling algorithms. Each panel is a heatmap displaying the Jaccard Index, from pairwise comparisons of tissues between ECA_UCD_AH1 and ECA_UCD_AH2. Darker blue indicates that there are more peaks that are shared by the two samples. The top row compares peaks called by MACS2 including the X chromosome (Panel 1) and without the repressed X chromosome (Panel 2). The bottom row compares peaks called by SICER including the X chromosome (Panel 3) and without the X chromosome (Panel 4).

Table S1: Concentration and catalog numbers for antibodies used during ChIP.

	Catalog Number	Adipose	Brain	Heart	Lamina	Liver	Lung	Muscle	Ovary
H3K4me1	C15410194	0.5	0.5	0.5	0.5	0.5	0.5	0.5	1
H3K4me3	C15410003	0.5	0.5	0.5	0.5	0.5	0.5	0.5	1

H3K27ac	C15410196	1	0.5	0.5	1	1	1	1	2
H3K27me3	C15410195	1	1	1	1	1	0.5	0.5	2
IgG	C15410206	0.5	0.5	0.5	0.5	0.5	0.5	0.5	1

Table S2.1: Quality metrics and bioinformatic summary of QC testing. The table lists the alignment summary of the QC data by mark. Alignment %, Filter %, and Dedup. % are the percent of reads from the previous processing step that were retained after alignment, filtering, and deduplication, respectively. Usable % is the percent of the raw reads that are usable for peak calling after processing.

Mark	Tissue	Antibody Concentr.	Raw Reads	Alignment %	Filter %	Dedup. %	Usable Reads	Usable %
H3K4me1	Adipose	0.25 ug	41533955	95.26	87.18	11.11	3829327	9.22
H3K4me1	Adipose	0.5 ug	25579328	95.77	89.00	22.38	4877999	19.07
H3K4me1	Brain	0.5 ug	28645138	96.92	88.89	80.01	19745330	68.93
H3K4me1	Brain	1.0 ug	31068455	96.56	88.96	76.62	20442934	65.80
H3K4me1	Heart	0.5 ug	34333726	96.72	92.72	55.99	17216104	50.14
H3K4me1	Heart	1.0 ug	34054263	96.84	92.86	57.31	17484791	51.34
H3K4me1	Lamina	0.5 ug	32877765	96.64	92.19	67.22	19685839	59.88
H3K4me1	Lamina	1.0 ug	37535048	96.59	92.11	74.20	24775236	66.01
H3K4me1	Liver	0.5 ug	34715017	97.88	90.95	81.80	25199799	72.59
H3K4me1	Liver	1.0 ug	33803219	97.89	90.64	73.78	22066658	65.28
H3K4me1	Lung	0.5 ug	31482650	97.17	88.39	78.19	21141408	67.15
H3K4me1	Lung	1.0 ug	34712022	97.01	88.57	69.80	20817914	59.97
H3K4me1	Muscle	0.5 ug	34866274	97.27	88.66	68.70	20650097	59.23
H3K4me1	Muscle	1.0 ug	28118912	97.26	88.83	70.33	17073795	60.72
H3K4me1	Ovary	1.0 ug	29851645	96.14	90.43	72.65	18854236	63.16
H3K4me1	Ovary	2.0 ug	26836588	96.27	90.09	73.90	17200901	64.09
H3K4me3	Adipose	0.25 ug	33019758	75.60	87.05	9.13	1984449	6.01
H3K4me3	Adipose	0.5 ug	28971178	76.22	87.48	12.24	2362691	8.16
H3K4me3	Brain	0.5 ug	32468247	83.19	87.25	70.56	16625919	51.21
H3K4me3	Brain	1.0 ug	34461807	83.34	87.26	71.46	17906655	51.96
H3K4me3	Heart	0.5 ug	33745101	77.83	92.17	58.07	14051998	41.64
H3K4me3	Heart	1.0 ug	31817029	78.93	91.65	58.18	13366182	42.01
H3K4me3	Lamina	0.5 ug	44077414	73.20	92.22	60.37	17959269	40.74
H3K4me3	Lamina	1.0 ug	40706683	73.88	91.82	63.56	17551985	43.12
H3K4me3	Liver	0.5 ug	31358288	90.17	89.37	71.20	17935573	57.20
H3K4me3	Liver	1.0 ug	34165010	91.98	87.77	72.13	19828768	58.04
H3K4me3	Lung	0.5 ug	36405123	81.63	88.21	71.96	18862690	51.81
H3K4me3	Lung	1.0 ug	34232569	81.99	88.44	65.13	16164051	47.22
H3K4me3	Muscle	0.5 ug	33479645	83.22	88.23	70.54	17333776	51.77
H3K4me3	Muscle	1.0 ug	28681805	83.79	87.77	53.94	11375345	39.66
H3K4me3	Ovary	1.0 ug	28705014	81.80	90.17	71.87	15215894	53.01
H3K4me3	Ovary	2.0 ug	26313116	79.90	90.91	70.47	13468533	51.19
H3K27ac	Adipose	0.25 ug	52539130	89.72	86.12	9.88	4010698	7.63
H3K27ac	Adipose	0.5 ug	42559254	91.16	88.05	15.23	5186417	12.19

H3K27ac	Brain	0.5 ug	34826845	97.10	73.30	72.57	17984772	51.64
H3K27ac	Brain	1.0 ug	34999603	96.96	72.15	54.12	13248416	37.85
H3K27ac	Heart	0.5 ug	39428944	87.10	94.66	51.49	16733089	42.44
H3K27ac	Heart	1.0 ug	36346242	87.41	94.64	47.53	14245431	39.19
H3K27ac	Lamina	0.5 ug	39630507	87.35	93.73	36.05	11695232	29.51
H3K27ac	Lamina	1.0 ug	37648978	89.23	93.81	68.07	21450213	56.97
H3K27ac	Liver	0.5 ug	26592944	95.72	90.28	70.47	16144814	60.71
H3K27ac	Liver	1.0 ug	34984296	95.51	91.41	75.42	22961435	65.63
H3K27ac	Lung	0.5 ug	33364892	88.63	92.19	58.70	16000329	47.96
H3K27ac	Lung	1.0 ug	65134357	89.51	91.74	54.19	28981017	44.49
H3K27ac	Muscle	0.5 ug	35671199	90.49	91.38	55.03	16212939	45.45
H3K27ac	Muscle	1.0 ug	41676921	89.83	92.92	63.80	22137306	53.12
H3K27ac	Ovary	1.0 ug	29641830	87.31	92.87	72.22	17358136	58.56
H3K27ac	Ovary	2.0 ug	28236515	88.15	92.45	74.46	17133727	60.68
H3K27me3	Adipose	0.25 ug	56875857	96.66	72.06	20.57	8147762	14.33
H3K27me3	Adipose	0.5 ug	52135622	97.22	72.89	55.67	20563401	39.44
H3K27me3	Brain	0.5 ug	28249874	97.24	73.66	76.36	15434252	54.63
H3K27me3	Brain	1.0 ug	33695472	97.32	73.07	75.82	18165407	53.91
H3K27me3	Heart	0.5 ug	31194828	97.25	78.01	47.46	11212668	35.94
H3K27me3	Heart	1.0 ug	33887908	97.35	78.53	52.91	13694961	40.41
H3K27me3	Lamina	0.5 ug	24325102	97.38	78.00	65.47	12092984	49.71
H3K27me3	Lamina	1.0 ug	27501665	97.37	77.78	65.01	13536980	49.22
H3K27me3	Liver	0.5 ug	47919881	96.35	79.56	62.14	22824430	47.63
H3K27me3	Liver	1.0 ug	55268603	97.15	79.28	64.76	27563233	49.87
H3K27me3	Liver	2.0 ug	37929627	97.28	78.68	62.66	18189681	47.96
H3K27me3	Lung	0.5 ug	34954280	97.51	81.33	71.76	19891811	56.91
H3K27me3	Lung	1.0 ug	34848942	97.52	81.37	74.03	20468725	58.74
H3K27me3	Muscle	0.5 ug	29469706	97.64	76.01	69.67	15194935	51.56
H3K27me3	Muscle	1.0 ug	32665616	97.66	76.09	62.20	15079631	46.16
H3K27me3	Ovary	1.0 ug	19706011	96.57	81.11	76.00	11731440	59.53
H3K27me3	Ovary	2.0 ug	35925294	96.51	81.31	68.82	19402590	54.01

Table S2.2: Quality metrics and bioinformatic summary of QC testing. The table lists six quality metrics by tissue: NRF is nonredundant (mapped) fraction; PBC1 is PCR bottleneck coefficient 1; PBC2 is PCR bottleneck coefficient 2; NSC is normalized strand cross-correlation coefficient; RSC is relative strand cross-correlation coefficient; and JSD is Jensen Shannon distance. NRF, PBC1, and PBC2 are all considered measures of library complexity, and NSC, RSC, and JSD are measures of ChIP enrichment.

Mark	Tissue	Antibody Concn.	Raw Reads	NRF (<=0.5)	PBC1 (<=0.5)	PBC2 (<=1)	NSC (<=1.1)	RSC (<=1)	JSD (<=0.1)	Peaks
H3K4me1	Adipose	0.25 ug	41533955	0.12	0.28	2.88	1.08	0.70	0.16	36943

H3K4me1	Adipose	0.5 ug	25579328	0.23	0.30	2.04	1.08	1.32	0.18	59577
H3K4me3	Adipose	0.25 ug	33019758	0.10	0.30	3.66	1.49	1.81	0.38	23240
H3K4me3	Adipose	0.5 ug	28971178	0.13	0.30	3.00	1.47	1.77	0.39	24611
H3K27ac	Adipose	0.25 ug	52539130	0.11	0.27	3.13	1.37	1.64	0.22	22293
H3K27ac	Adipose	0.5 ug	42559254	0.16	0.25	2.23	1.30	1.79	0.25	34407
H3K27me3	Adipose	0.25 ug	56875857	0.22	0.27	1.98	1.10	0.48	0.11	4692
H3K27me3	Adipose	0.5 ug	52135622	0.56	0.57	2.37	1.07	0.54	0.09	46491
H3K4me1	Brain	0.5 ug	28645138	0.81	0.81	5.23	1.06	1.31	0.21	112116
H3K4me1	Brain	1.0 ug	31068455	0.78	0.77	4.34	1.06	1.18	0.23	121851
H3K4me3	Brain	0.5 ug	32468247	0.72	0.73	3.80	1.26	1.32	0.37	39792
H3K4me3	Brain	1.0 ug	34461807	0.73	0.74	3.92	1.26	1.27	0.37	42057
H3K27ac	Brain	0.5 ug	34826845	0.74	0.74	3.75	1.07	0.40	0.09	5786
H3K27ac	Brain	1.0 ug	34999603	0.56	0.55	2.25	1.07	0.36	0.10	1511
H3K27me3	Brain	0.5 ug	28249874	0.77	0.77	4.42	1.08	0.43	0.09	7968
H3K27me3	Brain	1.0 ug	33695472	0.77	0.77	4.20	1.07	0.39	0.08	12267
H3K4me1	Heart	0.5 ug	34333726	0.57	0.56	2.30	1.05	1.81	0.30	118134
H3K4me1	Heart	1.0 ug	34054263	0.58	0.58	2.40	1.06	1.56	0.30	119918
H3K4me3	Heart	0.5 ug	33745101	0.59	0.60	2.56	1.36	1.59	0.48	44582
H3K4me3	Heart	1.0 ug	31817029	0.59	0.60	2.56	1.37	1.57	0.47	45830
H3K27ac	Heart	0.5 ug	39428944	0.52	0.52	2.11	1.32	2.34	0.41	97984
H3K27ac	Heart	1.0 ug	36346242	0.48	0.48	2.01	1.29	2.32	0.40	93594
H3K27me3	Heart	0.5 ug	31194828	0.48	0.46	1.80	1.10	0.61	0.11	39844
H3K27me3	Heart	1.0 ug	33887908	0.54	0.52	2.06	1.08	0.62	0.11	60793
H3K4me1	Lamina	0.5 ug	32877765	0.68	0.68	3.08	1.10	1.56	0.29	101838
H3K4me1	Lamina	1.0 ug	37535048	0.75	0.75	3.93	1.09	1.60	0.30	103366
H3K4me3	Lamina	0.5 ug	44077414	0.61	0.65	3.11	1.37	1.21	0.47	37739
H3K4me3	Lamina	1.0 ug	40706683	0.64	0.67	3.32	1.36	1.19	0.47	40597
H3K27ac	Lamina	0.5 ug	39630507	0.37	0.37	1.74	1.33	1.54	0.37	88110
H3K27ac	Lamina	1.0 ug	37648978	0.69	0.69	3.19	1.30	1.42	0.38	102573
H3K27me3	Lamina	0.5 ug	24325102	0.66	0.65	2.83	1.11	0.70	0.10	48723
H3K27me3	Lamina	1.0 ug	27501665	0.66	0.65	2.81	1.11	0.71	0.10	58568
H3K4me1	Liver	0.5 ug	34715017	0.82	0.82	5.44	1.08	1.57	0.32	119712
H3K4me1	Liver	1.0 ug	33803219	0.75	0.74	3.70	1.08	1.35	0.30	114010
H3K4me3	Liver	0.5 ug	31358288	0.72	0.72	3.41	1.17	1.61	0.38	52323
H3K4me3	Liver	1.0 ug	34165010	0.73	0.72	3.51	1.20	1.38	0.31	51597
H3K27ac	Liver	0.5 ug	26592944	0.71	0.70	3.25	1.16	1.46	0.28	79953
H3K27ac	Liver	1.0 ug	34984296	0.76	0.76	3.97	1.14	1.58	0.31	107647
H3K27me3	Liver	0.5 ug	47919881	0.63	0.63	2.72	1.08	0.70	0.08	759
H3K27me3	Liver	1.0 ug	55268603	0.65	0.65	2.92	1.08	0.68	0.07	633
H3K27me3	Liver	2.0 ug	37929627	0.63	0.63	2.76	1.09	0.64	0.09	5304
H3K4me1	Lung	0.5 ug	31482650	0.78	0.79	4.82	1.06	0.89	0.20	96576
H3K4me1	Lung	1.0 ug	34712022	0.70	0.70	3.40	1.07	1.01	0.22	101997
H3K4me3	Lung	0.5 ug	36405123	0.72	0.74	4.09	1.28	1.22	0.36	37468
H3K4me3	Lung	1.0 ug	34232569	0.66	0.67	3.14	1.30	1.17	0.38	38573
H3K27ac	Lung	0.5 ug	33364892	0.59	0.59	2.47	1.26	1.31	0.38	81078
H3K27ac	Lung	1.0 ug	65134357	0.55	0.54	2.11	1.20	1.21	0.35	100742
H3K27me3	Lung	0.5 ug	34954280	0.72	0.72	3.68	1.07	0.54	0.08	6867
H3K27me3	Lung	1.0 ug	34848942	0.74	0.75	4.01	1.05	0.44	0.07	6027

H3K4me1	Muscle	0.5 ug	34866274	0.69	0.69	3.19	1.06	0.88	0.17	77733
H3K4me1	Muscle	1.0 ug	28118912	0.71	0.70	3.32	1.06	0.87	0.19	78835
H3K4me3	Muscle	0.5 ug	33479645	0.71	0.72	3.63	1.38	1.28	0.38	45068
H3K4me3	Muscle	1.0 ug	28681805	0.55	0.55	2.22	1.38	1.30	0.40	41275
H3K27ac	Muscle	0.5 ug	35671199	0.56	0.55	2.22	1.33	1.51	0.35	79288
H3K27ac	Muscle	1.0 ug	41676921	0.65	0.64	2.79	1.31	1.47	0.39	98313
H3K27me3	Muscle	0.5 ug	29469706	0.70	0.70	3.26	1.08	0.51	0.09	17860
H3K27me3	Muscle	1.0 ug	32665616	0.63	0.62	2.58	1.08	0.49	0.09	15362
H3K4me1	Ovary	1.0 ug	29851645	0.73	0.73	3.75	1.07	1.21	0.23	89753
H3K4me1	Ovary	2.0 ug	26836588	0.74	0.75	3.95	1.07	1.13	0.24	87649
H3K4me3	Ovary	1.0 ug	28705014	0.73	0.74	3.93	1.30	1.28	0.38	31833
H3K4me3	Ovary	2.0 ug	26313116	0.71	0.72	3.74	1.33	1.19	0.43	35921
H3K27ac	Ovary	1.0 ug	29641830	0.73	0.73	3.79	1.25	1.34	0.42	70212
H3K27ac	Ovary	2.0 ug	28236515	0.75	0.75	4.10	1.25	1.33	0.40	72690
H3K27me3	Ovary	1.0 ug	19706011	0.76	0.77	4.30	1.10	0.53	0.07	22716
H3K27me3	Ovary	2.0 ug	35925294	0.69	0.69	3.29	1.07	0.52	0.05	39146

Table S3: Comparing peak numbers to ENCODE data. All peaks were called with MACS2 software. For combined peak calls for H3K27me3 by SICER, see Table 3. For ENCODE data, all samples were from adult females of middle age, except for brain (temporal lobe) which was from an elderly female individual. The same adult female biosample was used where possible, and ENCODE data are peaks called from one biological sample.

Mark	Tissue	Combined Peak Number	ENCODE Peak Number	ENCODE Accession
H3K4me1	Adipose	107318	260137	ENCFF503NNI
H3K4me1	Brain	95918	208634	ENCFF304IPZ
H3K4me1	Heart	121663	252397	ENCFF720SXQ
H3K4me1	Liver	11676	19538	ENCFF629FSX
H3K4me1	Lung	92972	371852	ENCFF271SCL
H3K4me1	Muscle	95816	199056	ENCFF286NIM
H3K4me1	Ovary	102986	290940	ENCFF423QUC
H3K4me3	Adipose	26905	103909	ENCFF711TJV

H3K4me3	Brain	27101	70004	ENCFF733MXP
H3K4me3	Heart	26475	3804	ENCFF765QKM
H3K4me3	Liver	28498	46726	ENCFF228VKE
H3K4me3	Lung	28546	53032	ENCFF890ESC
H3K4me3	Muscle	2811	44787	ENCFF178MGY
H3K4me3	Ovary	28378	39238	ENCFF652QTC
H3K27ac	Adipose	7962	119346	ENCFF140PPW
H3K27ac	Brain	78823	115692	ENCFF073BUA
H3K27ac	Heart	68728	107709	ENCFF283CXG
H3K27ac	Liver	87589	160542	ENCFF710URH
H3K27ac	Lung	69054	154303	ENCFF159KOZ
H3K27ac	Muscle	76495	107011	ENCFF094AJQ
H3K27ac	Ovary	64318	188716	ENCFF478NMO
H3K27me3	Adipose	25183	172266	ENCFF699CLI
H3K27me3	Brain	24243	152554	ENCFF067HQZ
H3K27me3	Heart	68113	91450	ENCFF647YSZ
H3K27me3	Liver	63874	188665	ENCFF134JJJ
H3K27me3	Lung	30191	45680	ENCFF784XKT
H3K27me3	Muscle	42610	72065	ENCFF654RZS
H3K27me3	Ovary	40825	143999	ENCFF165LTG

Author Contributions: conceptualization, C.J.F., R.R.B., J.L.P., T.S.K., and J.N.M.; methodology, C.C., C.K., R.R.B., C.J.F. J.L.P.; software, N.B.K. and C.K.; formal analysis, N.B.K.; investigation, N.B.K. and C.C.; resources, C.J.F., R.R.B., J.L.P., E.N.H., and H.Z.; data curation, N.B.K.; writing—original draft preparation, N.B.K., R.R.B.; writing—review and editing, C.J.F., J.L.P., J.N.M, T.S.K., C.K., C.C., E.N.H., and H.Z.; visualization, N.B.K.; supervision, R.R.B.; project administration, C.J.F., R.R.B., and J.L.P.; funding acquisition, C.J.F., R.R.B., J.L.P., T.S.K., and J.N.M.

Funding: Funding for investigator salaries, experimental materials, and other resources was provided by the Grayson Jockey Club Foundation, USDA NRSP-8 equine species coordinator funds, and the Center for Equine Health with funds provided by the State of California pari-mutuel fund and contributions by private donors. Support for N.B.K. was also provided by Morris Animal Foundation (D16-EQ-028) and a fellowship from the Center for Equine Health at the University of California - Davis. Support for C.J.F. was provided by the National Institutes of Health (NIH) to C.J.F. (K01OD015134 and L40 TR001136).

Acknowledgments: The authors would like to acknowledge members of the UC Davis FAANG group for providing their technical expertise and feedback. The authors would also like to acknowledge the contributions from horse owners that made this work possible.

Conflicts of Interest: Catherine Creppe is affiliated with Diagenode which is a leading provider of complete solutions for epigenetics research including end to end services.

References:

1. Rudolph, J.A.; Spier, S.J.; Byrans, G.; Hoffman, E.P. Linkage of hyperkalaemic periodic paralysis in Quarter horses to the horse adult skeletal muscle sodium channel gene. *Anim. Genet.* **1992**, *23*, 241-250.
2. Finno, C.J.; Bannasch, D.L. Applied equine genetics. *Equine Vet. J.* **2014**, *46*, 538-544.
3. Raudsepp, T.; Finno, C.J.; Bellone, R.R.; Petersen, J.J. Ten years of the horse reference genome: insights into equine biology, domestication, and population dynamics in the post-genome era. *Anim. Genet.* **2019**, *50*, 569-597.
4. OMIA – Online Mendelian Inheritance in Animals. Available online: <https://omia.org/home/> (accessed on 4 January 2019).
5. Wade, C.M.; Giulotto, E.; Sigurdsson, S.; Zoli, M.; Gnerre, S.; Imstrand, F.; Lear, T.L.; Adelson, D.L.; Bailey, E.; Bellone, R.R.; *et al.* Genome Sequence, Comparative Analysis, and Population Genetics of the Domestic Horse. *Science* **2009**, *326*, 865-867.
6. Mathelier, A.; Shi, W.; Wasserman, W.W. Identification of altered cis-regulatory elements in human disease. *Trends Genet.* **2015**, *31*, 67-76.
7. Koufariotis, L.; Chen, Y.P.; Bolormaa, S.; Hayes, B.J. Regulatory and coding genome regions are enriched for trait associated variants in dairy and beef cattle. *BMC Genomics* **2014**, *15*, 436.
8. Wang, M.; Hancock, T.P.; MacLeod, I.M.; Pryce, J.E.; Cocks, B.G.; Hayes, B.J. Putative enhancer sites in the bovine genome are enriched with variants affecting complex traits. *Genet. Sel. Evol.* **2017**, *49*, 56.
9. Danko, C.G.; Choate, L.A.; Marks, B.A.; Rice, E.J.; Wang, Z.; Chu, T.; Martins, A.L.; Dukler, N.; Coonrod, S.A.; Tait Wojno, E.D.; *et al.* Dynamic evolution of regulatory element ensembles in primate CD4+ T cells. *Nat. Ecol. Evol.* **2018**, *2*, 537-548.

10. Pennacchio, L.A.; Bickmore, W.; Dean, A.; Nobrega, M.A.; Bejerano, G. Enhancers: five essential questions. *Nat. Rev. Genet.* **2013**, *14*, 288-295.
11. Pasquali, L.; Gaulton, K.J.; Rodriguez-Segui, S.A.; Mularoni, L.; Miguel-Escalada, I.; Akerman, I.; Tena, J.J.; Moran, I.; Gomez-Marin, C.; van de Bunt, M.; *et al.* Pancreatic islet enhancer clusters enriched in type 2 diabetes risk-associated variants. *Nat. Genet.* **2014**, *46*, 136-143.
12. Sun, W.; Poschmann, J.; Cruz-Herrera Del Rosario, R.; Parikshak, N.N.; Hajan, H.S.; Kumar, V.; Ramasamy, R.; Belgard, T.G.; Elanggovan, B.; Wong, C.C.; *et al.* Histone Acetylome-wide Association Study of Autism Spectrum Disorder. *Cell* **2016**, *167*, 1385-1397.e11.
13. The FAANG Consortium, Andersson, L.; Archibald, A.L.; Bottema, C.D.; Brauning, R.; Burgess, S.C.; Burt, D.W.; Casas, E.; Cheng, H.H.; Clarke, L.; *et al.* Coordinated international action to accelerate genome-to-phenome with FAANG, the Functional Annotation of Animal Genomes project. *Genome Biol.* **2015**, *16*, 57.
14. Tuggle, C.K.; Guiffra, E.; White, S.N.; Clarke, L.; Zhou, H.; Ross, P.J.; Acloque, H.; Reecy, J.M.; Archibald, A.; Bellone, R.R.; *et al.* GO-FAANG meeting: a Gathering On Functional Annotation of Animal Genomes. *Anim. Genet.* **2016**, *47*, 528-533.
15. Guiffra, E.; Tuggle, C.K.; FAANG Consortium. Functional Annotation of Animal Genomes (FAANG): Current Achievements and Roadmap. *Annu. Rev. Anim. Biosci.* **2019**, *7*, 65-88.
16. Bannister, A.J.; Kouzarides, T. Regulation of chromatin by histone modifications. *Cell Res.* **2011**, *21*, 381-395.
17. Allfrey, V.G.; Faulkner, R.; Mirsky, A.E. Acetylation and methylation of histones and their possible role in the regulation of RNA synthesis. *PNAS* **1964**, *51*, 786-794.

18. Howe, F.S.; Fischl, H.; Murray, S.C.; Mellor, J. Is H3K4me3 instructive for transcription activation? *Bioessays* **2016**, *39*, 1-12.
19. Calo, E.; Wysocka, J. Modification of enhancer chromatin: what, how, and why? *Mol. Cell* **2013**, *49*, 825-837.
20. Entrevan, M.; Schuettengruber, B.; Cavalli, G. Regulation of Genome Architecture and Function by Polycomb Proteins. *Trends Cell Biol.* **2016**, *26*, 511-525.
21. Tie, F.; Banerjee, R.; Stratton, C.A.; Prasad-Sinha, J.; Stepanik, V.; Zlobin, A.; Diaz, M.O.; Scacheri, P.C.; Harte, P.J. CBP-mediated acetylation of histone H3 lysine 27 antagonizes *Drosophila* Polycomb silencing. *Development* **2009**, *136*, 3131-3141.
22. Spange, S.; Wagner, T.; Heinzl, T.; Kramer, O.H. Acetylation of non-histone proteins modulates cellular signaling at multiple levels. *Int. J. Biochem. Cell Biol.* **2009**, *41*, 185-198.
23. Creighton, M.P.; Cheng, A.W.; Welstead, G.G.; Kooistra, T.; Carey, B.W.; Steine, E.J.; Hanna, J.; Lodato, M.A.; Frampton, G.M.; *et al.* Histone H3K27ac separates active from poised enhancers and predicts developmental states. *PNAS* **2010**, *107*, 21931-21936.
24. Bernstein, B.E.; Humphrey, E.L.; Erlich, R.L.; Schneider, R.; Bouman, P.; Liu, J.S.; Kouzarides, T.; Schreiber, S.L. Methylation of histone H3 Lys 4 in coding regions of active genes. *PNAS* **2002**, *99*, 8695-8700.
25. Dai, H.; Wang, Z. Histone Modification Patterns and Their Responses to Environment. *Curr. Envir. Health Rpt.* **2014**, *1*, 11-21.
26. Burns, E.N.; Bordbari, M.H.; Mienaltowski, M.J.; Affolter, V.K.; Barro, M.V.; Gianino, F.; Gianino, G.; Giulotto E.; Kalbfleisch, T.S.; Katzman, S.A.; *et al.* Generation of an equine biobank to be used for Functional Annotation of Animal Genomes project. *Anim. Genet.* **2018**, *49*, 564-570.

27. Landt, S.G.; Marinov, G.K.; Kundaje, A.; Kheradpour, P.; Pauli, F.; Batzoglou, S.; Bernstein, B.E.; Bickel, P.; Brown, J.B.; Cayting, P.; Chen, Y.; *et al.* ChIP-seq guidelines and practices of the ENCODE and modENCODE consortia. *Genome Res.* **2012**, *22*, 1813-1831.
28. Ramirez, F.; Ryan, D.P.; Gruning, B.; Bhardwaj, V.; Kilpert, F.; Rickter, A.S.; Heyne, S.; Dundar, F.; Manke, T. deepTools2: a next generation web server for deep-sequencing data analysis. *Nucleic Acids Res.* **2016**, *44*, W160-W165.
29. Trim Galore. Available online: http://www.bioinformatics.babraham.ac.uk/projects/trim_galore/ (Version 0.4.0).
30. Martin, M. Cutadapt Removes Adapter Sequences from High-Throughput Sequencing Reads. *EMBnet.journal* **2011**, *17*, 10-12.
31. Kalbfleisch, T.S.; Rice, E.S.; DePriest, M.S.; Walenz, B.P.; Hestand, M.S.; Vermeesch, J.R.; O'Connell, B.L.; Fiddes, I.T.; Vershinina, A.O.; *et al.* Improved reference genome for the domestic horse increases assembly contiguity and composition. *Commun. Biol.* **2018**, *1*, 197.
32. Li, H.; Durbin, R. Fast and accurate short read alignment with Burrows-Wheeler transform. *Bioinformatics* **2009**, *25*, 1754-1760.
33. Li, H.; Handsaker, B.; Wysoker, A.; Fennell, T.; Ruan, J.; Homer, N.; Marth, G.; Abecasis, G.; Durbin, R.; 1000 Genome Project Data Processing Subgroup. The Sequence Alignment/Map format and SAMtools. *Bioinformatics* **2009**, *25*, 2078-2079.
34. Picard Toolkit, GitHub Repository. Available online: <http://broadinstitute.github.io/picard/> (Version 2.7.1).
35. Zhang, Y.; Liu, T.; Meyer, C.A.; Eeckhoute, J.; Johnson, D.S.; Berntein, B.E.; Nusbaum, C.; Myers, R.M.; Brown, M.; Wei, L.; *et al.* Model-based Analysis of ChIP-Seq (MACS). *Genome Biol.* **2008**, *9*, R137.

36. SICERpy, GitHub Repository. Available online: <https://github.com/dariober/SICERpy> (Accessed on 10 October 2019).
37. Zang, C.; Schones, D.E.; Zeng, C.; Cui, K.; Zhao, K.; Peng, W. A clustering approach for identification of enriched domains from histone modification ChIP-Seq data. *Bioinformatics* **2009**, *25*, 1952-1958.
38. Favorov, A.; Mularoni L.; Cope, L.M.; Medvedeva, Y.; Mironov, A.A.; Makeev, V.J., Wheelan, S.J. Exploring Massive, Genome Scale Datasets with the GenometriCorr Package. *PLoS Comput. Biol.* **2012**, *8*, e1002529.
39. Quinlan, A.R.; Hall, I.M. BEDTools: a flexible suite of utilities for comparing genomic features. *Bioinformatics* **2010**, *26*, 841-842.
40. Wickham, H. *ggplot2: Elegant Graphics for Data Analysis*. Springer-Verlag: New York, USA, 2016.
41. R Core Team. R: A language and environment for statistical computing. R Foundation for Statistical Computing. Accessed online: <https://www.r-project.org/> (Version 3.4.3).
42. McLeary, R.; Bailey, T.L. Motif Enrichment Analysis: A unified framework and method evaluation. *BMC Bioinformatics* **2010**, *11*, 165.
43. Khan, A.; Fornes, O.; Stigliani, A.; Gheorghe, M.; Castro-Mondragon, J.A.; van der Lee, R.; Bessy, A.; Cheneby, J.; Kulkarni, S.R.; Tan, G.; *et al.* JASPAR 2018: update of the open-access database of transcription factor binding profiles and its web framework. *Nucleic Acids Res.* **2018**, *46*, D260-D266.
44. The UniProt Consortium. UniProt: a worldwide hub of protein knowledge. *Nucleic Acids Res.* **2019**, *47*, D506-D515.

45. Robinson, J.T.; Thorvaldsdottir, H.; Winckler, W.; Guttman, M.; Lander, E.S.; Getz, G.; Mesirov, J.P. Integrative Genomics Viewer. *Nature Biotech.* **2011**, *29*, 24-26.
46. Aken, B.L.; Ayling, S.; Barrel, D.; Clarke, L.; Curwen, V.; Fairley, S.; Fernandez Banet, J.; Billis, K.; Garcia Giron, C.; Hourlier, T.; *et al.* The Ensembl gene annotation system. *Database* **2016**, *2016*, baw093.
47. Szklarczyk, D.; Gable, A.L.; Lyon, D.; Junge, A.; Wyder, S.; Huerta-Cepas, J.; Simonovic, M.; Doncheva, N.T.; Morris, J.H.; Bork, P.; *et al.* STRING v11: protein-protein association networks with increased coverage, supporting functional discovery in genome-wide experimental datasets. *Nucleic Acids Res.* **2019**, *47*, D607-D613.
48. Trefts, E.; Gannon, M.; Wasserman, D.H. The liver. *Curr. Biol.* **2017**, *27*, R1141-R1155.
49. Drogemuller, M.; Jagannathan, V.; Welle, M.M.; Graubner, C.; Straub, R.; Gerber, V.; Burger, D.; Signer-Hasler, H.; Poncet, P.A.; Klopfenstein, S. Congenital hepatic fibrosis in the Franches-Montagnes horse is associated with the polycystic kidney and hepatic disease 1 (*PKHD1*) gene. *PLoS ONE* **2014**, *9*, e110125.
50. Velie, B.D.; Lillie, M.; Fegraeus, K.J.; Rosengren, M.K.; Sole, M.; Wiklund, M.; Ihler, C.F.; Strand E.; Lindgren, G. Exploring the genetics of trotting racing ability in horses using a unique Nordic horse model. *BMC Genomics* **2019**, *20*, 104.
51. Guttman, M.; Amit, I.; Garber, M.; French, C.; Lin, M.F.; Feldser, D.; Huarte, M.; Zuk, O.; Carey, B.W.; Cassady, J.P.; *et al.* Chromatin signature reveals over a thousand highly conserved large non-coding RNAs in mammals. *Nature* **2009**, *458*, 223-227.
52. Ferraz-de-Souza, B.; Lin, L.; Achermann, J.C. Steroidogenic factor-1 (SF1, NR5A1) and human disease. *Mol. Cell. Endocrinol.* **2011**, *336*, 198-205.

53. Szalkowski, A.M.; Schmid, C.D. Rapid innovation in ChIP-seq peak-calling algorithms is outdistancing benchmarking efforts. *Brief. Bioinform.* **2010**, *12*, 626-633.
54. Steinhauser, S.; Kurzawa, N.; Eils, R.; Herrmann, C. A comprehensive comparison of tools for differential ChIP-seq analysis. *Brief. Bioinform.* **2016**, *17*, 953-966.
55. Xu, S.; Grullon, S.; Ge, K.; Peng, W. Spatial Clustering for Identification of ChIP-Enriched Regions (SICER) to Map Regions of Histone Methylation Patterns in Embryonic Stem Cells. In *Stem Cell Transcriptional Networks*; Kidder, B.; Humana Press: New York, USA, 2014; MIMB Volume 1150, pp. 97-111.
56. Masland, R.H. Neuronal cell types. *Curr. Biol.* **2004**, *14*, R497-R500.
57. Belknap, J.K. Genomics of laminitis. In *Equine Genomics*, 1st ed.; Chowdhary, B.P.; John Wiley & Sons, Inc: Iowa, USA, 2013; pp. 255-264.
58. Al-Agele, R.; Paul, E.; Kubale Dvojmoc, V.; Sturrock, C.J.; Rauch, C.; Rutland, C.S. The Anatomy, Histology and Physiology of the Healthy and Lamé Equine Hoof. In *Veterinary Anatomy and Physiology*; Rutland, C.; Kubale, V.; IntechOpen: London, UK, 2019; pp. 1-18.
59. Ogryzko, V.V.; Schiltz, R.L.; Russanova, V.; Howard, B.H.; Nakatani, Y.; The Transcriptional Coactivators p300 and CBP Are Histone Acetyltransferases. *Cell* **1996**, *87*, 953-959.
60. Song, C.; Keller, K.; Chen, Y.; Chen, Y.; Murata, K.; Stamatoyannopoulos, G. Transcription coactivator CBP has direct DNA binding activity and stimulates transcription factor DNA binding through small domains. *Biochem. Biophys. Res. Commun.* **2002**, *296*, 118-124.
61. Oster, S.K.; Ho, C.S.; Soucie, E.L.; Penn, L.Z. The myc oncogene: MarvelouslyY Complex. *Adv. Cancer Res.* **2002**, *84*, 81-154.

62. Mogi, A.; Kuwano, H. TP53 Mutations in Nonsmall Cell Lung Cancer. *J. Biomed. Biotechnol.* **2010**, *2011*, 9.
63. Widmann, M.; Nieß, A.M.; Munz, B. Physical Exercise and Epigenetic Modifications in Skeletal Muscle. *Sports Med.* **2019**, *49*, 509-523.
64. Fages, A.; Hanghoj, K.; Khan, N.; Gaunitz, C.; Seguin-Orlando, A.; Leonardi, M.; McCrory Constantz, C.; Gamba, C.; Al-Rasheid, K.A.S.; Albizuri, S.; *et al.* Tracking Five Millennia of Horse Management with Extensive Ancient Genome Time Series. *Cell* **2019**, *177*, 1419-1435.
65. Pujar, S.; Meyers-Wallen, V.N. Sequence variations in equine candidate genes for XX and XY inherited disorders of sexual development. *Reprod. Domest. Anim.* **2012**, *47*, 827-834.
66. Achermann, J.C.; Ozisik, G.; Ito, M.; Orun, U.A.; Harmanci, K.; Gurakan, B.; Jameson, J.L. Gonadal Determination and Adrenal Development Are Regulated by the Orphan Nuclear Receptor Steroidogenic Factor-1, in a Dose-Dependent Manner. *J. Clin. Endocrinol. Metab.* **2002**, *87*, 1829-1833.
67. Splinter, E.; Heath, H.; Kooren, J.; Palstra, R.; Klous, P.; Grosveld, F.; Galiart, N.; de Laat, W.L. CTCF mediates long-range chromatin looping and local histone modification in the β -globin locus. *Genes & Dev.* **2006**, *20*, 2349-2354.
68. Hou, C.; Dale, R.; Dean, A. Cell type specificity of chromatin organization mediated by CTCF and cohesion. *PNAS* **2010**, *107*, 3651-3656.

Chapter 3: Heritability of Insidious Uveitis in Appaloosa Horses

Authors: N. B. Kingsley, L. Sandmeyer, E. Norton, D. Speed, A. Dwyer, M. Lassaline, M. McCue, and R. R. Bellone.

Keywords: ERU, autoimmune, genetics, equine, ocular, inflammation

Reference: Kingsley, N.B.; Sandmeyer, L.; Norton, E.; Speed, D.; Dwyer, A.; Lassaline, M.; McCue, M.; and Bellone, R.R. Heritability of Insidious Uveitis in Appaloosa Horses. *Anim. Genet.* Submitted 2022.

Submitted: March 18, 2022

Summary:

Equine Recurrent Uveitis (ERU) is a blinding ocular disorder among horses, and the Appaloosa horse breed is disproportionately affected by a chronic form of this intraocular inflammatory disease known as insidious uveitis. Strong breed predisposition and previous investigations suggest that there is a genetic component to the pathology of insidious uveitis among Appaloosa horses; however, no estimates of the heritability of the disease have previously been determined. This study aimed to characterize the genetic underpinning of the disease by estimating the heritability for insidious uveitis among Appaloosas. After combining two genotyping array datasets from the Illumina Equine SNP70 BeadChip and the Axiom Equine 670K Genotyping Array, heritability was estimated for 59 affected and 83 unaffected horses using the Linkage Disequilibrium Adjusted Kinship (LDAK) software. Based on previous research, age and sex were used as covariates, and the allele responsible for the characteristic Appaloosa spotting coat pattern (LP), previously associated with ERU risk, was included as a fixed effect (“top predictor”). The heritability estimate for insidious uveitis was 1.09 (SE = 0.16, $P = 1.56 \times 10^{-4}$) with LP contributing 0.20 to the estimate.

This study suggests that insidious uveitis is highly heritable ($h^2 = 0.77-1.0$) and additional loci outside of *LP* are contributing to the genetic risk for insidious uveitis for Appaloosas. Once identified, these other genetic factors may lead to new disease mitigation efforts in veterinary care and breeding practices.

Main Text:

The Appaloosa horse breed is known to have an increased risk of developing a blinding inflammatory disease known as equine recurrent uveitis (ERU).¹ While several classifications have been described in horses, Appaloosas are most often diagnosed with insidious uveitis.^{2,3} Previous retrospective research determined that Appaloosas are approximately 8-10 times more likely to be affected by ERU than horses from other breeds commonly presenting at veterinary services in North America.¹ As an immune-mediated disease, ERU is thought to be a complex trait with both genetic and environmental risk factors.^{2,4,5} While breed predisposition suggests that there is a genetic component underlying the development of insidious uveitis among Appaloosas, estimating heritability of the disease trait has been limited due to small sample sizes.⁵ Previous investigations, however, have consistently identified age and homozygosity for the breed defining coat patterning allele (*LP*, for leopard complex spotting pattern) as risk factors for insidious uveitis.^{2,5,6} The *LP* allele is a retroviral insertion in the calcium ion channel gene known as *TRPM1*, and it is the cause of both the incomplete dominant coat pattern known as *LP* spotting and the associated recessive ocular condition known as congenital stationary night blindness (Fig. 1).⁷⁻⁹ It is suspected that additional genetic loci impact disease risk for ERU as age and *LP* genotype are not sufficient to explain the distribution of disease among Appaloosas.⁵ To better understand the role of genetics in this disease, we aimed to estimate the proportion of the phenotypic variation that is explained

by the additive genetic variation as captured by SNP markers from commercially available genotyping arrays in a combined cohort of Appaloosa horses.



Figure 1: Phenotypic expression of the *LP* variant. (A) Horses homozygous for *LP* have a white pattern that contains few or no pigmented spots, such as the horse with an extensive unpigmented coat pattern, known as fewspot. These horses are night blind and are at increased risk for insidious equine recurrent uveitis. (B) Heterozygous *LP* horses have a similar white pattern of variable size; however, the unpigmented region usually contains pigmented spots as seen in the leopard horse in panel B. (C) Horses without *LP* do not display the leopard complex spotting patterns and are considered true solid horses as shown in panel C. Photographs courtesy of Martha Mitchell (A and B).

All protocols were approved by the Institutional Animal Care and Use Committee at the University of California, Davis (protocol number 18851) or by the Animal Care Committee at the University of Saskatchewan (protocol number 20110053). All horses received a complete ocular examination including neuro-ophthalmic, transilluminator, slit-lamp biomicroscopic, indirect ophthalmoscopic, and tonometry assessments. Diagnosis of insidious uveitis was made for horses experiencing active uveitis (aqueous or vitreous flare, conjunctival hyperemia, miosis, blepharospasm, epiphora, and photophobia) with clinical evidence and/or history of past inflammation. A diagnosis of insidious uveitis was also made for horses with sequelae indicative of long-term inflammation within the eye, including lens luxation, synechiae, immature or mature cataracts, iris hyperpigmentation and/or color changes, corneal neovascularization, corpora nigra atrophy, retinal detachment or degeneration, glaucoma, or phthisis bulbi. Horses were considered controls in this study if they were at least eight years of age; appeared unaffected at the time of the

examination; had no history of eye disease; and did not display ocular pathology outside of normal limits. Mild conjunctival hyperemia, incipient cataracts, and pigmented peripapillary chorioretinal lesions demonstrating a “bullet hole” or “butterfly” pattern were not considered indicative of uveitis without additional pathology.⁶ Samples of blood and/or hair follicles were collected, and DNA was extracted using the Gentra Puregene DNA Isolation kit (Qiagen Inc.) using established protocols.¹⁰

All Appaloosa samples were described previously in Rockwell *et al.* (2020) and/or Sandmeyer *et al.* (2020), and samples were included in this study if age information was known and if control samples met a minimum age threshold of eight years old.^{2,5,6} Horses were genotyped on either the Illumina Equine SNP70 BeadChip (23 cases and 29 controls) or the Axiom Equine Genotyping Array with 670K markers (36 cases and 60 controls).^{5,11} Four horses (2 cases and 2 controls) were genotyped on both arrays, and these duplicates were used to ensure consistent genotyping across platforms and Appaloosa-specific validation of imputation. All data were remapped to the EquCab3.0 reference genome and imputed up to 2M markers using previously described methods.¹¹⁻¹⁴ SNP markers with less than 90% imputation accuracy based on the reference dataset and the four duplicate samples were removed from further analysis. After assessing concordance between the two arrays and proper merging using PLINK software,¹⁵ the four horses that were included in both the 70K array and the 670K array datasets were filtered to remove one of the duplicate entries for each horse. The combined dataset (n = 144) was pruned for linkage disequilibrium such that only one marker was randomly retained from every pair with $r^2 > 0.25$ in a 2 Mb sliding window.¹⁶ Data were also filtered based on the following parameters: minor allele frequency < 0.05, genotype call rate < 0.90, and sample call rate < 0.90. All pruning

and filtering was performed using PLINK software.¹⁵ After quality control, 142 horses (59 cases and 83 controls) and 71,537 markers remained for evaluation.

Heritability was estimated using a restricted maximum likelihood (REML) solver from Linkage Disequilibrium Adjusted Kinship (LDAK) software, which incorporates a weighted relationship matrix based on local LD.¹⁷ The LDAK REML solver uses an eigen-decomposition, making it potentially better for estimating heritability values near zero or one compared to similar software.¹⁷ Previous evaluations of heritability estimates from LDAK for tarsal osteochondrosis and metabolic syndrome illustrate the efficacy of this software for evaluating the genetic architecture of equine diseases.^{18,19} Given associations between *LP* and ERU,^{2,5-7} *LP* genotype was assayed by the Veterinary Genetics Laboratory (UC Davis) diagnostic services, and those genotypes were included as a fixed effect in the model. In LDAK, genetic markers like *LP* with large effect size (referred to as “top predictors” by LDAK) are treated as covariates (fixed effects), except the variance explained by these markers is added to the heritability estimate.²⁰ Specifically,

$$\frac{\sigma_G^2 + \sigma_T^2}{\sigma_G^2 + \sigma_T^2 + \sigma_E^2}$$

where σ_G^2 , σ_T^2 , and σ_E^2 are the variances explained by the kinship matrix, the “top predictors,” and the environment, respectively. As a previously implicated risk factor, age was considered a covariate (fixed effect) in the analysis.^{6,21} Sex was also used as a fixed effect covariate to prevent confounding from imbalances in the sex ratio (60 males to 82 females) between cases and controls in this cohort (Table 1). Based on previous investigations examining disease prevalence, an estimated population prevalence of 0.25 was used when creating the model.^{1,21-23} Heritability estimates were not constrained to values between zero and one to prevent over- or underestimating heritability values.

Table 1: Ratio of females to males among the cases and controls in the combined dataset of 142 horses (59 cases and 83 controls).

	Affected	Unaffected	Totals:
Females	31	51	82
Males	28	32	60
Totals:	59	83	142

After accounting for covariates, the heritability estimate for insidious uveitis was 1.09 (SE = 0.16, $P = 1.56 \times 10^{-4}$). Interestingly, the *LP* genotype accounted for 0.20 of the estimated heritability. While this finding provides additional support that *LP* is a major risk factor for predicting ERU disease status, it also suggests that other genetic factors are contributing to the development of insidious uveitis within the Appaloosa breed. Additionally, the estimated coefficients for sex ($\beta_{\text{sex}} = -0.12$, $P = 2.01 \times 10^{-1}$) and age ($\beta_{\text{age}} = 0.02$, $P = 6.07 \times 10^{-3}$) on the liability scale indicate that age, but not sex, significantly contributed to the phenotypic variation (i.e. whether a horse developed ERU or not) within our dataset. The effect of increased age is consistent with previous investigations.⁶

Although cryptic relatedness, sex, age, and *LP* genotype were incorporated within our model, we cannot exclude the possibility that other unknown risk factors, interactions, or biases exist in our dataset and were not included or mitigated in our analysis. Previous associations have implicated *Leptospira* exposure and other infectious agents in triggering ERU, but these environmental risk factors are difficult to assess in a meaningful manner due to long latency periods between infection and ERU onset, false negative and positive rates with titers, and difficult field sampling conditions.^{1,24} Additionally, several independent investigations indicate that horses affected with insidious uveitis are less likely to have *Leptospira* involvement compared to horses with more acute forms of the disease.²⁵⁻²⁷ Still, environmental factors were not assessed in this study and may have inflated the heritability estimate if they were correlated with the genetic data

due to chance or non-random sampling. Furthermore, uncharacterized gene-environment interactions (GxE) or genetic interactions (also known as epistatic and dominance variation) could have been inadvertently counted as part of the additive genetic variation and artificially increased our narrow-sense heritability estimate.

Despite the limitations described above for estimating h^2 , previous research supports a genetic component to the development of insidious uveitis among Appaloosas.¹ Although heritability estimates in this study were not constrained to values between zero and one for reasons outlined above, h^2 values greater than one are not possible. Therefore, the heritability for insidious uveitis in the combined dataset of 142 horses is expected to be between 0.77 and 1.0, based on the 95% confidence interval. Our estimate supports that insidious uveitis is highly heritable in the Appaloosa. Furthermore, the proportion of the estimate attributed to the genotype at the *LP* locus (0.20) suggests that variation in other regions of the genome outside of *LP* are also contributing to ERU, and identifying these other regions will be important for predicting disease risk. For this reason, additional research is needed to elucidate the genetic basis of insidious uveitis in Appaloosas, which may lead to advancements in medical prevention and treatment, as well as diagnostic tools for mate selection to reduce the impact of uveitis on horses in this breed.

Acknowledgements:

The authors would like to acknowledge Sheila Archer, Maura Mack, and Samantha Beeson for their technical assistance during the research. We would also like to thank the horse owners whose horses participated in this study. This work was supported by the Townsend Equine Health Research Fund (TEHRF) and the Morris Animal Foundation (D16EQ-028). The mission of the Morris Animal Foundation is to bridge science and resources to advance the health of animals. N.

B. Kingsley was also supported in part by the University of California – Davis, Center for Equine Health Fellowship.

Data Availability:

MAP and PED files from this study are available at Open Science Framework: <https://osf.io/v6s4f/>

Conflict of Interest:

N. B. Kingsley and R. R. Bellone are affiliated with the UC Davis Veterinary Genetics Laboratory, a service laboratory offering diagnostic genetic tests for horses and other animal species.

References:

1. Dwyer AE, Crockett RS, Kalsow CM. Association of leptospiral seroreactivity and breed with uveitis and blindness in horses: 372 cases (1986-1993). *J Am Vet Med Assoc.* 1995;207(10):1327-1331. <http://www.ncbi.nlm.nih.gov/pubmed/7591929>
2. Fritz KL, Kaese HJ, Valberg SJ, et al. Genetic risk factors for insidious equine recurrent uveitis in Appaloosa horses. *Anim Genet.* 2014;45(3):392-399. doi:10.1111/age.12129
3. McMullen RJ, Fischer BM. Medical and Surgical Management of Equine Recurrent Uveitis. *Vet Clin North Am - Equine Pract.* 2017;33(3):465-481. doi:10.1016/j.cveq.2017.07.003
4. Gilger BC, Deeg CA. Equine recurrent uveitis. In: Gilger BC, ed. *Equine Ophthalmology.* 2nd ed. Elsevier Saunders; 2011:317-349.
5. Rockwell H, Mack M, Famula T, et al. Genetic investigation of equine recurrent uveitis in Appaloosa horses. *Anim Genet.* 2020;51(1):111-116. doi:10.1111/age.12883
6. Sandmeyer LS, Kingsley NB, Walder C, et al. Risk factors for equine recurrent uveitis in a population of Appaloosa horses in western Canada. *Vet Ophthalmol.* 2020;23(3):515-525. doi:10.1111/vop.12749

7. Bellone RR, Holl H, Setaluri V, et al. Evidence for a Retroviral Insertion in *TRPM1* as the Cause of Congenital Stationary Night Blindness and Leopard Complex Spotting in the Horse. *PLoS One*. 2013;8(10):1-14. doi:10.1371/journal.pone.0078280
8. Bellone RR, Brooks SA, Sandmeyer L, et al. Differential gene expression of *TRPM1*, the potential cause of congenital stationary night blindness and coat spotting patterns (LP) in the Appaloosa horse (*Equus caballus*). *Genetics*. 2008;179(4):1861-1870. doi:10.1534/genetics.108.088807
9. Bellone RR, Forsyth G, Leeb T, et al. Fine-mapping and mutation analysis of *TRPM1*: A candidate gene for leopard complex (LP) spotting and congenital stationary night blindness in horses. *Briefings Funct Genomics Proteomics*. 2010;9(3): 193-207. doi:10.1093/bfgp/elq002
10. Bellone RR, Liu J, Petersen JL, et al. A missense mutation in damage-specific DNA binding protein 2 is a genetic risk factor for limbal squamous cell carcinoma in horses. *Int J Cancer*. 2017;141:342-353. doi:10.1002/ijc.30744
11. Schaefer RJ, Schubert M, Bailey E, et al. Developing a 670k genotyping array to tag ~2M SNPs across 24 horse breeds. *BMC Genomics*. 2017;18(1):1-18. doi:10.1186/s12864-017-3943-8
12. McCoy AM, McCue ME. Validation of imputation between equine genotyping arrays. *Anim Genet*. 2014;45(1):153. doi:10.1111/age.12093
13. Beeson SK, Schaefer RJ, Mason VC, McCue ME. Robust remapping of equine SNP array coordinates to EquCab3. *Anim Genet*. 2019;50(1):114-115. doi:10.1111/age.12745
14. Schaefer RJ, McCue ME. Equine Genotyping Arrays. *Vet Clin North Am - Equine Pract*. 2020;36(2):183-193. doi:10.1016/j.cveq.2020.03.001

15. Purcell S, Neale B, Todd-Brown K, et al. PLINK: A tool set for whole-genome association and population-based linkage analyses. *Am J Hum Genet.* 2007;81(3):559-575. doi:10.1086/519795
16. Weale ME. *Quality Control for Genome-Wide Association Studies.* Vol 628.; 2010. doi:10.1007/978-1-60327-367-1_19
17. Speed D, Hemani G, Johnson MR, Balding DJ. Improved heritability estimation from genome-wide SNPs. *Am J Hum Genet.* 2012;91(6):1011-1021. doi:10.1016/j.ajhg.2012.10.010
18. McCoy AM, Norton EM, Kemper AM, Beeson SK, Mickelson JR, McCue ME. SNP-based heritability and genetic architecture of tarsal osteochondrosis in North American Standardbred horses. *Anim Genet.* 2019;50(1):78-81. doi:10.1111/age.12738
19. Norton E, Schultz N, Geor R, McFarlane D, Mickelson J, McCue M. Genome-wide association analyses of equine metabolic syndrome phenotypes in welsh ponies and morgan horses. *Genes (Basel).* 2019;10(11):1-23. doi:10.3390/genes10110893
20. Speed D, Cai N, Johnson MR, Nejentsev S, Balding DJ. Reevaluation of SNP heritability in complex human traits. *Nat Genet.* 2017;49(7):986-992. doi:10.1038/ng.3865
21. Sandmeyer LS, Bauer BS, Feng CX, Grahn BH. Equine recurrent uveitis in western Canadian prairie provinces : A retrospective study (2002–2015). *Can Vet J.* 2017;58:717-722.
22. Deeg CA. Ocular immunology in equine recurrent uveitis. *Vet Ophthalmol.* 2008;11(SUPPL.1):61-65. doi:10.1111/j.1463-5224.2008.00625.x
23. Brooks D, Matthews AG. *Essentials of Veterinary Ophthalmology.* 2nd ed. (Gelatt K, ed.); 2008.

24. Williams RD, Morter RL, Freeman MJ, Lavignette AM. Experimental chronic uveitis. Ophthalmic signs following equine leptospirosis. *Invest Ophthalmol.* 1971;10(12):948-954.
25. Baumgart A, Gerhards H. Besonderheiten der Tigerschecken-Uveitis und möglicher Cyclosporin A-Einsatz in deren Therapie in Deutschland. *Pferdeheilkunde.* 2014;30(6):626-632.
26. Polle F, Storey E, Eades S, et al. Role of Intraocular *Leptospira* Infections in the Pathogenesis of Equine Recurrent Uveitis in the Southern United States. *J Equine Vet Sci.* 2014;34(11-12):1300-1306. doi:10.1016/j.jevs.2014.09.010
27. Gerding JC, Gilger BC. Prognosis and impact of equine recurrent uveitis. *Equine Vet J.* 2016;48(3):290-298. doi:10.1111/evj.12451

Chapter 4: Identifying Genetic Risk Loci for Insidious Uveitis in Appaloosa Horses

Authors: N. B. Kingsley, L. Sandmeyer, A. Dwyer, C. D. Langefeld, R. J. McMullen Jr., M. McCue, M. Lassaline, and R. R. Bellone.

Keywords: ERU, GWAS, inflammation, equine, moon blindness, Periodic Ophthalmia, panuveitis

Abstract:

Equine Recurrent Uveitis is the leading cause of blindness among horses, and the insidious form of the disease is especially pervasive within the Appaloosa breed. Previous research found that insidious uveitis is highly heritable ($h^2 = 0.77-1.0$, $P = 1.56 \times 10^{-4}$) with a previously identified risk locus, *LP*, contributing only 0.20 to the estimate. To characterize additional genetic risk factors for insidious uveitis, a genome-wide association study (GWAS) was performed in the first phase of the study on a sample of 96 Appaloosas (36 cases and 60 controls). Using relatedness, *LP* genotype, sex, and age as covariates, a 9.7 Kb region of association was identified on ECA X (chrX:14528106 – 14537812) as significantly associated ($P = 2.11 \times 10^{-8}$). A meta-analysis after sex stratification provided additional support for the association on ECA X ($P = 1.35 \times 10^{-8}$). To test for epistasis between *LP* and the locus on ECA X, an interaction analysis using the Cochran-Mantel-Haenszel was performed, and the results supported interaction between the two loci ($P = 2.94 \times 10^{-6}$). In the second phase of the study, single-nucleotide variants (SNVs) were identified in the region by whole genome sequencing (WGS) of 18 horses from the GWAS (9 cases and 9 controls). Five reference markers from the GWAS, two previously associated coat pattern loci, and 102 SNVs were further evaluated in a combined dataset of 157 horses (70 cases and 87 controls, including the original 96 horses from the GWAS). Using logistic regression, none of the

WGS SNVs were significantly associated with phenotype; however, *LP* and the top three SNP markers from ECA X (ECA X: 14.5 Mb) were significantly associated in the larger dataset ($P_{LP} = 2.34 \times 10^{-6}$ and $P_X = 4.06 \times 10^{-5}$). Thus, our investigation identified a locus on chromosome X with a strong association to ERU that interacts with the *LP* locus, and additional work is needed to characterize potential causative variants in the region.

Introduction:

Equine recurrent uveitis (ERU) is an inflammatory disease affecting critical tissues of the inner eye. As the leading cause of blindness for horses, ERU can have a detrimental impact on a horse's quality of life. Previous investigations found that the majority of affected horses could not return to pre-disease performance roles, and a large proportion of cases (15-53%) were euthanized during these studies as a direct result of ERU.^{1,2} Furthermore, diagnostic and treatment costs per case commonly reached \$1,000–3,000 and \$3,000–5,000, respectively.² Such financial burdens make this ocular disease a major concern for the horse industry.

ERU is characterized by inflammation within the vascular uveal tract, and it has been divided into several types based on location, such as posterior (behind lens) versus anterior (before lens), and type of inflammation, such as classic (episodic inflammation) versus insidious (continuous inflammation).³⁻⁵ In particular, the insidious form of ERU usually presents with subtle or even no outward signs of persistent intraocular inflammation, making this form of the disease difficult to recognize before cumulative damage has occurred.^{3,6}

Predisposition for insidious uveitis among the Appaloosa breed and a high heritability estimate ($h^2 = 0.77-1.0$) provide evidence of a strong genetic component underlying insidious uveitis in this breed.⁶⁻⁸ Interestingly, Appaloosa horses have been selected for a particular coat pattern known as leopard complex spotting pattern (LP). The LP phenotype is characterized by

white patterning over the hindquarters that can vary in size from minimal white markings to entirely unpigmented horses (Figure 1). The coat pattern is an incomplete dominant trait caused by an LTR insertion in an intron of the Transient Receptor Potential Cation M1 Channel (*TRPM1*) gene.^{9,10} The insertion allele, denoted as *LP*, acts in a dominant epistatic manner to produce a large variety of patterns with varying levels of unpigmented coat. In addition to influencing coat pattern, *LP* is also known to disrupt the function of the ON-bipolar cell signaling pathway that is necessary for proper nerve transmission of light detection from the rod cells of the retina to the ON-bipolar cell.^{9,11,12} As a result, horses homozygous for the insertion cannot transmit nerve impulses from the rods cells to see in low light conditions and, therefore, have a disorder known as Congenital Stationary Night Blindness (CSNB).¹⁰

Previous research using a candidate gene approach found that insidious uveitis in a sample of Appaloosas was associated with two markers in the set of immune genes known as the major histocompatibility complex (MHC) and one marker in the 11th intron of *TRPM1*, tagging *LP*.⁷ Subsequent testing on the SNP70 BeadChip genotyping array provided further support for the association with *TRPM1* but did not support the association to the MHC.¹³ It was suspected, however, that evaluation on an array with a higher marker density, such as the Axiom Equine 670K Genotyping Array, may be necessary to properly tag the notoriously variable MHC. Given the association between this region and ERU in German Warmbloods and similar associations between human autoimmune uveitis and the equivalent human region (ELA), the MHC has remained an important area of investigation for ERU risk factors.¹⁴⁻¹⁷

Two investigations further supported the association of the *LP* allele with disease risk among Appaloosas.^{13,18} One of these studies also detected an association between ERU and *PATNI*, an allele at the *RFWD3* gene that leads to more extensive white patterns for *LP* horses.¹³

The other investigation found that a larger amount of white patterning at birth was associated with increased risk for ERU, although *PATNI* was not tested directly in the study.¹⁸ Both *LP* and *PATNI* are of particular interest given the selection for the *LP* phenotype in the Appaloosa and other spotted breeds, and together these investigations indicate that *LP* and potentially *PATNI*, or closely linked variants, are involved in the development of insidious uveitis. However, further evaluation of *PATNI* is necessary to determine if the association from Rockwell et al. (2020) can be replicated.¹³ In the same investigation, a model with age, *LP*, and *PATNI* genotypes was not sufficient to fully explain the distribution of this disease among Appaloosas (AUC = 0.83),¹³ suggesting that additional genetic loci may be involved in the development of insidious uveitis in this breed. Based on previous research in horses and humans, as well as the immunogenic nature of the disease, we hypothesize that, in addition to the loci already mentioned, insidious uveitis in Appaloosas can be explained by additional genetic loci.

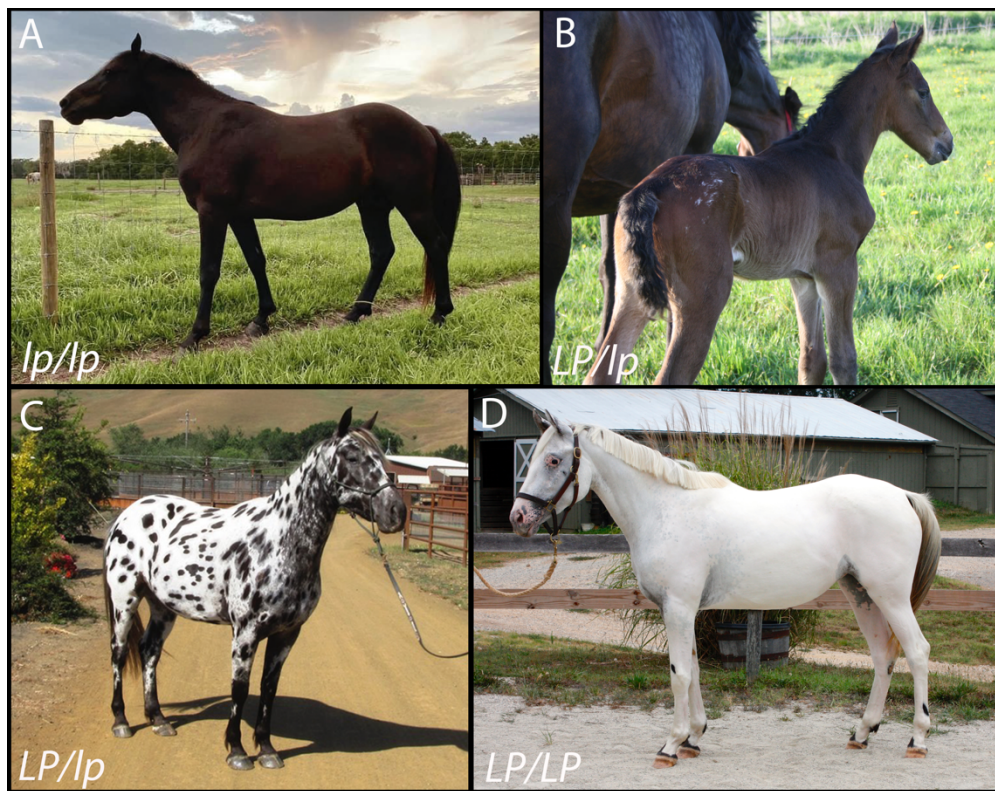


Figure 1: Leopard Complex Spotting Coat Patterns (LP). (A) A horse without any copies of *LP*. These horses are considered “true solids” as they do not display any phenotypic characteristics of the leopard complex spotting pattern. (B) A heterozygous *LP* horse with minimal white patterning over the rump. (C) Another heterozygous *LP* horse with a more extensive white patterning due to the *PATNI* locus. The horse's coat contains pigmented spots within the unpigmented region, which is characteristic of *LP/lp* horses. (D) A horse with two copies of *LP* that also displays extensive white patterning due to the combination of genotypes at the *LP* and *PATNI* loci. *LP* homozygous horses usually have a minimal number of pigmented spots within the white patterned area. Photographs courtesy of (A) Chelsea Thornton, (B) Dr. Sanna Hèden, (C) Cheryl Woods, and (D) Martha Mitchell.

Materials and methods:

Sample Collection

All protocols were approved by the Institutional Animal Care and Use Committee at the University of California, Davis (18851, 20699, and 22466) or by the Animal Care Committee at the University of Saskatchewan (20110053). All horses received a complete ocular examination from a Doctor of Veterinary Medicine (DVM), a diplomate or honorary member of the American College of Veterinary Ophthalmologist (ACVO), or a diplomate of the European College of Veterinary Surgeons (ECVS). The exams included neuro-ophthalmic, transilluminator, slit-lamp biomicroscopic, indirect ophthalmoscopic, and tonometry assessments. Horses experiencing active uveitis (aqueous or vitreous flare, conjunctivitis, miosis, blepharospasm, epiphora, and photophobia) with evidence of past inflammation received a diagnosis of insidious uveitis. Additionally, a diagnosis of insidious uveitis was given to horses with sequelae indicative of long-term inflammation within the eye, including lens luxation, synechiae, mature cataracts, phthisis bulbi, glaucoma, iris atrophy and color changes, corneal neovascularization, and retinal detachment or degeneration. Samples of blood and/or hair follicles were collected from each examined horse, and DNA was isolated using the Genra Puregene DNA Isolation kit (Qiagen Inc.), following previously validated protocols.¹⁹

An initial sample of 96 phenotyped Appaloosa horses from Kingsley *et al* (2022) was used in the GWAS analyses.⁸ Given the replicated association to *LP*, these horses were selected for inclusion to evaluate other potential risk variants for insidious uveitis; thus, the sample contains a high proportion of *LP* heterozygous horses (n = 58/96) among both the cases (n = 21/36) and controls (n = 37/60). DNA isolated from 96 samples was genotyped on the Axiom Equine 670K array, and genotyping was performed by Geneseek (Neogen Genomics, Lincoln, NE).²⁰ For variant investigation, an additional cohort of 61 phenotyped Appaloosas was combined with the dataset of 96 horses for a total sample set of 157 animals (70 cases and 87 controls). Given the progressive nature of this disease, controls horses had to be at least eight years of age with no clinical evidence of disease at the time of the examination and no history of eye disease. The *LP* and *PATN1* loci were assayed for all horses by the UC Davis Veterinary Genetics Laboratory diagnostic testing services.

Genome-Wide Association Study of Insidious Uveitis in 96 Appaloosas

After quality control filtering of the genotype data (minor allele frequency < 0.05, genotype call rate < 0.90, and sample call rate < 0.90), 96 horses (36 cases and 60 controls) and 426,343 markers remained for the analysis. Genome-wide association studies (GWAS) were performed using mixed linear models (MLM) from Genome-wide Efficient Mixed Model Association (GEMMA) software.^{21,22} GEMMA reduces the influence of genomic inflation by accounting for relatedness and population structure using a genetic relationship matrix as a covariate and performs a Wald statistical test of association. Statistical models with age, sex, and/or *LP* genotype as covariates were also evaluated. To correct for multiple testing in the GWAS, strict Bonferroni and modified Bonferroni adjusted thresholds were applied ($\alpha_{\text{bonf.}} = 1.17 \times 10^{-7}$ and $\alpha_{\text{mod.bonf.}} = 2.05 \times 10^{-7}$). The modified Bonferroni adjusted threshold was calculated using the effective number of

independent tests as determined by the Genetic Type 1 Error Calculator (GEC) software.²³ While simulation studies have not been performed specifically in horses to validate GEC, this approach has been successfully utilized in several studies in horses and many investigations in other animal and plant species.²⁴⁻⁴⁷

To ensure that an uneven distribution of males and females did not lead to false positive associations, an analysis with stratification by sex was performed. Separate MLMs from GEMMA software were used to analyze the data from the males (n = 45, 21 cases and 24 controls) and the females (n = 51, 15 cases and 36 controls). Both models included relatedness, age, and *LP* genotype as covariates. The sex-stratified associations were then evaluated by meta-analysis with METAL software v.20110325, which converted the p-values into Z-scores for each individual analysis before combining them into a single weighted Z-score for each marker.⁴⁸ Additionally, evidence of genetic interaction was assessed by the Cochran-Mantel-Haenszel test implemented in R v.4.1.3, using ERU phenotype as the stratifying category.^{49,50}

Whole Genome Sequencing of 18 Appaloosas

Whole genome sequencing (WGS) of nine cases and nine controls from the GWAS dataset was performed with Illumina NovaSeq 4000 technology (San Diego, CA) and targeted at least 20X coverage. Reads were trimmed and filtered for quality with HTStream v.1 software prior to alignment with BWA mem v0.7.16.^{51,52} SAMtools v.1.11 was used to sort and consolidate files, and both Freebayes v. 1.3.1 and BCFtools v1.10.2 were used for variant calling.^{53,54} Single-nucleotide variants were annotated for coding regions with SNPeff v.4.3 using GenBank (GCA_002863925.1) annotation from NCBI and annotated for non-coding functional elements specific to equine tissues using publicly available histone mark ChIP-Seq peaks from the Functional Annotation of Animal Genomes (FAANG) Initiative (PRJEB35307 and

PRJEB42315).^{55–58} All variants within the region of interest were filtered based on genotype frequency differences of at least 0.3 between cases and controls, and only variants identified by both variant calling software were investigated further. Genotyping of variants in a larger cohort of samples (n = 157, 70 cases and 87 controls) was performed on the Agena Bioscience MassARRAY system (San Diego, CA), and data were filtered using the same quality control parameters used previously (minor allele frequency < 0.05, genotype call rate < 0.90, and sample call rate < 0.90). Association testing of variants was performed using a logistic regression model from GEMMA.^{21,22} A strict Bonferroni adjusted threshold was used for multiple testing correction ($\alpha_{\text{bonf.}} = 4.59 \times 10^{-4}$).

Results:

Identifying Regions of Interest by Association Testing

Under a MLM with a relationship matrix, sex, and age as covariates, no regions reached genome-wide significance, although two regions on ECA 1 (ECA 1: 171.8 Mb, $P = 4.81 \times 10^{-7}$ and ECA 1: 2.5 Mb, $P = 5.74 \times 10^{-7}$) approached significance, based on multiple testing correction for the number of independent tests ($\alpha_{\text{mod.bonf.}} = 2.05 \times 10^{-7}$) (Figure 2A and Table 1). By including *LP* genotype as an additional covariate, a second MLM analysis did not support either locus on ECA 1 but instead identified a 9.7 Kb region reaching genome-wide significance on the X chromosome (ECA X: 14.5 Mb, $P = 2.11 \times 10^{-8}$) (Figure 2B). The genomic inflation factors for the two MLM analyses were 1.05 and 1.04, respectively (Figure 2C and 2D).

Table 1: Wald test (MLM) p-values for associations between ERU and five top SNP markers from the GWAS analyses in 96 horses (36 cases and 60 controls).

Locus	1_2453754	1_171786187	X_14530368	X_14537812	X_14528106
MLM with sex and age as covariates	5.74×10^{-7}	4.81×10^{-7}	4.33×10^{-5}	9.88×10^{-5}	1.53×10^{-4}

MLM with <i>LP</i> genotype, sex, and age as covariates	7.17×10^{-6}	7.08×10^{-6}	2.35×10^{-7}	$2.11 \times 10^{-8*}$	$2.11 \times 10^{-8*}$
--	-----------------------	-----------------------	-----------------------	------------------------	------------------------

* Denotes significance using a modified Bonferroni adjusted threshold ($\alpha_{\text{mod.bonf.}} = 2.05 \times 10^{-7}$).

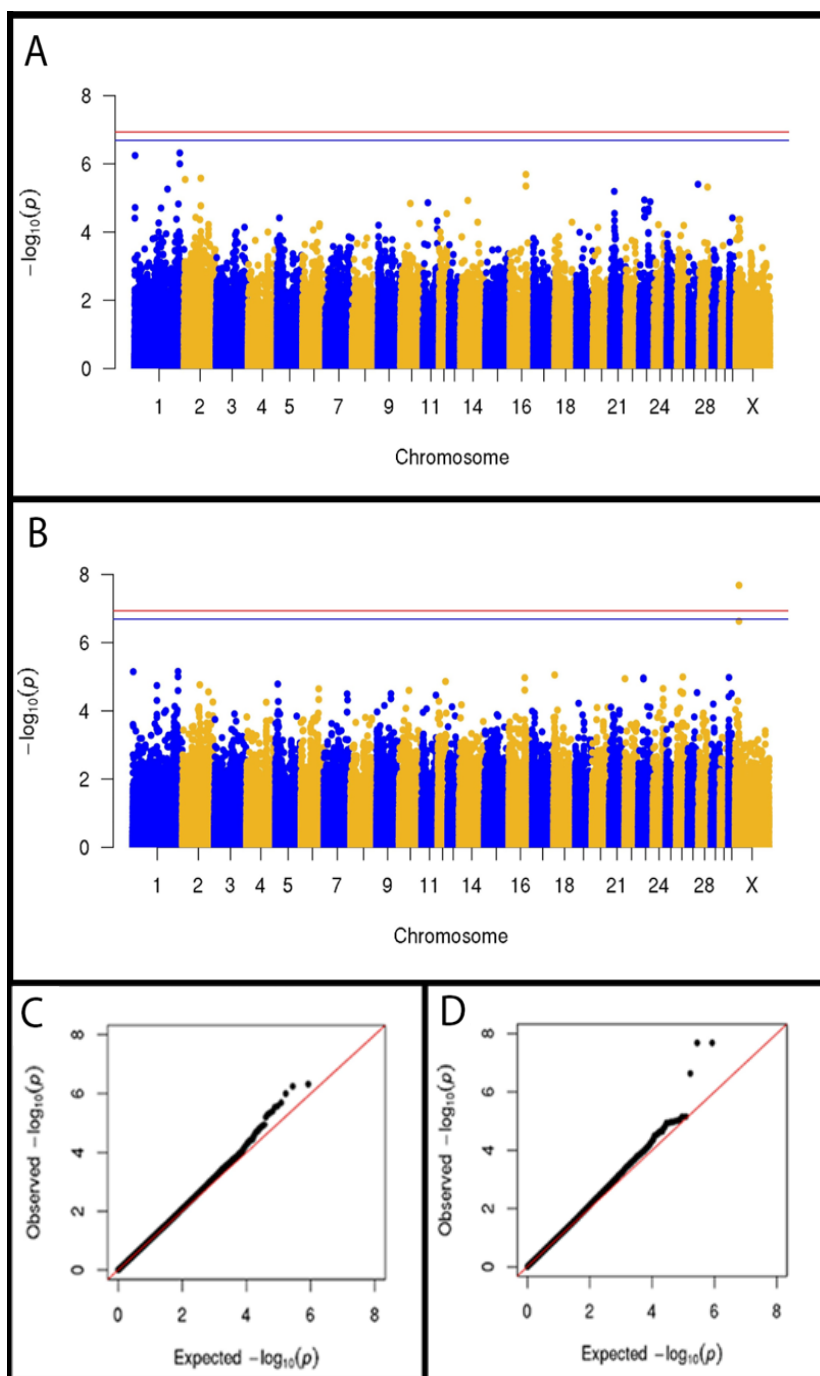


Figure 2: GWAS for insidious uveitis in a sample of 96 Appaloosa horses. (A) and (B) Red vertical line represents a Bonferroni threshold ($\alpha_{\text{bonf.}} = 1.17 \times 10^{-7}$) and blue vertical line represents a modified Bonferroni adjusted threshold ($\alpha_{\text{mod.bonf.}} = 2.05 \times 10^{-7}$). (A) Manhattan plot of Wald test p-values from a mixed linear model using GEMMA software. Sex and age were used as covariates in the analysis. (B) Manhattan plot of Wald test p-values from a mixed linear model using GEMMA software. *LP* genotype, sex, and age were used as covariates in the analysis. (C) and (D) Diagonal red line indicates perfect normality. (C) Quantile-quantile (QQ) plot of Wald test p-values from a mixed linear model using GEMMA software as in Panel A. The genomic inflation factor was 1.05. (D) QQ plot of Wald test p-values from a mixed linear model using GEMMA software as in Panel B. The genomic inflation factor was 1.04.

To further prevent confounding sex bias, a sex stratification analysis was performed, and the three associated SNP markers on the X chromosome continued to be significantly associated with insidious uveitis in the meta-analysis ($P = 1.35 \times 10^{-8}$) (Table 2). Furthermore, an interaction analysis between *LP* and the locus on ECA X, using female ECA X genotypes coded as 0 (homozygous reference), 1 (heterozygous), or 2 (homozygous alternate) and hemizygous male genotypes coded as 0 (reference) or 2 (alternate), identified a statistically significant interaction between the two loci ($P = 2.94 \times 10^{-6}$ and Table 3).

Table 2: Sex-stratified analysis of 96 Appaloosas. Distribution of females and males among the 36 cases and 60 controls and p-values for the associations of the three SNP markers on ECA X in the sex stratified analyses (GEMMA software) and meta-analysis (METAL software).

	Females	Males	Total:
Affected	15	21	36
Unaffected	36	24	60
Total:	51	45	96
Locus	Females Only	Males Only	Meta-Analysis
X_14530368	4.78×10^{-7}	1.31×10^{-2}	$7.97 \times 10^{-8*}$
X_14537812	1.93×10^{-4}	1.62×10^{-5}	$1.44 \times 10^{-8*}$
X_14528106	1.93×10^{-4}	1.62×10^{-5}	$1.44 \times 10^{-8*}$

* Denotes significance using a modified Bonferroni adjusted threshold ($\alpha_{\text{mod.bonf.}} = 2.05 \times 10^{-7}$).

Table 3: Distribution of combined genotypes for *LP* and locus on ECA X in dataset of 96 Appaloosas (36 cases and 60 controls).

	ECA X:	ref/ref	ref/alt	alt/alt	Totals:
Unaffected	<i>lp/lp</i>	5	5	5	15
	<i>LP/lp</i>	3	13	21	37
	<i>LP/LP</i>	0	1	7	8
	Totals:	8	19	33	60
Affected	<i>lp/lp</i>	0	0	0	0
	<i>LP/lp</i>	14	6	1	21
	<i>LP/LP</i>	6	2	7	15
	Totals:	20	8	8	36
Combined Total:		28	27	41	96

Investigating Region of Interest by Whole Genome Sequencing

The region of interest on ECA X including 150 Kb up- and downstream of the associated locus (ECA X: 14.37-14.68 Mb) was evaluated for variants by WGS. Based on filtering by genotype frequency difference of 0.3 or greater between cases and controls, 130 SNVs from ECA X were further investigated by genotyping in a larger cohort of samples (n = 157, 70 cases and 87 controls) (Table S1). Of the 1,552 variants identified in the investigated region through WGS, only five variants had an allele frequency difference in the nine cases and nine controls of 50% or greater. Furthermore, one coding variant was identified in the region, but it was not predicted to have a deleterious impact on protein function. Four variants were identified within the boundaries of histone mark ChIP-Seq peaks, indicating a potential role in gene regulation.^{55,56} To better assess associations, seven additional markers (*LP*, *PATNI*, two markers on ECA 1 approaching genome-

wide significance in the first MLM, and three significant markers on ECA X identified in the second MLM,) were also evaluated in the larger cohort.

After quality filtering, 109 variants and 157 samples (70 cases and 87 controls) remained for further analysis. Using a logistic model from GEMMA with sex and age as covariates, only associations with the *LP* locus reached significance using multiple testing correction with a strict Bonferroni adjusted threshold (*LP*, $P = 2.34 \times 10^{-6}$) (Table 4). After adding *LP* genotype as a covariate, the three SNP markers from ECA X reached significance (*X_14530368*, $P = 4.06 \times 10^{-5}$; *X_14537812*, $P = 4.13 \times 10^{-5}$; *X_14528106*, $P = 4.14 \times 10^{-5}$). *PATN1* was not significantly associated to insidious uveitis in any analysis, and none of the 102 chromosome X SNVs identified by WGS showed a significant association to disease phenotype, even after inclusion of *LP* as a covariate (Table S2).

Table 4: Investigating *LP*, *PATN1*, and five SNP markers by genotyping in a larger dataset of 157 Appaloosas (70 cases and 87 controls). Wald test p-values for associations between insidious uveitis and *LP*, *PATN1*, and the five SNP markers identified in the original GWAS.

Locus	<i>LP</i>	<i>PATN1</i>	1_2453754	1_171786187	X_14530368	X_14537812	X_14528106
Logistic model with age and sex as covariates	2.34x10-6*	0.52	0.083	0.102	0.072	0.61	0.71
Logistic model with age, sex, and <i>LP</i> genotype as covariates	N/A	0.65	0.037	4.22x10-3	4.06x10-5*	4.13x10-5*	4.14x10-5*

* Denotes significance using a Bonferroni corrected threshold ($\alpha_{\text{bonf}} = 4.59 \times 10^{-4}$).

Discussion:

Previous investigations in Appaloosas characterized the *LP* insertion as a pleiotropic locus, conferring both the defining coat pattern of the Appaloosa breed and the ocular condition known as CSNB.^{9,10,12} As seen in previous investigations, the *LP* locus was significantly associated with

insidious uveitis when evaluated within the larger dataset.^{13,18} In horses with CSNB, the *LP* insertion contains an early poly-adenylation signal that prevents transcription of the entire *TRPM1* gene within retinal tissues.¹⁰ Investigations in humans have also found novel mutations in *TRPM1* associated with CSNB, often in conjunction with myopia and strabismus phenotypes, and molecular investigations indicate that it is the absence of functional TRPM1 that is the cellular mechanism leading to an inability to see in scotopic conditions.^{18,59–63} Evaluation of *TRPM1* expression in homozygous (*LP/LP*) and heterozygous (*LP/lp*) horses indicate that both experience a decrease relative to *lp/lp* individuals (*LP/LP* = 0.0005 and *LP/lp* = 0.31), yet heterozygotes produce enough wild-type TRPM1 for a normal light detection response after dark adaptation.¹²

Although *LP/LP* horses have been identified as having the highest risk for developing ERU compared to *lp/lp* (OR = 19), heterozygous individuals are also affected by insidious uveitis.^{13,18} Furthermore, *LP* genotype has been found to explain part, but not all, of the phenotypic distribution of ERU among Appaloosas.^{8,13} While it is valuable to use *LP* genotype as a risk factor, it is not clear if the association with insidious uveitis is the result of linkage or causality, and further interrogation of the region by haplotype analysis is needed to refine the locus. Additional investigations are also needed to characterize the cellular ramifications of the *LP* insertion to determine what role it may play in the etiology of insidious uveitis.

Evaluation of *PATNI* genotypes in the larger cohort of 157 horses did not identify an association with disease status. Thus, our investigation did not support previous findings from Rockwell *et al.*¹³ Yet, the previous associations with *PATNI* genotype and with high amounts of white patterning suggest that *PATNI* may play a minor role in the genetic contribution to ERU risk, and a larger cohort may be needed to identify a pleiotropic effect from this locus or other pigmentation modifiers in cases of insidious uveitis.^{13,18}

To account for the known risk associated with the *LP* locus, the *LP* genotype was used as a covariate to identify additional risk loci. Using a MLM with only sex and age as covariates, two regions on ECA 1 approached genome-wide significance; however, the associations on ECA 1 became less significant after accounting for *LP* genotype in the GWAS. Additionally, the two markers on ECA 1 were not as concordant with ERU phenotype as *LP* when genotyped in the larger cohort (n = 157, 70 cases and 87 controls). Since these markers were not significantly associated after accounting for *LP* as a covariate, it is suspected that these loci were tagging the *LP* insertion, and further interrogation of SNVs from these ECA 1 regions was not performed at this time.

When accounting for relatedness, *LP* genotype, sex, and age in the MLM analysis, three SNP markers tagging a 9.7 Kb region on ECA X reached genome-wide significance, and the same markers continued to be significantly associated with disease in a sex-stratified analysis. Although we cannot completely exclude the possibility that the association is the result of sampling bias due to non-random sampling and small sample size, the repeated associations while correcting for sex indicate that the association is not driven by an imbalanced sex ratio in the dataset. Additional work is needed to assess the replicability of these associations in an independent dataset.

The three significantly associated X chromosome SNP markers in this study are all located within introns of the cyclin dependent kinase like 5 (*CDKL5*) gene. This gene is associated with neurologic disorders in humans and is, therefore, not an obvious functional candidate gene for insidious uveitis.⁶⁴ Protein phosphatase with EF hand domain-1 (*PPEF-1*), located 30 Kb downstream of our GWAS hit, is also an unlikely functional candidate gene. It has limited expression within human ocular tissues, and knockout experiments of *PPEF-1* and its paralog *PPEF-2* did not lead to retinal degeneration in mice.^{65,66} One synonymous coding variant of *PPEF-*

I was identified in the WGS cohort, but the mutation was not concordant with ERU in the larger dataset. A potentially intriguing functional candidate gene, retinoschisin 1 (*RS1*), is located between *CDKL5* and *PPEF-1*, and mutations in the gene are associated with a retinal delaminating disease known as retinoschisis in humans.⁶⁷ The protein is necessary for proper retinal structure by mediating cell adhesion and interactions between photoreceptors and bipolar cells.⁶⁸ Humans with dysfunctional *RS1* generally experience progressive visual loss with retinal lesions and schisis, as well as retinal detachment or degeneration.⁶⁷

Although uveitis in humans has not been associated with mutations in *RS1*, investigations of knockout mice demonstrated that TRPM1 positioning within the membranes of bipolar cells is altered in the absence of *RS1* protein, indicating a potential functional link between *TRPM1* and *RS1* in normal ocular tissue.⁶⁹ Since the associated region on ECA X was only significant in our investigations when *LP* genotype was considered, we suspected that the pathogenic impact of the X locus may depend on the presence of the *LP* allele. An interaction analysis that stratified by ERU phenotype supported the hypothesis that *LP* is epistatic with the X locus. Although no single-nucleotide coding variants were identified in *RS1* based on WGS of 18 horses, the role of this gene suggests that alterations in expression may have an impact on TRPM1 positioning, which could influence the pathophysiology of ERU. Future investigations to explore expression of *RS1* in affected and unaffected ocular tissues from *LP* horses are needed to understand the potential interaction of these loci and their role in conferring risk for insidious uveitis.

Additionally, none of the 102 SNVs investigated from the associated X locus and 150 Kb flanking regions was perfectly concordant with phenotype in the full dataset of 157 horses. Further testing of the WGS variants with a logistic regression did not support a significant association with any of the 102 SNVs, even when *LP* was used as a covariate. Yet, the three SNP markers on ECA

X from the GWAS remained significantly associated with ERU in the larger dataset when *LP* was included in the model as a covariate. Together, these findings suggest that these markers may be tagging an uncharacterized mutation, such as a structural variant; however, more work is needed to investigate this hypothesis further.

Similar to other investigations of diseases in domesticated animals, the sample size in this study limited the ability to detect loci with small effect size. Future investigations should aim to utilize larger cohorts or combine complimentary datasets to harness more statistical power. Additionally, unknown environmental risk factors may have affected the analyses. Whenever feasible, cohabitating cases and controls were used to mitigate the effect of environmental variation within the analyses; however, perfectly paired cases and controls were not available from every farm. Further work is needed to determine environmental contributors specific to insidious uveitis pathology to build robust risk models and understand disease progression.

Conclusion

The analyses in this investigation identified an additional locus on ECA X as a risk factor for insidious uveitis among Appaloosas. In particular, the effect of the X locus appears to depend on *LP* genotype, such that it only confers additional risk for horses with the *LP* allele. Additional work is needed to identify and investigate potential causal variants from the ECA X locus and to characterize the functional roles of the *LP* insertion in the etiology of insidious uveitis.

Table S1: Annotation and sequence information for the 102 prioritized single-nucleotide variants and three top SNP markers from associated locus on ECA X for further investigation in a larger dataset (n = 157, 70 cases and 87 controls).

Location	REF	ALT	Variant Type	Predicted Effect	Gene(s)	Transcripts	Genomic Region	Variant
chrX_14378866	C	T	intergenic region	MODIFIER	SCML2-CDKL5	ENSECAG0000002 2025- ENSECAG0000000 7008	intergenic_region	n.14378866C>T
chrX_14379600	T	C	intergenic region	MODIFIER	SCML2-CDKL5	ENSECAG0000002 2025- ENSECAG0000000 7008	intergenic_region	n.14379600T>C

chrX_14379712	G	A	intergenic region	MODIFIER	SCML2-CDKL5	ENSECAG00000022025-ENSECAG00000007008	intergenic_region	n.14379712G>A
chrX_14415514	A	G	intergenic region	MODIFIER	SCML2-CDKL5	ENSECAG00000022025-ENSECAG00000007008	intergenic_region	n.14415514A>G
chrX_14421398	G	A	intergenic region	MODIFIER	SCML2-CDKL5	ENSECAG00000022025-ENSECAG00000007008	intergenic_region	n.14421398G>A
chrX_14422436	G	A	intergenic region	MODIFIER	SCML2-CDKL5	ENSECAG00000022025-ENSECAG00000007008	intergenic_region	n.14422436G>A
chrX_14423939	A	G	intergenic region	MODIFIER	SCML2-CDKL5	ENSECAG00000022025-ENSECAG00000007008	intergenic_region	n.14423939A>G
chrX_14424436	C	T	intergenic region	MODIFIER	SCML2-CDKL5	ENSECAG00000022025-ENSECAG00000007008	intergenic_region	n.14424436C>T
chrX_14427781	C	T	intergenic region	MODIFIER	SCML2-CDKL5	ENSECAG00000022025-ENSECAG00000007008	intergenic_region	n.14427781C>T
chrX_14443946	G	A	intergenic region	MODIFIER	SCML2-CDKL5	ENSECAG00000022025-ENSECAG00000007008	Heart_H3K4me1; intergenic_region	n.14443946G>A
chrX_14474144	C	A	upstream_gene_variant	MODIFIER	CDKL5	ENSECAG00000007008	transcript	c.-4499C>A
chrX_14527569	A	G	intron_variant	MODIFIER	CDKL5	ENSECAG00000007008	transcript	c.668-659A>G
chrX_14528106*	C	T	intron_variant	MODIFIER	CDKL5	ENSECAG00000007008	transcript	c.668-122C>T
chrX_14530368*	A	G	intron_variant	MODIFIER	CDKL5	ENSECAG00000007008	transcript	c.728-1024A>G
chrX_14533344	G	A	intron_variant	MODIFIER	CDKL5	ENSECAG00000007008	transcript	c.819-1471G>A
chrX_14533844	A	G	intron_variant	MODIFIER	CDKL5	ENSECAG00000007008	transcript	c.819-971A>G
chrX_14537812*	T	G	intron_variant	MODIFIER	CDKL5	ENSECAG00000007008	transcript	c.1008+2808T>G
chrX_14588444	A	G	intron_variant	MODIFIER	RS1	ENSECAG000000012117	transcript	c.327-307T>C
chrX_14598048	A	G	intron_variant	MODIFIER	RS1	ENSECAG000000012117	transcript	c.79-18T>C
chrX_14600567	C	G	intron_variant	MODIFIER	RS1	ENSECAG000000012117	transcript	c.53-1948G>C
chrX_14607334	T	A	upstream_gene_variant	MODIFIER	RS1	ENSECAG000000012117	transcript	c.-956A>T
chrX_14614535	G	A	intergenic region	MODIFIER	RS1-PPEF1	ENSECAG000000012117-ENSECAG000000013892	intergenic_region	n.14614535G>A
chrX_14622857	T	C	intergenic region	MODIFIER	RS1-PPEF1	ENSECAG000000012117-ENSECAG000000013892	intergenic_region	n.14622857T>C
chrX_14625236	C	T	intergenic region	MODIFIER	RS1-PPEF1	ENSECAG000000013892	transcript	n.14625236C>T
chrX_14627363	G	A	intergenic region	MODIFIER	RS1-PPEF1	ENSECAG000000013892	transcript	n.14627363G>A
chrX_14630923	G	T	intron_variant	MODIFIER	PPEF1	ENSECAG000000013892	transcript	c.-217-600G>T

chrX_146355	C	A	intron_variant	MODIFIER	PPEF1	ENSECAG0000001 3892	transcript	c.-116-3181C>A
chrX_146399	T	C	intron_variant	MODIFIER	PPEF1	ENSECAG0000001 3892	transcript	c.49+1115T>C
chrX_146414	C	G	intron_variant	MODIFIER	PPEF1	ENSECAG0000001 3892	transcript	c.49+2590C>G
chrX_146440	G	A	intron_variant	MODIFIER	PPEF1	ENSECAG0000001 3892	transcript	c.49+5209G>A
chrX_146443	A	G	intron_variant	MODIFIER	PPEF1	ENSECAG0000001 3892	transcript	c.49+5499A>G
chrX_146447	T	C	intron_variant	MODIFIER	PPEF1	ENSECAG0000001 3892	transcript	c.49+5855T>C
chrX_146462	A	G	intron_variant	MODIFIER	PPEF1	ENSECAG0000001 3892	transcript	c.49+7394A>G
chrX_146467	T	G	intron_variant	MODIFIER	PPEF1	ENSECAG0000001 3892	transcript	c.49+7844T>G
chrX_146478	C	T	intron_variant	MODIFIER	PPEF1	ENSECAG0000001 3892	transcript	c.50-8847C>T
chrX_146480	T	C	intron_variant	MODIFIER	PPEF1	ENSECAG0000001 3892	transcript	c.50-8635T>C
chrX_146486	T	G	intron_variant	MODIFIER	PPEF1	ENSECAG0000001 3892	transcript	c.50-8056T>G
chrX_146491	T	C	intron_variant	MODIFIER	PPEF1	ENSECAG0000001 3892	transcript	c.50-7550T>C
chrX_146496	T	C	intron_variant	MODIFIER	PPEF1	ENSECAG0000001 3892	transcript	c.50-7058T>C
chrX_146508	T	C	intron_variant	MODIFIER	PPEF1	ENSECAG0000001 3892	transcript	c.50-5809T>C
chrX_146509	C	G	intron_variant	MODIFIER	PPEF1	ENSECAG0000001 3892	transcript	c.50-5723C>G
chrX_146509	T	C	intron_variant	MODIFIER	PPEF1	ENSECAG0000001 3892	transcript	c.50-5685T>C
chrX_146510	A	G	intron_variant	MODIFIER	PPEF1	ENSECAG0000001 3892	transcript	c.50-5590A>G
chrX_146515	T	G	intron_variant	MODIFIER	PPEF1	ENSECAG0000001 3892	transcript	c.50-5140T>G
chrX_146522	A	G	intron_variant	MODIFIER	PPEF1	ENSECAG0000001 3892	transcript	c.50-4431A>G
chrX_146532	G	A	intron_variant	MODIFIER	PPEF1	ENSECAG0000001 3892	transcript	c.50-3464G>A
chrX_146537	A	G	intron_variant	MODIFIER	PPEF1	ENSECAG0000001 3892	transcript	c.50-2907A>G
chrX_146539	A	G	intron_variant	MODIFIER	PPEF1	ENSECAG0000001 3892	transcript	c.50-2707A>G
chrX_146548	C	T	intron_variant	MODIFIER	PPEF1	ENSECAG0000001 3892	transcript	c.50-1855C>T
chrX_146548	C	T	intron_variant	MODIFIER	PPEF1	ENSECAG0000001 3892	transcript	c.50-1828C>T
chrX_146554	A	T	intron_variant	MODIFIER	PPEF1	ENSECAG0000001 3892	transcript	c.50-1220A>T
chrX_146565	T	C	intron_variant	MODIFIER	PPEF1	ENSECAG0000001 3892	transcript	c.50-73T>C
chrX_146570	A	C	intron_variant	MODIFIER	PPEF1	ENSECAG0000001 3892	transcript	c.177+248A>C
chrX_146579	C	T	intron_variant	MODIFIER	PPEF1	ENSECAG0000001 3892	transcript	c.177+1157C>T
chrX_146583	A	G	intron_variant	MODIFIER	PPEF1	ENSECAG0000001 3892	transcript	c.178-976A>G
chrX_146591	A	G	intron_variant	MODIFIER	PPEF1	ENSECAG0000001 3892	transcript	c.178-191A>G
chrX_146591	C	G	intron_variant	MODIFIER	PPEF1	ENSECAG0000001 3892	transcript	c.178-171C>G
chrX_146597	G	C	intron_variant	MODIFIER	PPEF1	ENSECAG0000001 3892	transcript	c.238+334G>C
chrX_146598	T	C	intron_variant	MODIFIER	PPEF1	ENSECAG0000001 3892	transcript	c.238+501T>C
chrX_146600	C	T	intron_variant	MODIFIER	PPEF1	ENSECAG0000001 3892	transcript	c.238+650C>T

chrX_146623 20	G	A	intron_variant	MODIFIER	PPEF1	ENSECAG0000001 3892	Spleen_H3K4 me3; transcript	c.238+2925G >A
chrX_146624 58	C	T	intron_variant	MODIFIER	PPEF1	ENSECAG0000001 3892	Ovary_H3K4 me3; Spleen_H3K4 me3; transcript	c.238+3063C >T
chrX_146627 16	T	C	intron_variant	MODIFIER	PPEF1	ENSECAG0000001 3892	Lung_H3K4m e3; Ovary_H3K4 me3; Spleen_H3K4 me3; transcript	c.238+3321T >C
chrX_146645 03	A	G	intron_variant	MODIFIER	PPEF1	ENSECAG0000001 3892	transcript	c.239- 4549A>G
chrX_146647 68	G	A	intron_variant	MODIFIER	PPEF1	ENSECAG0000001 3892	transcript	c.239- 4284G>A
chrX_146648 39	C	T	intron_variant	MODIFIER	PPEF1	ENSECAG0000001 3892	transcript	c.239- 4213C>T
chrX_146651 60	T	C	intron_variant	MODIFIER	PPEF1	ENSECAG0000001 3892	transcript	c.239- 3892T>C
chrX_146682 06	A	G	intron_variant	MODIFIER	PPEF1	ENSECAG0000001 3892	transcript	c.239- 846A>G
chrX_146685 71	G	A	intron_variant	MODIFIER	PPEF1	ENSECAG0000001 3892	transcript	c.239- 481G>A
chrX_146696 35	A	C	intron_variant	MODIFIER	PPEF1	ENSECAG0000001 3892	transcript	c.402+420A> C
chrX_146709 19	A	G	intron_variant	MODIFIER	PPEF1	ENSECAG0000001 3892	transcript	c.402+1704A >G
chrX_146711 11	T	C	intron_variant	MODIFIER	PPEF1	ENSECAG0000001 3892	transcript	c.402+1896T >C
chrX_146714 32	T	C	intron_variant	MODIFIER	PPEF1	ENSECAG0000001 3892	transcript	c.402+2217T >C
chrX_146720 73	A	T	intron_variant	MODIFIER	PPEF1	ENSECAG0000001 3892	transcript	c.402+2858A >T
chrX_146736 15	T	C	intron_variant	MODIFIER	PPEF1	ENSECAG0000001 3892	transcript	c.403- 2784T>C
chrX_146738 37	G	A	intron_variant	MODIFIER	PPEF1	ENSECAG0000001 3892	transcript	c.403- 2562G>A
chrX_146741 83	T	C	intron_variant	MODIFIER	PPEF1	ENSECAG0000001 3892	transcript	c.403- 2216T>C
chrX_146743 71	C	G	intron_variant	MODIFIER	PPEF1	ENSECAG0000001 3892	transcript	c.403- 2028C>G
chrX_146765 09	T	C	synonymous_variant	LOW	PPEF1	ENSECAG0000001 3892	transcript	c.513T>C; p.Ile171Ile
chrX_146766 62	G	C	intron_variant	MODIFIER	PPEF1	ENSECAG0000001 3892	transcript	c.517+149G> C
chrX_146783 38	A	C	intron_variant	MODIFIER	PPEF1	ENSECAG0000001 3892	transcript	c.518- 1460A>C
chrX_146783 65	T	C	intron_variant	MODIFIER	PPEF1	ENSECAG0000001 3892	transcript	c.518- 1433T>C
chrX_146789 97	T	C	intron_variant	MODIFIER	PPEF1	ENSECAG0000001 3892	transcript	c.518- 801T>C
chrX_146790 24	C	A	intron_variant	MODIFIER	PPEF1	ENSECAG0000001 3892	transcript	c.518- 774C>A
chrX_146790 99	C	T	intron_variant	MODIFIER	PPEF1	ENSECAG0000001 3892	transcript	c.518- 699C>T
chrX_146796 30	A	G	intron_variant	MODIFIER	PPEF1	ENSECAG0000001 3892	transcript	c.518- 168A>G
chrX_146800 53	C	T	intron_variant	MODIFIER	PPEF1	ENSECAG0000001 3892	transcript	c.564+209C> T
chrX_146809 03	A	G	intron_variant	MODIFIER	PPEF1	ENSECAG0000001 3892	transcript	c.564+1059A >G
chrX_146815 48	T	C	intron_variant	MODIFIER	PPEF1	ENSECAG0000001 3892	transcript	c.564+1704T >C
chrX_146815 68	G	A	intron_variant	MODIFIER	PPEF1	ENSECAG0000001 3892	transcript	c.564+1724G >A
chrX_146817 56	T	C	intron_variant	MODIFIER	PPEF1	ENSECAG0000001 3892	transcript	c.564+1912T >C

chrX_14682696	G	A	intron_variant	MODIFIER	PPEF1	ENSECAG00000013892	transcript	c.564+2852G>A
chrX_14683719	T	G	intron_variant	MODIFIER	PPEF1	ENSECAG00000013892	transcript	c.564+3875T>G
chrX_14683765	G	A	intron_variant	MODIFIER	PPEF1	ENSECAG00000013892	transcript	c.564+3921G>A
chrX_14684127	C	T	intron_variant	MODIFIER	PPEF1	ENSECAG00000013892	transcript	c.564+4283C>T
chrX_14684419	T	A	intron_variant	MODIFIER	PPEF1	ENSECAG00000013892	transcript	c.564+4575T>A
chrX_14684820	T	C	intron_variant	MODIFIER	PPEF1	ENSECAG00000013892	transcript	c.564+4976T>C
chrX_14685052	T	C	intron_variant	MODIFIER	PPEF1	ENSECAG00000013892	transcript	c.564+5208T>C
chrX_14685324	T	G	intron_variant	MODIFIER	PPEF1	ENSECAG00000013892	transcript	c.564+5480T>G
chrX_14685338	T	C	intron_variant	MODIFIER	PPEF1	ENSECAG00000013892	transcript	c.564+5494T>C
chrX_14686000	A	G	intron_variant	MODIFIER	PPEF1	ENSECAG00000013892	transcript	c.564+6156A>G
chrX_14686145	T	C	intron_variant	MODIFIER	PPEF1	ENSECAG00000013892	transcript	c.564+6301T>C
chrX_14686546	C	G	intron_variant	MODIFIER	PPEF1	ENSECAG00000013892	transcript	c.564+6702C>G
chrX_14686598	A	G	intron_variant	MODIFIER	PPEF1	ENSECAG00000013892	transcript	c.564+6754A>G
chrX_14686738	T	A	intron_variant	MODIFIER	PPEF1	ENSECAG00000013892	transcript	c.565-6793T>A

* Denotes significantly associated SNPs from MLM with *LP*, sex, age, and relatedness as covariates

Table S2: Results from logistic regression analysis for 102 prioritized single-nucleotide variants, two SNP markers from ECA 1, *LP*, *PATN1*, and three SNP markers from associated locus on ECA X investigated in a larger dataset (n = 157, 70 cases and 87 controls). Beta, standard error, and p-value from Wald test of significance were reported for logistic regression with age and sex as covariates (denoted with “1”) and for logistic regression with age, sex, and *LP* genotype as covariates (denoted with “2”).

chr	position	N miss	Minor Allele	Major Allele	Allele freq	beta_1	se_1	p_wald_1	beta_2	se_2	p_wald_2
1	2453754	0	T	C	0.092	2.31E-01	1.32E-01	8.29E-02	2.06E-01	9.82E-02	3.71E-02
1	109211964	0	<i>lp</i>	<i>LP</i>	0.478	-3.20E-01	6.53E-02	2.34E-06	n/a	n/a	n/a
1	171786187	0	G	A	0.204	1.58E-01	9.60E-02	1.02E-01	1.88E-01	6.47E-02	4.22E-03
3	24352525	0	<i>PATN1</i>	<i>patn1</i>	0.207	6.50E-02	1.01E-01	5.20E-01	3.45E-02	7.50E-02	6.46E-01
X	14325195	0	A	G	0.197	-2.99E-02	8.57E-02	7.28E-01	-1.18E-02	6.25E-02	8.51E-01
X	14348894	0	T	C	0.35	2.52E-02	7.11E-02	7.24E-01	2.68E-02	5.18E-02	6.06E-01
X	14378866	0	T	C	0.255	7.10E-02	1.23E-01	5.64E-01	6.70E-02	8.75E-02	4.45E-01
X	14379600	0	C	T	0.255	7.10E-02	1.23E-01	5.64E-01	6.70E-02	8.75E-02	4.45E-01
X	14379712	0	A	G	0.067	1.15E-02	1.59E-01	9.42E-01	-2.60E-02	1.12E-01	8.17E-01
X	14415514	0	G	A	0.175	5.32E-02	1.94E-01	7.85E-01	-8.16E-03	1.36E-01	9.52E-01
X	14421398	0	A	G	0.344	-1.00E-01	1.13E-01	3.76E-01	-7.53E-02	7.68E-02	3.28E-01
X	14422436	0	A	G	0.226	-7.74E-03	1.39E-01	9.56E-01	-5.10E-03	9.01E-02	9.55E-01
X	14423939	0	G	A	0.223	-7.25E-02	1.36E-01	5.95E-01	-3.40E-02	8.95E-02	7.05E-01
X	14424436	0	T	C	0.223	4.25E-02	1.38E-01	7.58E-01	1.85E-02	8.95E-02	8.36E-01
X	14427781	0	T	C	0.318	-2.68E-02	1.05E-01	7.99E-01	-3.45E-02	7.27E-02	6.36E-01

X	14443946	0	A	G	0.344	-7.43E-02	1.11E-01	5.05E-01	-7.11E-02	7.63E-02	3.53E-01
X	14474144	0	A	C	0.175	5.32E-02	1.94E-01	7.85E-01	-8.16E-03	1.36E-01	9.52E-01
X	14502474	0	G	A	0.303	-7.49E-02	9.12E-02	4.13E-01	-5.26E-02	6.45E-02	4.16E-01
X	14505483	1	G	C	0.394	4.63E-02	8.73E-02	5.97E-01	4.29E-02	6.21E-02	4.90E-01
X	14527569	0	G	A	0.175	5.32E-02	1.94E-01	7.85E-01	-8.16E-03	1.36E-01	9.52E-01
X	14528106	0	C	T	0.379	4.20E-02	1.11E-01	7.07E-01	1.74E-01	4.12E-02	4.14E-05
X	14530368	1	G	A	0.41	-1.78E-01	9.85E-02	7.23E-02	-2.00E-01	4.74E-02	4.06E-05
X	14533344	0	A	G	0.166	8.51E-02	1.38E-01	5.39E-01	8.59E-02	8.85E-02	3.34E-01
X	14533844	0	G	A	0.169	3.04E-02	1.33E-01	8.20E-01	5.85E-02	8.72E-02	5.03E-01
X	14537812	0	T	G	0.382	5.76E-02	1.12E-01	6.08E-01	1.73E-01	4.10E-02	4.13E-05
X	14588444	0	G	A	0.357	-7.98E-02	9.81E-02	4.18E-01	-8.94E-02	6.38E-02	1.63E-01
X	14590603	0	T	C	0.299	1.35E-02	1.05E-01	8.98E-01	-4.01E-03	7.25E-02	9.56E-01
X	14598048	0	A	G	0.287	-1.64E-02	1.27E-01	8.97E-01	3.25E-05	8.63E-02	1.00E+00
X	14600092	0	T	C	0.455	-7.23E-02	1.17E-01	5.36E-01	-5.12E-02	7.75E-02	5.09E-01
X	14600567	0	C	G	0.455	-7.23E-02	1.17E-01	5.36E-01	-5.12E-02	7.75E-02	5.09E-01
X	14607334	0	T	A	0.28	-6.14E-02	1.35E-01	6.49E-01	-1.86E-02	9.00E-02	8.36E-01
X	14614535	0	A	G	0.331	-1.30E-01	1.08E-01	2.30E-01	-1.16E-01	6.89E-02	9.43E-02
X	14622857	0	C	T	0.303	2.63E-01	2.86E-01	3.60E-01	1.89E-01	1.85E-01	3.08E-01
X	14625236	0	T	C	0.255	2.17E-01	1.79E-01	2.26E-01	1.69E-01	1.37E-01	2.19E-01
X	14627363	0	A	G	0.268	1.28E-01	1.23E-01	3.01E-01	1.14E-01	9.93E-02	2.53E-01
X	14630923	0	G	T	0.497	-7.69E-03	1.68E-01	9.64E-01	-4.59E-02	1.11E-01	6.81E-01
X	14635535	0	C	A	0.49	-5.05E-02	1.97E-01	7.98E-01	-6.42E-02	1.20E-01	5.92E-01
X	14639995	0	C	T	0.115	2.08E-01	1.72E-01	2.29E-01	1.53E-01	1.19E-01	2.02E-01
X	14641470	0	G	C	0.296	-9.81E-02	1.31E-01	4.56E-01	-7.57E-02	1.01E-01	4.55E-01
X	14644089	0	A	G	0.303	2.63E-01	2.86E-01	3.60E-01	1.89E-01	1.85E-01	3.08E-01
X	14644379	0	G	A	0.303	2.63E-01	2.86E-01	3.60E-01	1.89E-01	1.85E-01	3.08E-01
X	14644735	0	C	T	0.268	-3.54E-02	1.98E-01	8.58E-01	3.22E-03	1.34E-01	9.81E-01
X	14646274	0	G	A	0.28	-9.56E-03	1.77E-01	9.57E-01	1.04E-02	1.35E-01	9.39E-01
X	14646724	0	G	T	0.303	2.63E-01	2.86E-01	3.60E-01	1.89E-01	1.85E-01	3.08E-01
X	14647817	0	C	T	0.49	-5.05E-02	1.97E-01	7.98E-01	-6.42E-02	1.20E-01	5.92E-01
X	14648029	0	C	T	0.264	-3.46E-03	2.15E-01	9.87E-01	1.43E-02	1.41E-01	9.19E-01
X	14648608	0	G	T	0.303	2.63E-01	2.86E-01	3.60E-01	1.89E-01	1.85E-01	3.08E-01
X	14649114	0	T	C	0.315	6.82E-02	1.32E-01	6.06E-01	5.58E-02	8.98E-02	5.35E-01
X	14649606	0	T	C	0.481	-8.97E-02	1.56E-01	5.66E-01	-9.41E-02	1.06E-01	3.75E-01
X	14650855	0	C	T	0.268	-5.99E-02	2.27E-01	7.92E-01	1.40E-03	1.48E-01	9.92E-01
X	14650941	0	G	C	0.306	1.69E-01	2.85E-01	5.53E-01	1.65E-01	1.84E-01	3.70E-01
X	14650979	0	C	T	0.306	1.69E-01	2.85E-01	5.53E-01	1.65E-01	1.84E-01	3.70E-01
X	14651074	0	G	A	0.306	1.69E-01	2.85E-01	5.53E-01	1.65E-01	1.84E-01	3.70E-01
X	14651524	0	G	T	0.309	7.62E-02	2.45E-01	7.57E-01	1.25E-01	1.68E-01	4.61E-01

X	14652233	0	G	A	0.306	1.69E-01	2.85E-01	5.53E-01	1.65E-01	1.84E-01	3.70E-01
X	14653200	0	G	A	0.417	9.98E-02	1.23E-01	4.18E-01	1.33E-01	7.57E-02	8.06E-02
X	14653757	0	G	A	0.293	2.44E-01	2.63E-01	3.54E-01	1.41E-01	1.85E-01	4.45E-01
X	14653957	0	G	A	0.296	1.11E-01	3.39E-01	7.44E-01	6.01E-02	2.09E-01	7.74E-01
X	14654809	0	T	C	0.258	-1.38E-01	2.45E-01	5.75E-01	-8.48E-02	1.59E-01	5.95E-01
X	14654836	0	T	C	0.296	1.11E-01	3.39E-01	7.44E-01	6.01E-02	2.09E-01	7.74E-01
X	14655444	0	T	A	0.296	1.11E-01	3.39E-01	7.44E-01	6.01E-02	2.09E-01	7.74E-01
X	14656591	0	C	T	0.293	4.60E-02	2.71E-01	8.65E-01	3.10E-02	1.87E-01	8.69E-01
X	14657039	2	C	A	0.261	-2.95E-01	2.32E-01	2.06E-01	-1.65E-01	1.59E-01	3.00E-01
X	14657948	0	T	C	0.296	1.11E-01	3.39E-01	7.44E-01	6.01E-02	2.09E-01	7.74E-01
X	14658359	0	G	A	0.252	-3.88E-01	1.82E-01	3.41E-02	-2.70E-01	1.40E-01	5.62E-02
X	14659144	0	A	G	0.5	-8.60E-03	2.00E-01	9.66E-01	-1.42E-02	1.20E-01	9.06E-01
X	14659164	0	G	C	0.296	1.11E-01	3.39E-01	7.44E-01	6.01E-02	2.09E-01	7.74E-01
X	14659729	0	C	G	0.277	-1.35E-01	1.93E-01	4.86E-01	-9.61E-02	1.51E-01	5.24E-01
X	14659896	0	C	T	0.258	-1.38E-01	2.45E-01	5.75E-01	-8.48E-02	1.59E-01	5.95E-01
X	14660045	0	T	C	0.296	1.11E-01	3.39E-01	7.44E-01	6.01E-02	2.09E-01	7.74E-01
X	14662320	0	A	G	0.296	1.11E-01	3.39E-01	7.44E-01	6.01E-02	2.09E-01	7.74E-01
X	14662458	0	T	C	0.258	-1.38E-01	2.45E-01	5.75E-01	-8.48E-02	1.59E-01	5.95E-01
X	14662716	0	C	T	0.296	1.11E-01	3.39E-01	7.44E-01	6.01E-02	2.09E-01	7.74E-01
X	14664503	0	G	A	0.258	-1.38E-01	2.45E-01	5.75E-01	-8.48E-02	1.59E-01	5.95E-01
X	14664768	0	A	G	0.296	1.11E-01	3.39E-01	7.44E-01	6.01E-02	2.09E-01	7.74E-01
X	14664839	0	C	T	0.5	-8.60E-03	2.00E-01	9.66E-01	-1.42E-02	1.20E-01	9.06E-01
X	14665160	0	C	T	0.296	1.11E-01	3.39E-01	7.44E-01	6.01E-02	2.09E-01	7.74E-01
X	14668206	0	G	A	0.287	-2.93E-01	2.39E-01	2.21E-01	-2.29E-01	1.81E-01	2.08E-01
X	14668571	0	A	G	0.287	-2.93E-01	2.39E-01	2.21E-01	-2.29E-01	1.81E-01	2.08E-01
X	14669635	0	C	A	0.204	-1.86E-01	4.08E-01	6.50E-01	-1.58E-01	2.31E-01	4.95E-01
X	14670919	0	G	A	0.236	-4.05E-02	1.52E-01	7.90E-01	-8.41E-02	1.20E-01	4.83E-01
X	14671111	0	C	T	0.204	-1.86E-01	4.08E-01	6.50E-01	-1.58E-01	2.31E-01	4.95E-01
X	14671432	0	C	T	0.204	-4.59E-01	2.55E-01	7.39E-02	-2.94E-01	1.89E-01	1.23E-01
X	14672073	0	T	A	0.204	-1.86E-01	4.08E-01	6.50E-01	-1.58E-01	2.31E-01	4.95E-01
X	14673615	0	C	T	0.204	-1.86E-01	4.08E-01	6.50E-01	-1.58E-01	2.31E-01	4.95E-01
X	14673837	0	A	G	0.204	-1.86E-01	4.08E-01	6.50E-01	-1.58E-01	2.31E-01	4.95E-01
X	14674183	0	C	T	0.204	-1.86E-01	4.08E-01	6.50E-01	-1.58E-01	2.31E-01	4.95E-01
X	14674371	0	G	C	0.204	-1.86E-01	4.08E-01	6.50E-01	-1.58E-01	2.31E-01	4.95E-01
X	14676509	0	T	C	0.49	-5.05E-02	1.97E-01	7.98E-01	-6.42E-02	1.20E-01	5.92E-01
X	14676662	0	C	G	0.204	-1.86E-01	4.08E-01	6.50E-01	-1.58E-01	2.31E-01	4.95E-01
X	14678338	0	C	A	0.204	-1.86E-01	4.08E-01	6.50E-01	-1.58E-01	2.31E-01	4.95E-01
X	14678365	0	C	T	0.204	-1.86E-01	4.08E-01	6.50E-01	-1.58E-01	2.31E-01	4.95E-01
X	14678997	0	C	T	0.204	-1.86E-01	4.08E-01	6.50E-01	-1.58E-01	2.31E-01	4.95E-01

X	14679024	0	A	C	0.204	-1.86E-01	4.08E-01	6.50E-01	-1.58E-01	2.31E-01	4.95E-01
X	14679099	0	T	C	0.207	-3.14E-01	2.99E-01	2.95E-01	-2.41E-01	2.05E-01	2.42E-01
X	14679630	0	G	A	0.204	-1.86E-01	4.08E-01	6.50E-01	-1.58E-01	2.31E-01	4.95E-01
X	14680053	0	T	C	0.204	-1.86E-01	4.08E-01	6.50E-01	-1.58E-01	2.31E-01	4.95E-01
X	14680903	0	A	G	0.5	-8.60E-03	2.00E-01	9.66E-01	-1.42E-02	1.20E-01	9.06E-01
X	14681548	0	C	T	0.21	-4.84E-01	2.57E-01	6.12E-02	-3.36E-01	1.93E-01	8.25E-02
X	14681568	0	G	A	0.5	-8.60E-03	2.00E-01	9.66E-01	-1.42E-02	1.20E-01	9.06E-01
X	14681756	0	C	T	0.207	1.63E-01	3.06E-01	5.95E-01	1.75E-02	2.07E-01	9.33E-01
X	14682696	0	A	G	0.204	-1.86E-01	4.08E-01	6.50E-01	-1.58E-01	2.31E-01	4.95E-01
X	14683719	0	G	T	0.204	-1.86E-01	4.08E-01	6.50E-01	-1.58E-01	2.31E-01	4.95E-01
X	14683765	0	A	G	0.204	-1.86E-01	4.08E-01	6.50E-01	-1.58E-01	2.31E-01	4.95E-01
X	14684127	0	T	C	0.201	-3.61E-01	3.00E-01	2.30E-01	-2.57E-01	2.02E-01	2.04E-01
X	14684419	0	A	T	0.207	1.63E-01	3.06E-01	5.95E-01	1.75E-02	2.07E-01	9.33E-01
X	14684820	0	C	T	0.204	-1.86E-01	4.08E-01	6.50E-01	-1.58E-01	2.31E-01	4.95E-01
X	14685052	0	C	T	0.204	-1.86E-01	4.08E-01	6.50E-01	-1.58E-01	2.31E-01	4.95E-01
X	14685324	0	G	T	0.204	-1.86E-01	4.08E-01	6.50E-01	-1.58E-01	2.31E-01	4.95E-01
X	14685338	0	C	T	0.204	-1.86E-01	4.08E-01	6.50E-01	-1.58E-01	2.31E-01	4.95E-01
X	14686000	0	G	A	0.204	-1.86E-01	4.08E-01	6.50E-01	-1.58E-01	2.31E-01	4.95E-01
X	14686145	0	T	C	0.5	-8.60E-03	2.00E-01	9.66E-01	-1.42E-02	1.20E-01	9.06E-01
X	14686546	1	G	C	0.205	-3.58E-01	3.85E-01	3.54E-01	-2.43E-01	2.29E-01	2.90E-01
X	14686598	0	A	G	0.5	-8.60E-03	2.00E-01	9.66E-01	-1.42E-02	1.20E-01	9.06E-01
X	14686738	0	T	A	0.5	-8.60E-03	2.00E-01	9.66E-01	-1.42E-02	1.20E-01	9.06E-01
X	14722726	2	A	G	0.423	2.79E-02	1.18E-01	8.14E-01	6.41E-02	8.43E-02	4.48E-01
X	14724832	2	C	T	0.406	5.16E-02	9.99E-02	6.07E-01	3.26E-02	7.13E-02	6.48E-01

Acknowledgements:

The authors would like to acknowledge the horse owners who participated in this research project and made this study possible. The authors would also like to recognize the technical assistance from Maura Mack, Hrair Zeitounian, Elizabeth Esdaile, and other members of the UC Davis Veterinary Genetics Laboratory. We graciously acknowledge the contribution of Drs. Henneke Hermans and Thomas Launois who provided clinical cases for this investigation. The research was supported by the Townsend Equine Health Research Fund (TEHRF) and the Morris Animal Foundation (D16EQ-028). The mission of the Morris Animal Foundation is to bridge science and

resources to advance the health of animals. N. B. Kingsley was also supported in part by the University of California – Davis, Center for Equine Health Fellowship.

Conflict of Interest:

N. B. Kingsley and R. R. Bellone are affiliated with the UC Davis Veterinary Genetics Laboratory, a service laboratory offering diagnostic genetic tests for horses and other animal species.

Availability of data:

The genotyping data from 96 Appaloosas used in this study are available at Open Science Framework (MAP and PED files originally from Kingsley *et al.* 2022)⁸: <https://osf.io/v6s4f/>. WGS data are available upon reasonable request from the corresponding author.

References:

1. Sandmeyer LS, Bauer BS, Feng CX, Grahn BH. Equine recurrent uveitis in western Canadian prairie provinces : A retrospective study (2002–2015). *Can Vet J.* 2017;58:717-722.
2. Gerding JC, Gilger BC. Prognosis and impact of equine recurrent uveitis. *Equine Vet J.* 2016;48(3):290-298. doi:10.1111/evj.12451
3. Gilger BC, Deeg CA. Equine recurrent uveitis. In: Gilger BC, ed. *Equine Ophthalmology*. 2nd ed. Elsevier Saunders; 2011:317-349.
4. Dwyer A, Gilger BC. Equine Recurrent Uveitis. In: Gilger BC, ed. *Equine Ophthalmology*. 2nd ed. Elsevier Saunders; 2005:285-322. doi:10.1016/B0-72-160522-2/50010-8
5. Gilger BC. Recurrent Uveitis. In: Felipe M, ed. *Equine Clinical Immunology*. John Wiley & Sons, Ltd; 2016:121-126.
6. Dwyer AE, Crockett RS, Kalsow CM. Association of leptospiral seroreactivity and breed with uveitis and blindness in horses: 372 cases (1986-1993). *J Am Vet Med Assoc.* 1995;207(10):1327-1331. <http://www.ncbi.nlm.nih.gov/pubmed/7591929>
7. Fritz KL, Kaese HJ, Valberg SJ, et al. Genetic risk factors for insidious equine recurrent uveitis in Appaloosa horses. *Anim Genet.* 2014;45(3):392-399. doi:10.1111/age.12129
8. Kingsley NB, Sandmeyer LS, Norton E, et al. Heritability of Insidious Uveitis in Appaloosa Horses. *Anim Genet.* 2022; Accepted.

9. Bellone RR, Forsyth G, Leeb T, et al. Fine-mapping and mutation analysis of *TRPM1*: A candidate gene for leopard complex (LP) spotting and congenital stationary night blindness in horses. *Briefings Funct Genomics Proteomics*. 2010;9(3):193-207. doi:10.1093/bfgp/elq002
10. Bellone RR, Holl H, Setaluri V, et al. Evidence for a Retroviral Insertion in *TRPM1* as the Cause of Congenital Stationary Night Blindness and Leopard Complex Spotting in the Horse. *PLoS One*. 2013;8(10):1-14. doi:10.1371/journal.pone.0078280
11. Schneider FM, Mohr F, Behrendt M, Oberwinkler J. Properties and functions of TRPM1 channels in the dendritic tips of retinal ON-bipolar cells. *Eur J Cell Biol*. 2015;94(7-9):420-427. doi:10.1016/j.ejcb.2015.06.005
12. Bellone RR, Brooks SA, Sandmeyer L, et al. Differential gene expression of *TRPM1*, the potential cause of congenital stationary night blindness and coat spotting patterns (LP) in the Appaloosa horse (*Equus caballus*). *Genetics*. 2008;179(4):1861-1870. doi:10.1534/genetics.108.088807
13. Rockwell H, Mack M, Famula T, et al. Genetic investigation of equine recurrent uveitis in Appaloosa horses. *Anim Genet*. 2020;51(1):111-116. doi:10.1111/age.12883
14. Brewerton DA, Nicholls A, Caffrey M, Walters D, James DCO. ACUTE ANTERIOR UVEITIS AND HL-A 27. *Lancet*. 1973;302(7836):994-996. doi:10.1016/S0140-6736(73)91090-8
15. Deeg CA, Marti E, Gaillard C, Kaspers B. Equine recurrent uveitis is strongly associated with the MHC class I haplotype ELA-A9. *Equine Vet J*. 2004;36(1):73-75. doi:10.2746/0425164044864651
16. Martin TM, Rosenbaum JT. An update on the genetics of HLA-B27 associated acute anterior uveitis. *Ocul Immunol Inflamm*. 2011;19(2):108-114. doi:10.3109/09273948.2011.559302
17. Kulbrock M, Lehner S, Metzger J, Ohnesorge B, Distl O. A Genome-Wide Association Study Identifies Risk Loci to Equine Recurrent Uveitis in German Warmblood Horses. *PLoS One*. 2013;8(8):1-6. doi:10.1371/journal.pone.0071619
18. Sandmeyer LS, Kingsley NB, Walder C, et al. Risk factors for equine recurrent uveitis in a population of Appaloosa horses in western Canada. *Vet Ophthalmol*. 2020;23(3):515-525. doi:10.1111/vop.12749

19. Bellone RR, Liu J, Petersen JL, et al. A missense mutation in damage-specific DNA binding protein 2 is a genetic risk factor for limbal squamous cell carcinoma in horses. *Int J Cancer*. 2017;141:342-353. doi:10.1002/ijc.30744
20. Schaefer RJ, Schubert M, Bailey E, et al. Developing a 670k genotyping array to tag ~2M SNPs across 24 horse breeds. *BMC Genomics*. 2017;18(1):1-18. doi:10.1186/s12864-017-3943-8
21. Purcell S, Neale B, Todd-Brown K, et al. PLINK: A tool set for whole-genome association and population-based linkage analyses. *Am J Hum Genet*. 2007;81(3):559-575. doi:10.1086/519795
22. Zhou X, Stephens M. Genome-wide Efficient Mixed Model Analysis for Association Studies. *Nat Genet*. 2012;44(7):821-824. doi:10.1038/ng.2310
23. Li MX, Yeung JMY, Cherny SS, Sham PC. Evaluating the effective numbers of independent tests and significant p-value thresholds in commercial genotyping arrays and public imputation reference datasets. *Hum Genet*. 2012;131(5):747-756. doi:10.1007/s00439-011-1118-2
24. McCoy AM, Norton EM, Kemper AM, Beeson SK, Mickelson JR, McCue ME. SNP-based heritability and genetic architecture of tarsal osteochondrosis in North American Standardbred horses. *Anim Genet*. 2019;50(1):78-81. doi:10.1111/age.12738
25. Norton E, Schultz N, Geor R, McFarlane D, Mickelson J, McCue M. Genome-wide association analyses of equine metabolic syndrome phenotypes in welsh ponies and morgan horses. *Genes (Basel)*. 2019;10(11):1-23. doi:10.3390/genes10110893
26. Deng M, Li D, Luo J, et al. The genetic architecture of amino acids dissection by association and linkage analysis in maize. *Plant Biotechnol J*. 2017;15(10):1250-1263. doi:10.1111/pbi.12712
27. Cui Z, Luo J, Qi C, et al. Genome-wide association study (GWAS) reveals the genetic architecture of four husk traits in maize. *BMC Genomics*. 2016;17(1). doi:10.1186/s12864-016-3229-6
28. Yang W, Guo Z, Huang C, et al. Combining high-throughput phenotyping and genome-wide association studies to reveal natural genetic variation in rice. *Nat Commun*. 2014;5:1-9. doi:10.1038/ncomms6087
29. Zhao H, Nyholt DR, Yang Y, Wang J, Yang Y. Improving the detection of pathways in

- genome-wide association studies by combined effects of SNPs from Linkage Disequilibrium blocks. *Sci Rep.* 2017;7(1):1-8. doi:10.1038/s41598-017-03826-2
30. Bovo S, Mazzoni G, Bertolini F, et al. Genome-wide association studies for 30 haematological and blood clinical-biochemical traits in Large White pigs reveal genomic regions affecting intermediate phenotypes. *Sci Rep.* 2019;9(1):1-17. doi:10.1038/s41598-019-43297-1
 31. Norton EM, Avila F, Schultz NE, Mickelson JR, Geor RJ, McCue ME. Evaluation of an HMGA2 variant for pleiotropic effects on height and metabolic traits in ponies. *J Vet Intern Med.* 2019;33(2):942-952. doi:10.1111/jvim.15403
 32. Hayward JJ, White ME, Boyle M, et al. Imputation of canine genotype array data using 365 whole-genome sequences improves power of genome-wide association studies. *PLoS Genet.* 2019;15(9):1-21. doi:10.1371/journal.pgen.1008003
 33. Hess R, Henthorn P, Devoto M, Wang F, Feng R. An exploratory association analysis of the insulin gene region with diabetes mellitus in two dog breeds. *J Hered.* 2019;110(7):793-800. doi:10.1093/jhered/esz059
 34. Han H, McGivney BA, Farries G, et al. Selection in Australian Thoroughbred horses acts on a locus associated with early two-year old speed. *PLoS One.* 2020;15(2):1-21. doi:10.1371/journal.pone.0227212
 35. Guo S, Zhao S, Sun H, et al. Resequencing of 414 cultivated and wild watermelon accessions identifies selection for fruit quality traits. *Nat Genet.* 2019;51(11):1616-1623. doi:10.1038/s41588-019-0518-4
 36. Lai E, Danner AL, Famula TR, Oberbauer AM. Genome-wide association studies reveal susceptibility loci for digital dermatitis in holstein cattle. *Animals.* 2020;10(11):1-22. doi:10.3390/ani10112009
 37. Jiang S, Zhang H, Ni P, et al. Genome-Wide Association Study Dissects the Genetic Architecture of Maize Husk Tightness. *Front Plant Sci.* 2020;11. doi:10.3389/fpls.2020.00861
 38. Gershony LC, Belanger JM, Hytönen MK, Lohi H, Famula TR, Oberbauer AM. Genetic characterization of Addison's disease in Bearded Collies. *BMC Genomics.* 2020;21(1):1-13. doi:10.1186/s12864-020-07243-0
 39. Lai E, Danner AL, Famula TR, Oberbauer AM. Genome-Wide Association Studies Reveal

- Susceptibility Loci for Noninfectious Claw Lesions in Holstein Dairy Cattle. *Front Genet.* 2021;12. doi:10.3389/fgene.2021.657375
40. Hisey EA, Hermans H, Lounsberry ZT, et al. Whole genome sequencing identified a 16 kilobase deletion on ECA13 associated with distichiasis in Friesian horses. *BMC Genomics.* 2020;21(1):1-13. doi:10.1186/s12864-020-07265-8
 41. Ricard A, Duluard A. Genomic analysis of gaits and racing performance of the French trotter. *J Anim Breed Genet.* 2021;138(2):204-222. doi:10.1111/jbg.12526
 42. Bitaraf Sani M, Zare Harofte J, Banabazi MH, et al. Genomic prediction for growth using a low-density SNP panel in dromedary camels. *Sci Rep.* 2021;11(1):1-14. doi:10.1038/s41598-021-87296-7
 43. Lai E, Danner AL, Famula TR, Oberbauer AM. Pleiotropic Loci Associated With Foot Disorders and Common Periparturient Diseases in Holstein Cattle. *Front Genet.* 2021;12:1-11. doi:10.3389/fgene.2021.742934
 44. Norton EM, Minor KM, Taylor SM, McCue ME, Mickelson JR. Heritability and genomic architecture of episodic exercise-induced collapse in border collies. *Genes (Basel).* 2021;12(12). doi:10.3390/genes12121927
 45. Zhao J, Sauvage C, Bitton F, Causse M. Multiple haplotype-based analyses provide genetic and evolutionary insights into tomato fruit weight and composition. *Hortic Res.* 2022;9. doi:10.1093/hr/uhab009
 46. Hu D, He S, Jia Y, et al. Genome-wide association study for seedling biomass-related traits in *Gossypium arboreum* L. *BMC Plant Biol.* 2022;22(1):1-12. doi:10.1186/s12870-022-03443-w
 47. Li H, Wang S, Chai S, et al. Graph-based pan-genome reveals structural and sequence variations related to agronomic traits and domestication in cucumber. *Nat Commun.* 2022;13(1):1-14. doi:10.1038/s41467-022-28362-0
 48. Willer CJ, Li Y, Abecasis GR. METAL: Fast and efficient meta-analysis of genomewide association scans. *Bioinformatics.* 2010;26(17):2190-2191. doi:10.1093/bioinformatics/btq340
 49. Zhang J, Boos DD. Generalized Cochran-Mantel-Haenszel test statistics for correlated categorical data. *Commun Stat - Theory Methods.* 1997;26(8):1813-1837. doi:10.1080/03610929708832016

50. Team RC. R: A language and environment for statistical computing. Published online 2018.
51. Settles M. HTStream. <https://github.com/s4hts/HTStream>
52. Li H, Durbin R. Fast and accurate short read alignment with Burrows-Wheeler transform. *Bioinformatics*. 2009;25(14):1754-1760. doi:10.1093/bioinformatics/btp324
53. Li H, Handsaker B, Wysoker A, et al. The Sequence Alignment/Map format and SAMtools. *Bioinformatics*. 2009;25(16):2078-2079. doi:10.1093/bioinformatics/btp352
54. Garrison E, Marth G. Haplotype-based variant detection from short-read sequencing. *arXiv*. Published online 2012:1-9. <http://arxiv.org/abs/1207.3907>
55. Kingsley NB, Kern C, Creppe C, et al. Functionally Annotating Regulatory Elements in the Equine Genome Using Histone Mark ChIP-Seq. *Genes (Basel)*. 2020;11(1):3. doi:10.3390/genes11010003
56. Kingsley NB, Hamilton NA, Lindgren G, et al. “Adopt-a-Tissue” Initiative Advances Efforts to Identify Tissue-Specific Histone Marks in the Mare. *Front Genet*. 2021;12(March):1-9. doi:10.3389/fgene.2021.649959
57. Cingolani P, Platts A, Wang LL, et al. A program for annotating and predicting the effects of single nucleotide polymorphisms, SnpEff. *Fly (Austin)*. 2012;6(2):80-92. doi:10.4161/fly.19695
58. Benson DA, Cavanaugh M, Clark K, et al. GenBank. *Nucleic Acids Res*. 2013;41(D1):36-42. doi:10.1093/nar/gks1195
59. van Genderen MM, Bijveld MMC, Claassen YB, et al. Mutations in *TRPM1* Are a Common Cause of Complete Congenital Stationary Night Blindness. *Am J Hum Genet*. 2009;85(5):730-736. doi:10.1016/j.ajhg.2009.10.012
60. AlTalbish A, Zelinger L, Zeitz C, et al. TRPM1 Mutations are the Most Common Cause of Autosomal Recessive Congenital Stationary Night Blindness (CSNB) in the Palestinian and Israeli Populations. *Sci Rep*. 2019;9(1):1-6. doi:10.1038/s41598-019-46811-7
61. Hirsch Y, Zeevi DA, Lam BL, et al. A founder deletion in the *TRPM1* gene associated with congenital stationary night blindness and myopia is highly prevalent in Ashkenazi Jews. *Hum Genome Var*. 2019;6(1). doi:10.1038/s41439-019-0076-4
62. Koike C, Obara T, Uriu Y, et al. TRPM1 is a component of the retinal ON bipolar cell transduction channel in the mGluR6 cascade. *Proc Natl Acad Sci U S A*. 2010;107(1):332-337. doi:10.1073/pnas.0912730107

63. Chiang J, Pei W, Luo H, Duan J, Ekstein J, Hirsch Y. Founder Ashkenazi Jewish mutations of large deletion in the inherited retinal dystrophy genes. *Ophthalmic Genet.* 2018;39(1):135-136. doi:10.1080/13816810.2017.1318928
64. Amendola E, Zhan Y, Mattucci C, et al. Mapping pathological phenotypes in a mouse model of CDKL5 disorder. *PLoS One.* 2014;9(5):5-16. doi:10.1371/journal.pone.0091613
65. Ramulu P, Kennedy M, Xiong W-H, et al. Normal Light Response, Photoreceptor Integrity, and Rhodopsin Dephosphorylation in Mice Lacking Both Protein Phosphatases with EF Hands (PPEF-1 and PPEF-2). *Mol Cell Biol.* 2001;21(24):8605-8614. doi:10.1128/mcb.21.24.8605-8614.2001
66. Sherman PM, Sun H, Macke JP, Williams J, Smallwood PM, Nathans J. Identification and characterization of a conserved family of protein serine/threonine phosphatases homologous to Drosophila retinal degeneration C (rdgC). *Proc Natl Acad Sci U S A.* 1997;94(21):11639-11644. doi:10.1073/pnas.94.21.11639
67. Wang T, Waters CT, Rothman AMK, Jankins TJ, Römisch K, Trump D. Intracellular retention of mutant retinoschisin is the pathological mechanism underlying X-linked retinoschisis. *Hum Mol Genet.* 2002;11(24):3097-3105. doi:10.1093/hmg/11.24.3097
68. Reid SNM, Yamashita C, Farber DB. Retinoschisin, a photoreceptor-secreted protein, and its interaction with bipolar and Müller cells. *J Neurosci.* 2003;23(14):6030-6040. doi:10.1523/jneurosci.23-14-06030.2003
69. Ou J, Vijayasarathy C, Ziccardi L, et al. Synaptic pathology and therapeutic repair in adult retinoschisis mouse by AAV-RS1 transfer. *J Clin Invest.* 2015;125(7):2891-2903. doi:10.1172/JCI81380

Chapter 5: Risk Factors for Equine Recurrent Uveitis in the Knabstrupper Breed

Authors: N. B. Kingsley*, Lynne Sandmeyer*, Sarah Parker, Ann Dwyer, Sanna Heden, Camilla Reilly, Anna Hallendar-Edman, Sheila Archer, and Rebecca R. Bellone

Keywords: insidious uveitis, horse, ocular, leopard complex, ERU, inflammation

Reference: Kingsley, N.B.*; Sandmeyer, L.*; Parker, S.; Dwyer, A.; Heden, S.; Reilly, C.; Hallendar-Edman, A.; Archer, S.; Bellone, R.R. Risk Factors for Equine Recurrent Uveitis in the Knabstrupper Breed. *EVJ*. Submitted 2022.

* Denotes equal contributions

Submitted: April 29, 2022

Summary

Background

Equine recurrent uveitis (ERU) is the leading cause of blindness for horses; previous research implicated the leopard complex spotting allele (*LP*) as a genetic risk factor in the Appaloosa. There is limited information about risk in the Knabstrupper.

Objective

To evaluate clinical manifestations, disease frequency, and potential risk factors for ERU in Knabstrupper horses.

Study Design

Cross-sectional study

Methods

Ocular examinations were performed on 116 horses and identified anomalies classified horses as suspect, ERU-affected, or having no clinical signs. MAT of serum assessed exposure to *Leptospira* spp. Clinical signs, age, sex, base colour, coat pattern, *LP* and *PATN1* genotypes, percent white at birth, progressive roaning, and *Leptospira* were assessed as risk factors using multivariable exact logistic regression, accounting for clustering at the barn level. Additionally, a pedigree analysis was performed (n = 20 cases and 21 controls), and coefficients of coancestry (CC) and inbreeding were calculated.

Results

Prevalence of ERU in this sample of Knabstrappers was 20.7%. Similar to findings for Appaloosas, *LP* homozygotes had higher odds of uveitis compared to true solid (*N/N*) horses (*LP/LP* OR = 7.64, 95% CI [0.8 - +INF], P = 0.04) and age was also identified as a risk factor. After accounting for *LP*, the 16-20 age group had higher odds compared to the youngest group (OR = 13.36, 95% CI [1.4 – 213.4], P = 0.009). The distributions of average CC were significantly different between cases and controls (P = 0.01).

Main Limitations

Small sample size decreased the power for detecting additional associations. The progressive nature of ERU may have prevented identification of younger affected horses.

Conclusions

Our data support genotyping for *LP* to assess risk of ERU in Knabstruppers. Additional studies are necessary to develop more robust risk models across LP breeds for earlier detection and improved clinical management.

1. Introduction

Equine recurrent uveitis (ERU) is a disease complex with a long history and global distribution, making it a major concern for equine health.¹ Specifically, certain horse breeds, such as the Knabstrupper, have a predisposition for developing ERU.² This Danish breed has been strongly selected for a white coat spotting pattern known as leopard complex spotting (LP) that is also a characteristic of the Appaloosa breed (Figure 1).³ Both breeds are recognized as having a predisposition for the insidious form of ERU,^{2,4} however, limited information is available in the scientific literature to characterize ERU in the Knabstrupper horse. In a large retrospective study at the University of Munich, researchers evaluated indicators and sequelae of ERU among a group of LP-spotted horses from the Appaloosa, Knabstrupper, and unknown breeds in comparison to non-LP horses.⁴ The LP horses had a higher rate of bilateral inflammation as well as higher incidences of lens luxation, diffuse cataract, and phthisis bulbi compared to the non-LP group. However, breed specific prevalence and risk factors were not evaluated in the study.

Insidious uveitis is characterized by chronic, low-grade intraocular inflammation that gradually damages structures of the eye, while usually lacking the outwardly painful episodes that characterize other forms of ERU.⁵ Previous research identified the mutation causing the LP spotting pattern, a 1,378 base-pair insertion in the *Transient Receptor Potential Cation Channel M1 (TRPM1)* gene, as a risk marker for insidious uveitis in the Appaloosa breed.⁶⁻⁹ In homozygotes the *LP* allele was already shown to have a pleiotropic effect within the eye by causing congenital stationary night blindness (CSNB).⁹ While the mechanism connecting *TRPM1* function

to CSNB has been extensively characterized, the link between the *LP* allele and ERU has not been fully elucidated. In particular, the role of the *LP* insertion as either a causative factor or a marker in linkage disequilibrium with the true causal mutation remains unclear. Additionally, a second coat colour allele known to modify the LP coat pattern, called *Pattern 1 (PATN1)* was also found to be associated with insidious uveitis in the Appaloosa (Figure 1).⁶

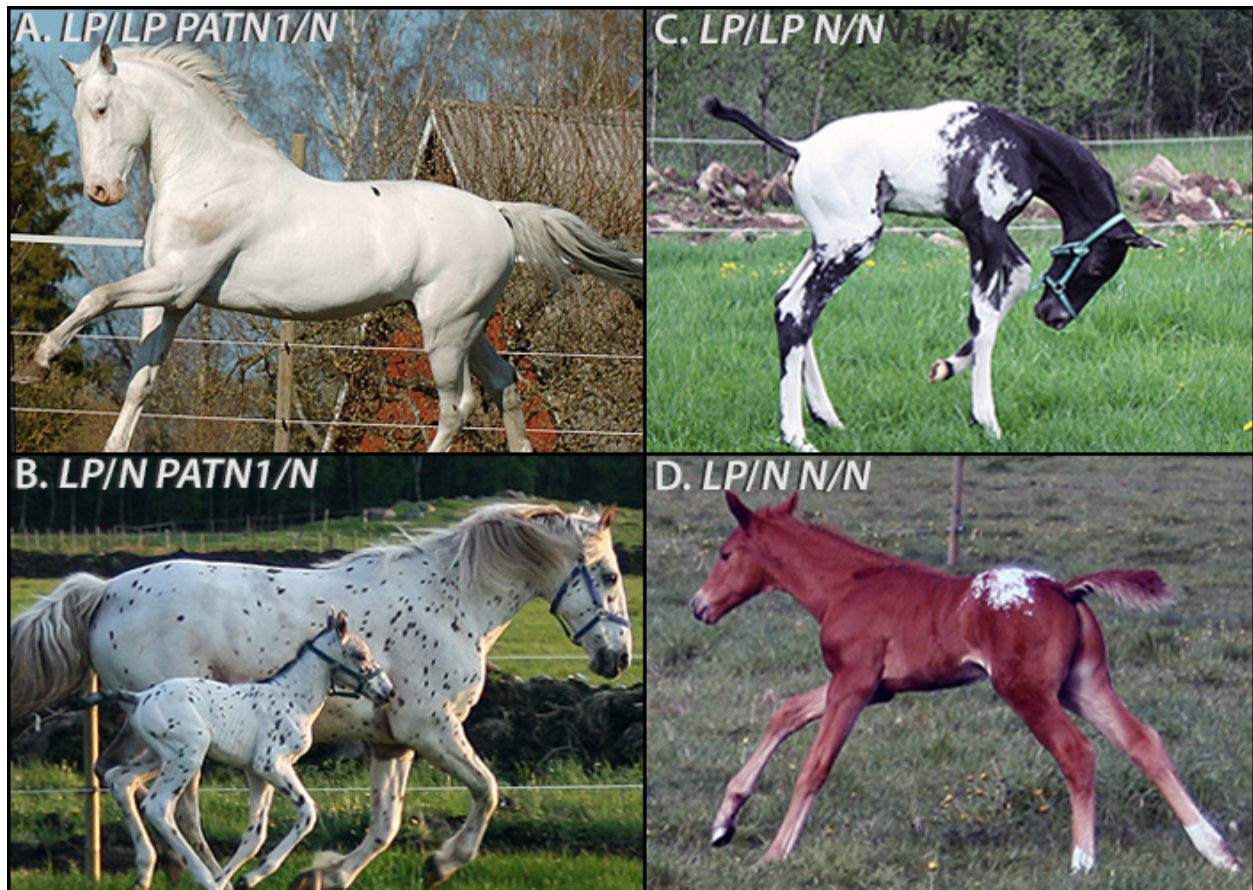


Figure 1: The coat colour patterning in the Knabstrupper and ERU genetic risk factors investigated. (A) Horses with two copies of the *LP* allele and at least one copy of *PATN1* have extensive white patterning (typically >50% at birth) with a few or no pigmented spots in the white patterned area (A = few spot) (B) Horses with one copy of *LP* and at least one copy of *PATN1* also have extensive white patterning but typically have numerous pigmented spots in the white patterned area (B = leopard). (C and D) Horses with at least one copy of *LP* and no copies of *PATN1* generally have less patterning than panels A and B, although the amount ranges on a continuum from C (snowcap) to less than panel D (lace blanket). Photos courtesy of Sofie Aronsson (A) and Anna Larsson (C).

In addition to genetic risk loci, other risk factors have been identified for ERU such as age and certain environmental conditions. In particular, an association between infection with *Leptospira* species and ERU has been described previously; however, the precise role of *Leptospira* in ERU risk is incompletely understood.^{5,10–19} Infection with *Leptospira* is considered sufficient to incite disease,²⁰ but it does not appear to be a necessary component of ERU onset in all cases, particularly for insidious disease.^{4,12,21–23} Previous retrospective research found that affected LP horses generally have less evidence of concurrent *Leptospira* infection compared with affected horses in other breeds.^{4,12}

The aim of this study was to investigate ERU specifically in the Knabstrupper breed by studying horses within Denmark, Sweden, and the United States. The investigation was performed to measure disease frequency, to characterize clinical manifestations of ERU, and to evaluate several putative risk factors for association with ERU in the Knabstrupper.

2. Methods

2.1 Horses

Horses registered with the Knabstrupperforeningen for Danmark (KNN) in Denmark, Sweden, and the United States were recruited to this study by voluntary owner participation. Information about participating in the study was made available to all owners through the breed registry and voluntary participation was coordinated by local contacts (CR – Denmark; SH – Sweden; AD and RRB – USA). In some cases, to maximize exam efficiency and inclusion in the study, horses were trailered to a centrally located barn for examination, and barns were selected for having at least three horses available to participate. Where possible, all Knabstrupper horses at a given barn were included in the study, except for animals under two years of age.

2.2 Ophthalmic examination

Ocular evaluations were performed under field conditions at privately owned barns. The examinations included a neuro-ophthalmic examination prior to administration of any sedation, rebound tonometry, direct transilluminator, slit-lamp biomicroscopic, and indirect ophthalmoscopic assessments. Horses in Denmark and Sweden were sedated with a combination of detomidine hydrochloride (0.008-0.02 mg/kg body weight) and butorphanol (0.008-0.025 mg/kg body weight). Horses examined in the USA were sedated, if needed, with xylazine (0.5 mg/kg body weight). Examinations were performed by a Diplomate of the American College of Veterinary Ophthalmologists (DACVO) (LS, n = 90 in Sweden and Denmark), Honorary Member of the American College of Veterinary Ophthalmologists (AD, n = 22 in USA), or a Doctor of Veterinary Medicine (DVM) (AHE, n = 4 in Denmark).

A diagnosis of confirmed ERU was assigned to horses with presence of active inflammation in addition to historical or clinical evidence of continuous or episodic inflammation. Eyes were classified as unaffected by having no clinical signs of current or previous uveitis (i.e. lacking aqueous or vitreous flare and minimal to no ocular abnormalities) or as ERU-affected by displaying mild clinical signs of inflammation, moderate damage, or severe damage from ERU as previously described.⁷ Mild clinical signs of ERU consisted of eyes with conjunctival hyperemia, aqueous flare, miosis and ocular hypotony (defined as ≤ 10 mm Hg for an eye or at least 10 mm Hg difference between eyes). Moderate damage from ERU consisted of eyes with signs of mild ERU and one or more of posterior synechia, cataract, vitritis, or uveal pigmentation changes (depigmentation or hyperpigmentation). Severe damage from ERU consisted of eyes with secondary glaucoma, phthisis bulbi, retinal detachment, and/or blindness due to sequelae of ERU. Bilaterally affected horses were assigned a classification based on the most severely affected eye.

Uveitis was considered “active” if inflammation, as evidenced by aqueous flare and/or vitritis, was confirmed in either the anterior or posterior segment of at least one eye, and it was considered “quiescent” if inflammation was not observed at the time of the exam. Horses with clinical manifestations of subtle active uveitis or quiescent eyes with changes suggesting previous inflammation, for which continuous or episodic inflammation could not be confidently diagnosed either as ERU affected or unaffected as defined above, were marked as suspect.

All clinical abnormalities, in addition to age (years), sex (male or female), base coat colour as confirmed by genotyping (bay, black, or chestnut), coat pattern phenotypes (few spot, snowcap, lace blanket, leopard, spotted blanket, white flecks, no pattern, unknown, or true solid), amount of progressive roaning (none/unknown, low, moderate, or high), and percentage of white in the coat (none, <50%, or ≥50%) were recorded. Progressive roaning is a characteristic of LP in which white hairs replace dark hairs while a horse ages. Coat pattern phenotyping was performed by one rater (SA) and was based on photographic record taken at the time of examination or foal pictures when extensive varnish roaning obscured the original pattern. Percent white phenotype was determined for horses with *LP* by examining the photographic record, and progressive roaning was also determined for horses with *LP* by comparing the photographic record at the time of examination with foal pictures, except four horses for which photographic records were not complete.

2.3 Coat colour genotype testing

Whole blood and/or mane hair follicles were collected from each horse. The Gentra Puregene DNA Isolation kit (Qiagen Inc.) was used to extract total genomic DNA from blood, or from hair if blood was not available, using previously described protocols.²³ All horses were tested at the UC Davis Veterinary Genetics Laboratory for the known LP spotting pattern loci (*LP* and

PATNI) and the loci affecting the base coat colour phenotypes (*Agouti* and *Extension*) using the commercially available genetic tests. Alleles are reported as *LP* for the leopard complex spotting allele or *N* for the reference allele at the same locus. For the *PATNI* locus, the LP pattern modifying allele is reported as *PATNI*, while *N* was used for the reference allele.

2.4 *Leptospira* MAT testing

Blood samples for serum isolation were collected at the time of the ocular exam for 89/116 horses examined. Serum was isolated by allowing approximately 3 mL of whole blood to clot at room temperature for at least 15 minutes prior to cold storage (approximately 4°C without freezing) in order to process samples at the end of each day. The clotted blood was separated from serum by centrifugation at 2,000 xg for 10 minutes. All 89 serum samples were evaluated for six serovars of *Leptospira* (*bratislava*, *canicola*, *grippotyphosa*, *hardjo*, *icterohemorrhagiae*, and *pomona*) by microagglutination testing (MAT) at the California Animal Health and Food Safety Laboratory System Diagnostic Services (UC Davis). Titers of greater than 1:100 were considered positive for exposure to the antigen.

2.5 Pedigree analysis

To investigate the genetic architecture and the role of shared ancestry in ERU risk, a pedigree analysis was performed using Pedigraph software.²⁴ Given the progressive nature of ERU and previous implications for age as a risk factor for Appaloosas,⁷ a minimum age threshold of 12 was used to categorize an unaffected horse with no confounding ocular pathology as a control. Only horses with at least four known generations were used to calculate coefficients of coancestry (CC) and inbreeding (COI). The CC is the estimated pairwise probability of sharing the same allele from a common ancestor, and the COI is the estimated probability of an individual possessing a

pair of identical alleles by descent from a common ancestor.²⁵ The average pairwise CC values were calculated from all horses in the affected group and all horses in the control group, and the average COI values were calculated from each individual COI in both affected and control groups. Wilcoxon rank-sum tests were then used to compare the average CC and COI between the two groups. Dominant, recessive, and X-linked modes of inheritance for ERU risk were evaluated.

To investigate the genetic architecture and the role of shared ancestry in ERU risk, a pedigree analysis was performed using Pedigraph software.²⁴ Given the progressive nature of ERU and previous implications for age as a risk factor for Appaloosas,⁷ a minimum age threshold of 12 was used to categorize an unaffected horse with no confounding ocular pathology as a control. Only horses with at least four known generations were used to calculate coefficients of coancestry (CC) and inbreeding (COI). The CC is the estimated pairwise probability of sharing the same allele from a common ancestor, and the COI is the estimated probability of an individual possessing a pair of identical alleles by descent from a common ancestor.²⁵ The average pairwise CC values were calculated from all horses in the affected group and all horses in the control group, and the average COI values were calculated from each individual COI in both affected and control groups. Wilcoxon rank-sum tests were then used to compare the average CC and COI between the two groups. Dominant, recessive, and X-linked modes of inheritance for ERU risk were evaluated.

2.6 Statistical analysis

Ocular anomalies, horse attributes, phenotypes and genotypes were compared between confirmed ERU affected and horses classified as unaffected. Assessment of risk factors for ERU included the following factors: age, sex, base coat colour, specific coat pattern, amount of progressive roaning, percentage of white patterning at birth, *Leptospira* MAT positivity, and *LP*

and *PATNI* genotypes. *PATNI* genotype was dichotomized to consider horses as having at least one copy of *PATNI* present or not. Initial univariable analysis with exact logistic regression was employed to determine which variables to consider for inclusion in the final model. Where categories for a variable did not include more than five horses, that category was dropped from the analysis. Significance test threshold for inclusion consideration was $P \leq 0.2$. Since horses were recruited from barns in three countries, accounting for clustering was required. Since the main risk factor of interest (*LP* genotype) predicted the outcome perfectly, ordinary multilevel logistic regression models failed to converge, and exact logistic regression models including barn as a group variable to control for the effect of clustering were used to examine potential risk factors. Since barns are nested within countries, control for clustering effects due to country was included when accounting for barn effect.

Multivariable exact logistic regression analysis was conducted using forward stepwise model building. The linearity assumption for logistic regression and continuous variables was tested with inclusion of a squared term in the model. A variable was considered a confounder of the model if coefficients changed by >20% when including or excluding that variable from the model. Collinearity between variables was determined based on a biological explanation, their correlation, and/or the model building results. Where sets of variables failed any of the assessments of collinearity, alternative models using either variable were compared. Since the goal of the study was to investigate if *LP* was a risk factor, the model including *LP* was kept as the final model when comparing variables collinear with *LP*. Results from exact logistic regression analyses were reported as odds ratios (OR) with 95% confidence intervals (95% CI) computed from the exact conditional distribution, along with p-values. Given exact logistic regression and accounting for clustering effects at barn level, it was not possible to calculate predicted probabilities for

occurrence of ERU across all three *LP* genotypes using the final model. Instead, to determine how well *LP* genotype predicts risk for ERU in the Knabstrupper, probabilities were estimated using a simplified analysis (no adjustment for barn clustering) for horses with the *LP* allele (heterozygous or homozygous). Additionally, evaluating whether *LP* genotype was associated with different proportions of ERU severity in affected horses was evaluated with a Fisher's exact test.

Since almost all affected horses were bilateral for ERU, analysis at the level of the eye, even when accounting for repeated measures within each horse, was not possible. Clinical findings were, therefore, summarized at the level of the horse, and clinical manifestations were compared across uveitis status using exact logistic regression. Horses with unilateral ERU or unilateral symptoms were included as positive for ERU and/or for those symptoms. Significance testing was conducted with exact logistic regression (conditional scores test). Since description and analysis of the association between clinical signs and occurrence of ERU is exploratory, p-values are presented as uncorrected for multiple comparisons. P-values < 0.05 were considered significant. All statistical tests and modeling for ERU risk factors and symptoms was performed with Stata, a commercial statistics software package.²⁶

3. Results

From 2017-2019, a sample of 116 Knabstrupper horses were examined in Denmark (n = 46), Sweden (n = 48), and the USA (n = 22). Demographics, horse attributes, and phenotypic information are summarized in Table 1. Horses were evaluated on one occasion at six barns in Denmark and at three barns in both Sweden and the USA. From the overall sample, 69 horses were female and 47 were male. Horses varied in age from 2 - 26 years with an average age of 10.3 (\pm 5.6) years. Equine recurrent uveitis was diagnosed in 24/116 (20.7%) horses (ERU-affected), and

it was not diagnosed in 81/116 (69.8%) horses (unaffected). A designation of suspect was assigned to 11/116 horses, and these animals were excluded from further risk factor analysis. Altogether, 105 phenotyped Knabstrupper horses remained for further evaluation of pedigrees and potential risk factors. Overall, the affected classification included eight horses with mild clinical signs of ERU, five horses with moderate, and eleven with severe damage from ERU. Uveitis was bilateral in 22/24 (91.7%) horses and unilateral in two horses (8.3%). One horse in the bilateral group previously had one eye enucleated due to ERU, and only symptoms from the remaining eye were evaluated and considered for this horse.

Table 1. Summary of demographic information and univariable exact logistic regression analysis for potential risk factors for a sample of Knabstrupper horses in three countries evaluated for ERU.

	Affected (n = 24)	Unaffected (n = 81)	Total (n = 105)	OR	95% CI	p- value
Average age (± SD)	12.88 (5.21)	9.48 (5.73)	10.26 (5.77)	n/a	n/a	n/a
Country:						
Denmark	12	26	38	n/a	n/a	n/a
Sweden	10	36	46	n/a	n/a	n/a
USA	2	19	21	n/a	n/a	n/a
Barn:						
1	3	11	14	n/a	n/a	n/a
2	7	19	26	n/a	n/a	n/a
3	0	6	6	n/a	n/a	n/a
4	2	6	8	n/a	n/a	n/a
5	0	3	3	n/a	n/a	n/a
6	3	5	8	n/a	n/a	n/a
7	0	5	5	n/a	n/a	n/a
8	5	3	8	n/a	n/a	n/a
9	2	4	6	n/a	n/a	n/a
10	2	8	10	n/a	n/a	n/a
11	0	4	4	n/a	n/a	n/a
12	0	7	7	n/a	n/a	n/a
Sex (P = 0.8):						
females	16	48	64	Reference	n/a	n/a
males	8	33	41	0.84	0.25 - 2.64	0.8
Age Groups						

(P = 0.02):						
0-5 years	2	24	26	Reference	n/a	n/a
6-10 years	6	32	38	2.09	0.32 - 23.7	0.5
11-15 years	7	13	20	6.79	1.01 - 80.84	0.03
16-20 years	8	5	13	10.55	1.23 - 153.96	0.02
> 20 years	1	7	8	0.93	0.01 - 20.27	1.0
<i>Leptospira</i>						
MAT*						
(P = 0.6):						
negative	11	24	35	Reference	n/a	n/a
positive	8	37	45	0.65	0.19 - 2.23	0.6
unknown	5	20	25	Excluded	n/a	n/a
Base Coat						
Colour						
(P = 0.5):						
bay	13	47	60	Reference	n/a	n/a
black	2	12	14	0.38	0.03 - 2.22	0.3
chestnut	9	22	31	0.97	0.27 - 3.25	1.0
Coat Pattern*						
(P = 0.02):						
spotted blanket	2	22	24	Reference	n/a	n/a
few spot	7	8	15	2.44	0.2 - 5.19	0.02
leopard	10	23	33	1.75	-0.31 - 4.36	0.1
snowcap	2	5	7	2.05	-0.98 - 5.15	0.1
true solid	0	12	12	0.31 [§]	-INF - 2.93	1.0
no pattern	1	2	3	Excluded	n/a	n/a
white flecks	1	3	4	Excluded	n/a	n/a
lace blanket	0	5	5	Excluded	n/a	n/a
unknown	1	1	2	Excluded	n/a	n/a
LP Genotype						
(P = 0.03):						
N/N	0	12	12	Reference	n/a	n/a
LP/N	15	56	71	2.98	0.39 - +INF	0.3
LP/LP	9	13	22	8.62	1.04 - +INF	0.05
PATN1						
Genotype*						
(P > 0.9):						
N/N	5	23	28	Reference	n/a	n/a
PATN1/N	12	41	53	1.19	0.32 - 5.01	1.0
PATN1/PATN1	7	17	24			
Percent White						
Patterning (P						
= 0.2):						
0%	0	12	12	Reference	n/a	n/a
<50%	4	19	23	4.74	0.63 - +INF	0.09

≥50%	20	50	70	3.02	0.31 - +INF	0.3
Varnish Roaning* (P = 0.2):						
low	4	22	26	Reference	n/a	n/a
moderate	8	26	34	1.63	0.33 - 9.67	0.7
high	11	18	29	3.73	0.74 – 23.51	0.09
none or unknown	1	15	16	Excluded	n/a	n/a

* Restricted analysis was performed for: i) *Leptospira* MAT – tested horses only (n = 80); ii) base coat pattern – included pattern categories with more than 5 horses only (n = 91); iii) *PATN1* genotype – analyzed as dominant mode of inheritance (*PATN1/PATN1* and *PATN1/N* verses *N/N*); iv) varnish roaning – does not include ‘none or unknown’ category (n = 89).

§ True solid category used the median unbiased estimator (MUE) for OR.

The clinical manifestations of uveitis are summarized in Table 2. The most common clinical manifestations in the ERU-affected horses included aqueous flare (23/24), and iris hyperpigmentation (19/24), followed by conjunctival hyperemia (15/24), miosis (14/24), iris depigmentation (11/24), immature cataract (10/24), and corpora nigra atrophy (10/24). Blindness was present in 41.7% of the affected horses due to glaucoma, phthisis bulbi, cataract, or a combination of these sequelae. Most clinical manifestations were significantly more common in ERU-affected horses compared to unaffected horses with the exception of incipient cataract (P > 0.9), “bullet hole” retinal lesions (P = 0.7), “butterfly” retinal lesions (P = 0.3), and vitreous degeneration (P = 0.1). Furthermore, the presence of enophthalmos (P = 0.05), lens luxation (P = 0.2), glaucoma (P = 0.05), and phthisis bulbi (P = 0.05) occurred infrequently in both groups (once or twice in affected and none in unaffected horses).

Table 2. Evaluating clinical ocular manifestations in a sample of Knabstrupper horses (n = 116) from three countries based on diagnosis. Horses were identified as affected, unaffected, or suspect for ERU. P-values estimated with exact logistic regression are reported for association of ERU status (affected compared to unaffected) with clinical signs.

Clinical Manifestations	Affected horses	Unaffected horses	Suspect horses	Affected: Unaffected p-values
	(n = 24)	(n = 81)	(n = 11)	

Enophthalmos	2	0	0	0.05
Blepharospasm	3	0	0	0.01
Conjunctival hyperemia	15	4	1	<0.001
Epiphora	5	0	0	<0.001
Hypotony	5	0	2	<0.001
Aqueous flare	23	0	7	<0.001
Miosis	14	0	0	<0.001
Corneal edema	7	0	1	<0.001
Corneal vascularization	3	0	0	0.01
Corneal fibrosis	5	2	0	0.007
Iris hyperpigmentation	19	8	1	<0.001
Iris depigmentation	11	13	4	0.004
Corpora nigra atrophy	10	0	0	<0.001
Pupillary fibrosis	7	0	0	<0.001
Pupillary fibrin	9	0	2	<0.001
Posterior synechia	8	0	1	<0.001
Pupillary occlusion	5	0	0	<0.001
Anterior lens pigment	3	0	0	0.01
Incipient cataract	8	29	4	1.00
Immature cataract	10	0	0	<0.001
Mature cataract	5	0	0	<0.001
Lens luxation	1	0	0	0.2
Vitreous degeneration	5	7	3	0.1
Vitritis	7	0	0	<0.001
Bullet hole lesions	2	9	1	1.00
Butterfly lesions	0	5	0	0.3
Blind	10	0	0	<0.001
Glaucoma	2	0	0	0.05
Phthisis bulbi	2	0	0	0.05

* One horse with ERU had only one eye examined due to a previous enucleation. All results are reported at the level of the horse, almost all horses were bilateral for ERU and for symptoms.

The mean age for affected horses was 12.9 ± 5.2 years and for unaffected horses was 9.5 ± 5.7 years. The allele frequency of *LP* was 0.55 and that of *PATN1* was 0.48 in this sample. Since none of the horses homozygous for the reference allele (*N/N*) at the *LP* locus were affected, exact logistic regression analysis was required to assess association of the *LP* genotype, and it was utilized in all risk factor analysis steps. For specific coat pattern, four pattern types (n = 14 horses) had few observations (≤ 5 horses) and were not included in that analysis. Potentially associated

factors ($P \leq 0.2$) considered in the multivariable analysis were age ($P = 0.02$), specific coat pattern ($P = 0.02$), amount of progressive roan ($P = 0.2$), and *LP* genotype ($P = 0.03$) (Table 1). *PATN1* genotypes ($P > 0.9$) were considered in further model building due to a previously described association with ERU in Appaloosas.⁸ *Leptospira* MAT positivity ($P = 0.6$), sex ($P = 0.8$), percentage of white patterning at birth ($P = 0.2$), and base coat colour ($P = 0.5$) were not considered further. The regression model including age as a continuous predictor failed the linearity assumption. Thus, age was categorized into groups based on 5-year intervals.

Amount of progressive roaning, specific coat pattern, and percentage of white patterning at birth are biologically related to the genotypes for *LP* and *PATN1*. Additionally, specific coat pattern and progressive roaning could not be fit in the same model as *LP* due to collinearity. The model fit with progressive roaning was not as good (i.e. overall model significance was less) compared to the model built with *LP* genotype. Furthermore, progressive roaning does not occur in horses with the *N/N* genotype, resulting in a restricted model ($n = 89$). The model fit with specific coat pattern was similar (i.e. overall model significance similar) compared to the model built with *LP* genotype; two specific coat patterns include almost all of the *N/N* and *LP/LP* horses. However, this model also failed to include all horses as only patterns with more than five horses were included ($n = 91$). For these reasons, the final overall model included the genotype for *LP*, as it had a high model significance and utilized information from all horses in the study. However, in a subset analysis of the *LP* heterozygous horses (*LP/N*, $n = 56$), specific coat pattern explained some of the occurrence of ERU. The subset exact logistic regression analysis suggests that horses with the leopard pattern have increased odds of ERU occurrence compared to horses with the spotted blanket pattern after adjusting for age (OR = 12.6, 95% CI [0.6 – 1134.0], $P = 0.1$), although this was not significant at the $P < 0.05$ threshold.

Following multivariable exact logistic regression, only *LP* genotype ($P = 0.04$) and age ($P = 0.03$) were significantly associated with the odds of ERU overall (Table 3). *LP/LP* horses had higher odds of ERU compared to *N/N* horses (*LP/LP* OR = 7.39, 95% CI [0.8 - +INF], $P = 0.05$). When accounting for *LP* genotype, horses from age 16-20 had higher odds of ERU compared to the less than five years age group (OR = 12.11, 95% CI [1.3 – 181.8], $P = 0.01$). The 11-15 years age category also had significantly higher odds of ERU compared to the youngest age group (>5 years) (OR = 7.34, 95% CI [1.0 – 97.6], $P = 0.04$). The age groups 6-10 and older than 20 did not have higher odds of ERU compared to the less than five years group (age 6-10 OR = 2.27, 95% CI [0.3 – 26.6], $P = 0.4$ and age > 20 OR = 1.91, 95% CI [0.03 – 49.0], $P > 0.9$). In the multivariate exact logistic regression model with *LP* genotype and age, there was no significant effect of *PATNI* genotype ($P = 0.7$, Table 4). Eleven of 24 affected horses were graded as having severe damage from ERU, and these cases were distributed over the five age groupings (Table S1). No evidence of severe damage being more frequent among the older age groups was observed. Additionally, differences in the distribution of severity scores were not observed for *LP/LP* versus *LP/N* affected horses ($P > 0.9$, Table S2). Using a restricted, simplified full model, the predicted probabilities for *LP/N* and *LP/LP* horses in the 16-20 age category are 0.7 (95% CI [0.3 - 0.9]) and 0.9 (95% CI [0.5 - 0.98]), respectively (Figure 2). It was not possible to include clustering for this prediction, but the odds ratios for *LP* genotype and age were similar from both the clustered and simple analyses for this subset of horses (Table S3). Thus, a simplified analysis is expected to build a similar model to the overall full model with barn clustering.

Table 3. The final model as determined by multivariable exact logistic regression analysis accounting for effect of clustering at the barn level. *LP* genotype and age categories were identified as risk factors for ERU in a group of Knabstrupper horses from three different countries.

Uveitis	<i>N/N</i>	<i>LP/N</i>	<i>LP/LP</i>	Age ≤ 5	Age 6 - 10	Age 11 - 15	Age 16 - 20	Age > 20
Affected	0	15	9	2	6	7	8	1
Unaffected	12	56	13	24	32	13	5	7
Totals	12	71	22	26	38	20	13	8
Odds Ratio	reference	2.52	7.39	reference	2.27	7.34	12.11	1.91
95% CI	n/a	0.3 - +INF	0.8 - +INF	n/a	0.3 - 26.6	1.0 - 97.6	1.3 - 181.8	0.03 - 49.0
p-value	n/a	0.3	0.05	n/a	0.4	0.04	0.01	1.0
	For genotype: P = 0.04			For age: P = 0.03				
Model. Exact logistic regression (grouped by barn): Model score = 17.6, P = 0.005								

Table 4. Combined *LP* and *PATN1* genotypes in sample of Knabstrupper horses evaluated for ERU from three countries.

<i>LP</i> genotype	<i>LP/LP</i>	<i>LP/L</i> <i>P</i>	<i>LP/N</i>	<i>LP/N</i>	<i>N/N</i>	<i>N/N</i>	
<i>PATN1</i> genotype	<i>PATN1/-</i>	<i>N/N</i>	<i>PATN1/-</i>	<i>N/N</i>	<i>PATN1/-</i>	<i>N/N</i>	Totals
Affected	8	1	11	4	0	0	24
Unaffected	12	1	38	18	8	4	81
Totals	20	2	49	22	8	4	105

* In the multivariate exact logistic regression model with *LP* genotype and age, there was no significant effect of *PATN1* genotype (P = 0.7).

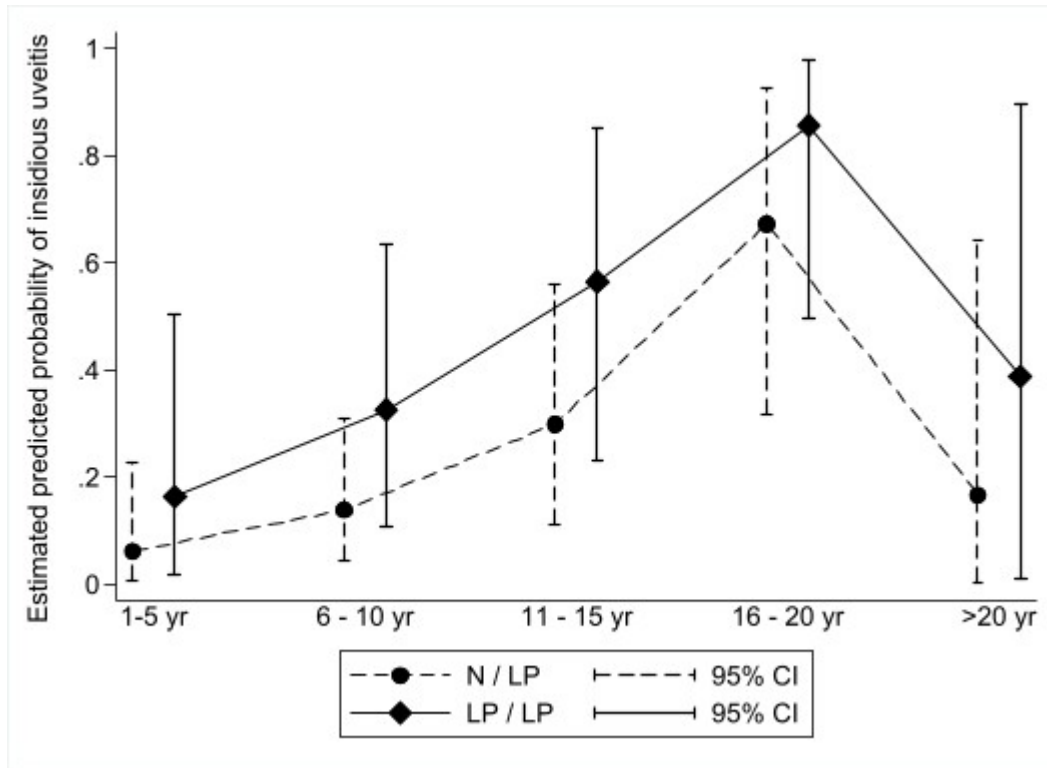


Figure 2: Estimated predicted probability of developing insidious uveitis for Knabstrupper horses that are heterozygous (*N/LP*) and homozygous (*LP/LP*) from an exact logistic regression model. The predicted probabilities were calculated based on those horses that had one or two copies of the *LP* allele ($n = 93$). This analysis did not account for clustering by barn which was not computationally possible with exact logistic regression. The model accounting for barn level provided similar odds ratios to the simplified model without clustering; a minimal effect on probabilities is anticipated.

For the pedigree analysis, 21 out of 81 unaffected horses were considered “controls” based on the age inclusion criteria for controls (≥ 12 years old). Pedigrees with at least four generations were available for 20/24 affected horses and 16/21 horses identified as controls. A common ancestor shared by all affected horses was not identified in the pedigree analysis. One ancestral sire (GS18, denoted in yellow Figure 3A) was shared by 14/20 affected horses for which pedigrees were available for four generations. Two of the affected horses were inbred to this ancestor, while the other twelve horses can be traced back to him from either the sire or dam lines. Of the control horses with available pedigree information, 11/21 horses were also found to descend from GS18. Similar to the affected horses, two controls were inbred to GS18, while the remaining nine control

horses trace back only on one side of their pedigrees. Five affected Knabstruppers that all descended from GS18 were seen at the same location (denoted as Barn 8). The two remaining horses over 12 years old residing at Barn 8 for more than 10 years did not show any evidence of inflammation and were unrelated to GS18 (Figure 3B).

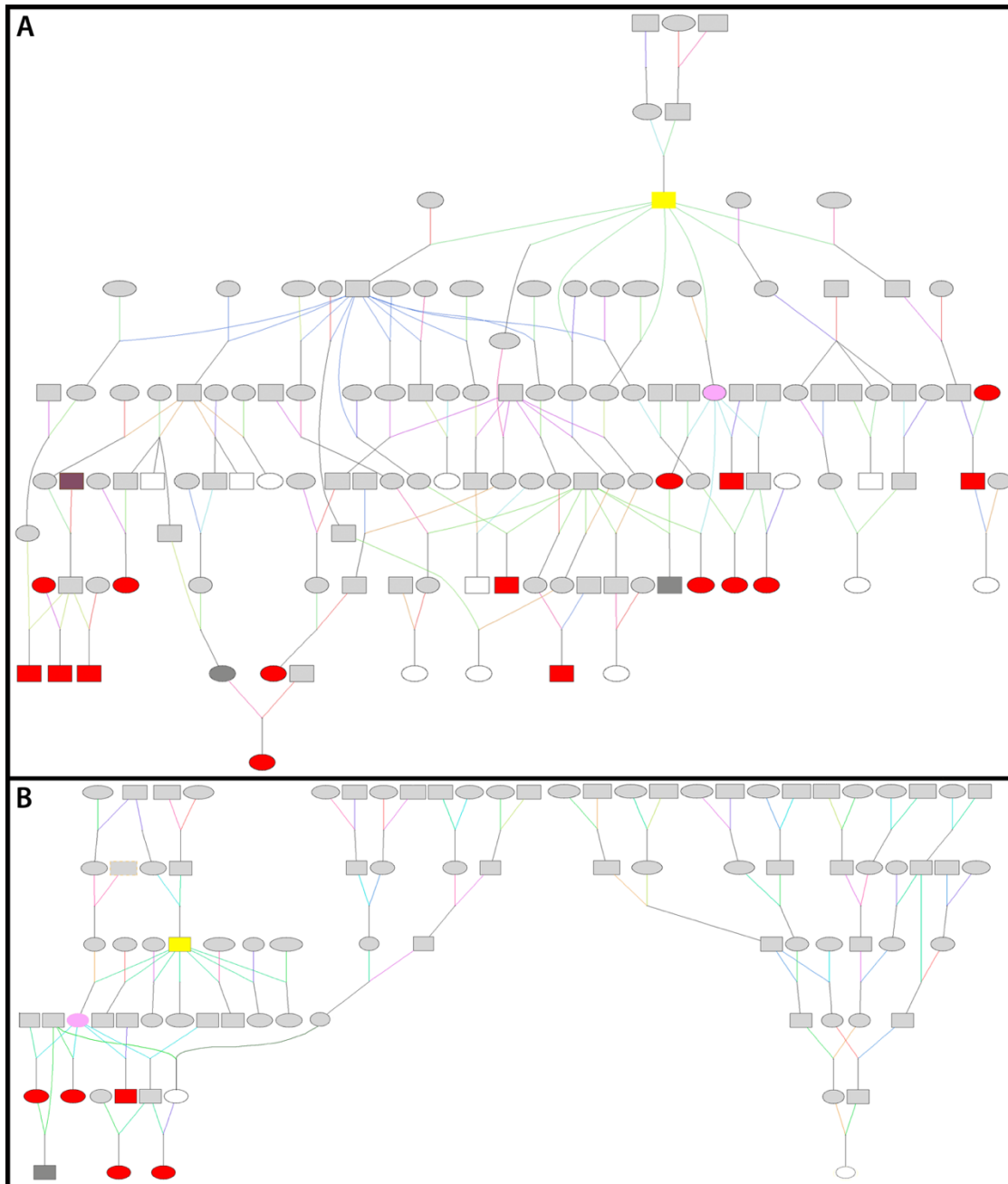


Figure 3: Pedigree analysis for insidious uveitis in the Knabstrupper. Red shading signifies diagnosis of ERU, and white shading indicates a control horse (unaffected upon examination, no history of inflammation, and at least 12 years of age). Grey shading signifies horses that were either unaffected by ocular examination but younger than the age threshold (dark grey) or horses not available for ocular examination (light grey). (A) The pedigree analysis identified the common ancestor of 14 out of 24 ERU affected horses. This ancestor (GS18) is highlighted in yellow shading. (B) Pedigrees of all horses seen at one barn (denoted as Barn 8). Shaded in pink is one dam descending from GS18 that is a shared ancestor of all affected horses but neither of the controls at Barn 8. One of the control horses produced an affected offspring from a cross with a stallion descending from GS18. The stallion was known to have produced at least one other affected offspring with a different mare.

The average CC for the 20 affected horses with pedigrees ($CC_{avg} = 0.025$) was significantly different from that of the control group ($n = 16$, $CC_{avg} = 0.014$, $P = 0.01$). Conversely, the distribution of the COI was not significantly different between affected and control horses ($n = 35$, $P > 0.9$). Out of the full analyzed sample ($n = 105$), we did not detect an imbalanced distribution of disease between the sexes (16/64 females and 8/41 males affected) that would be indicative of simple X-linked inheritance. Limited information was available to investigate other modes of inheritance as there were only three cases for which the disease status was known for one parent and no cases for which disease status was known for both parents. One sire, whose phenotype was unknown but whose own sire (Figure 3A, highlighted in brown) was reported to have ERU, produced affected offspring when crossed with two unrelated mares and one distantly related mare. However, two of the dams have unknown disease status and the third is affected.

4. Discussion

We recorded several clinical manifestations that may be associated with ERU in the Knabstrupper. Active inflammation was more common than quiescent disease and overt signs of discomfort such as blepharospasm and epiphora were uncommon in ERU-affected horses. Similar to ERU in the Appaloosa,⁷ the most common clinical manifestations of uveitis in the Knabstrupper were subtle signs that may not be noticed without careful ocular examination, such as aqueous

flare, iris hyperpigmentation, conjunctival hyperemia, miosis, iris depigmentation, immature cataract, and corpora nigra atrophy.

Recorded clinical manifestations were more likely to be present in ERU-affected horses compared to unaffected horses with the exception of incipient cataract, “bullet hole” lesions, “butterfly” retinal lesions, vitreous degeneration, enophthalmos, lens luxation, glaucoma, and phthisis bulbi. With regard to retinal lesions, ERU has been suggested as a possible cause of peripapillary chorioretinitis and the finding of “bullet-hole” and, in particular, “butterfly lesions” has been suggested as an indication of ERU.^{27–29} However, “bullet hole” and “butterfly” retinal lesions were not significantly associated with ERU-affected horses in our study. This result is similar to findings in the Appaloosa,⁷ and our data further support that the presence of these lesions in an otherwise normal eye should not signify a diagnosis of ERU. It is important to note that our ability to detect a significant association for enophthalmos, lens luxation, glaucoma, and phthisis bulbi may have been limited by a small sample size as these symptoms only occurred in a small number of affected horses. Since lens luxation, glaucoma, and phthisis bulbi are considered characteristics of end-stage disease, survivor bias may have diminished our power to detect a significant relationship between these sequelae and ERU in the Knabstrupper.

Blindness, resulting from glaucoma, phthisis bulbi, cataract, or a combination of these conditions, was recorded in 41.7% of the affected horses. This is consistent with the proportion reported in a similar study of Appaloosas in which 41% of eyes with ERU were blind.⁷ The proportion of confirmed ERU in this sample of horses was 20.7%, which is only slightly higher than that reported in the most recent studies of the Appaloosa breed with approximately 14% prevalence.^{7,30} All except two of the confirmed cases of ERU in our investigation were bilateral. Taken together, the clinical evaluations in this study support that ERU in the Knabstrupper horse

has several similarities to ERU in the Appaloosa including prevalence, commonly being bilateral and insidious in nature, and frequently resulting in blindness.

Diagnosis of ERU requires a combination of clinical signs, in addition to signalment and history, and our criteria for an ERU diagnosis was the presence of active inflammation in addition to a clinical history of continuous or episodic inflammation.^{7,19} We did, therefore, classify 11 horses as “suspect” as they had suggestive clinical manifestations indicative of uveitis, including various combinations of conjunctival hyperemia, aqueous flare, hypotony, iris depigmentation, and pupillary fibrin, but their clinical signs and history, together, did not fit our criteria to confirm ERU diagnosis. While they were not included in the disease prevalence estimates or in our risk models, we speculate that the suspect horses displayed subtle or early disease. However, follow-up examinations are required to confirm ERU diagnosis, and a longitudinal study may help to confirm if these signs are early symptoms of insidious uveitis in this breed.

The mean age (12.9 years) of ERU-affected horses was similar to that reported for the Appaloosa (12.3 years).^{7,30} In both the Knabstrupper and the Appaloosa, risk of ERU diagnosis increases with advancing age.³⁰ However, when accounting for *LP* genotype, horses under ten and over 20 years old did not show increased odds of disease in the Knabstruppers in this study. Previous investigations of ERU have indicated that euthanasia is a common outcome for affected horses.^{12,19} Survivor bias may, therefore, have impacted our results for the older age categories. The subtle nature of insidious uveitis often makes it difficult to determine an accurate age of onset for most horses, and we suspect that some horses in the younger age groups may go on to develop disease. As a result, we may inherently overestimate the average age of affection and underestimate the effect of age on insidious uveitis onset. In contrast to the Appaloosa, age was not a risk factor for severity of damage from ERU in this population of Knabstruppers. The relatively small sample

size and possible survivor bias may have impacted our ability to detect a relationship, and therefore, a longitudinal study following a group of affected horses would provide further insights.

Previous work in Appaloosas supported *LP* or a closely linked marker as a genetic risk factor for insidious uveitis.⁶⁻⁸ Investigating this locus in the Knabstrupper provided further support that *LP* is a risk locus for insidious uveitis across breeds, with homozygotes (*LP/LP*) being at greatest risk. The Rockwell *et al* (2020) study found that *LP* was an additive risk factor.⁸ While in this investigation of Knabstrupper, homozygotes (*LP/LP*), but not heterozygotes (*LP/N*), had significantly higher odds of ERU compared to *N/N* horses. However, 38 of 56 unaffected *LP/N* horses were younger than ten years of age. Examination of a large older cohort of Knabstrupper, particularly in the age range identified at risk in this study (11-20), may help to thoroughly delineate the relationship between insidious uveitis and *LP*.

To make recommendations on screening for ERU, the predicted probability of ERU for horses with *LP* was estimated using a simplified model that did not account for clustering by barn. Estimated probabilities greater than 0.6 indicate a high-risk group, thus the data support regular clinical evaluation of *LP/LP* horses that are 11-20 years old and *LP/N* horses that are 16-20 years for ERU. Future investigations of the etiology of the disease will enable further refinement of the clinical recommendations in the Knabstrupper.

Previous work in Appaloosas also identified suggestive significance for *PATNI* as an additive genetic risk factor using a logistic regression model.⁸ In our analysis, however, we did not detect a significant association between *PATNI* genotype and ERU affection status. Given the relatively small sample size and the high frequency of the *PATNI* allele in the Knabstrupper, it is possible that we did not have enough power to detect an association with the locus. Alternatively,

PATNI may not be informative for ERU in this breed. Further evaluation of *PATNI* in other cohorts of Knabstrappers, as well as other breeds, will help to assess this putative risk factor.

Consistent with a previous investigation in Appaloosas and Knabstrappers,⁴ positive results for *Leptospira* exposure were not associated with higher odds of ERU in our sample. In fact, a higher proportion of unaffected horses were positive for *Leptospira* exposure than affected animals. It is suspected that *Leptospira* spp. may play a larger role in ERU for non-LP horses. A recent investigation suggests that cryptic biofilm formation within the eye may occur in horses that test negative for *Leptospira* in serum and even ocular fluid evaluations.¹¹ Our assessments of *Leptospira* exposure were limited in this dataset as serum was not available from four horses in Sweden or any of the horses seen in the USA. Our investigation was also limited from evaluating ocular fluids as the risk of ocular damage was considered too high to justify sampling of ocular fluids in the examination settings.

Similar to previous findings within the Appaloosa breed,⁷ the distributions of CC values indicate that the affected Knabstrappers are more likely to share a greater proportion of their genomes with one another than with the control horses. It was not possible to definitively investigate simple Mendelian modes of inheritance in this study because the disease status of most sires and dams was unknown. However, the approximately equal proportion of affected males and females indicates that a simple X-linked mode of inheritance is unlikely. The identification of a common ancestor (GS18) within five generations among the majority of the cases (56%) without inbreeding in most cases suggests that multiple genetic factors may be contributing to ERU, which is consistent with the genetic architecture of ERU identified among Appaloosas.⁶⁻⁸ Approximately one third of the affected individuals ($n = 5$) that traced back to GS18 resided within the same environment at Barn 8 (Figure 3). Despite long-term (10+ years) cohabitation within the same

environment, the two Knabstrappers that were not descended from GS18 at Barn 8 had not developed insidious uveitis at ages 20 and 22. Although the horses at barn 8 suggest that genetics may play an important role, further work with larger cohorts from the same environment is needed to better refine genetic architecture of ERU.

One of the major limitations of our investigation is the small sample size relative to the frequency of ERU, which limited the capacity for multivariable analysis and decreased the power of the study to evaluate all potentially important risk factors. Additionally, the diagnosis of ERU based on one examination can lead to phenotyping bias and requires consideration of the medical history and the clinical signs observed. To decrease the effect of this bias, horses that did not meet strict classification as an affected individual were grouped into a “suspect” category and excluded from the risk factor analysis. Another limitation is the effect of age as described above with the risk of falsely diagnosing a young horse as an unaffected and survivor bias of old horses imposing challenges. Nevertheless, this is the first study to investigate disease occurrence and specific risk factors in the Knabstrupper breed, and the results have important implications for designing further studies aimed at unraveling the causes of this blinding disorder across horse breeds.

Since *LP* genotype has been identified as a risk factor in two breeds, genetic testing for *LP* should help inform clinical management decisions. More frequent examinations are recommended for Knabstrupper horses with the *LP* allele, especially for those between 11 and 20 years old and *LP/LP* horses, in particular. Furthermore, performing a genomic investigation using a combined breed approach to overcome sample size limitations may help to unravel additional genetic risk factors for insidious uveitis in *LP* patterned horses in the future.

Supplementary Materials:

Table S1. Severity classification of ERU for each age category in a sample of ERU-affected Knabstrupper horses in three countries.

Age:	≤ 5	6-10	11-15	16-20	>20	Totals
Mild	0	3	3	1	1	8
Moderate	0	0	0	5	0	5
Severe	2	3	4	2	0	11
Totals	2	6	7	8	1	24

Table S2. Severity classification of ERU for *LP/N* and *LP/LP* genotypes in a sample of ERU-affected Knabstrupper horses in three countries.

	<i>LP/N</i>	<i>LP/LP</i>	Totals
Mild	5	3	8
Moderate	3	2	5
Severe	7	4	11
Totals	15	9	24

Table S3. Comparison of the clustered and simplified multivariable exact logistic regression model for the horses with *LP* (i.e. accounting or not accounting for effect of clustering at the barn level, respectively).

	<i>LP/N</i>	<i>LP/LP</i>	Age ≤ 5	Age 6 - 10	Age 11 - 15	Age 16 - 20	Age > 20
Affected	15	9	2	6	7	8	1
Unaffected	56	13	24	32	13	5	7
Totals	71	22	26	38	20	13	8
Clustered <i>LP</i> model - exact logistic regression (grouped by barn): Model score = 13.9, P = 0.01							
Odds Ratio	reference	1.15	reference	0.88	1.99	2.49	0.65
95% CI	n/a	-0.3 – 2.8	n/a	-1.1 – 3.3	-0.02 – 4.6	0.3 – 5.2	-3.6 – 3.9
p-value	n/a	0.1	n/a	0.4	0.04	0.01	1.0
Simplified <i>LP</i> model - exact logistic regression: Model score = 21.6, P < 0.001							
Odds Ratio	reference	1.07	reference	0.90	1.85	3.30	1.10
95% CI	n/a	-0.3 – 2.4	n/a	-1.0 – 3.3	-0.03 – 4.3	1.2 – 6.0	-3.2 – 4.3
p-value	n/a	0.07	n/a	0.4	0.05	0.0002	0.4

Authorship:

Study design – R.R. Bellone, L.S. Sandmeyer, and N.B. Kingsley; data collection – L.S. Sandmeyer, N.B. Kingsley, R.R. Bellone, A. Dwyer, A. Hallendar-Edman, S. Heden, C. Reilly, and S. Archer; data integrity – L.S. Sandmeyer, N.B. Kingsley, S. Parker, and R.R. Bellone; data analysis and interpretation – S. Parker, N.B. Kingsley, R.R. Bellone, and L.S. Sandmeyer; and all authors contributed to the preparation and approval of the manuscript.

Sources of Funding:

The research was supported by funding from the Knabstrupperforeningen for Danmark, the UC Davis Center for Equine Health (18-17), and the Morris Animal Foundation (D16EQ-028). The mission of the Morris Animal Foundation is to bridge science and resources to advance the health of animals. N. B. Kingsley was also supported in part by a University of California – Davis, Center for Equine Health Fellowship.

Competing Interests:

N. B. Kingsley and R. R. Bellone are affiliated with the UC Davis Veterinary Genetics Laboratory, a service laboratory offering diagnostic genetic tests for horses and other animal species.

Ethical Animal Research:

All protocols were approved by the Institutional Animal Care and Use Committee at the University of California, Davis (protocol number 18851).

Informed Consent:

All owners provided written informed consent for study participation prior to examinations and sample collection.

Acknowledgements:

The authors gratefully acknowledge all horse owners who participated in this research project. In addition, we are grateful for the assistance of the members of the Knabstrupperforeningen for Danmark registry, in particular Ena Sparre and Poul Gerhard Pedersen, who made this study possible.

Data Availability Statement:

The data that support the findings of this study are available from the corresponding author upon reasonable request.

References

1. Spiess BM. Equine recurrent uveitis: The European viewpoint. *Equine Vet J.* 2010;42(SUPPL.37):50-56. doi:10.1111/j.2042-3306.2010.tb05635.x
2. McMullen RJ, Fischer BM. Medical and Surgical Management of Equine Recurrent Uveitis. *Vet Clin North Am - Equine Pract.* 2017;33(3):465-481. doi:10.1016/j.cveq.2017.07.003
3. Thirstrup JP, Pertoldi C, Loeschke V. Genetic analysis, breed assignment and conservation priorities of three native Danish horse breeds. *Anim Genet.* 2008;39(5):496-505. doi:10.1111/j.1365-2052.2008.01767.x
4. Baumgart A, Gerhards H. Besonderheiten der Tigerschecken-Uveitis und möglicher Cyclosporin A-Einsatz in deren Therapie in Deutschland. *Pferdeheilkunde.* 2014;30(6):626-632.

5. Gilger BC. Equine recurrent uveitis: The viewpoint from the USA. *Equine Vet J.* 2010;42(SUPPL.37):57-61. doi:10.1111/j.2042-3306.2010.tb05636.x
6. Fritz KL, Kaese HJ, Valberg SJ, et al. Genetic risk factors for insidious equine recurrent uveitis in Appaloosa horses. *Anim Genet.* 2014;45(3):392-399. doi:10.1111/age.12129
7. Sandmeyer LS, Kingsley NB, Walder C, et al. Risk factors for equine recurrent uveitis in a population of Appaloosa horses in western Canada. *Vet Ophthalmol.* 2020;23(3):515-525. doi:10.1111/vop.12749
8. Rockwell H, Mack M, Famula T, et al. Genetic investigation of equine recurrent uveitis in Appaloosa horses. *Anim Genet.* 2020;51(1):111-116. doi:10.1111/age.12883
9. Bellone RR, Holl H, Setaluri V, et al. Evidence for a Retroviral Insertion in *TRPM1* as the Cause of Congenital Stationary Night Blindness and Leopard Complex Spotting in the Horse. *PLoS One.* 2013;8(10):1-14. doi:10.1371/journal.pone.0078280
10. Davidson MG, Nasiss MP, Roberts SM. Immunodiagnosis of leptospiral uveitis in two horses. *Equine Vet J.* 1987;19(2):155-157. doi:10.1111/j.2042-3306.1987.tb02615.x
11. Ackermann K, Kenngott R, Settles M, Gerhards H, Maierl J, Wollanke B. In vivo biofilm formation of pathogenic *Leptospira* spp. In the vitreous humor of horses with recurrent uveitis. *Microorganisms.* 2021;9(9):1-14. doi:10.3390/microorganisms9091915
12. Dwyer AE, Crockett RS, Kalsow CM. Association of leptospiral seroreactivity and breed with uveitis and blindness in horses: 372 cases (1986-1993). *J Am Vet Med Assoc.* 1995;207(10):1327-1331. <http://www.ncbi.nlm.nih.gov/pubmed/7591929>

13. Wollanke B, Gerhards H, Brem S, Kopp H, Meyer P. Intraocular and serum antibody titers to *Leptospira* in 150 horses with equine recurrent uveitis (ERU) subjected to vitrectomy. *Berl Munch Tierarztl Wochenschr.* 1998;111(4):134-139.
14. Brem S, Gerhards H, Wollanke B, Meyer P, Kopp H. 35 *Leptospira* isolated from the vitreous body of 32 horses with recurrent uveitis (ERU). *Berl Munch Tierarztl Wochenschr.* 1999;112(10-11):390-393.
15. Faber NA, Crawford M, LeFebvre RB, Buyukmihci NC, Madigan JE, Willits NH. Detection of *Leptospira* spp. in the aqueous humor of horses with naturally acquired recurrent uveitis. *J Clin Microbiol.* 2000;38(7):2731-2733. doi:10.1128/jcm.38.7.2731-2733.2000
16. Niedermaier G, Wollanke B, Hoffmann R, Brem S, Gerhards H. Detection of *Leptospira* in the vitreous body of horses without ocular diseases and of horses with equine recurrent uveitis (ERU) using transmission-electron microscopy. *Dtsch Tierarztl Wochenschr.* 2006;113(11):418-422.
17. Brandes K, Wollanke B, Niedermaier G, Brem S, Gerhards H. Recurrent uveitis in horses: Vitreal examinations with ultrastructural detection of leptospire. *J Vet Med Ser A Physiol Pathol Clin Med.* 2007;54(5):270-275. doi:10.1111/j.1439-0442.2007.00921.x
18. Pearce JW, Galle LE, Kleiboeker SB, et al. Detection of *Leptospira interrogans* DNA and antigen in fixed equine eyes affected with end-stage equine recurrent uveitis. *J Vet Diagnostic Investig.* 2007;19(6):686-690. doi:10.1177/104063870701900611
19. Gerding JC, Gilger BC. Prognosis and impact of equine recurrent uveitis. *Equine Vet J.* 2016;48(3):290-298. doi:10.1111/evj.12451

20. Williams RD, Morter RL, Freeman MJ, Lavignette AM. Experimental chronic uveitis. Ophthalmic signs following equine leptospirosis. *Invest Ophthalmol.* 1971;10(12):948-954.
21. Gilger BC, Salmon JH, Yi NY, et al. Role of bacteria in the pathogenesis of recurrent uveitis in horses from the southeastern United States. *Am J Vet Res.* 2008;69(10):1329-1335. doi:10.2460/ajvr.69.10.1329
22. Matthews AG, Palmer MF. Serological study of leptospiral infections and endogenous uveitis among horses and ponies in the United Kingdom. *Equine Vet J.* 1987;19(2):125-128. doi:10.1111/j.2042-3306.1987.tb02605.x
23. Wollanke B, Gerhards H, Ackermann K. Infectious Uveitis in Horses and New Insights in Its Leptospiral. *Microorganisms.* 2022;10(2):387.
24. Garbe J, Da Y. Pedigraph: A Software Tool for the Graphing and Analysis of Large Complex Pedigree. User manual. Published online 2008.
25. Cunningham EP, Dooley JJ, Splan RK, Bradley DG. Microsatellite diversity, pedigree relatedness and the contributions of founder lineages to thoroughbred horses. *Anim Genet.* 2001;32(6):360-364. doi:10.1046/j.1365-2052.2001.00785.x
26. StataCorp. Stata Statistical Software. Published online 2017.
27. Cutler T, Brooks D, Andrew S, et al. Disease of the equine posterior segment. *Vet Ophthalmol.* 2000;3(2-3):73-82. doi:10.1046/j.1463-5224.2000.00138.x
28. Roberts S. Fundus lesion in equine periodic ophthalmia. *J Am Vet Med.* 1962;141:229-239.
29. Lavach J. Pupil, iris, and ciliary body. In: *Large Animal Ophthalmology.* Mosby Company;

1990:150-177.

30. Sandmeyer LS, Bauer BS, Feng CX, Grahn BH. Equine recurrent uveitis in western Canadian prairie provinces : A retrospective study (2002–2015). *Can Vet J.* 2017;58:717-722.

Chapter 6: Genome-wide Investigation of Genetic Risk Factors for Insidious Uveitis in Horses with LP Spotting

Authors: N. B. Kingsley, L. Sandmeyer, A. Dwyer, M. McCue, M. Lassaline, and R. R. Bellone

Keywords: ERU, Appaloosa, Knabstrupper, Pony of the Americas, *TRPM1*, ocular, inflammation

Summary:

Equine recurrent uveitis (ERU) is a devastating ocular disease that is characterized by inflammation of the uvea within the eye. Horses with the leopard complex spotting pattern (LP) have been identified as being at a higher risk of developing a form of this disease known as insidious uveitis, which features continuous and often subtle inflammation. Based on previous genetic investigations, it was hypothesized that multiple genetic loci influence risk for insidious uveitis. Here, we conducted a genome-wide association study utilizing a combined dataset with genotyping data from 250 horses (111 cases and 139 controls) to identify genetic risk factors shared by three LP spotted horse breeds (Appaloosa, Knabstrupper, and Pony of the Americas). In the combined breed analysis, the locus responsible for LP spotting (*LP*) was the only region to reach genome-wide significance ($P = 6.58 \times 10^{-9}$). Haplotype investigation of the SNP markers within the region of interest refined the association to 76 Kb surrounding the *LP* insertion site. These data support that *LP* or a tightly linked variant is the major genetic risk factor across breeds and suggest that the previously implicated risk factor on the X chromosome (ECA X: 14.5 Mb) identified in Appaloosas may be a breed-specific risk locus.

Main Text:

Insidious uveitis is a form of equine recurrent uveitis (ERU) that is known to affect horses from the Appaloosa, Pony of the Americas (POA), and Knabstrupper breeds, which have been

selected for the leopard complex spotting pattern (LP) (Figure 1).¹⁻⁵ Previous genetic investigations found that the *LP* insertion in *TRPM1*, the variant leading to the LP pattern, was associated with insidious uveitis in both Appaloosa and Knabstrupper horses.⁴⁻⁸ *LP* genotype, however, is not sufficient to explain the distribution of the disease within either breed.^{5,8,9} While the estimated heritability for ERU in Appaloosas was high ($h^2 = 0.77 - 1.0$), *LP* genotype only accounted for 0.20 of the overall estimate.⁹ Thus, it is suspected that additional genetic loci may impact disease predisposition for ERU.

Additional work in Appaloosas identified a modifying locus on the X chromosome (ECA X: 14528106 – 14537812) that was associated with disease status only when accounting for *LP* genotype. This association was further supported by a sex-stratification analysis, and an interaction analysis indicated that *LP* is epistatic to the X locus (Chapter 4). However, none of the single-nucleotide variants identified by whole genome sequencing (WGS) analysis of the region of interest was strongly concordant with phenotype (Chapter 4). Thus, the causal variant from this locus remains to be identified. Furthermore, it is unknown if the association on ECA X is specific to the Appaloosa breed or if the region is also a risk factor in other LP horses. Therefore, a genome-wide association study (GWAS) was performed on a combined dataset of horses from the Appaloosa, Knabstrupper, and POA breeds to identify loci that may confer a predisposition for insidious uveitis across LP spotted breeds.



Figure 1: Leopard Complex Spotting Patterns and *LP* genotype in Appaloosa, Pony of the Americas, and Knabstrupper Breeds. Horses without *LP* do not display the leopard complex spotting patterns and are considered true solid horses as shown in panel A. Horses with one or two copies of the *LP* allele usually have unpigmented areas of coat that can vary in size from minimal white markings (B) through moderate white blankets (C and D) up to extensive unpigmented regions (E and F). In particular, *LP* heterozygotes usually have an unpigmented region that contains pigmented spots (C and E), while *LP/LP* horses have a white pattern area that contains few or no pigmented spots (D and F). Photographs courtesy of Chelsea Thornton (A), Sanna Hedén (B), Cheryl Woods (E), and Ann Dwyer (F).

All protocols were approved by the Institutional Animal Care and Use Committee at the University of California, Davis (18851, 20699, and 22466) or by the Animal Care Committee at the University of Saskatchewan (20110053). All phenotyping followed previously described methods (Chapter 4).⁹ In short, all horses received a complete ocular examination that included neuro-ophthalmic, transilluminator, slit-lamp biomicroscopic, indirect ophthalmoscopic, and tonometry assessments. Horses with evidence of active uveitis (aqueous or vitreous flare, conjunctivitis, miosis, blepharospasm, epiphora, and photophobia) with sequelae from past inflammation received a diagnosis of insidious uveitis. Additionally, horses with signs of chronic inflammation within the eye, including lens luxation, synechiae, mature cataracts, phthisis bulbi, glaucoma, iris atrophy and color changes, corneal neovascularization, and retinal detachment or degeneration, were also diagnosed as affected. Unaffected horses were considered true controls if they were over the age of eight years, had no signs of active uveitis, and no history of ocular disease. Samples of blood and/or hair follicles were collected from each examined horse, and DNA was isolated using the Genra Puregene DNA Isolation kit (Qiagen Inc.), following previously described protocols.¹⁰

A combined dataset of 250 horses (111 cases and 139 controls) included 69 Knabstrappers, 26 POAs, and 155 Appaloosas. All 69 Knabstrupper horses in this dataset were clinically evaluated for ERU as part of a cross-sectional clinical study,⁸ and the samples were either assayed with the GeneSeek Genomic Profiler (GGP) 80K equine genotyping array (48 horses), the Axiom Equine 670K Genotyping (670K) Array (three horses),¹¹ or by whole genome sequencing (WGS) on an Illumina Nova-Seq 4000 (San Diego, CA) with variant-calling that followed previously described methods (18 horses) (Chapter 4). Similarly, the POA horses were genotyped either on the GGP Array (22 horses) or on the 670K Array (4 horses). Of the Appaloosa data, 96 samples were

obtained from Kingsley *et al.* (2022) and were originally assayed on the 670K Array (San Diego, CA).^{9,11} An additional set of 54 Appaloosas were genotyped on the GGP Array, and data from five samples were obtained from WGS on the Illumina Nova-Seq 4000 platform with variants called using the previously described protocol (Chapter 4). Data were remapped to EquCab3.0, if needed.¹² All data were downsampled to the same shared set of 65,673 markers and merged using PLINK, prior to filtering using minor allele frequency < 0.05 , genotype call rate < 0.90 , and sample call rate < 0.90 .¹³ After quality control, the final combined dataset contained 111 affected and 139 unaffected horses and 58,855 SNP markers.

The combined dataset was evaluated with a mixed linear model (MLM) from Genome-wide Efficient Mixed Model Association (GEMMA) software and a SNP-based relationship matrix was used as a covariate to account for relatedness and population substructure.¹⁴ As a previously identified risk factor in Appaloosas and Knabstrappers (Chapter 4),⁷ age was used as a numeric covariate to account for the progressive nature of recurrent uveitis. Additionally, sex was used as a covariate to account for imbalances in the ratio of females to males in the dataset (affected: $\hat{p}_{\text{females}} = 0.39$ and $\hat{p}_{\text{males}} = 0.52$). *LP* genotype was used as a covariate with *LP* genotyping performed by the UC Davis Veterinary Genetics Laboratory diagnostic services. To prevent erroneous associations related to breed difference, breed was also used as a covariate in the analysis of the combined dataset. To adjust for multiple testing correction, strict Bonferroni and modified Bonferroni adjusted thresholds were used in the GWAS analyses. The modified Bonferroni adjusted threshold was calculated with the effective number of independent tests as determined by the Genetic Type 1 Error Calculator (GEC) software.¹⁵ To further assess associations, haplotype phasing was performed using SHAPEIT v2.r904 software. Haplotypes of interest were identified

in the affected horses, and concordance between cases and controls was compared using a chi-squared test.^{16,17}

Investigating breed-specific risk factors in Knabstrupper and POA horses was not feasible due to small sample sizes ($n = 69$ and 26 , respectively). In the combined breed analysis, the only locus to reach genome-wide significance was a region on ECA 1, flanking the *LP* insertion site (chr1_109280171 , $P = 6.58 \times 10^{-9}$) (Figure 2A). When *LP* genotype was used as a covariate in a subsequent analysis, the association on ECA 1 was no longer significant ($P = 0.13$), suggesting that the associated SNPs on ECA 1 were in linkage disequilibrium (LD) with the *LP* locus (Figure 2B).

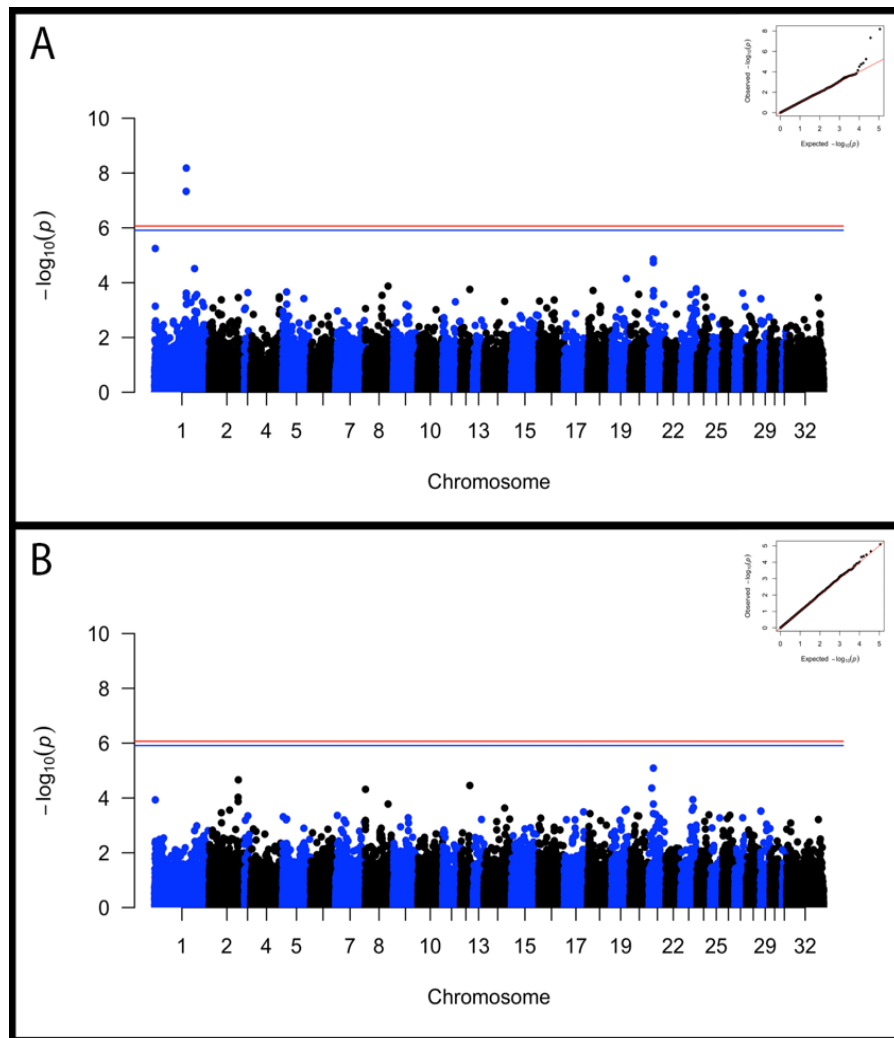


Figure 2: GWAS for insidious uveitis in a combined dataset with 250 samples (111 cases and 139 controls) from the Appaloosa, Pony of the Americas, and Knabstrupper horse breeds. Red vertical line represents a Bonferroni threshold ($\alpha_{\text{bonf.}} = 8.50 \times 10^{-7}$) and blue vertical line represents a modified Bonferroni threshold adjusted for the effective number of independent tests ($\alpha_{\text{mod.bonf.}} = 1.22 \times 10^{-6}$). Quantile-quantile (QQ) plots of p-values are arranged in the upper right corners with the diagonal red line representing perfect normality. (A) Manhattan plot of Wald test p-values from a mixed linear model using GEMMA software. Sex, age, and breed were used as covariates in the analysis. The genomic inflation was 1.02. (B) Manhattan plot of Wald test p-values from a mixed linear model using GEMMA software. *LP* genotype, sex, age, and breed were used as covariates in the analysis. The genomic inflation was 1.04.

To investigate the ECA 1 association further, phased haplotypes were evaluated (Table 1). No haplotypes from the region were perfectly concordant with phenotype. However, one haplotype, designated “Haplotype A” and spanning 76 Kb, was found in 80/80 chromosomes for the affected *LP/LP* horses and all affected *LP/lp* horses had at least one copy (87/142) (Table 2). However, it was also present in 31/32 and 9/47 phased haplotypes from *LP/LP* unaffected and *lp/lp* unaffected horses, respectively. Based on the distribution, we suspect that Haplotype A represents the background haplotype for the *LP* insertion, and any potential causal variants tightly linked with *LP* will also reside on Haplotype A. Although significantly associated with ERU, Haplotype A was not more concordant with disease status than *LP* ($P_{\text{HapA}} = 9.04 \times 10^{-21}$ versus $P_{\text{LP}} = 1.08 \times 10^{-27}$).

Table 1: Refining the Associated Region on ECA 1 from the 111 Affected Horses. Using phased haplotypes, the association within the region of interest on chromosome 1 (ECA 1: 104222042 - 114132959) was found to extend for 76 Kb based on identified recombination within the affected horses (ECA 1: 109204337 – 109280171, termed Haplotype A). Presented are the recombinant haplotypes used to define the boundaries of Haplotype A. An asterisk denotes the most concordant GWAS marker ($P = 6.58 \times 10^{-9}$).

Horse ID:	109137810	109141476	109204337	109221223	109254391	109257750	109280171*	109334984	109385060	Count:
17-502	0	1	1	1	1	1	1	1	1	64
05-102	1	1	1	1	1	1	1	1	0	54
17-432	1	1	1	1	1	1	1	1	1	41
16-274	0	1	1	1	1	1	1	1	0	5
20-14	1	1	1	1	1	1	1	0	1	1
16-287	1	0	1	1	1	1	1	1	0	1
16-259	1	1	1	1	1	1	1	0	0	1

Table 2: Distribution of Haplotype A by *LP* genotype. Haplotype A extends for 76 Kb (ECA 1: 109204337 – 109280171). Haplotype frequencies are listed in parentheses and an asterisk denotes the most concordant GWAS marker.

		Horses	Haplotype A	Other Haplotypes	Total
Affected	<i>LP/LP</i>	40	80	0	80
	<i>LP/lp</i>	71	87	55	142
	<i>lp/lp</i>	0	0	0	0
	Total	111	167 (0.752)	55 (0.248)	222
Unaffected	<i>LP/LP</i>	16	31	1	32
	<i>LP/lp</i>	86	102	70	172
	<i>lp/lp</i>	37	9	65	74
	Total	139	142 (0.511)	136 (0.489)	278
	109204337	109221223	109254391	109257750	109280171*
Haplotype A	T	T	A	T	C

The current results support that *LP* or a variant within the surrounding 76 Kb defined haplotype is a major additive risk factor with incomplete penetrance for insidious uveitis. In particular, we found that none of the true solid (*lp/lp*) horses (n = 37) were affected, yet not every horse with an *LP* allele or Haplotype A is affected (affected: $\hat{p}_{LP} = 0.52$ and $\hat{p}_{HapA} = 0.50$). While it has been suspected that the discordance between *LP* genotype and disease status are mainly explained by other genetic loci, limited work has investigated environmental risk factors or gene by environment (GxE) interactions that may impact disease onset and lead to reduced penetrance of the *LP* locus. Identification of non-genetic risk factors was not within the scope of this study; however, additional research is needed to identify potential environmental risk factors and GxE interactions that are specific to insidious uveitis in LP spotted breeds.

In this study, the region containing *LP* was identified as the only major risk locus that is shared across the Appaloosa, Knabstrupper, and POA breeds. The X locus that was previously associated with insidious uveitis in a cohort of Appaloosas was not significantly associated in our

multibreed GWAS, indicating that the ECA X locus may contain an Appaloosa-specific risk factor (Chapter 4). Additional work is needed to further characterize potential breed-specific risk factors within each of the LP breeds. Yet, the significant association on ECA 1 in the multibreed GWAS indicates that *LP* genotype is a valuable diagnostic tool for assessing risk of developing insidious uveitis across horse breeds. Although *LP* has been repeatedly implicated as a risk factor, it is not clear if the associations are the result of a functional link between *LP* and ERU or if they are due to a tightly linked causal variant. Investigation of the haplotypes surrounding the top associated markers did not identify a haplotype that was more concordant with phenotype than the *LP* genotype. Yet, one haplotype was identified in all affected horses, and it refined the association to 76 Kb, including the site of the *LP* insertion. Further evaluation of additional variants within this region by WGS is necessary to definitively identify the causal variant.

The functional role of *TRPM1* in vision under scotopic conditions was initially identified through investigations of the pleiotropic effect of the *LP* insertion in triggering Appaloosa spotting and congenital stationary night blindness (CSNB).^{6,18,19} Since those discoveries, molecular investigations have confirmed that TRMP1 is a necessary cation channel for hyperpolarizing (no light detection) or depolarizing (light detection) of the ON-bipolar cells, which are the post-synaptic partners for the rod cells within the mammalian eye.²⁰ *LP/LP* horses are not expected to have any functional TRPM1 protein produced, yet lack of TRMP1 in knockout experiments has not been reported to lead to ocular inflammation or coat color changes in mice.^{6,21} For these reasons, it is suspected that the 1,378 bp insertion of the *LP* allele may directly contribute to the etiology of uveitis in LP patterned horses. During the original identification of the insertion, it was characterized as a long-terminal repeat (LTR) from a past retroviral insertion, and the LTR, itself, contains at least nine predicted open reading frames.⁶ Additionally, several members of the TRP

protein family play key roles in the function of immune cells.²² For example, TRPM2 impacts cytokine secretion and proliferation of T-cells, as well as playing key roles in other immune cells, and mice deficient for TRPM2 were more susceptible to infection with *Listeria monocytogenes*, due to a diminished innate immune response.^{23,24} Thus, functional assessments of the *LP* insertion and TRPM1 are necessary future directions for investigating the etiology of insidious uveitis.

Acknowledgments:

authors would like to thank the horses and owners who made this research possible. The authors would also like to thank Drs. Thomas Launois, Henneke Hermans, Sanna Hedèn, Anna Hallendar-Edman, and Richard McMullen for contributing samples to this investigation. The research was supported by the KNN, the Center for Equine Health at the University of California – Davis, the Townsend Equine Health Research Fund (TEHRF), and the Morris Animal Foundation (D16EQ-028). The mission of the Morris Animal Foundation is to bridge science and resources to advance the health of animals. N. B. Kingsley was also supported in part by the University of California – Davis, Center for Equine Health Fellowship.

Conflict of Interest:

N. B. Kingsley and R. R. Bellone are affiliated with the UC Davis Veterinary Genetics Laboratory, a service laboratory offering diagnostic genetic tests for horses and other animal species.

References:

1. Sandmeyer LS, Bauer BS, Feng CX, Grahn BH. Equine recurrent uveitis in western Canadian prairie provinces : A retrospective study (2002–2015). *Can Vet J.* 2017;58:717-722.

2. Dwyer AE, Crockett RS, Kalsow CM. Association of leptospiral seroreactivity and breed with uveitis and blindness in horses: 372 cases (1986-1993). *J Am Vet Med Assoc.* 1995;207(10):1327-1331. <http://www.ncbi.nlm.nih.gov/pubmed/7591929>
3. Baumgart A, Gerhards H. Besonderheiten der Tigerschecken-Uveitis und möglicher Cyclosporin A-Einsatz in deren Therapie in Deutschland. *Pferdeheilkunde.* 2014;30(6):626-632.
4. Fritz KL, Kaese HJ, Valberg SJ, et al. Genetic risk factors for insidious equine recurrent uveitis in Appaloosa horses. *Anim Genet.* 2014;45(3):392-399. doi:10.1111/age.12129
5. Rockwell H, Mack M, Famula T, et al. Genetic investigation of equine recurrent uveitis in Appaloosa horses. *Anim Genet.* 2020;51(1):111-116. doi:10.1111/age.12883
6. Bellone RR, Holl H, Setaluri V, et al. Evidence for a Retroviral Insertion in *TRPM1* as the Cause of Congenital Stationary Night Blindness and Leopard Complex Spotting in the Horse. *PLoS One.* 2013;8(10):1-14. doi:10.1371/journal.pone.0078280
7. Sandmeyer LS, Kingsley NB, Walder C, et al. Risk factors for equine recurrent uveitis in a population of Appaloosa horses in western Canada. *Vet Ophthalmol.* 2020;23(3):515-525. doi:10.1111/vop.12749
8. Kingsley NB, Sandmeyer LS, Parker S, et al. Risk Factors for Equine Recurrent Uveitis in Knabstrupper Horses. *Equine Vet J.* 2022; Submitted.
9. Kingsley NB, Sandmeyer LS, Norton E, et al. Heritability of Insidious Uveitis in Appaloosa Horses. *Anim Genet.* 2022; Accepted.
10. Bellone RR, Liu J, Petersen JL, et al. A missense mutation in damage-specific DNA binding protein 2 is a genetic risk factor for limbal squamous cell carcinoma in horses. *Int J Cancer.* 2017;141:342-353. doi:10.1002/ijc.30744

11. Schaefer RJ, Schubert M, Bailey E, et al. Developing a 670k genotyping array to tag ~2M SNPs across 24 horse breeds. *BMC Genomics*. 2017;18(1):1-18. doi:10.1186/s12864-017-3943-8
12. Beeson SK, Schaefer RJ, Mason VC, McCue ME. Robust remapping of equine SNP array coordinates to EquCab3. *Anim Genet*. 2019;50(1):114-115. doi:10.1111/age.12745
13. Purcell S, Neale B, Todd-Brown K, et al. PLINK: A tool set for whole-genome association and population-based linkage analyses. *Am J Hum Genet*. 2007;81(3):559-575. doi:10.1086/519795
14. Zhou X, Stephens M. Genome-wide Efficient Mixed Model Analysis for Association Studies. *Nat Genet*. 2012;44(7):821-824. doi:10.1038/ng.2310
15. Li MX, Yeung JMY, Cherny SS, Sham PC. Evaluating the effective numbers of independent tests and significant p-value thresholds in commercial genotyping arrays and public imputation reference datasets. *Hum Genet*. 2012;131(5):747-756. doi:10.1007/s00439-011-1118-2
16. Delaneau O, Zagury JF, Marchini J. Improved whole-chromosome phasing for disease and population genetic studies. *Nat Methods*. 2013;10(1):5-6. doi:10.1038/nmeth.2307
17. Delaneau O, Marchini J, Zagury JF. A linear complexity phasing method for thousands of genomes. *Nat Methods*. 2012;9(2):179-181. doi:10.1038/nmeth.1785
18. Bellone RR, Brooks SA, Sandmeyer L, et al. Differential gene expression of *TRPM1*, the potential cause of congenital stationary night blindness and coat spotting patterns (LP) in the Appaloosa horse (*Equus caballus*). *Genetics*. 2008;179(4):1861-1870. doi:10.1534/genetics.108.088807
19. Bellone RR, Forsyth G, Leeb T, et al. Fine-mapping and mutation analysis of *TRPM1*: A

- candidate gene for leopard complex (LP) spotting and congenital stationary night blindness in horses. *Briefings Funct Genomics Proteomics*. 2010;9(3):193-207. doi:10.1093/bfgp/elq002
20. Xu Y, Orlandi C, Cao Y, et al. The TRPM1 channel in ON-bipolar cells is gated by both the α and the β 13 subunits of the G-protein G_o. *Sci Rep*. 2016;6(September 2015). doi:10.1038/srep20940
 21. Morgans CW, Brown RL, Duvoisin RM. TRPM1: The endpoint of the mGluR6 signal transduction cascade in retinal ON-bipolar cells. *BioEssays*. 2010;32(7):609-614. doi:doi:10.1002/bies.200900198
 22. Parenti A, De Logu F, Geppetti P, Benemei S. What is the evidence for the role of TRP channels in inflammatory and immune cells? *Br J Pharmacol*. 2016;173(6):953-969. doi:10.1111/bph.13392
 23. Melzer N, Hicking G, Göbel K, Wiendl H. TRPM2 Cation Channels Modulate T Cell Effector Functions and Contribute to Autoimmune CNS Inflammation. *PLoS One*. 2012;7(10):1-6. doi:10.1371/journal.pone.0047617
 24. Knowles H, Heizer JW, Li Y, et al. Transient Receptor Potential Melastatin 2 (TRPM2) ion channel is required for innate immunity against *Listeria monocytogenes*. *Proc Natl Acad Sci U S A*. 2011;108(28):11578-11583. doi:10.1073/pnas.1010678108

Conclusion:

Insidious uveitis is a devastating form of ERU that is particularly common among horses with the leopard complex spotting pattern (LP). It is clear from this work and proceeding studies that the *LP* allele—involved in LP coat color patterning and CSNB— or a tightly linked variant is a major risk factor for insidious uveitis in horses. Yet, *LP* genotype is not sufficient to explain the distribution of insidious uveitis in Appaloosas or Knabstrappers as some, but not all, heterozygous and *LP* homozygous individuals are affected by the disease. While the SNP-based heritability estimate suggests that ERU is highly heritable, *LP* only contributed 0.20 to the overall estimate ($h^2 = 0.77 - 1.0$). For these reasons, the over-arching aim of this dissertation work was to characterize the missing genetic contribution by identifying and investigating additional variants leading to ERU, which we suspected to impact relevant gene pathways, such as pigmentation, immunity, or ocular function.

Using genotyping array data from 96 Appaloosas, a GWAS with *LP* genotype, sex, and age as covariates identified a significant association between disease status and a 9.7 Kb region on ECA X. This region encompasses a promising candidate gene, *RSI*, has been implicated in ocular function in mammals. However, none of the 102 SNVs investigated following WGS sequencing of the associated locus were as concordant or more concordant with phenotype than *LP* or the original ECA X SNP markers in a larger dataset ($n = 157$). In the future, additional mutations such as indels and structural variants will be evaluated from this locus to identify potential causative variants associated with ERU phenotype for further investigation.

Furthermore, a GWAS of 250 combined Appaloosa, POA, and Knabstrupper horses identified the region on ECA 1 containing *LP* as the only shared risk locus across LP breeds. Despite extensive replication, it is still not clear if the associations to the *LP* insertion are causal

or the result of linkage. Through haplotype phasing, we were not able to identify a haplotype in the region that was perfectly concordant with the disease phenotype. The distribution of the most associated haplotype suggests, instead, that the locus on ECA 1 displays incomplete penetrance for ERU. Still, additional fine mapping and functional assessments of the region of interest are needed to determine the underlying role of *LP* in this disease.

Similar to risk loci for other complex diseases that have incomplete penetrance, many factors likely affect the probability that an individual with *LP* will experience onset of insidious uveitis, as well as influencing disease progression. For example, uncharacterized environmental factors or GxE interactions could explain the discrepancy. While such factors can be difficult to assess, attempts should be made to identify additional non-genetic risk factors in the future through longitudinal and twin studies of insidious uveitis in *LP* spotted breeds. In addition to environmental factors, other genetic variants can also contribute to incomplete penetrance of a major locus. Given the role of the immune system in ERU and the complexity of immunogenetics, many loci of small effect, even to the point of genetic background, may influence disease risk. Furthermore, loci may impact ERU onset at the level of the individual, the family, the subpopulation, or the breed. This can make identification of the missing risk factors especially challenging as private variation usually cannot be identified by leveraging large sample sizes. However, our discovery of the X chromosome locus specific to the Appaloosa breed suggests that breed-specific loci are informative for disease risk, and breed-specific investigations of genetic and non-genetic risk factors in the Knabstrupper and POA breeds should be a priority for future research.

Addendum 1: "Adopt-a-Tissue" Initiative Advances Efforts to Identify Tissue-Specific Histone Marks in the Mare

Authors: N. B. Kingsley, Natasha Hamilton, Gabriella Lindgren, Ludovic Orlando, Ernie Bailey, Samantha Brooks, Molly McCue, T. S. Kalbfleisch, James N. MacLeod, Jessica L. Petersen, Carrie J. Finno, and Rebecca R. Bellone.

Keywords: genome, annotation, epigenetics, horse, chromatin, consortium, collaboration, regulation

Reference: Kingsley, N.B.; Hamilton, N.; Lindgren, G.; Orlando, L.; Bailey, E.; Brooks, S.; McCue, M.; Kalbfleisch, T.S.; MacLeod, J.N.; Petersen, J.L.; Finno, C.J.; Bellone, R.R. "Adopt-a-Tissue" Initiative Advances Efforts to Identify Tissue-Specific Histone Marks in the Mare. *Front. Genet.* **2021**, *12*, 649959. <https://doi.org/10.3389/fgene.2021.649959>.

Accepted: March 1, 2021

1. Introduction

The equine genetics and genomics research community has a long history of synergistic collaborations for developing tools and resources to advance equine biology. Starting in 1995 with the first International Equine Gene Mapping Workshop supported by the Dorothy Russell Havemeyer Foundation Inc. (Bailey, 2010), researchers collaborated to build comprehensive equine linkage maps (Guérin et al., 1999, 2003; Penedo et al., 2005; Swinburne et al., 2006), radiation hybrid and comparative maps (Caetano et al., 1999; Chowdhary et al., 2002), physical marker and BAC contig maps (Raudsepp et al., 2004, 2008; Leeb et al., 2006), reference genomes for the horse (Wade et al., 2009; Kalbfleisch et al., 2018), and genotyping arrays to economically map and study traits of interest for horse owners and breeders (McCue et al., 2012;

McCoy and McCue, 2014; Schaefer et al., 2017). Continuing the legacy of community-based advancements, a new collective effort began in 2015 to functionally annotate DNA elements in the horse as part of the international Functional Annotation of Animal Genomes (FAANG) Consortium (Andersson et al., 2015; Tuggle et al., 2016; Burns et al., 2018).

Reminiscent of the ENCODE project in humans and mice (Dunham et al., 2012), the ultimate goal of the FAANG consortium is to annotate the major functional elements in the genomes of domesticated animal species (Andersson et al., 2015). In particular, four histone modifications were chosen by the consortium to characterize the genomic locations of enhancers (H3K4me1), promoters and transcription start sites (H3K4me3), open chromatin with active regulatory elements (H3K27ac), and facultative heterochromatin with inaccessible or repressed regulatory elements (H3K27me3) (Andersson et al., 2015; Giuffra and Tuggle, 2019). The initial equine FAANG efforts identified putative regulatory regions in eight prioritized tissues of interest (TOI) by performing Chromatin Immuno-Precipitation Sequencing (ChIP-Seq) for the four target histone marks (Kingsley et al., 2020). In that investigation, more than one million putative regulatory sites were characterized across the equine genome. With more than 80 tissues, cell lines, and body fluids stored in the equine biobank (Burns et al., 2018), further opportunities to expand the scope of the annotation work exist. To leverage the benefits of the biobank, a collaborative sponsorship program titled “Adopt-a-Tissue” was created to enable researchers from across the globe to select and support annotation of a tissue by the equine FAANG group. Through this effort, four additional “Adopted” tissues— spleen, metacarpal 3 (MC3), sesamoid, and full thickness skin— were assayed by histone mark ChIP-Seq to expand the tissue-specific annotation resources available to the entire equine research community.

2. Methods

All ChIP-Seq assays were performed by Diagenode ChIP-Seq Profiling Service (Diagenode, Cat# G02010000, Liège, Belgium). Summarized experimental procedures are available in more detail at the FAANG FTP site hosted by EBI (<ftp://ftp.faang.ebi.ac.uk/faang/ftp/protocols/assays/> and <ftp://ftp.faang.ebi.ac.uk/faang/ftp/protocols/experiments/>). Spleen samples were processed following the assay procedures outlined in [UCD_SOP_ChIP-Seq_for_Histone_Marks_20191101.pdf](#). Skin and both bone tissues were processed following the experimental protocols outlined in [UCD_SOP_ChIP-seq_for_Histone_Marks_Skin_20201218.pdf](#) and [UCD_SOP_ChIP-seq_for_Histone_Marks_Bone_20201218.pdf](#), respectively. “Adopted” tissues, as summarized in Supplementary Table 1, were collected from two Thoroughbred mares (denoted as ECA_UCD_AH1 for SAMEA104728862 and ECA_UCD_AH2 for SAMEA104728877) as part of the FAANG equine biobank (Burns et al., 2018) following protocols approved by the University of California, Davis Institutional Animal Care and Use Committee (Protocol #19037).

Chromatin was isolated from the two bone tissues using the TrueMicro ChIP-Seq kit (Diagenode Cat# C01010140) and from spleen and skin using the iDeal ChIP-Seq kit for Histones (Diagenode Cat# C01010059). Starting amounts for each replicate varied by tissue with ~100 mg for spleen, 375-770 mg for MC3, 445-650 mg for sesamoid, and ~125 mg for skin. After homogenization, fixed samples were sheared with the Bioruptor® Pico (Diagenode Cat# B01060001) for 12 (spleen), 10-12 (MC3 and sesamoid), and 8 (skin) cycles of 30 seconds on and 30 seconds off. The amount of chromatin yield and thus chromatin per IP varied by tissue. Spleen and skin had the greatest amounts (1.5 µg and 600 ng, respectively) per IP and MC3 and sesamoid had the least (350 ng each). The following antibody concentrations were used for MC3, sesamoid, and skin: 0.5 µg for H3K4me1, 0.5 µg for H3K4me3, 1 µg for H3K27ac, and 1 µg for H3K27me3.

To account for the greater amount of chromatin from spleen, twice the amount of antibody was used for each mark compared to the other three tissues. For all tissues, 10% of the total chromatin from each replicate was saved for the input.

Libraries were prepared with the IP-Star® Compact Automated System (Diagenode Cat# B03000002) using the MicroPlex Library Preparation Kit v2 (Diagenode Cat# C05010013). Spleen, MC3, and sesamoid were sequenced as 50 basepair single-end (SE) reads on the HiSeq 4000 platform (Illumina, San Diego, CA, USA). For these tissues, the broad mark (H3K27me3) was sequenced to a minimum of 50M raw reads while the remaining marks (H3Kme1, H3K4me3, and H3K27ac) and the input were sequenced to a minimum depth of 30M raw reads. Methods for analyzing SE reads followed the procedures described previously (Kingsley et al., 2020). Due to advancements in sequencing technology, skin tissue was sequenced as 50 basepair paired-end (PE) reads on the NovaSeq 6000 (Illumina, San Diego, CA, USA). For skin, the broad mark (H3K27me3) was sequenced to a minimum of 100M raw fragments while the remaining marks (H3Kme1, H3K4me3, and H3K27ac) and the input were sequenced to a minimum depth of 40M raw fragments.

Methods for analyzing SE reads followed the procedures described previously (Kingsley et al., 2020), and modifications were made to the SE analysis methods to accommodate PE data generated from skin. After trimming with Trim-Galore version 0.4.0 (Martin, 2011; Andrews et al., 2012), reads were aligned to EquCab3.0 (Kalbfleisch et al., 2018) with BWA-MEM version 0.7.9a (Li and Durbin, 2009). Alignments in BAM format were filtered using SAMtools version 1.9 (Li et al., 2009). Reads were removed if they did not map, had secondary alignments (including split hits), failed platform/vendor quality tests, were identified as optical duplicates, or had an alignment quality score less than 30. PE reads were also removed if the mates did not map. PCR

duplicates were marked with PicardTools version 2.7.1 (Picard toolkit, 2019) and removed with SAMtools. For peak-calling, MACS2 version 2.1.1.20160309 (Zhang et al., 2008) was used to call peaks for all marks with PE data denoted by a PE flag (-f BAMPE). SICERpy version 0.1.1 was also used to call peaks for H3K27me3 as it specializes in broad peak calling (SICERpy, GitHub Repository.; Zang et al., 2009). To use SICERpy with the PE data, the second read in each pair was removed and data were processed as SE based on recommendations from the software developers. Peak-calls were combined by identifying overlapping regions of enrichment in both biological replicates where at least one replicate was significantly enriched for a given mark. Heatmaps and quality metrics were generated using deepTools 2.4.2 (Ramírez et al., 2016), SPP 1.13 (Kharchenko et al., 2008), and custom scripts. Detailed bioinformatic workflows are available at <ftp://ftp.faang.ebi.ac.uk/faang/ftp/protocols/analysis/>.

3. Quality Assessment

3.1 Library Complexity

Data were assessed for library complexity with metrics established by ENCODE and endorsed by FAANG, including nonredundant fraction (NRF), PCR bottleneck coefficient 1 (PBC1), and PCR bottleneck coefficient 2 (PBC2) (Landt et al., 2012; Kingsley et al., 2020). All of the libraries prepared surpassed the quality threshold for the PBC2 metric ($PBC2 > 1$), however, several marks and tissues fell below the quality threshold for NRF and PBC1 (Table 1). For example, three of the four marks for spleen passed all library complexity measures while the H3K27me3 data from both biological replicates failed NRF and PBC1. Additionally, both replicates for sesamoid and MC3 passed all three metrics for H3K4me1 and H3K27me3 but fell below threshold for H3K4me3 and H3K27ac. All skin libraries passed NRF and PBC1 thresholds

with three exceptions: both replicates for H3K4me3 and ECA_UCD_AH2 replicate for H3K4me1.

In addition to quality metrics, sequencing data were evaluated at several processing stages of the analysis including alignment and PCR deduplication. All datasets generated high mapping quality scores (> 35) and exceeded the minimum sequencing targets as described in the methods (Supplementary Table 2). Skin and spleen tissues retained a high number of reads for H3K4me1, H3K4me3, and H3K27ac after alignment, filtering, and deduplication (> 20 M reads per replicate). Although all three activating marks were sequenced to the same target for both bone tissues, H3K4me1 retained more than 20M reads per replicate while H3K4me3 and H3K27ac fell below 20M processed reads per replicate with the majority of reads removed by deduplication. More than 40M reads remained for each H3K27me3 replicate after processing with the exception of ECA_UCD_AH2 for sesamoid.

3.2 IP Enrichment

Data were also evaluated for IP enrichment using a variety of metrics to determine signal quality. For normalized strand cross-correlation (NSC) and relative strand cross-correlation (RSC) assessments as established by ENCODE (Landt et al., 2012), all marks for skin tissue exceeded the minimum quality threshold (Table 1). Additionally, the biological replicates for H3K4me3 and H3K27ac from spleen and MC3, as well as the H3K4me3 replicates for sesamoid, passed both cross-correlation measures. Similar to the library complexity metrics, several tissues fell below the quality thresholds (NCS > 1.05 and RSC > 0.8) including H3K4me1 from sesamoid and MC3; H3K27ac from ECA_UCD_AH2 sesamoid; and H3K27me3 from spleen, sesamoid, and MC3. Alignments were also assessed using the Jensen Shannon distance (JSD) to compare the

distribution of reads with that of the background (input). Using JSD, H3K27me3 from both spleen replicates had values below 0.05, which is indicative of insufficient IP enrichment.

The final measure of IP enrichment evaluated the fraction of reads in peaks (FRiP) by comparing the peak calls with the read distribution for each sample. All tissues produced a high proportion of aligned reads within peaks for H3K4me3, ranging from 0.21 for sesamoid to 0.69 for skin. Similarly, MC3, skin, and spleen generated high FRiP scores for H3K27ac (0.47-0.19), and peaks from skin and spleen also scored well for H3K4me1 (0.47-0.29). Although lower than the values from skin and spleen, FRiP scores from MC3 indicated sufficient enrichment was obtained for H3K4me1 (0.07-0.09). For sesamoid tissue, the ECA_UCD_AH2 replicate generated peaks with comparable enrichment for H3K4me1, H3K27ac, and H3K27me3, while the ECA_UCD_AH2 replicate scored below threshold for both H3K4me1 and H3K27me3 (0.0005 and 0.0043, respectively). Further, H3K27me3 peaks from skin generated a substantially higher fraction of reads compared with MC3 and spleen (0.21-0.24 versus 0.05-0.10), although all three of these tissues obtained sufficient enrichment based on this assessment.

3.3 Replicate Comparison

In addition to quality assessments for the read alignments, peaks called from the biological replicates were compared. For most of the marks, the percentage of genome covered by peaks was consistent with previously reported values for the TOI (Table 1). For sesamoid tissue, at least one replicate for H3K4me1, H3K27ac, and H3K27me3 generated fewer peak calls than expected based on results from the other replicate and the MC3 replicates. Additionally, the initial data for H3K27me3 from both spleen replicates yielded fewer peaks in accordance with the low complexity and enrichment scores for those libraries. The Jaccard similarity coefficient identified the highest correlation between the biological replicates for H3K4me3 across all “Adopted” tissues, ranging

from 0.65 to 0.84 (Table 2), and data from skin also showed high correlation for all marks (0.44 to 0.84). Replicates for spleen and MC3 had moderate levels of similarity for H3K4me1 and H3K27ac (0.32 to 0.58), while the biological replicates for H3K4me1 and H3K27me3 from sesamoid had no identity detected, consistent with the low-scoring quality assessments.

Table 1: Quality metrics and peak-calling summary for each biological replicate. The summary includes six quality metrics—Non-Redundant Fraction (NRF), PCR Bottleneck Coefficient 1 and 2 (PBC1 and PBC2), Normalized Strand Cross-Correlation Coefficient (NSC), Relative Strand Cross-Correlation Coefficient (RSC), and Fraction of Reads in Peaks (FRiP)—and thresholds originally established by ENCODE, and the Jensen Shannon Distance (JSD). Samples include all of the original spleen IP, the repeated spleen IP for H3K27me3, and the merged (original + repeated) spleen IPs for H3K27me3. Peaks used to determine FRiP and peak numbers for H3K27me3 were called with SICER. All other peaks were generated with MACS2. Biological replicates are denoted as AH1 for SAMEA104728862 and AH2 for SAMEA104728877.

Mark	Tissue	Replicate	NRF	PBC1	PBC2	NSC	RSC	JSD	FRiP	Peak
		Threshold:	(>0.5)	(>0.5)	(>1)	(>1.05)	(>0.8)	(>0.05)	(>0.01)	Calls
K4me1	Spleen	AH1	0.65	0.64	2.82	1.03	0.98	0.39	0.20	84146
K4me1	Spleen	AH2	0.74	0.74	3.80	1.04	0.96	0.39	0.25	113447
K4me3	Spleen	AH1	0.62	0.64	2.98	2.67	1.44	0.62	0.57	28735
K4me3	Spleen	AH2	0.57	0.60	2.67	2.53	1.34	0.62	0.57	31198
K27ac	Spleen	AH1	0.65	0.66	2.96	1.34	1.54	0.46	0.29	50977
K27ac	Spleen	AH2	0.70	0.70	3.40	1.31	1.46	0.45	0.29	60281
K27me3	OriginalSpleen	AH1	0.43	0.42	1.79	1.01	0.64	0.02	0.05	1136
K27me3	RepeatSpleen	AH1	0.13	0.28	2.94	1.03	0.33	0.20	0.02	164
K27me3	MergedSpleen	AH1	0.32	0.40	1.86	1.01	0.59	0.50	0.05	6297
K27me3	OriginalSpleen	AH2	0.44	0.43	1.82	1.01	0.67	0.05	0.08	6647
K27me3	RepeatSpleen	AH2	0.66	0.67	3.02	1.02	0.74	0.06	0.10	32492
K27me3	MergedSpleen	AH2	0.53	0.55	2.40	1.01	0.83	0.06	0.11	37629
K4me1	Sesamoid	AH1	0.63	0.63	2.64	1.02	0.63	0.31	0.08	43397
K4me1	Sesamoid	AH2	0.84	0.85	6.46	1.01	0.49	0.21	0.00	4
K4me3	Sesamoid	AH1	0.37	0.39	1.79	2.33	1.26	0.57	0.48	19617
K4me3	Sesamoid	AH2	0.39	0.40	1.78	1.40	1.20	0.41	0.21	16524
K27ac	Sesamoid	AH1	0.42	0.42	1.81	1.16	1.19	0.40	0.19	34223

K27ac	Sesamoid	AH2	0.34	0.34	1.67	1.02	0.60	0.31	0.02	5013
K27me3	Sesamoid	AH1	0.68	0.68	3.11	1.01	0.48	0.25	0.06	1840
K27me3	Sesamoid	AH2	0.75	0.75	3.97	1.01	0.56	0.18	0.00	0
K4me1	MC3	AH1	0.74	0.74	3.76	1.02	0.68	0.12	0.09	56238
K4me1	MC3	AH2	0.77	0.77	4.28	1.02	0.63	0.13	0.07	47452
K4me3	MC3	AH1	0.14	0.27	2.91	2.73	1.22	0.48	0.50	19209
K4me3	MC3	AH2	0.32	0.34	1.71	2.56	1.20	0.48	0.50	21339
K27ac	MC3	AH1	0.27	0.29	1.65	1.25	1.19	0.30	0.23	36022
K27ac	MC3	AH2	0.09	0.26	4.56	1.38	0.95	0.32	0.19	16638
K27me3	MC3	AH1	0.57	0.58	2.36	1.01	0.55	0.25	0.10	17001
K27me3	MC3	AH2	0.65	0.65	2.88	1.01	0.51	0.22	0.08	13790
K4me1	Skin	AH1	0.43	0.47	2.14	1.15	2.85	0.29	0.34	115470
K4me1	Skin	AH2	0.53	0.55	2.39	1.13	3.06	0.25	0.29	109322
K4me3	Skin	AH1	0.41	0.46	2.12	3.14	1.27	0.60	0.69	24442
K4me3	Skin	AH2	0.32	0.40	2.12	3.19	1.30	0.60	0.68	23584
K27ac	Skin	AH1	0.50	0.53	2.30	1.51	1.45	0.41	0.47	58278
K27ac	Skin	AH2	0.58	0.59	2.57	1.47	1.46	0.40	0.47	57737
K27me3	Skin	AH1	0.50	0.53	2.36	1.06	3.20	0.14	0.24	95788
K27me3	Skin	AH2	0.50	0.54	2.40	1.06	4.09	0.11	0.21	77151

3.4 Additional Data Collection

Due to insufficient enrichment and replicate identity, IP and sequencing were repeated for H3K27me3 from both spleen replicates. Unfortunately, the repeated ECA_UCD_AH1 data had low library complexity and IP enrichment (Table 1 and Supplementary Table 2). To achieve sufficient data for accurate peak calling from spleen tissue, the first round of IP and sequencing from ECA_UCD_AH1 for H3K27me3 and both rounds from ECA_UCD_AH2 were used for combined peak calling. Reads from the two input files for ECA_UCD_AH2 were also merged. The number of combined peaks increased from 4,955 covering 1.98% from the first round of

sequencing to 5,267 covering 2.18% of the genome when data were merged (Table 2). Similar issues with enrichment prevented sufficient signal for peak calling in sesamoid for three of the four marks, and therefore, a second round of IP and quality evaluation of ECA_UCD_AH2 sesamoid is underway for H3K4me1, H3K27ac, and H3K27me3.

Table 2: Summary of the combined peak calls and replicate comparison. The summary includes the combined number of peaks and the percentage of the genome covered by those peaks. The Jaccard Similarity Coefficient compares the two biological replicates with 1 being perfectly concordant and 0 being entirely discordant. Peaks for H3K4me1, H3K4me3, and H3K27ac were called with MACS2.

Mark	Tissue	Combined Peak Number	% Covered	Jaccard Similarity Coefficient
H3K4me1	Spleen	73528	2.98	0.44
H3K4me3	Spleen	28661	1.56	0.80
H3K27ac	Spleen	51427	1.82	0.58
H3K27me3 MACS2	Spleen	7349	0.09	0.01
H3K27me3 SICER	Spleen	449	0.22	0.03
H3K4me1	MC3	46511	1.16	0.32
H3K4me3	MC3	20556	1.10	0.75
H3K27ac	MC3	31547	1.08	0.38
H3K27me3 MACS2	MC3	15304	0.40	0.28
H3K27me3 SICER	MC3	5628	2.57	0.28
H3K4me1	Sesamoid	750	0.01	0.00
H3K4me3	Sesamoid	17361	1.07	0.65
H3K27ac	Sesamoid	13160	0.67	0.08
H3K27me3 MACS2	Sesamoid	390	0.01	0.00
H3K27me3 SICER	Sesamoid	703	0.26	0.00
H3K4me1	Skin	92971	4.56	0.50
H3K4me3	Skin	24353	1.60	0.84
H3K27ac	Skin	54946	3.38	0.67

H3K27me3 MACS2	Skin	51480	6.02	0.44
H3K27me3 SICER	Skin	11764	6.28	0.44

4. Data Metrics

After combining replicates, the number of retained peaks for each mark from the SE data ranged from 4,933 to 73,528 for spleen and from 5,628 to 46,511 for MC3 (Table 2). For both tissues, H3K4me1—the mark indicative of enhancers—was found to have the highest number of peaks while the repressive mark was found to have the lowest. This pattern is also consistent with the TOI data (Kingsley et al., 2020). For PE skin data, the number of combined peaks varied from 24,353 to 92,971 regions, and H3K4me3, which denotes promoters, was the mark with the lowest number of peaks. Additionally, the amount of the genome covered by H3K27me3 peaks was substantially higher for skin compared to the other equine FAANG tissues analyzed to date (6.28% versus 2.94%), while the number of reads retained for H3K27me3 from the PE data after filtering (42.8%) was comparable to the average retained for all of the equine H3K27me3 SE data (41.3%, PRJEB42315 and PRJEB35307).

Evaluating general enrichment patterns revealed that the “adopted” tissues detected mark distributions for the activating marks that were consistent with those identified previously for the TOI (Supplementary Figures 1-3). Data for H3K27me3 from skin, however, generated strong enrichment around the TSS and upstream of an average gene, while still maintaining a similar level of relative enrichment for H3K27me3 distributed throughout the rest of the gene body and downstream as seen for other tissues (Supplementary Figure 4). Evaluation of the spleen datasets detected the strongest H3K27me3 enrichment when combining the original ECA_UCD_AH1 dataset and the merged ECA_UCD_AH2 dataset (denoted as “spleen” on Supplementary Figure 4). While enrichment distributions for sesamoid tissue detected consistent patterns for H3K4me1,

H3K27ac, and H3K27me3, the relative level of enrichment is lower than expected based on the other tissues. In addition to genome-wide evaluations, the replicate-combined peak calls were also manually evaluated across a small number of well characterized regions. Consistent with expectations, activating marks were detected at the TSS and upstream of ubiquitously expressed genes such as *ACTB* for all tissues (Supplementary Figure 5A and 5B). Additionally, all “adopted” tissues lacked peaks indicative of active transcription for a liver-specific gene known as *CYP2E1* (Supplementary Figure 5C and 5D).

5. Data Accessibility

Data were submitted to the European Nucleotide Archive following the best practices established by the FAANG Metadata and Data Sharing Committee and the FAANG Data Coordination Centre (Harrison et al., 2018). All of the new data referenced in the manuscript were submitted under project ID PRJEB42315. The following file types were submitted for all high quality data: raw fastq for each mark and input from both replicates (38 files), processed BAM files for each mark and input from both replicates (34 files), bed files with peak calls per replicate including both SICERpy and MACS2 calls for H3K27me3 (32 files), and bed files with combined peak calls including those from both SICERpy and MACS2 for H3K27me3 (16 files). All files and metadata can be accessed from the FAANG Data Portal (<https://data.fang.org/home>). Previously published FAANG data used in the comparisons are also available from the FAANG data portal under project ID PRJEB35307 (Kingsley et al., 2020).

6. Discussion

The ENCODE project profoundly impacted scientific understanding of genome function in humans by enabling researchers to explore previously impossible challenges, such as charting genomic landscape shifts during development and uncovering enhancer networks associated

with disease (Nord et al., 2013; Rhie et al., 2016). The advancements made by ENCODE paved a path for the FAANG consortium to characterize genomic function in numerous agricultural species (Andersson et al., 2015; Tuggle et al., 2016; Giuffra and Tuggle, 2019), which will expand research opportunities across diverse genera. As a part of the larger consortium, the equine FAANG group established a community-based initiative to “adopt” additional tissues for annotation. As a result of that expansive collaborative effort, characterization of putative regulatory regions was performed in spleen, sesamoid, MC3, and skin. The four additional tissues are of major importance for equine health and traits of economic impact. Specifically, research on catastrophic fracture involving sesamoid and MC3 can benefit from bone-specific annotations as recent advances in treatment have focused on transgenically modified stem cell therapeutics (Ball et al., 2019). Similarly, many diseases and traits under artificial selection in horses, such as melanoma, insect bite hypersensitivity, and coat colors including Appaloosa spotting among others, involve skin tissue (Rieder et al., 2000, 2001; Bellone et al., 2008, 2013; Rosengren Pielberg et al., 2008; Curik et al., 2013; Lanz et al., 2017). Several of these characterized phenotypes have been associated with mutations affecting gene expression (Rieder et al., 2000; Rosengren Pielberg et al., 2008; Bellone et al., 2013), making regulatory regions identified from whole skin a valuable resource for equine researchers. The “Adopt-a-Tissue” effort fits into a broader legacy of collaborative resource development that has historically led to rapid advancements for equine genomics and will continue to push equine science toward new frontiers. In concordance with past community efforts, the high-quality data generated from the “Adopted” tissues are publicly available to benefit all investigators and lead to further progress in equine research.

Using quality metrics first standardized by ENCODE (Dunham et al., 2012), we identified low IP enrichment for the broad mark in spleen, sesamoid, and MC3 tissues. Unlike the SE datasets, the skin replicates sequenced with PE reads generated a higher enrichment signal for H3K27me3 as determined by quality metrics and enrichment topology plots. In particular, enrichment near the TSS was more strongly detected for skin than for any of the TOI or the other “adopted” tissues, suggesting that PE reads may better evaluate the broad repressive mark than SE datasets. With only one tissue evaluated as PE, we cannot exclude the possibility that this enrichment pattern may be skin-specific rather than evidence of a better method for detecting H3K27me3. Although enrichment difficulties have been previously recognized for the broad domains like those of H3K27me3 (Landt et al., 2012; Carelli et al., 2017), investigation of specific ChIP methods for broad histone marks appear to be rare. O’Geen et al. (2011) used both short and long sonication periods to account for the different rates of shearing efficiency for compact versus open chromatin. They found that the larger DNA fragments after sonication were more enriched for broad repressive histone marks while smaller fragments were more likely to contain active chromatin modifications (O’Geen et al., 2011). Their work suggests that shorter sonication times and stringent size selection may bias ChIP samples toward higher enrichment of regions containing narrow marks at the expense of more condensed areas with broad marks, yet current ChIP-Seq standards do not encourage separate protocols for the different mark topologies (Landt et al., 2012; ENCODE Guidelines for Experiments Generating ChIP-seq Data, 2017). Instead, advances in ChIP-Seq methods have focused on analysis and software development to accommodate the different enrichment levels expected from broad and narrow domains assayed with the same protocol (Zhang et al., 2008; Zang et al., 2009). Future investigations involving

H3K27me3 and other broad histone modifications may benefit from developing bench protocols, including sequencing parameters, that are specific for broad marks.

To account for insufficient H3K27me3 signal from spleen tissue, IP and sequencing were repeated for both biological replicates. By combining the reads from both sets of data for ECA_UCD_AH2, we were able to obtain sufficient enrichment for peak identification. These data support that combining results from different IPs performed on the same tissue sample can be a useful approach to obtain the enrichment needed for annotation purposes. Study of the best means for combining information from biological and technical replicates for differential enrichment analyses suggests that combining ChIP datasets without accounting for enrichment levels may lead to more false negatives (Bao et al., 2013). Although our data may not have captured all possible peaks, combining data enabled detection of more H3K27me3 peak calls with higher consistency than possible with the first dataset alone. Therefore, the current peak calls can serve as the starting point for spleen-specific annotations, which can be improved upon with characterization of heterochromatin regions from additional equine spleen samples.

The low-quality metrics for three of the four marks from ECA_UCD_AH1 sesamoid tissue indicated there was low IP enrichment. To the best of the authors' knowledge, the MC3 and sesamoid data generated here represent the first histone mark peak calls from healthy, whole bone tissue. The overall lower quality metrics for bone tissues support the difficulty of working with these tissues, however, one of the two replicates for sesamoid showed sufficient quality for all four marks, suggesting the issue may be sample specific. To determine if any issues arose during chromatin extraction or IP, further evaluation of H3K4me1, H3K27ac, and H3K27me3 marks in sesamoid tissue from ECA_UCD_AH1 is warranted. Additional data generated from ECA_UCD_AH1 sesamoid tissue will be added to PRJEB42315 when available.

Previous equine annotations were developed based on homology and transcriptomics, leaving much of the genome, especially noncoding regions, uncharacterized (Hestand et al., 2015; Aken et al., 2016; Mansour et al., 2017). While valuable, annotation of regulatory regions based solely on homology with other species is not expected to be sufficient given the evolutionary role of these elements within and among species (Schmidt et al., 2010; McLean et al., 2011; Shibata et al., 2012; Lowdon et al., 2016). With the first publication of the equine FAANG data from eight prioritized tissues (Kingsley et al., 2020) and the four “Adopted” tissues presented in this manuscript, researchers can begin to interrogate the role of regulatory regions in equine traits, such as the recent investigation of a novel 16 KB deletion associated with an ocular disorder known as distichiasis (Hisey et al., 2020). Future annotations for the horse will include maps of regulatory states characteristic of healthy tissue, making it a vital resource to compare against disease states. The histone ChIP-Seq data from the horse have already been integrated into a useable annotation resource by a new project known as FAANGMine (FAANGMine.). Similar to FlyMine (Lyne et al., 2007), the project aims to combine the results from all of the genomic assays used by the FAANG consortium into a single resource for easier use. Thanks to these integration effort, additional equine FAANG datasets including the “Adopted” tissue peak calls will open up opportunities for variant investigations in previously uncharacterized noncoding regions and expand research opportunities in equine omics.

7. Conflict of Interest

The authors declare that the research was conducted in the absence of any commercial or financial relationships that could be construed as a potential conflict of interest.

8. Author Contributions

Conceptualization, C.J.F., R.R.B., J.L.P., T.S.K., J.N.M., N.H., G.L., O.L., S.B., M.M., and E.B.; methodology, N.B.K., R.R.B., C.J.F., and J.L.P.; formal analysis, N.B.K.; investigation, N.B.K.; resources, C.J.F., R.R.B., J.L.P.; data curation, N.B.K.; writing—original draft preparation, N.B.K., R.R.B.; writing—review and editing, C.J.F., J.L.P., J.N.M., T.S.K., N.H., G.L., O.L., S.B., M.M., and E.B.; visualization, N.B.K.; supervision, R.R.B.; project administration, C.J.F., R.R.B., and J.L.P.; funding acquisition, C.J.F., R.R.B., J.L.P., T.S.K., and J.N.M. All authors have read and agreed to the published version of the manuscript.

9. Funding

Funding for experimental materials, and other resources was provided by the Grayson Jockey Club Foundation, United States Department of Agriculture (USDA) NRSP-8 equine species coordinator funds, a Priority Partnership Collaboration Award from the University of Sydney and University of California, Davis, and the Center for Equine Health (CEH) at UC Davis with funds provided by the State of California pari-mutuel fund and contributions by private donors. Support for N.B.K. was provided by the Grayson Jockey Club Foundation, USDA (2018-06530), Morris Animal Foundation (D16-EQ-028), and a CEH fellowship. Support for C.J.F. was provided by the National Institutes of Health (L40 TR001136). Publication fees supplied by UC Davis Open Access Publication Fund.

10. Acknowledgments

The authors would like to acknowledge Drs. Colin Kern, Huaijun Zhou, Pablo Ross, Ying Wang, and the other members of the UC Davis FAANG group for providing technical expertise and feedback. The authors would also like to recognize the contributions from horse owners that made this work possible.

11. Supplemental Material

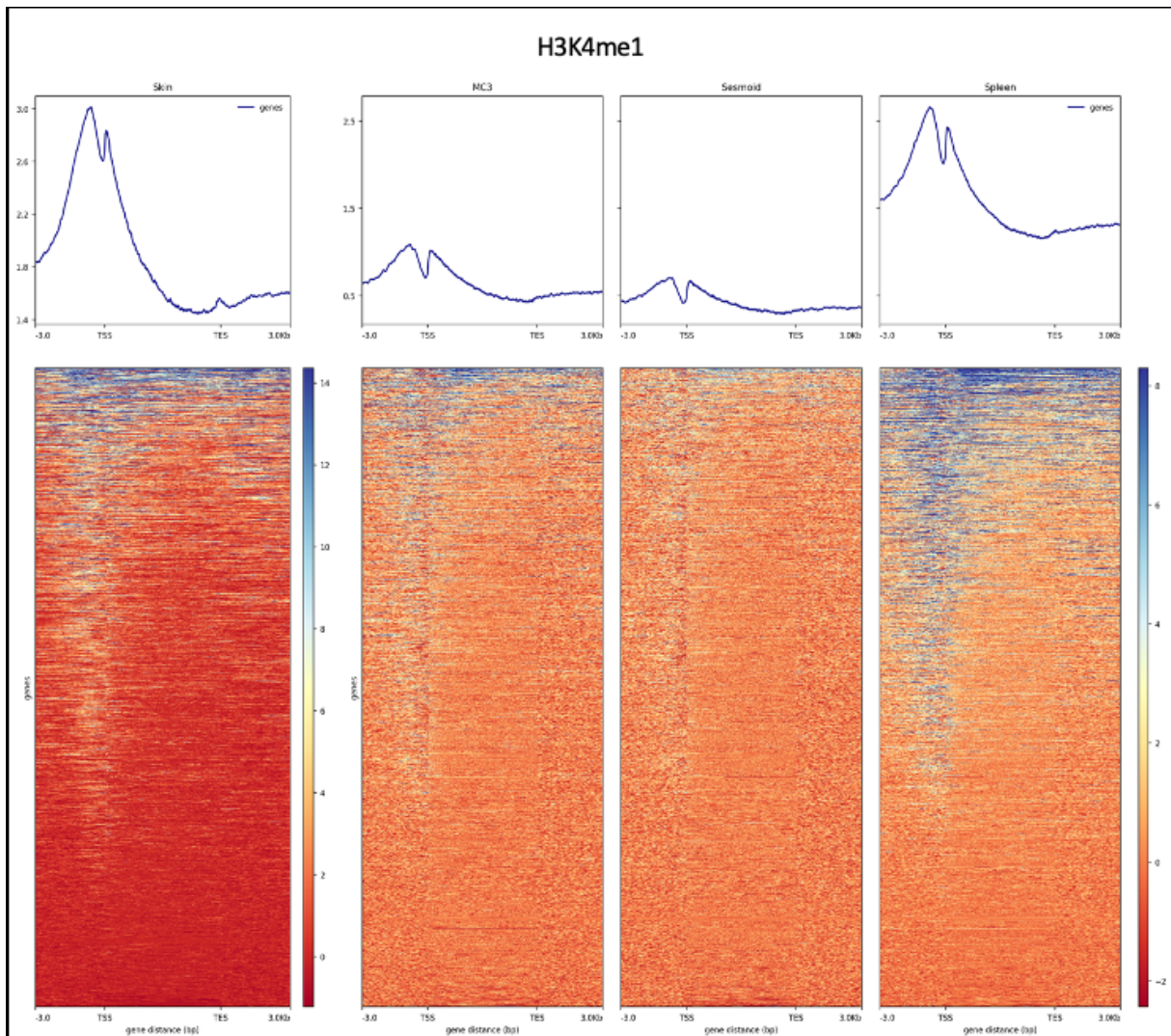
Supplementary Table 1: Metadata for the four “adopted” tissues including specimen details and dissection locations. The identifiers listed for each biological replicate are the ENA Biosample ID for each tissue specimen.

General Term	Specimen Details	ECA_UCD_AH1 Location	ECA_UCD_AH1 Identifier	ECA_UCD_AH2 Location	ECA_UCD_AH2 Identifier
MC3	diaphysis of metacarpal 3 bone	right forelimb	SAMEA104728737	left forelimb	SAMEA104728803
Sesamoid	sesmoid bone	right forelimb	SAMEA104728750	left forelimb	SAMEA104728908
Skin	full thickness skin	dorsal	SAMEA104728773	dorsal	SAMEA104728858
Spleen	spleen	tail of spleen	SAMEA104728847	tail of spleen	SAMEA104728710

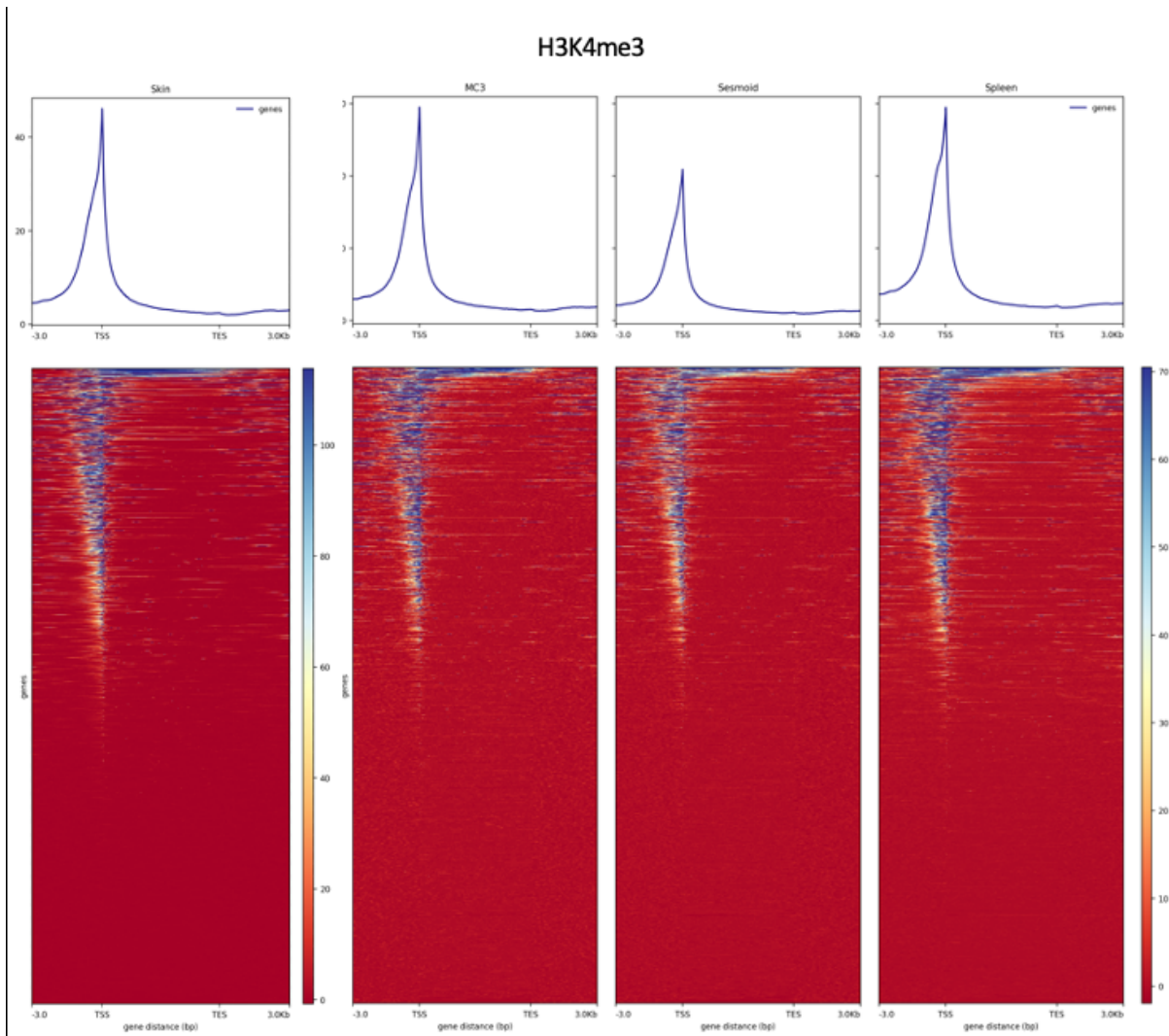
Supplementary Table 2: Alignment statistics for all “Adopted” tissue datasets. Values represent the number or percent of reads retained after each major processing step.

Mark	Tissue	Rep	Raw Reads	Aligned Reads	Fraction Aligned	Filtered Reads	Fraction Retained	Duplicates Removed	Fraction Retained	Mapping Quality
H3K4me1	MC3	AH1	54299480	53060859	0.977	44609686	0.822	32624171	0.601	39.3
H3K4me1	MC3	AH2	44609955	43483449	0.975	36581241	0.820	27841274	0.624	39.3
H3K4me3	MC3	AH1	48073400	46951130	0.977	40820791	0.849	5048151	0.105	39.2
H3K4me3	MC3	AH2	51681338	50427310	0.976	43965079	0.851	13702423	0.265	39.2
H3K27ac	MC3	AH1	54107393	52847451	0.977	45540327	0.842	11875218	0.219	39.3
H3K27ac	MC3	AH2	43737105	42737401	0.977	36508428	0.835	2732504	0.062	39.3
H3K27me3	MC3	AH1	119854288	116591477	0.973	90227468	0.753	51165282	0.427	39.3
H3K27me3	MC3	AH2	110859932	107874788	0.973	84810177	0.765	54593706	0.492	39.4
Input	MC3	AH1	84572411	82335647	0.974	65019158	0.769	55694485	0.659	39.2
Input	MC3	AH2	84672593	82497961	0.974	65810982	0.777	56895483	0.672	39.2
H3K4me1	Sesamoid	AH1	45891896	44875523	0.978	38004664	0.828	23620876	0.515	39.2
H3K4me1	Sesamoid	AH2	52938667	51796071	0.978	44032184	0.832	37019848	0.699	39.3
H3K4me3	Sesamoid	AH1	40078088	39146935	0.977	34082271	0.850	12181511	0.304	39.1
H3K4me3	Sesamoid	AH2	46893954	45848365	0.978	39158317	0.835	14945410	0.319	39.2
H3K27ac	Sesamoid	AH1	63131652	61674003	0.977	51954351	0.823	21191826	0.336	39.2
H3K27ac	Sesamoid	AH2	60028953	58736109	0.978	49880778	0.831	16159281	0.269	39.3
H3K27me3	Sesamoid	AH1	57868687	56320918	0.973	44163981	0.763	29691030	0.513	39.3
H3K27me3	Sesamoid	AH2	110579568	108193972	0.978	90068940	0.815	66772818	0.604	39.3

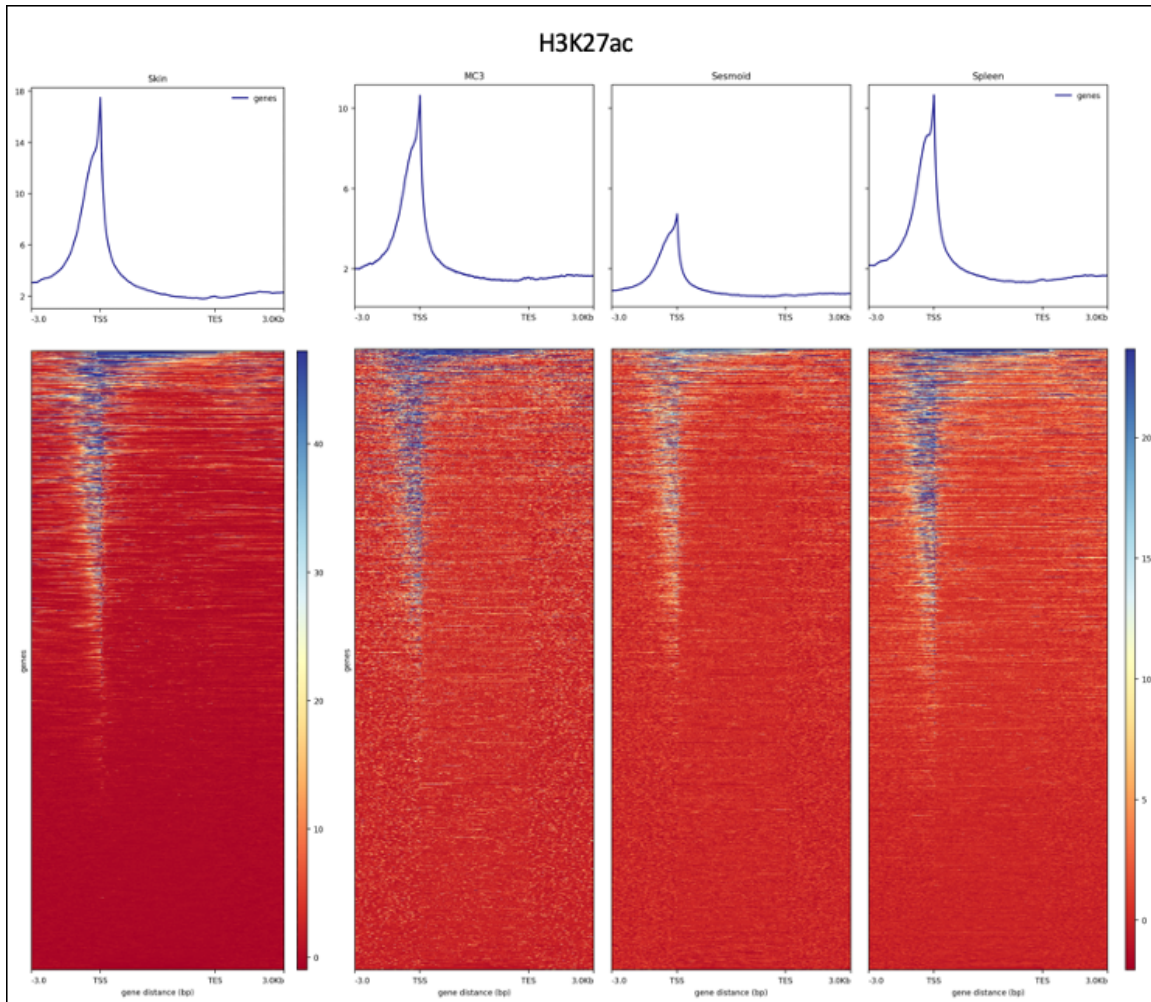
Input	Sesamoid	AH1	76829554	74802343	0.974	59669571	0.777	49465708	0.644	39.2
Input	Sesamoid	AH2	80363657	78426988	0.976	65639004	0.817	54494081	0.678	39.2
H3K4me1	Skin	AH1	101045990	98504165	0.975	91318474	0.904	38495428	0.381	36.0
H3K4me1	Skin	AH2	87209338	85457820	0.980	79459886	0.911	41741916	0.479	36.1
H3K4me3	Skin	AH1	93328152	91165019	0.977	85519746	0.916	43212672	0.463	36.0
H3K4me3	Skin	AH2	108342810	106140174	0.980	99067992	0.914	36666768	0.338	35.9
H3K27ac	Skin	AH1	98203170	96404211	0.982	90251692	0.919	47614788	0.485	36.0
H3K27ac	Skin	AH2	84671932	83069754	0.981	78463594	0.927	47724734	0.564	36.1
H3K27me3	Skin	AH1	235278636	230117904	0.978	199467262	0.848	99953752	0.425	35.8
H3K27me3	Skin	AH2	216721712	211810391	0.977	186085566	0.859	93574734	0.432	35.8
Input	Skin	AH1	237940562	233135467	0.980	198923286	0.836	125342988	0.527	35.8
Input	Skin	AH2	215686900	211396863	0.980	184358841	0.855	111272071	0.516	35.8
H3K4me1	Spleen	AH1	63601827	62745768	0.987	56773348	0.893	36256567	0.570	39.4
H3K4me1	Spleen	AH2	51272309	50434535	0.984	45441490	0.886	33243566	0.648	39.4
H3K4me3	Spleen	AH1	50031817	49263669	0.985	44735618	0.894	27289907	0.545	39.2
H3K4me3	Spleen	AH2	65293465	64232543	0.984	58089426	0.890	32607222	0.499	39.2
H3K27ac	Spleen	AH1	51164015	50539219	0.988	46131632	0.902	29939731	0.585	39.4
H3K27ac	Spleen	AH2	51069779	50403653	0.987	45860424	0.898	31815423	0.623	39.4
H3K27me3	Original Spleen	AH1	120011603	117467034	0.979	98010079	0.817	41090124	0.342	39.4
H3K27me3	Original Spleen	AH2	115571539	113036495	0.978	93613695	0.810	40155514	0.347	39.4
Input	Original Spleen	AH1	46798298	45825840	0.979	38503667	0.823	29042532	0.621	39.4
Input	Original Spleen	AH2	54580462	53467507	0.980	44863485	0.822	33878779	0.621	39.4
H3K27me3	Repeated Spleen	AH1	65517848	62189426	0.949	50991577	0.778	6163159	0.094	39.3
H3K27me3	Repeated Spleen	AH2	83105559	81166884	0.977	66009598	0.794	43415707	0.522	39.3
Input	Repeated Spleen	AH1	96690152	94676056	0.979	78272613	0.810	57791568	0.598	39.3
Input	Repeated Spleen	AH2	77069273	75488501	0.979	62505669	0.811	49284477	0.639	39.3
H3K27me3	Merged Spleen	AH1	185529451	179656466	0.968	149001655	0.803	47153968	0.254	39.4
H3K27me3	Merged Spleen	AH2	198677098	194203397	0.977	159623293	0.803	82873895	0.417	39.4
Input	Merged Spleen	AH1	143488450	140501900	0.979	116776284	0.814	86230894	0.601	39.3
Input	Merged Spleen	AH2	131649735	128956013	0.980	107369154	0.816	82571243	0.627	39.4



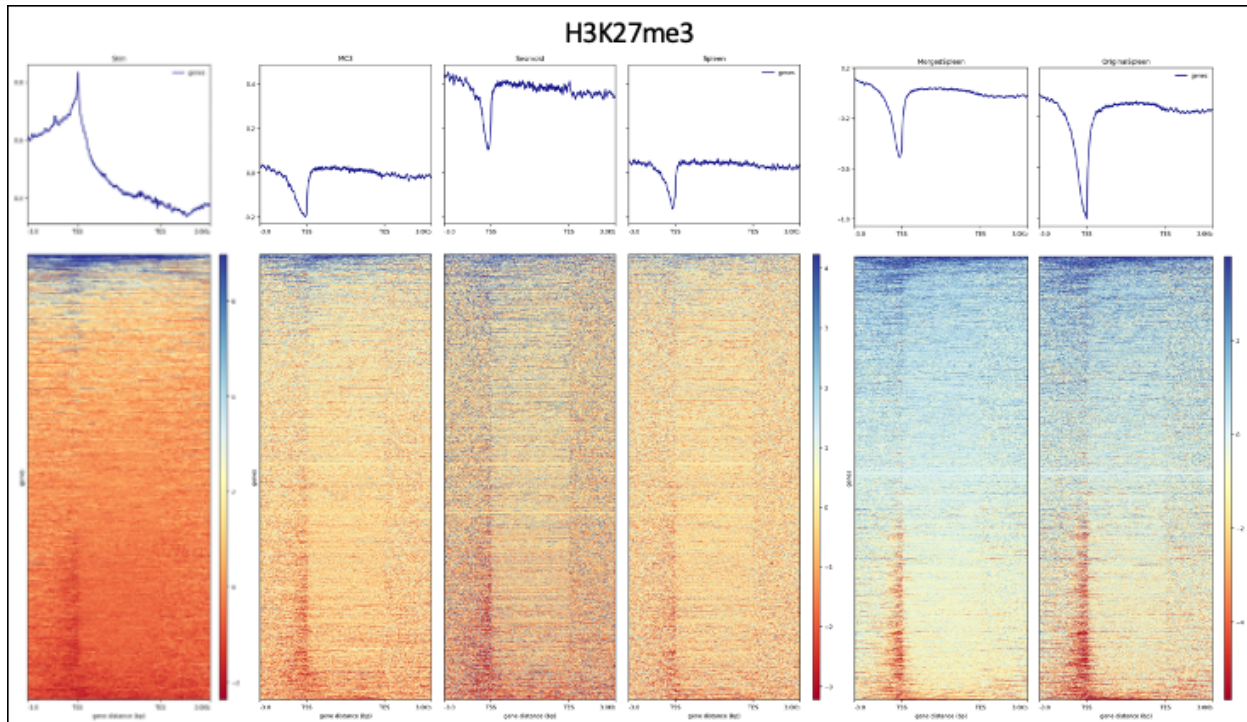
Supplementary Figure 1: H3K4me1 histone mark enrichment across the average gene body. For each panel, topology plots (top) and heat maps (bottom) display the average enrichment for this mark in each of the corresponding tissues across a size-normalized gene distribution based on ENSEMBL annotation (release 95) for EquCab3. Each line in the heatmap represents relative enrichment across a given gene. Presented are the enrichment topologies for skin, MC3, sesmoid, and spleen.



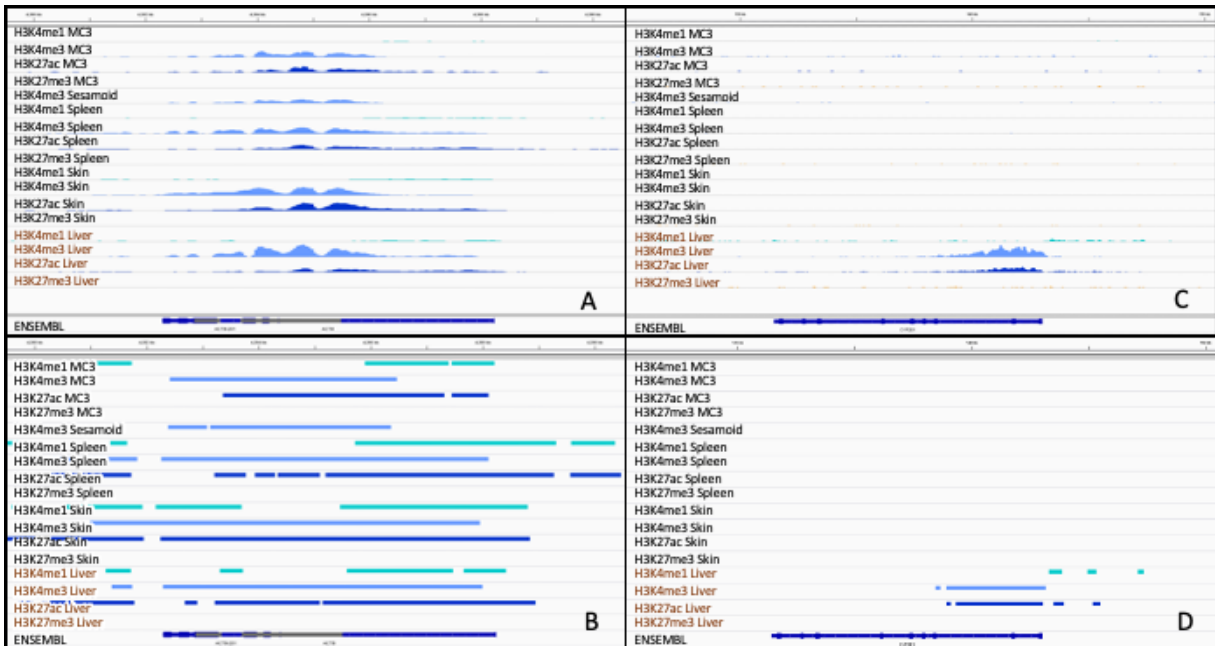
Supplementary Figure 2: H3K4me3 histone mark enrichment across the average gene body. For each panel, topology plots (top) and heat maps (bottom) display the average enrichment for this mark in each of the corresponding tissues across a size-normalized gene distribution based on ENSEMBL annotation (release 95) for EquCab3. Each line in the heatmap represents relative enrichment across a given gene. Presented are the enrichment topologies for skin, MC3, sesamoid, and spleen.



Supplementary Figure 3: H3K27ac histone mark enrichment across the average gene body. For each panel, topology plots (top) and heat maps (bottom) display the average enrichment for this mark in each of the corresponding tissues across a size-normalized gene distribution based on ENSEMBL annotation (release 95) for EquCab3. Each line in the heatmap represents relative enrichment across a given gene. Presented are the enrichment topologies for skin, MC3, sesamoid, and spleen.



Supplementary Figure 4: H3K27me3 histone mark enrichment across the average gene body. For each panel, topology plots (top) and heat maps (bottom) display the average enrichment for this mark in each of the corresponding tissues across a size-normalized gene distribution based on ENSEMBL annotation (release 95) for EquCab3. Each line in the heatmap represents relative enrichment across a given gene. Presented are the enrichment topologies for skin, MC3, sesamoid, spleen. Given that this mark performed poorly for spleen tissue initially, the experiments were repeated, and the data were analyzed multiple ways. The plot noted as “Spleen” represents the AH1 data from initial IP and AH2 merged data for both the initial and repeat IP experiments. “MergedSpleen” represents merged data (initial IP and repeat IP experiments) from both replicates. The “OriginalSpleen” plot represents data only from the initial IP and sequencing experiment for both biological replicates.



Supplementary Figure 5: Histone mark enrichment and peak calls from four “adopted” tissues and previously characterized liver data for one house-keeping gene and one liver-specific gene. Evaluation of high-quality data was performed using Integrated Genome Viewer. ChIP enrichment tracks were generated as bigWig files in which the input alignments were subtracted from the IP read distributions prior to combining both biological replicates for each mark. All peak calls were visualized from BED files. H3K27me3 peaks were called with SICER, and all other marks were called with MACS2. (A) ChIP enrichment detected in region surrounding house-keeping gene, *ACTB*. (B) Replicate-combined peak calls for the same region from panel A. (C) Enrichment of ChIP and (D) replicate-combined peaks detected for tissue-specific gene previously identified for liver tissue, *CYP2E1*.

12. References

- Aken, B. L., Ayling, S., Barrell, D., Clarke, L., Curwen, V., Fairley, S., et al. (2016). The Ensembl gene annotation system. *Database (Oxford)*. 2016, 1–19. doi:10.1093/database/baw093.
- Andersson, L., Archibald, A. L., Bottema, C. D., Brauning, R., Burgess, S. C., Burt, D. W., et al. (2015). Coordinated international action to accelerate genome-to-phenome with FAANG, the Functional Annotation of Animal Genomes project. *Genome Biol.* 16, 4–9. doi:10.1186/s13059-015-0622-4.

- Andrews, S., Krueger, F., Segonds-Pichon, A., Biggins, L., Krueger, C., and Wingett, S. (2012). Trim Galore. Available at: https://www.bioinformatics.babraham.ac.uk/projects/trim_galore/.
- Bailey, E. (2010). Horse genomics and the Dorothy Russell Havemeyer Foundation. *Anim. Genet.* 41, 1. doi:10.1111/j.1365-2052.2010.02136.x.
- Ball, A. N., Phillips, J. N., McIlwraith, C. W., Kawcak, C. E., Samulski, R. J., and Goodrich, L. R. (2019). Genetic modification of scAAV-equine-BMP-2 transduced bone-marrow-derived mesenchymal stem cells before and after cryopreservation: An “off-the-shelf” option for fracture repair. *J. Orthop. Res.* 37, 1310–1317. doi:10.1002/jor.24209.
- Bao, Y., Vinciotti, V., Wit, E., and 't Hoen, P. A. C. (2013). Accounting for immunoprecipitation efficiencies in the statistical analysis of ChIP-seq data. *BMC Bioinformatics* 14. doi:10.1186/1471-2105-14-169.
- Bellone, R. R., Brooks, S. A., Sandmeyer, L., Murphy, B. A., Forsyth, G., Archer, S., et al. (2008). Differential gene expression of *TRPM1*, the potential cause of congenital stationary night blindness and coat spotting patterns (LP) in the Appaloosa horse (*Equus caballus*). *Genetics* 179, 1861–1870. doi:10.1534/genetics.108.088807.
- Bellone, R. R., Holl, H., Setaluri, V., Devi, S., Maddodi, N., Archer, S., et al. (2013). Evidence for a Retroviral Insertion in *TRPM1* as the Cause of Congenital Stationary Night Blindness and Leopard Complex Spotting in the Horse. *PLoS One* 8, 1–14. doi:10.1371/journal.pone.0078280.
- Burns, E. N., Bordbari, M. H., Mienaltowski, M. J., Affolter, V. K., Barro, M. V., Gianino, F., et al. (2018). Generation of an equine biobank to be used for Functional Annotation of Animal Genomes project. *Anim. Genet.* 49, 564–570. doi:10.1111/age.12717.

- Caetano, A. R., Shiue, Y. L., Lyons, L. A., O'Brien, S. J., Laughlin, T. F., Bowling, A. T., et al. (1999). A comparative gene map of the horse (*Equus caballus*). *Genome Res.* 9, 1239–1249. doi:10.1101/gr.9.12.1239.
- Carelli, F. N., Sharma, G., and Ahringer, J. (2017). Broad Chromatin Domains: An Important Facet of Genome Regulation. *BioEssays* 39, 1–7. doi:10.1002/bies.201700124.
- Chowdhary, B. P., Raudsepp, T., Honeycutt, D., Owens, E. K., Piumi, F., Guérin, G., et al. (2002). Construction of a 5000rad whole-genome radiation hybrid panel in the horse and generation of a comprehensive and comparative map for ECA11. *Mamm. Genome* 13, 89–94. doi:10.1007/s00335-001-2089-8.
- Curik, I., Druml, T., Seltenhammer, M., Sundström, E., Pielberg, G. R., Andersson, L., et al. (2013). Complex Inheritance of Melanoma and Pigmentation of Coat and Skin in Grey Horses. *PLoS Genet.* 9. doi:10.1371/journal.pgen.1003248.
- Dunham, I., Kundaje, A., Aldred, S. F., Collins, P. J., Davis, C. A., Doyle, F., et al. (2012). An integrated encyclopedia of DNA elements in the human genome. *Nature* 489, 57–74. doi:10.1038/nature11247.
- ENCODE Guidelines for Experiments Generating ChIP-seq Data (2017). Available at: <https://www.encodeproject.org/about/experiment-guidelines/>.
- FAANGMine. Available at: <http://faangmine.org>.
- Giuffra, E., and Tuggle, C. K. (2019). Functional Annotation of Animal Genomes (FAANG): Current Achievements and Roadmap. *Annu. Rev. Anim. Biosci.* 7, 65–88. doi:10.1146/annurev-animal-020518-114913.

- Guérin, G., Bailey, E., Bernoco, D., Anderson, I., Antczak, D. F., Bell, K., et al. (1999). Report of the international equine gene mapping workshop: Male linkage map. *Anim. Genet.* 30, 341–354. doi:10.1046/j.1365-2052.1999.00510.x.
- Guérin, G., Bailey, E., Bernoco, D., Anderson, I., Antczak, D. F., Bell, K., et al. (2003). The second generation of the International Equine Gene Mapping Workshop half-sibling linkage map. *Anim. Genet.* 34, 161–168. doi:10.1046/j.1365-2052.2003.00973.x.
- Harrison, P. W., Fan, J., Richardson, D., Clarke, L., Zerbino, D., Cochrane, G., et al. (2018). FAANG, establishing metadata standards, validation and best practices for the farmed and companion animal community. *Anim. Genet.* 49, 520–526. doi:10.1111/age.12736.
- Hestand, M. S., Kalbfleisch, T. S., Coleman, S. J., Zeng, Z., Liu, J., Orlando, L., et al. (2015). Annotation of the protein coding regions of the equine genome. *PLoS One* 10, 1–13. doi:10.1371/journal.pone.0124375.
- Hisey, E. A., Hermans, H., Lounsberry, Z. T., Avila, F., Grahn, R. A., Knickelbein, K. E., et al. (2020). Whole genome sequencing identified a 16 kilobase deletion on ECA13 associated with distichiasis in Friesian horses. *BMC Genomics* 21, 1–13. doi:10.1186/s12864-020-07265-8.
- Kalbfleisch, T. S., Rice, E. S., DePriest, M. S., Walenz, B. P., Hestand, M. S., Vermeesch, J. R., et al. (2018). Improved reference genome for the domestic horse increases assembly contiguity and composition. *Commun. Biol.* 1, 1–8. doi:10.1038/s42003-018-0199-z.
- Kharchenko, P. V., Tolstorukov, M. Y., and Park, P. J. (2008). Design and analysis of CHIP-seq experiments for DNA-binding proteins. *Nat. Biotechnol.* 26, 1351–1359. doi:10.1038/nbt.1508.

- Kingsley, N. B., Kern, C., Creppe, C., Hales, E. N., Zhou, H., Kalbfleisch, T. S., et al. (2020). Functionally Annotating Regulatory Elements in the Equine Genome Using Histone Mark ChIP-Seq. *Genes (Basel)*. 11, 3. doi:10.3390/genes11010003.
- Landt, S. G., Marinov, G. K., Kundaje, A., Kheradpour, P., Pauli, F., Batzoglou, S., et al. (2012). ChIP-seq guidelines and practices of the ENCODE and modENCODE consortia. *Genome Res.* 22, 1813–1831. doi:10.1101/gr.136184.111.
- Lanz, S., Brunner, A., Graubner, C., Marti, E., and Gerber, V. (2017). Insect Bite Hypersensitivity in Horses is Associated with Airway Hyperreactivity. *J. Vet. Intern. Med.* 31, 1877–1883. doi:10.1111/jvim.14817.
- Leeb, T., Vogl, C., Zhu, B., de Jong, P. J., Binns, M. M., Chowdhary, B. P., et al. (2006). A human-horse comparative map based on equine BAC end sequences. *Genomics* 87, 772–776. doi:10.1016/j.ygeno.2006.03.002.
- Li, H., and Durbin, R. (2009). Fast and accurate short read alignment with Burrows-Wheeler transform. *Bioinformatics* 25, 1754–1760. doi:10.1093/bioinformatics/btp324.
- Li, H., Handsaker, B., Wysoker, A., Fennell, T., Ruan, J., Homer, N., et al. (2009). The Sequence Alignment/Map format and SAMtools. *Bioinformatics* 25, 2078–2079. doi:10.1093/bioinformatics/btp352.
- Lowdon, R. F., Jang, H. S., and Wang, T. (2016). Evolution of Epigenetic Regulation in Vertebrate Genomes. *Trends Genet.* 32, 269–283. doi:10.1016/j.tig.2016.03.001.
- Lyne, R., Smith, R., Rutherford, K., Wakeling, M., Varley, A., Guillier, F., et al. (2007). FlyMine: An integrated database for Drosophila and Anopheles genomics. *Genome Biol.* 8. doi:10.1186/gb-2007-8-7-r129.

- Mansour, T. A., Scott, E. Y., Finno, C. J., Bellone, R. R., Mienaltowski, M. J., Penedo, M. C., et al. (2017). Tissue resolved, gene structure refined equine transcriptome. *BMC Genomics* 18, 1–12. doi:10.1186/s12864-016-3451-2.
- Martin, M. (2011). Cutadapt removes adapter sequences from high-throughput sequencing reads. *EMBnet J.* 17, 10–12. doi:https://doi.org/10.14806/ej.17.1.200.
- McCoy, A. M., and McCue, M. E. (2014). Validation of imputation between equine genotyping arrays. *Anim. Genet.* 45, 153. doi:10.1111/age.12093.
- McCue, M. E., Bannasch, D. L., Petersen, J. L., Gurr, J., Bailey, E., Binns, M. M., et al. (2012). A high-density SNP array for the domestic horse and extant Perissodactyla: Utility for association mapping, genetic diversity, and phylogeny studies. *PLoS Genet.* 8. doi:10.1371/journal.pgen.1002451.
- McLean, C. Y., Reno, P. L., Pollen, A. A., Bassan, A. I., Capellini, T. D., Guenther, C., et al. (2011). Human-specific loss of regulatory DNA and the evolution of human-specific traits. *Nature* 471, 216–219. doi:10.1038/nature09774.
- Nord, A. S., Blow, M. J., Attanasio, C., Akiyama, J. A., Holt, A., Hosseini, R., et al. (2013). Rapid and pervasive changes in genome-wide enhancer usage during mammalian development. *Cell* 155, 1521–1531. doi:10.1016/j.cell.2013.11.033.
- O’Geen, H., Echipare, L., and Farnham, P. J. (2011). “Using ChIP-Seq Technology to Generate High-Resolution Profiles of Histone Modifications,” in *Epigenetics Protocols - Methods in Molecular Biology 2nd Ed*, ed. Trygve O. Tollefsbol (Springer US), 265–286. doi:10.1007/978-1-61779-316-5.
- Penedo, M. C. T., Millon, L. V., Bernoco, D., Bailey, E., Binns, M., Cholewinski, G., et al. (2005). International equine gene mapping workshop report: A comprehensive linkage map

- constructed with data from new markers and by merging four mapping resources. *Cytogenet. Genome Res.* 111, 5–15. doi:10.1159/000085664.
- Picard toolkit (2019). *Broad Institute, GitHub Repos*. Available at: <http://broadinstitute.github.io/picard/>.
- Ramírez, F., Ryan, D. P., Grüning, B., Bhardwaj, V., Kilpert, F., Richter, A. S., et al. (2016). deepTools2: a next generation web server for deep-sequencing data analysis. *Nucleic Acids Res.* 44, W160–W165. doi:10.1093/nar/gkw257.
- Raudsepp, T., Gustafson-Seabury, A., Durkin, K., Wagner, M. L., Goh, G., Seabury, C. M., et al. (2008). A 4,103-marker integrated physical and comparative map of the horse genome. *Cytogenet. Genome Res.* 122, 28–36. doi:10.1159/000151313.
- Raudsepp, T., Santani, A., Wallner, B., Kata, S. R., Ren, C., Zhang, H. Bin, et al. (2004). A detailed physical map of the horse Y chromosome. *Proc. Natl. Acad. Sci. U. S. A.* 101, 9321–9326. doi:10.1073/pnas.0403011101.
- Rhie, S. K., Guo, Y., Tak, Y. G., Yao, L., Shen, H., Coetzee, G. A., et al. (2016). Identification of activated enhancers and linked transcription factors in breast, prostate, and kidney tumors by tracing enhancer networks using epigenetic traits. *Epigenetics and Chromatin* 9, 1–17. doi:10.1186/s13072-016-0102-4.
- Rieder, S., Stricker, C., Joerg, H., Dummer, R., and Stranzinger, G. (2000). A comparative genetic approach for the investigation of ageing grey horse melanoma. *J. Anim. Breed. Genet.* 117, 73–82. doi:10.1111/j.1439-0388.2000x.00245.x.
- Rieder, S., Taourit, S., Mariat, D., Langlois, B., and Guérin, G. (2001). Mutations in the agouti (*ASIP*), the extension (*MC1R*), and the brown (*TYRP1*) loci and their association to coat color

- phenotypes in horses (*Equus caballus*). *Mamm. Genome* 12, 450–455. doi:10.1007/s003350020017.
- Rosengren Pielberg, G., Golovko, A., Sundström, E., Curik, I., Lennartsson, J., Seltenhammer, M. H., et al. (2008). A cis-acting regulatory mutation causes premature hair graying and susceptibility to melanoma in the horse. *Nat. Genet.* 40, 1004–1009. doi:10.1038/ng.185.
- Schaefer, R. J., Schubert, M., Bailey, E., Bannasch, D. L., Barrey, E., Bar-Gal, G. K., et al. (2017). Developing a 670k genotyping array to tag ~2M SNPs across 24 horse breeds. *BMC Genomics* 18, 1–18. doi:10.1186/s12864-017-3943-8.
- Schmidt, D., Wilson, M. D., Ballester, B., Schwalie, P. C., Brown, G. D., Marshall, A., et al. (2010). Transcription Factor Binding. 1036, 1036–1040. doi:10.1126/science.1186176.
- Shibata, Y., Sheffield, N. C., Fedrigo, O., Babbitt, C. C., Wortham, M., Tewari, A. K., et al. (2012). Extensive evolutionary changes in regulatory element activity during human origins are associated with altered gene expression and positive selection. *PLoS Genet.* 8. doi:10.1371/journal.pgen.1002789.
- SICERpy, GitHub Repository. Available at: <https://github.com/dariober/SICERpy>.
- Swinburne, J. E., Boursnell, M., Hill, G., Pettitt, L., Allen, T., Chowdhary, B., et al. (2006). Single linkage group per chromosome genetic linkage map for the horse, based on two three-generation, full-sibling, crossbred horse reference families. *Genomics* 87, 1–29. doi:10.1016/j.ygeno.2005.09.001.
- Tuggle, C. K., Giuffra, E., White, S. N., Clarke, L., Zhou, H., Ross, P. J., et al. (2016). GO-FAANG meeting: a Gathering on Functional Annotation of Animal Genomes. *Anim. Genet.* 47, 528–533. doi:10.1111/age.12466.

Wade, C. M., Giulotto, E., Sigurdsson, S., Zoli, M., Gnerre, S., Imsland, F., et al. (2009). Genome sequence, comparative analysis, and population genetics of the domestic horse. *Science* 326, 865–867. doi:10.1126/science.1178158.

Zang, C., Schones, D. E., Zeng, C., Cui, K., Zhao, K., and Peng, W. (2009). A clustering approach for identification of enriched domains from histone modification ChIP-Seq data. *Bioinformatics* 25, 1952–1958. doi:10.1093/bioinformatics/btp340.

Zhang, Y., Liu, T., Meyer, C. A., Eeckhoute, J., Johnson, D. S., Bernstein, B. E., et al. (2008). Model-based analysis of ChIP-Seq (MACS). *Genome Biol.* 9. doi:10.1186/gb-2008-9-9-r137.

Addendum 2: Risk factors for equine recurrent uveitis in a population of Appaloosa horses in western Canada

Authors: Lynne S. Sandmeyer, Nicole B. Kingsley, Cheryl Walder, Sheila Archer, Marina L. Leis, Rebecca R. Bellone, and Bianca S. Bauer

Keywords: Appaloosa, ERU, genotype, leopard complex, *TRPM1*, uveitis

Reference: Sandmeyer LS, Kingsley NB, Walder C, Archer S, Leis ML, Bellone RR, and Bauer BS. Risk factors for equine recurrent uveitis in a population of Appaloosa horses in western Canada. *Vet Ophthalmol.* 2020;23:515–525. <https://doi.org/10.1111/vop.12749>.

Accepted: January 23, 2020

Abstract

Objective: To characterize clinical manifestations, measure frequency, and evaluate risk factors for equine recurrent uveitis (ERU) in Appaloosa horses in western Canada.

Animals: 145 Appaloosa horses.

Procedures: Ophthalmic examinations were completed, and eyes were classified as having no or mild clinical signs, or moderate, or severe damage from ERU. Clinical signs, age, sex, base coat color, and pattern were recorded. Whole blood and/or mane hair follicles were collected for DNA extraction, and all horses were tested for the leopard complex (LP) spotting pattern allele. Pedigree analysis was completed on affected and unaffected horses, and coefficients of coancestry (CC) and inbreeding (COI) were determined.

Results: Equine recurrent uveitis was confirmed in 20 (14%) horses. The mean age of affected horses was 12.3 years (± 5.3 ; range 3–25). Age was a significant risk factor for ERU diagnosis ($OR_{year} = 1.15$) and classification ($OR_{year} = 1.19$). The fewspot coat pattern was significantly

associated with increased risk for ERU compared to horses that were minimally patterned or true solids. The LP/LP genotype was at a significantly greater risk for ERU compared to lp/lp (OR = 19.4) and LP/lp (OR = 6.37). Classification of ERU was greater in the LP/LP genotype compared to LP/lp. Affected horses had an average CC of 0.066, and there was a significant difference in the distribution of CC for affected horses versus the control group (P = .021). One affected horse was the sire or grandsire of nine other affected.

Conclusions: Age, coat pattern, and genetics are major risk factors for the diagnosis and classification of ERU in the Appaloosa.

1 | Introduction

Equine recurrent uveitis (ERU) is a common ocular disease with worldwide distribution and is the foremost cause of blindness in horses.¹ ERU is typified by chronic insidious or recurring bouts of inflammation of the uveal tissue which contribute to secondary ocular changes that ultimately result in blindness.¹ Three clinical varieties of ERU, classic, insidious, and posterior, have been described.¹ The insidious variety of ERU is distinguished by persistent low-grade intra-ocular inflammation with a gradual and cumulative destructive effect rather than outwardly painful episodes and is most commonly seen in both the Appaloosa and draft breeds.¹

The pathophysiology of ERU is multifaceted and is not completely understood. It is believed to be a complex autoimmune disease, involving both genetic and environmental components; however, the mechanisms of the inciting cause and recurrence of inflammation are not established. The association of *Leptospira* spp. with ERU has been widely documented and is thought to be a contributor in some cases; however, the role of *Leptospira* spp. in ERU risk is also insufficiently understood.¹⁻¹³ Th-1 and Th-17 cells play overlapping roles in auto-immune inflammation and are both significant directors of the immune response in ERU.¹⁴⁻¹⁷ Additionally,

greater expression of IFN γ in CD4⁺ T cells from horses with ERU was observed indicating a pro-inflammatory Th1 ERU phenotype.¹⁸ Genetic associations for ERU have been identified in the Appaloosa and the German warmblood horse breeds.¹⁹⁻²² In both Appaloosa and Draft breeds, genetic associations with the markers near the major histocompatibility complex (MHC) have been re-reported.^{19,23} However, in subsequent studies, association with this region in the Appaloosa breed was not replicated; thus, the role of the MHC in ERU risk needs further investigation.²⁴

The frequency of ERU in the Appaloosa horse is reportedly much higher than in the general population, and uveitis is thought to be more severe and more likely to cause blindness in this breed than in non-Appaloosa horses.^{2,11,22} Investigations using a candidate gene approach identified genetic markers significantly associated with insidious ERU in Appaloosa horses.¹⁹ Two microsatellites in the MHC region, as described above, were associated with ERU risk. Additionally, a single nucleotide polymorphism (SNP) in an intron of a calcium ion channel gene, *TRPM1* (transient receptor potential cation channel, subfamily M, member 1) on ECA1 (rs1140413009), which had been linked to the breed defining leopard complex coat spotting pattern (LP), as shown in Figure 1, was associated with ERU risk.^{19,25} Subsequently, a nearby 1378 bp insertion in this calcium ion channel gene (*TRPM1*) was shown to be responsible for the leopard complex spotting (LP) pattern.²⁶ *TRPM1* expression is reduced in the retina and skin of Appaloosa horses.²⁷ Reduced expression in the retina of horses homozygous for this insertion has been shown to also cause congenital stationary night blindness (CSNB). However, the exact biochemical mechanism by which this insertion disrupts normal pigmentation to result in Appaloosa patterning is not understood.²⁷ Recently, the association with this LP causal mutation and ERU was confirmed.²⁴

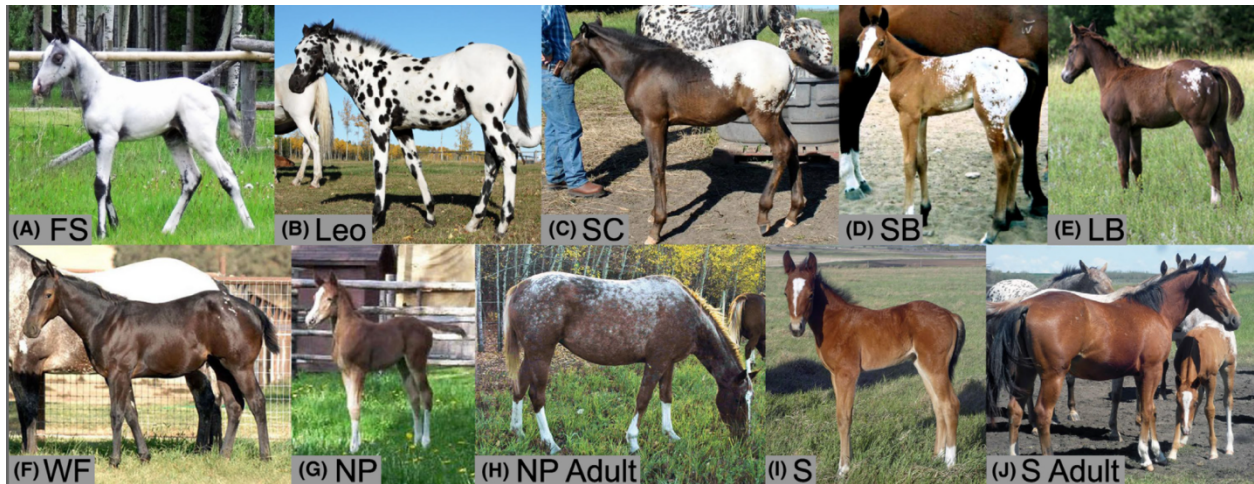


Figure 1: Leopard Complex Spotting Patterns in the Appaloosa horse. Appaloosas with the *LP* mutation have white spotting patterns that range on a continuum as displayed in A-H. The most extensive pattern is known as fewspot, denoted as FS (A). Leopard horses (denoted as Leo) are nearly all white with pigmented spots in the white area (B). Snowcap blankets (denoted as SC) have a variable size white pattern over the rump without pigmented spots (C). Spotted blankets (denoted as SB) will also have a variable size white pattern over the rump but will have pigmented spots (D). Lace blanket horses (denoted as LB) have a small white pattern over the rump (E). Horses with the white flecks pattern (denoted as WF) will have a small amount of discontinuous white pattern over the rump (F). Some horses with *LP* will have no patterning at birth (G, denoted as NP) but will roan with age (H). Horses that do not have an *LP* allele are true solids (denoted as S). They are born without a leopard complex spotting pattern (I) and they do not roan with age (J). Photos courtesy of Linda Hokanson (A, B, G, H), Joanne Greenwood (C), Sheila Archer (D), Kim Utke (E), Cassidy Cobarr (F), and Vicki Johnson (I,J).

Leopard complex spotting behaves as an incompletely dominant trait. Horses homozygous for *LP* tend to have few to no pigmented spots whereas heterozygotes typically have leopard spots in their white patterned area.^{28,29} The amount of white in the coat varies and can range from minimally patterned with white flecks on the rump, to horses that are almost completely white and known as leopard if they are *LP/lp* or fewspot if they are *LP/LP* (Figure 1). Modifier genes are responsible for determining the amount of white patterning that is inherited.²⁸⁻³⁰ A major dominant modifier, named *PATNI* (first pattern modifier), has been shown to interact with *LP* and cause white pattern levels of 60% or greater at birth thus resulting in the leopard and fewspot patterns.

Anecdotally, it is thought that Appaloosa horses with more extensive white patterning are at greater risk to develop ERU and subsequent blindness; however, this requires further investigation.

In a retrospective study of horses diagnosed with ERU at the Western College of Veterinary Medicine (WCVN), the prevalence of ERU in the hospital population was much higher in the Appaloosa (13.8%) compared to other breeds (0.24%).³¹ Appaloosas represented 62.5% of the horses diagnosed with ERU which was more than two times higher than previous studies where the proportion of Appaloosa horses with ERU was reported to be 24-25%.^{2,11} Thus, Appaloosas were identified as being at higher risk for ERU in western Canada.

Most objective data available on ERU in the Appaloosa are gleaned from retrospective studies which have inherent limitations.^{2,11,31} The purpose of this study was to prospectively investigate ERU in the Appaloosa breed in western Canada. The objectives were to characterize the clinical manifestations of the disease, to measure frequency of ERU in the Appaloosa, and to evaluate multiple risk factors for ERU in this population.

2 | Materials and Methods

2.1 Animals:

During the period of 2005 to 2017, a total of 145 Appaloosa horses on 11 breeding barns were examined. Forty-nine of these horses were also used in cohort 2 of the Rockwell *et al.* genomic study.²⁴ In Saskatchewan, 88 horses were examined on eight barns. In Alberta, 57 horses were examined on three barns. Of these, 29 horses were examined on two occasions: 1 year apart (n = 1), 2 years apart (n = 26), and 8 years apart (n = 2). Horses ranged in age from 0.5 to 26 years at the last examination. Ninety-nine were female and 46 were male. The Canadian Council on Animal Care guidelines for experimental animal use was followed, and the University of Saskatchewan Animal Care Committee approved the animal use protocol (#20110053).

2.2 Ocular examination:

Ocular examinations were completed at the horses' stables and included neuroophthalmic examination, followed by sedation with intravenous xylazine hydrochloride, 0.5-1.0 mg/kg (Rompun, Bayer, Inc). Rebound tonometry (Tonovet, Tiolat), direct transilluminator, slit-lamp biomicroscopic (Osram 64222, Carl Zeiss Canada or SL-14, Kowa) and indirect ophthalmoscopic (Heine Omega 200, Heine Instruments Canada) examinations were completed following mydriasis with tropicamide 1% solution (Mydriacyl, Alcon Canada). All examinations were completed by a Diplomate of the American College of Veterinary Ophthalmologists (DACVO).

Equine recurrent uveitis was confirmed if there was presence of active uveitis in addition to historical or clinical evidence of previous episodes or continuous uveal inflammation. Eyes were classified based on the clinical manifestations and amount of observed damage as having no clinical signs of ERU, mild clinical signs of ERU, moderate or severe damage from ERU. Mild clinical signs of ERU consisted of eyes with conjunctival hyperemia, aqueous flare, miosis and ocular hypotony (defined as ≤ 10 mm Hg or 10 mm Hg difference between eyes). Moderate damage from ERU consisted of eyes with signs of mild ERU and one or more of posterior synechia, cataract, vitritis, or uveal pigmentation changes (depigmentation or hyperpigmentation). Severe damage from ERU consisted of eyes with secondary glaucoma, phthisis bulbi, retinal detachment, and/or blindness due to sequela of ERU. In bilateral cases, horses were assigned an overall ERU classification based on the most severely affected eye. ERU was considered to be "active" if current inflammation of either the anterior or posterior segment was confirmed in at least one eye, as indicated by the presence of aqueous flare and/or vitritis, and "quiescent" if aqueous flare or vitritis was absent. All clinical abnormalities, in addition to age, sex, base coat color phenotypes (bay, black or chestnut), and coat pattern phenotypes (fewspot, snowcap, lace blanket, leopard,

spotted blanket, white flecks, no pattern, and solid) were recorded. Coat patterning was based on photographic record at time of examination or foal pictures when extensive roaning (progressive coat color change where dark hairs are replaced by white hairs) had occurred such that the original white pattern level of the horse was not obvious.

2.3 *LP* genotype testing:

Whole blood samples were collected in EDTA tubes, and/or mane hair follicles were collected from all horses for DNA extraction. Total genomic DNA was extracted from blood or by hair if blood was not available using the Gentra Puregene DNA Isolation kit (Qiagen Inc) following previously described protocols.³² All horses were tested for the leopard complex spotting pattern allele (*LP*) by the commercially available assay at the Veterinary Genetics Laboratory (UC Davis).

2.4 Pedigree analysis:

To investigate possible mechanisms of inheritance for ERU risk and to determine whether shared ancestors existed among affected individuals compared to a control group, a pedigree analysis was performed using Pedigraph software.³³ A recent retrospective study found that the mean age of presentation for insidious uveitis among Appaloosas was 12.1 (± 4.6) years,³¹ and, therefore, 12 years of age was the threshold applied to the pedigree analysis to characterize an unaffected horse as a control (25/125).

Pedigrees were available for 18/20 affected horses and 24/25 horses identified as controls (unaffected upon examination and at least 12 years of age). Additionally, coefficients of coancestry (CC) and inbreeding (COI) were calculated for horses with complete six-generation pedigrees (14/20 affected and 14/25 control horses). The CC is the estimated probability that two individuals share the same allele from a common ancestor, and the COI estimates the probability that an individual has a pair of alleles that are identical by descent from a common ancestor.³⁴ The

pairwise CC was calculated for all horses in the affected group and all horses in the control group, and a COI was calculated for each individual in both affected and control groups. Wilcoxon rank-sum tests were used to compare the distribution of CC and the average COI of the two groups.

2.5 Statistical analysis of risk factors:

Horse attributes and genotype markers were compared between horses with and without ERU and among horses with different ERU severity (mild, moderate, and severe). The diagnosis and classification of ERU at the last examination were used in all statistical comparisons. Risk factors of interest for these analyses included age (years), sex (male, female), base coat color phenotype, coat pattern phenotype, and LP genotype. Mixed logistic regression models with random intercepts for barn were used to examine risk factors for ERU. Mixed ordinal logistic regression with a random intercept for barn was used to examine the association between age and classification of ERU. Exact logistic regression or other nonparametric statistics (Kruskal-Wallis with post-hoc pairwise Wilcoxon rank sum) were used for all other associations with severity and where multilevel models would not converge for ERU (coat pattern, genotype). Because of the relatively small sample size, the capacity for multivariable analysis was limited. Therefore, age was adjusted for when examining the effect of genotype using exact logistic regression in the final model. The linearity of the association between age and the log odds of ERU was established by testing the significance of a squared term in a model with age and age squared. Results from regression analyses were reported as odds ratios (OR) with 95% confidence intervals (95% CI). Clinical manifestations were compared between ERU-affected and unaffected eyes with a generalized estimating equation (GEE) with a logit link function to account for repeated measures within horse and adjusted for left or right eyes. Alternatively, where the GEE analysis would not

converge due to small numbers of observations in one group, the data were summarized at the level of the horse and analyzed using exact logistic regression.

3 | Results

3.1 Characterization of ERU in the population:

Equine recurrent uveitis was confirmed in 20/145 (14%) horses at the last examination. Eighteen horses were diagnosed with ERU in Saskatchewan and two were diagnosed in Alberta. Horses in Saskatchewan were more likely to be diagnosed with ERU than in Alberta with an odds ratio (OR) of 4.3 (P = 0.02; 95% CI 1.2-16).

ERU was bilateral in 19/20 horses. ERU was considered to be “active” in 18/20 (90%) affected horses and “quiescent” in 2/20 (10%). Overall, the classification was mild clinical signs (n = 5), moderate (n = 4) and severe (n = 11) damage from ERU. In the horse with unilateral ERU, the affected eye was classified as mild. Horses with “quiescent” disease were all bilateral and were classified as having mild clinical signs (n = 1) and moderate (n = 1) damage from ERU. In horses that were examined on more than one occasion (n = 29), one horse went from a classification of mild clinical signs to severe damage from ERU when reexamined 8 years later. Two horses went from moderate to severe damage from ERU 2 years later. Two horses went from unaffected to severe damage from ERU, one at 2 years and one 8 years after the first examination. In 24/29 horses that were re-examined the ERU status did not change.

3.2 Clinical manifestations of ERU:

The clinical manifestations of ERU are summarized in Table 1. The most common clinical manifestations included aqueous flare (72%), conjunctival hyperemia (62%), miosis (56%), and iris hyperpigmentation (56%), followed by immature or mature cataract (39%), corpora nigra atrophy (41%), incipient cataract (38%), vitreous degeneration (36%), enophthalmos (36%), iris

depigmentation (33%), hypotony (31%), corneal vascularization (31%), and posterior synechia (26%). Sixteen eyes were blind (41%) due to cataract, glaucoma, phthisis bulbi, or a combination of these. Most of the clinical manifestations except for glaucoma ($P = 0.3$), “bullet-hole” ($P = 0.2$), and “butterfly” ($P > 0.9$) retinal lesions were statistically more common in the ERU-affected eyes.

Table 1. Clinical manifestations in ERU and non-ERU eyes

Clinical Manifestations	ERU eyes (n=39)	Non-ERU eyes (n=251)	P-value
Enophthalmos	14 (36%)	1 (0.4%)	<0.001*
Blepharospasm	10 (26%)	3 (1%)	<0.001*
Conjunctival hyperemia	24 (62%)	5 (2%)	<0.001*
Epiphora	6 (15%)	3 (1%)	0.005*
Hypotony	12 (31%)	0	<0.001**
Aqueous flare	28 (72%)	0	<0.001**
Miosis	22 (56%)	1 (0.4%)	<0.001*
Corneal edema	7 (18%)	1 (0.4%)	<0.001*
Corneal vascularization	12 (31%)	4 (2%)	0.026*
Corneal fibrosis	6 (15%)	3 (1%)	<0.001*
Iris hyperpigmentation	22 (56%)	3 (1%)	<0.001*
Iris depigmentation	13 (33%)	7 (3%)	<0.001*
Corpora nigra atrophy	16 (41%)	0	<0.001**
Pupillary fibrosis	13 (33%)	1 (0.4%)	<0.001*
Pupillary fibrin	7 (18%)	2 (0.8%)	0.002*
Posterior synechia	10 (26%)	0	<0.001**
Pupillary occlusion	7 (18%)	0	<0.001**
Anterior lens pigment	11 (28%)	2 (8%)	<0.001*
Incipient cataract	15 (38%)	22 (9%)	<0.001*
Immature cataract	3 (7.6%)	0	0.0328**
Mature cataract	12 (31%)	0	<0.001**
Vitreous degeneration	14 (36%)	4 (2%)	<0.001*
Vitritis	10 (26%)	0	<0.001**
Bullet hole lesions	1 (3%)	32 (13%)	0.2*
Butterfly lesions	1 (3%)	6 (2%)	0.943*
Blind	16 (41%)	0	<0.001**
Glaucoma	2 (5%)	0	0.262**
Phthisis bulbi	7 (18%)	0	<0.001**

*P-values based on generalized estimating equations with a logit link function to account for repeated measures within horse and adjusted for left or right eyes. **Due to small numbers GEE did not converge. P-values based on analysis completed for horse-level observations with exact logistic regression.

3.3 Risk factors for ERU:

Sex and base coat color in the population are summarized in Tables 2 and 3. There was no association between either sex or base coat color and the diagnosis of ERU. The mean age of affected horses at first detection of ERU was 12.3 years (± 5.3 ; range 3-25). Age was a significant risk factor for the presence of ERU with an OR_{year} of 1.15 ($P = 0.001$; 95% CI [1.06-1.24]), signifying that for every year of increase in age, the odds of ERU increased 1.15 times. Age was also a significant risk for classification of clinical signs and damage from ERU with an OR_{year} of 1.19 ($P < 0.001$; 95% CI [1.11-1.29]).

Table 2. Sex and ERU in the population

ERU	Male	Female	Total
Positive	9 (19%)	11 (11%)	20
Negative	39 (81%)	86 (89%)	125
Total	48	97	145

Table 3. Base coat colour and ERU in the population

ERU	Bay	Black	Chestnut	Unknown	Total
Positive	7 (11%)	3 (11%)	8 (15%)	2 (67%)	20
Negative	56 (89%)	24 (89%)	44 (85%)	1 (33%)	125
Total	63	27	52	3	145

Coat pattern in the population is summarized in Table 4. The fewspot coat pattern phenotype (Figure 1A) was significantly associated with increased risk for ERU compared to solid phenotype (solid horses do not have the *LP* allele (Figure 1I and J), $n = 33$, $OR 31$, 95% CI [4.1 to ∞], $P = 0.0003$) and white flecks phenotype (only a small amount of white patterning at birth, Figure 1F), all of which were *LP/lp* in this data set ($n = 11$, $OR 10$, 95% CI [1.3 to ∞], $P = 0.03$).

Table 4. Coat pattern and ERU in the Population. Abbreviations: FS=fewspot, SC=snowcap, LB=lace blanket, Leo=leopard, SB=spotted blanket, WF=white flecks, NP=no pattern, S=Solid, and 2 unknown. Note that “no pattern” is a horse with at least one copy of *LP* (genotype is either *LP/lp* or *LP/LP*) but is born with no white pattern. “True solid” is a horse that does not have *LP* (genotype is *lp/lp*). Illustrations provided and copyrighted by Sheila Archer.









ERU	FS 	SC 	LB 	Leo 	SB 	WF 	NP 	S 	Total
Positive	7(44%)	5(29%)	0	3(15%)	2(11%)	0	3(13%)	0	20
Negative	9(56%)	12(71%)	5(100%)	17(85%)	16(89%)	11(100%)	20(87%)	33(100%)	123
Total	16	17	5	20	18	11	23	33	143

Table 5 summarizes the available genotypes in the population (144/145). The confirmed genotypes for the leopard complex spotting locus in this population were *LP/LP* (n = 31), *LP/lp* (n = 81) and *lp/lp* (n = 32). Mean age for *LP/LP* (10.0 years), *LP/lp* (8.2 years), and *lp/lp* (6.5 years) did not significantly differ (P = 0.07). Overall, the *LP/LP* genotype cohort was at a significantly greater risk for ERU compared to the *lp/lp* horses (OR: 26; 95% CI [4.0 to ∞], P < 0.001). When adjusted for age, the *LP/LP* genotype was at significantly greater risk for ERU than *lp/lp* (OR: 19; 95% CI [2.8 to ∞], P = 0.009) and *LP/lp* (OR: 6.4; 95% CI [1.9 to 24], P = 0.002) genotypes. Based on this cohort, *LP/lp* was not at a significantly greater risk than *lp/lp* (OR 3.1; 95% CI [0.4 to ∞], P = 0.30). Furthermore, the classification of clinical signs and severity of damage from ERU was greater in the *LP/LP* genotype compared to *LP/lp* (P = 0.002) based on Wilcoxon rank-sum analysis.

Table 5. Genotype and ERU in the population

ERU	<i>LP/LP</i>	<i>LP/lp</i>	<i>lp/lp</i>	Unknown	Total
Positive	12 (39%)	7 (9%)	0	1 (100%)	20
Negative	19 (61%)	74 (91%)	32 (100%)	0	125
Total	31	81	32	1	145

3.4 Pedigree analysis:

A single common ancestor was not identified among affected horses for whom pedigrees were available (n = 18/20). However, a common ancestor was discovered for 15/18 affected horses within eight generations (Figure 2A). Five of the affected horses were inbred to this ancestor, while the other ten horses can be traced back to him from either the sire or dam lines. Of the control

horses with available pedigrees, only 5/24 were found to descend from the same ancestor identified in the affected horses, and all five of these horses trace back only on the sire line. Additionally, one affected horse (14-10) that descended from the common ancestor (14-10) was the sire or grandsire of nine other affected Appaloosas, and two of those horses, 14-18 and 17-15, were inbred to 14-10 suggesting additive genetic risk factors may be implicated in disease (COI = 0.25 and 0.13, respectively) (Figure 2B). In contrast, only one out of eight unaffected offspring of 14-10 (specifically 14-21) met the age threshold to be considered a control. In terms of coancestry, the affected horses had an average CC of 0.066, and there was a significant difference in the distribution of CC for the affected horses versus the control group ($P = 0.02$). On the other hand, the distribution of COI for horses with full six-generation pedigrees was not significantly different between affected and control horses ($n = 28$, $P = 0.8$).

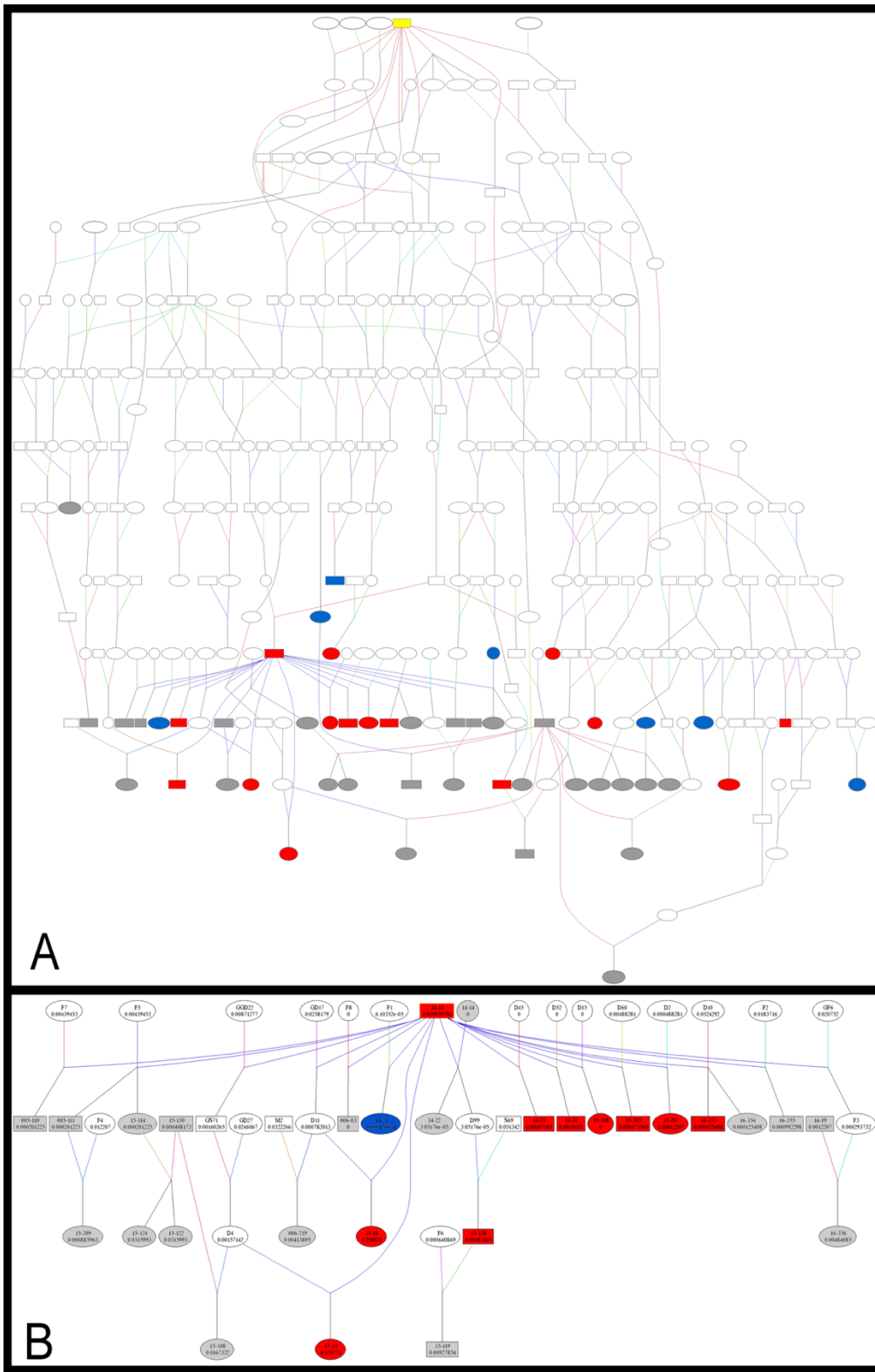


Figure 2: Pedigree Analysis for Equine Recurrent Uveitis. Red shading indicates clinical diagnosis of ERU, and blue shading indicates a horse was considered a control (unaffected upon examination and at least 12 years of age). Grey shading signifies unaffected individuals determined by ocular examination but younger than the age threshold utilized in final pedigree analysis. White

shading indicates that individuals were not available for examination. A) The pedigree analysis identified the common ancestor of 15 out of 18 ERU affected horses. This ancestor is highlighted in yellow shading. B) Enlarged view of the half-sibling family identified from this analysis shown in panel A. For each individual, the identification number and the estimated coefficient of inbreeding (COI) are listed.

4 | Discussion

This study confirms that genetics and age are major contributors of risk for ERU in the Appaloosa breed. The study provides further evidence that homozygosity for *LP* (*LP/LP*) carries the highest risk for presence of and classification of ERU, supporting two previous genetic investigations.^{19,24} It is important to note that our classification scheme of mild clinical signs, and moderate, or severe damage from ERU describes the presence of inflammation (mild) and the degree of resultant damage within the eye (moderate and severe) rather than severity of the disease as resultant damage could be due to the degree of inflammation, the chronicity of inflammation, or a combination of these factors.

When correcting for age, we did not find the *LP/lp* genotype had a significantly greater risk for ERU than *lp/lp*. This differs from other recent findings supporting an additive role for *LP* in risk for ERU with heterozygotes being at greater risk than horses that do not harbor the leopard complex allele (*lp/lp*).²⁴ However, 9% of the 81 *LP/lp* horses in the study were affected, while none of the 32 horses with the *lp/lp* genotype were affected. Therefore, we suspect that either low power in this study influenced the ability to detect a statistical difference between these two groups, or that the disease risk for the *LP/lp* genotype may be related to disease progression rather than onset. Additional work is needed to determine if *LP* or a variant “hitch-hiking” with *LP* is the causal risk factor. A careful analysis of sequencing data to identify variants around the *LP* locus may help to further address this question.

The *LP/LP* genotype results in coat patterns with little to no pigmented spots (also known as leopard spots) in white patterned areas and the fewspot coat pattern is the extreme manifestation of this phenomenon (Figure 1A). The fewspot coat pattern phenotype carried significantly more risk for ERU in this population compared to solid or minimally patterned horses (white flecks). This finding supports the anecdotal evidence that horses with more extensive white patterning are more likely to be affected by ERU. Additionally, this result supports recent work that found *PATNI* may also contribute to ERU risk, as horses with the fewspot pattern (in addition to being homozygous for *LP*) have at least one copy of the *PATNI* allele.²⁴ Horses with *LP* undergo a process called roaning where they lose pigment with age, displaying more white hairs over time; however, extent of depigmentation with age does not appear to be a risk factor for ERU.²⁴ This current investigation was the first to investigate the relationship between ERU and the specific white patterning levels at birth and supports extensive white pattern level, that is the horses with the fewspot pattern (Figure 1A) as being at elevated risk. Therefore, it is advisable to examine these horses more frequently for active inflammation. Additional work is needed to further investigate the role of *PATNI* and/or the absence of pigment in ERU risk.

Identification of a common ancestor within eight generations among 83% of the cases suggests that additional genetic factors are contributing to ERU risk. We also found a large half-sibling family of affected horses from a sire with ERU (14-10) which supports a major additive risk locus within this family. Additionally, by comparing the distribution of the co-efficient of ancestry values, we found that the affected horses likely share a greater proportion of their genomes with one another compared with the control group, which adds further support that there is a strong genetic predisposition to the development of insidious uveitis.

Location could also be considered a risk factor as horses in Saskatchewan were at higher risk compared to Alberta. However, this may relate more to genetics, as 14-10, the affected sire of eight other affected horses, resided in Saskatchewan, and all offspring were also examined in this region. Further, one of the affected horses in Alberta was the grand-offspring of 14-10 that had been sold and moved to the neighboring province prior to re-examination.

Age is another major risk factor for diagnosis and classification of clinical signs and severity of damage from ERU. The mean age (12.3 years) of affected horses was similar to previous studies.³¹ Diagnosis of ERU and severity of damage increase with increasing age. However, a 3-year-old horse was identified with mild clinical signs (16-353). This particular horse was a fewspot gelding and an offspring of 14-10, which further supports the influence of additive genetic risk factors in the condition.

Clinical manifestations of ERU noted in the population, and the low number of horses considered to have “quiescent” disease, support the insidious nature of the condition in the Appaloosa. Only a small number of affected eyes showed overt signs of discomfort in the form of blepharospasm (26%), or epiphora (15%). The majority of eyes diagnosed with ERU had more subtle manifestations including conjunctival hyperemia (62%), aqueous flare (72%), miosis (56%), and iris hyperpigmentation (56%). These chronic, low-grade clinical signs may not be noticed without careful ocular examination. The insidious nature of the disease likely contributes to delayed diagnosis and to the challenge of treating the condition in the Appaloosa horse.

We attempted to record all clinical manifestations that may be associated with ERU. We recognize that the presence of one or more of these manifestations does not equate to a diagnosis of ERU, but rather emphasizes that a combination of signs in addition to signalment and history is required. Clinical manifestations for which there was no significant difference between horses with

and without ERU were glaucoma (5% versus 0% of affected and unaffected horses, respectively, $P = 0.3$), “bullet-hole” (3% versus 13% of affected and unaffected horses, respectively, $P = 0.2$), and “butterfly” retinal lesions (3% versus 2% of affected and unaffected horses, respectively, $P > 0.9$). ERU is reported to be a common cause of secondary glaucoma in horses.¹¹ In this population, glaucoma was noted in two ERU-affected eyes and lack of statistical power may account for the lack of statistical significance. “Bullet-hole” retinal lesions are often discovered in the non-tapetal, peripapillary region. They appear as circular focal to multifocal areas of depigmented tissue with a hyperpigmented center and are thought to represent regions of inactive chorioretinitis. They are common in the horse population and one survey documented such lesions in 52.5% of Thoroughbred race-horses.³⁵ “Butterfly” lesions, which are noted in the region flanking the margins of the optic disk, are less common.³⁶ They appear as a pair of geographic areas of depigmented tissue, that, when combined with the appearance of the optic disk, look like a pair of butterfly wings, and are sometimes called “alar lesions.” They are thought to represent regions of inactive chorioretinitis and were observed in approximately 5% of adult horses as an incidental observation.³⁶ ERU has been suggested as a possible cause of peripapillary chorioretinitis and older references list the finding of “bullet-hole” and, in particular, “butterfly lesions” as being indications of ERU.³⁷⁻³⁹ However, the relationship between these findings and ERU is not well-established and, in fact, our data indicate that “bullet-hole” and “butterfly” lesions are not clinical manifestations of ERU. Other manifestations of ERU, such as cataract or vitritis, may mask detection of “butterfly” or “bullet-hole” retinal lesions in ERU-affected horses. Nevertheless, finding these lesions in an otherwise normal eye should not signify a diagnosis of ERU.

There are several limitations that should be acknowledged in this study. First, the sample size is small relative to the frequency of ERU which limits the power of the study to evaluate all

potentially important risk factors. Second, the diagnosis of ERU based on one examination can be problematic and requires consideration of the signalment, history, and clinical signs observed. We initially wanted to re-evaluate all horses within a 2-year time frame; however, horses were often sold and lost to follow-up, making re-examination impossible. Another major limitation is the effect of age. As the condition manifests with age, there is always a risk of falsely diagnosing a young horse as an unaffected control. The true average age of onset of the condition is unknown.

Older horses likely had the condition for several years prior to our examinations as most had end-stage disease. Determination of the mean age of onset of disease would require long-term study of a population of at-risk horses. Finally, we did not test for leptospirosis in this population. Serology alone may not be helpful in the definitive diagnosis of *Leptospira*-associated uveitis and in order to have strong evidence that leptospirosis plays a role in the development of ERU, sampling of ocular fluids for PCR, antibody detection, and/or culture is required.⁴⁰⁻⁴² Sampling ocular fluids is invasive and requires aseptic preparation which was not practical under field study conditions. The potential role of leptospirosis in insidious uveitis of the Appaloosa in western Canada is, therefore, still unclear.

To our knowledge, this is the first long-term prospective study to characterize ERU in the Appaloosa breed in Canada. The study supports the insidious nature of the condition and identifies age, coat pattern phenotype, and genetics to be major risk factors for diagnosis and classification of clinical signs and severity of damage from ERU in the Appaloosa. Based on this study, it is advisable to examine at-risk horses more frequently, especially after 12 years of age. Future studies to identify causal genetic variants for ERU are underway.

5 | Acknowledgments

We thank the horse owners who allowed their animals to participate in this study. This study was made possible with support from the Townsend Equine Health Research Fund (TEHRF) and the Morris Animal Foundation D16EQ-028. The mission of the Morris Animal Foundation is to bridge science and resources to advance the health of animals.

6 | Conflict of Interest

Nicole B. Kingsley and Rebecca R. Bellone are affiliated with the Veterinary Genetics Laboratory, a laboratory offering diagnostic tests in horses and other species.

7 | References

1. Gilger BC. Equine recurrent uveitis. The viewpoint from the USA. *Equine Vet J Suppl.* 2010;37:57-61.
2. Dwyer AE, Crockett RS, Kalsow CM. Association of leptospiral seroreactivity and breed with uveitis and blindness in horses: 372 cases (1986–1993). *J Am Vet Med Assoc.* 1995;207:1327-1331.
3. Davidson MG, Nasisse MP, Roberts SM. Immunodiagnosis of leptospiral uveitis in two horses. *Equine Vet J.* 1987;19:155-157.
4. Wollanke B, Gerhards H, Brem S, Kopp H, Meyer P. Intraocular and serum antibody titers to *Leptospira* in 150 horses with equine recurrent uveitis (ERU) subjected to vitrectomy. *Berl Munch Tierarztl Wochenschr.* 1998;111:134-139.
5. Wollanke B, Rohrbach BW, Gerhards H. Serum and vitreous humor antibody titers in and isolation of *Leptospira interrogans* from horses with recurrent uveitis. *J Am Vet Med Assoc.* 2001;219:795-800.

6. Pearce JW, Galle LE, Kleiboeker SB, et al. Detection of *Leptospira interrogans* DNA and antigen in fixed equine eyes affected with end-stage equine recurrent uveitis. *J Vet Diagn Invest.* 2007;19:686-690.
7. Deeg CA, Ehrenhofer M, Thureau SR, Reese S, Wildner G, Kaspers B. Immunopathology of recurrent uveitis in spontaneously diseased horses. *Exp Eye Res.* 2002;75:127-133.
8. Faber NA, Crawford M, LeFebvre RB, Buyukmihci NC, Madigan JE, Willits NH. Detection of *Leptospira* spp. in the aqueous humor of horses with naturally acquired recurrent uveitis. *J Clin Microbiol.* 2000;38:2731-2733.
9. Brandes K, Wollanke B, Niedermaier G, Brem S, Gerhards H. Recurrent uveitis in horses: vitreal examinations with ultrastructural detection of leptospire. *J Vet Med Ser.* 2007;54:270-275.
10. Brem S, Gerhards H, Willanke B, Meyer P, Kopp H. 35 *Leptospira* isolated from the vitreous body of 32 horses with recurrent uveitis (ERU). *Berl Munch Tierarztl Wochenschr* 1999;112:390-393.
11. Gerding JC, Gilger BC. Prognosis and impact of equine recurrent uveitis. *Equine Vet J.* 2016;48:290-298.
12. Gilger BC, Salmon JH, Yi NY, et al. Role of bacteria in the pathogenesis of recurrent uveitis in horses from the southeastern United States. *Am J Vet Res.* 2008;69:1329-1335.
13. Niedermaier G, Wollanke B, Hoffmann R, Brem S, Gerhards H. Detection of *Leptospira* in the vitreous body of horses without ocular disease and of horses with ERU using transmission-electron microscopy. *Deutsche Tierarztliche Wochenschrift.* 2006;113:418-422.
14. Romeike A, Brugmann M, Drommer W. Immunohistochemical studies in equine recurrent uveitis (ERU). *Vet Pathol.* 1998;35:515-526.

15. Gilger BC, Malok E, Cutter KV, Stewart T, Horohov DW, Allen JB. Characterization of T-lymphocytes in the anterior uvea of eyes with chronic equine recurrent uveitis. *Vet Immunol Immunopathol.* 1999;71:17-28.
16. Deeg CA, Thurau SR, Gerhards H, Ehrenhofer M, Wildner G, Kaspers B. Uveitis in horses induced by interphotoreceptor retinoid-binding protein is similar to the spontaneous disease. *Eur J Immunol.* 2002;32:2598-2606.
17. Deeg CA, Pompetzki D, Raith AJ, *et al.* Identification and functional validation of novel autoantigens in equine uveitis. *Mol Cell Proteomics.* 2006;5:1462-1470.
18. Saldinger LK, Nelson SG, Bellone RR, *et al.* Horses with equine recurrent uveitis have an activated CD4+ T-Cell phenotype that can be modulated by mesenchymal stem cells *in vitro.* *Vet Ophthalmol* (2019 Accepted). 2020;23(1):160-170.
19. Fritz KL, Kaese HJ, Valberg SJ, *et al.* Genetic risk factors for insidious equine recurrent uveitis in Appaloosa horses. *Anim Genet.* 2014;45:392-399.
20. Kulbrock M, Lehner S, Metzger J, Ohnesorge B, Distl O. A genome-wide association study identifies risk loci to equine recurrent uveitis in German warmblood horses. *PLoS ONE.* 2013;8(8):e71619.
21. Kulbrock M, von Borstel M, Rohn K, Distl O, Ohnesorge B. Occurrence and severity of equine recurrent uveitis in warmblood horses – a comparative study. *Pferdeheilkunde.* 2013;29:27-36.
22. Angelos J, Oppenheim Y, Rebhun W, Mohammed H, Antczak DF. Evaluation of breed as a risk factor for sarcoid and uveitis in horses. *Anim Genet.* 1998;19:417-425.
23. Deeg CA, Marti E, Gaillard C, Kaspers B. Equine recurrent uveitis is strongly associated with the MHC class I haplotype ELA-A9. *Equine Vet J.* 2004;36:73-75.

24. Rockwell H, Mack M, Famula T, *et al.* Genetic investigation of equine recurrent uveitis in Appaloosa horses. *Anim Gen.* 2019;51(1):111-116.
25. Bellone RR, Forsyth G, Leeb T, *et al.* Fine-mapping and mutation analysis of *TRPM1*: a candidate gene for leopard complex (LP) spotting and congenital stationary night blindness. *Brief Funct Genomics.* 2010;9:193-207.
26. Bellone RR, Holl H, Setaluri V DS, *et al.* Evidence for a retroviral insertion in *TRPM1* as the cause of congenital stationary night blindness and leopard complex spotting in the horse. *PLoS ONE.* 2013;8(10):e78280.
27. Bellone RR, Brooks SA, Sandmeyer L, *et al.* Differential gene expression of *TRPM1*, the potential cause of congenital stationary night blindness and coat spotting patterns (LP) in the Appaloosa horse (*Equus caballus*). *Genetics.* 2008;179:1861-1870.
28. Sponenberg DP, Carr G, Simak E, Schwink K. The inheritance of the leopard complex of spotting patterns in horses. *J Hered.* 1990;81:323-331.
29. Miller RW. Appaloosa coat color inheritance. Ph.D. Thesis, Animal Science Department, Montana State University, Bozeman, MT. 1965.
30. Holl HM, Brooks SA, Archer S, *et al.* Variant in the *RFWD3* gene associated with *PATN1*, a modifier of leopard complex spotting. *Anim Genet.* 2016;47:91-101.
31. Sandmeyer LS, Bauer BS, Feng CX, Grahn BH. Equine recurrent uveitis in western Canadian prairie provinces: A retrospective study (2002–2015). *Can Vet J.* 2017;58:717-722.
32. Bellone RR, Liu J, Petersen JL, *et al.* A missense mutation in damage-specific DNA binding protein 2 is a genetic risk factor for limbal squamous cell carcinoma in horses. *Int J Cancer.* 2017;141:342-353.

33. Garbe JR, Da Y. Pedigraph: A Software Tool for the Graphing and Analysis of Large Complex Pedigree. User manual Version 2.4. Department of Animal Science, University of Minnesota. 2008.
34. Cunningham EP, Dooley JJ, Splan RK, Bradley DG. Microsatellite diversity, pedigree relatedness and the contributions of founder lineages to thoroughbred horses. *Anim Genet.* 2001;32:360-364.
35. Hurn SD, Turner AG. Ophthalmic examination findings of Thoroughbred racehorses in Australia. *Vet Ophthalmol.* 2006;9:95-100.
36. Barnett KC, Crispin SM, Lavach JD, Matthews AG. *Equine Ophthalmology: An Atlas and Text*, 2nd edn. Edinburgh: W.B. Saunders; 2004.
37. Roberts SR. Fundus lesion in equine periodic ophthalmia. *J Am Vet Med Assoc.* 1962;141:229-239.
38. Lavach JD. Pupil, iris, and ciliary body. In: *Large Animal Ophthalmology*. C.V. Mosby Company, St. Louis, 1990:150-177.
39. Cutler TJ, Brooks DE, Andrew SE, *et al.* Disease of the equine posterior segment. *Vet Ophthalmol.* 2000;3:73-82.
40. Sauvage AC, Monclin SJ, Elansary M, Hansen P, Grauwels MF. Detection of intraocular *Leptospira spp.* by real-time polymerase chain reaction in horses with recurrent uveitis in Belgium. *Equine Vet J.* 2019;51:299-303.
41. Malalana F, Blundell RJ, Pinchbeck GL, McGowan CM. The role of *Leptospira spp.* in horses affected with recurrent uveitis in the UK. *Equine Vet J.* 2017;49:706-709.
42. Dorrego-Keiter E, Toth J, Dikker L, Sielhorst J, Schusser GF. Detection of *Leptospira* by culture of vitreous humor and detection of antibodies against *Leptospira* in vitreous humor and

serum of 225 horses with equine recurrent uveitis. *Berl Munch Tierarztl Wochenschr.*
2016;129:209-215.